Manipulating immune checkpoint signalling pathways with antibodies

Christopher Paluch

Jesus College

Supervisors: Prof Simon J. Davis and Prof Richard J. Cornall

Thesis submitted for the degree of Doctor of Philosophy
in Biomedical and Clinical Sciences



The work described in this thesis was supported by the Wellcome Trust (grant number [109029/Z/15/Z]) and the Medical Research Council (grant number [MC_UU-12010/4]).





Abstract

Manipulating immune checkpoint signalling pathways with antibodies
Christopher Paluch, Jesus College
Thesis submitted for the degree of Doctor of Philosophy in Biomedical and Clinical Sciences, Trinity Term 2019

Immune checkpoint receptors are critical regulators of immune tolerance. Antibodies blocking these pathways can enhance immune responses and in recent years have revolutionised the treatment of cancer. The converse approach of developing agonistic antibodies against checkpoint receptors to dampen immune responses has not been widely explored, and whether this could present an effective new approach for the treatment of autoimmune disease remains an open question. We have characterised panels of antibodies against three human immune checkpoint receptors: BTLA, TIGIT and CD200R. For each of these targets we have also characterised a transgenic mouse strain expressing the human form of the protein in a functional pathway, allowing for the assessment of translatable anti-human antibodies in the physiological context of an intact immune system. Using these transgenic mice we demonstrated that a BTLA agonist antibody can inhibit T cell responses *in vitro* and *in vivo* and that this can have a meaningful therapeutic impact in murine models of autoimmune disease. Utilising a collection of engineered antibodies as tool reagents we showed that antibody agonism of checkpoint receptors is dependent on Fc receptor engagement and sensitive to the dimensions of the antibody. This supports a mechanism of antibody agonism compatible with the kinetic-segregation model of receptor triggering, in which an immobilised antibody induces triggering by holding the receptor in the contact between two cells, leading to physical exclusion of the bulky receptor-type phosphatases that normally restrain signalling. Our results set the scene for the future clinical development of checkpoint agonists as a novel class of immunosuppressive therapeutic and provide insights into how such agents can be designed and optimised for maximal efficacy.

Acknowledgements

First and foremost, I would like to thank my two supervisors, Simon Davis and Richard Cornall for giving me the opportunity to work in two such fantastic labs and to be part of such an exciting project, as well as for your guidance and mentorship. Heather Brouwer for training me from scratch in molecular biology techniques and for your tireless assistance in cloning, protein production and purification. Tanya Cheetham for your super efficient colony management and equally efficient management of the coffee club biscuit cupboard. Consuelo Anzilotti for your mentorship at the beginning of my time in the lab, and invaluable training in flow cytometry and *in vivo* experimental protocols, and for all your work prior to my arrival in the lab that made this project possible. Oliver Lui for your never ending willingness to help with all problems great or small. To all other members of the Cornall and Davis labs for your help and support, and for creating such a fun environment to work in, as well as for putting up with my liberal approach to marker pen ownership.

Finally, my wife Amy for putting up with the recent omnipresence of my laptop on weekends, evenings and holidays, for fitting your life and work around my attachment to Oxford, and for your rigorous proofreading of this acknowledgements section.

Contents

Chapter 1 Introduction 1
1.1. Introduction to the immune system 1
1.1.1. Mechanical and chemical barriers to infection 2
1.1.2. Innate immune cells 3
1.1.3. The adaptive immune system 5
1.1.4. Orchestration of an adaptive immune response 6
1.2. Antibody isotypes and Fc receptors 8
1.3. Immune tolerance 11
1.3.1. Central tolerance 12
1.3.2. Peripheral tolerance and co-stimulatory receptors 12
1.3.3. The breakdown of tolerance leading to autoimmune disease 13
1.3.4. Existing therapies for autoimmune disease 14
1.4. Immunoreceptors 18
1.5. Models of immunoreceptor triggering 20
1.5.1. Aggregation models 21
1.5.2. Conformational change models 21
1.5.3. Segregation models 22
1.6. Immunoreceptor triggering by antibodies 26
1.7. Targeting immunoreceptors in cancer 28
1.8. Inhibitory immunoreceptor associations with autoimmune disease 31
1.9. Targeting inhibitory receptors for the treatment of autoimmunity 33
1.9.1. Natural ligand based inhibitory agonists 34
1.9.2. Agonist antibodies targeting inhibitory receptors 36
1.9.3. Novel engineered agonist constructs 41
1.10. The inhibitory receptors explored in this thesis 44
1.10.1. PD1 44
1.10.2. BTLA 46
1.10.3. TIGIT 50
1.10.4. CD200R 52
1.11. Work leading up to this project 54

Chapter 2 Materials and Methods 58
2.1. Buffers and reagents 58
2.1.1. General reagents 58
2.1.2. Cell culture media 59
2.2. Generation of B-cell hybridomas 60
2.3. Molecular biology techniques 61
2.3.1. Molecular Cloning 61
2.3.2. Antibody Isotyping 63
2.3.3. Hybridoma sequencing to obtain variable domain sequences 63
2.3.4. Cell culture 64
2.3.5. Hybridoma culture for the production of murine antibodies 64
2.3.6. Lentiviral transduction of HEK293T cells 65
2.3.7. Stable transfection of CHOK1 cells 66
2.3.8. Transient transfection of HEK293T cells using POPIN and pFUSE vectors 67
2.3.9. Creation of epitope mapping panels by site directed mutagenesis 68
2.3.10. Epitope mapping by flow cytometry of the mutant panels 71
2.3.11. Creation of lower affinity antibody variants by CDR mutagenesis 72
2.3.12. Nickel purification 72
2.3.13. Protein G purification 74

2.3.14. Protein A purification 74
2.3.15. Thrombin cleavage of Fc-fusion proteins 75
2.3.16. Quantification of protein concentrations 75
2.3.17. Gel electrophoresis 76
2.3.18. FPLC 76
2.3.19. Biotinylation 77
2.4. Surface plasmon resonance assays 77
2.5. Flow cytometry 79
2.6. Experiments using transgenic humanised mice 81
2.6.1. Genotyping of transgenic mice 82
2.7. Mouse mixed lymphocyte reaction 83
2.8. Assessing upregulation of checkpoint receptors on stimulation 84
2.9. Phenotyping immune cell subsets in humanised mice 84
2.10. Immunisation protocols 86
2.10.1. Sheep red blood cell (SRBC) immunisations 86
2.10.2. NPCGG immunisations and NPCGG specific ELISA 86
2.11. Adoptive transfer assays 87
2.12. Complement mediated cytotoxicity (CDC) assay 88
2.13. Antibody-dependent cell mediated cytotoxicity (ADCC) assay 89
2.14. *In vivo* cytotoxicity assessment 89
2.15. T-cell transfer model of colitis 89
2.16. Graft versus host disease model 91
2.17. MC38 colorectal cancer model 91
2.18. Statistical analysis 92

Chapter 3 Characterisation of the humanised mice 93
3.1. Introduction 93
3.2. Assessing cross-reactivity of human receptors with mouse ligands 95
3.3. Expression of the chimeric receptors in the transgenic mice 102
3.4. Immune system development in the transgenic mice 106
3.5. Response to immune challenge 114
3.6. Discussion 119

Chapter 4 Characterisation of antibody panels 121
4.1. Introduction 121
4.2. Assessment of antibody affinities 122
4.3. Assessment of ligand blockade 125
4.4. Epitope mapping 128
4.5. Generation of lower affinity mutants 138
4.6. Generation of Fc receptor knockout antibodies 141
4.7. Discussion 142

Chapter 5 Assessment of BTLA antibody effects on T cell responses 144
5.1. Introduction 144
5.2. Mixed lymphocyte reaction 144
5.3. SRBC and NPCGG immunisations 149
5.4. Adoptive transfer experiments 152
5.5. *In vitro* and *in vivo* cytotoxicity of anti-BTLA antibodies 154
5.6. Importance of antibody size to agonist function 159
5.7. Improving PD1 blockade by removal of antibody agonism 162
5.8. Discussion 165

Chapter 6 Assessment of BTLA antibodies in models of disease 168

6.1. Introduction ... **168**
6.2. T-cell transfer model of colitis ... **169**
6.3. Graft versus host disease ... **175**
6.4. MC38 model of colorectal cancer ... **179**
6.5. Discussion ... **182**

Chapter 7 General Discussion ... **185**
7.1. The humanised mice provide a tool for therapeutic antibody assessment ... **185**
7.2. BTLA agonist antibodies inhibit immune responses ... **187**
7.3. Antibody agonism of checkpoint receptors is FcR dependent ... **190**
7.4. Agonist activity does not require mimicry of ligand binding ... **193**
7.5. Agonism of checkpoints is sensitive to antibody dimensions ... **194**
7.6. Efficacy of checkpoint inhibitors could be limited by agonist activity ... **196**
7.7. Concluding remarks ... **197**

Chapter 8 Appendix ... **198**
8.1. Sequences of chimeric transcripts expressed in the transgenic mice ... **198**
8.1.1. BTLA ... 198
8.1.2. TIGIT ... 199
8.1.3. CD200R ... 200
8.2. Sequences of soluble proteins used for surface plasmon resonance ... **201**
8.2.1. hCD200RmFc-His ... 201
8.2.2. mCD200RmFc-His ... 201
8.2.3. hTIGITmFC-His ... 201
8.2.4. mTIGITmFc-His ... 201
8.2.5. His-hTIGIT (bacterial expression and refold) ... 202
8.2.6. His-hTIGIT-BirA (bacterial expression and refold) ... 202
8.2.7. His-mTIGIT (bacterial expression and refold) ... 202
8.2.8. hBTLAmFc-His ... 202
8.2.9. mBTLAmFc-His ... 202
8.2.10. hBTLA-His-BirA (bacterial expression and refold) ... 202
8.2.11. hHVEMmFc-His ... 203
8.2.12. mHVEMmFc-His ... 203
8.2.13. hPVR-BirA-His ... 203
8.2.14. mPVR-BirA-His ... 203
8.2.15. hCD200-BirA-His ... 203
8.2.16. mCD200-BirA-His ... 204
8.3. Constructs for epitope mapping ... **204**
8.3.1. Wildtype hBTLAmCD28-GFP^2 (cloned into pGFP^2-N3 vector) ... 204
8.3.2. Wildtype hTIGITmCD28-GFP^2 ... 204
8.3.3. Wildtype hCD200RmCD28-GFP^2 ... 204

Chapter 9 References ... **205**

List of Figures

Figure 1-1: Structure of a human IgG1 antibody 9
Figure 1-2: Immunoreceptor triggering in the physiological context and by agonist antibodies 25
Figure 1-3: Ligand interactions and signalling pathways of PD1 45
Figure 1-4: Ligand interactions and signalling pathways of BTLA 49
Figure 1-5: Ligand interactions and signalling pathways of TIGIT 51
Figure 1-6: Ligand interactions and signalling pathways of CD200R 53
Figure 1-7: Design of the chimeric receptor in the humanised BTLA mice. 55
Figure 1-8: Design of the chimeric receptor in the humanised CD200R mice. 56
Figure 1-9: Design of the chimeric receptor in the humanised TIGIT mice 56
Figure 3-1: SPR assessment of CD200R-CD200 cross-species interactions 98
Figure 3-2: SPR assessment of TIGIT-PVR cross-species interactions 99
Figure 3-3: SPR assessment of BTLA-HVEM cross-species interactions 100
Figure 3-4: Chimeric BTLA expression 104
Figure 3-5: Chimeric TIGIT expression 104
Figure 3-6: Chimeric CD200R expression 105
Figure 3-7: Flow cytometry gating strategies for immunophenotyping of transgenic mice 108
Figure 3-8: Flow cytometry gating strategies for phenotyping of B-cell populations and development 109
Figure 3-9: Flow cytometry gating strategies for myeloid cell populations and NK cells 110
Figure 3-10: Humanised BTLA mice immune system development 111
Figure 3-11: Humanised CD200R mice immune system development 112
Figure 3-12: Humanised TIGIT mice immune system development 113
Figure 3-13: SRBC response FACS gating 116
Figure 3-14: SRBC response in humanised strains 117
Figure 3-15: NP-CGG response in humanised strains 118
Figure 4-1: Example SPR data showing single cycle kinetics analysis of antibody binding to target receptor 123
Figure 4-2: Two different methods for SPR assessment of ligand blockade by checkpoint antibodies 127
Figure 4-3: Hypothesised relevance of epitope position to agonist activity 130
Figure 4-4: Example epitope mapping data for antibodies against BTLA 133
Figure 4-5: Epitope maps of membrane proximal binding antibodies to each of the three inhibitory receptors 134
Figure 4-6: Binding of antibody 2.8.6 to BTLA 137
Figure 4-7: Generation of an affinity series of mutant variants of the anti-BTLA clone 8.3.1 140
Figure 5-1: Mixed lymphocyte reaction 146
Figure 5-2: BTLA antibody impact on SRBC and NP-CGG immunisations 151
Figure 5-3: Adoptive transfers 153
Figure 5-4: *In vitro* cytotoxicity assessment. 157
Figure 5-5: *In vivo* cytotoxicity assessment 158
Figure 5-6: Impact of antibody size on agonistic function. 161
Figure 5-7: Effect of antibody size and FcR interaction on PD1 blockade 164

Figure 6-1: T-cell transfer model of colitis set up 171
Figure 6-2: Antibody effects in T-cell transfer model of colitis 174
Figure 6-3: Parent-to-F1 model of GVHD 178
Figure 6-4: MC38 model of colorectal cancer 181

List of Tables

Table 2-1: Mutants produced for epitope mapping 70
Table 2-2: Flow cytometry panels used for phenotyping of immune cell subsets in the transgenic mice. 85
Table 3-1: Summary of interaction affinities for each of the cross-species receptor-ligand interactions 101
Table 4-1: Summary of binding kinetics and ligand blockade for each antibody, as determined by surface plasmon resonance 124

Abbreviations

APC	Antigen-presenting cell
BCR	B-cell receptor
BLAST	Basic local alignment search tool
BTLA	B- and T-lymphocyte attenuator
C-terminus	Carboxy-terminus
CD	Cluster of differentiation
CD200R	CD200 receptor
cDNA	Complementary DNA
CDR	Complementarity-determining region
CHO	Chinese hamster ovary
CMV	Cytomegalovirus
CRO	Contract research organisation
CTLA4	Cytotoxic T-lymphocyte-associated protein 4
DC	Dendritic cell
DMEM	Dulbecco's modified eagle medium
DNA	Deoxyribonucleic acid
dNTP	Deoxynucleotide
EDTA	Ethylenediaminetetraacetic acid
ELISA	Enzyme-linked immunosorbent assay
Fab	Fragment antigen-binding
FACS	Fluorescence-activated cell sorting
Fc	Fragment crystallisable
FcR	Fragment crystallisable receptor
FPLC	Fast protein Liquid Chromatography
GPCR	G-protein coupled receptor
h	Human
HAT medium	Hypoxanthine-aminopterin-thymidine medium
HBS	HEPES-buffered saline
HEK	Human embryonic kidney
HEPA	High-efficiency particulate air
HEPES	(4-(2-hydroxyethyl)-1-piperazineethanesulfonic acid
hi	High
His	Histidine
HIV	Human immunodeficiency virus
HRP	Horse radish peroxidase
IC50	Half maximal inhibitory concentration
ICOS	Inducible T-cell costimulator
IFN	Interferon
Ig	Immunoglobulin
IgSF	Immunoglobulin superfamily
IL-2	Interleukin-2
ILC	Innate lymphoid cell
ITAM	Immunoreceptor tyrosine-based activation motif
ITIM	Immunoreceptor tyrosine-based inhibitory motif
ITSM	Immunoreceptor tyrosine-based switch motif

K_d	Dissociation constant
k_{off}	Dissociation rate constant
k_{on}	Association rate constant
KS	Kinetic segregation
Lck	Lymphocyte-specific protein tyrosine kinase
LIGHT	Homologous to lymphotoxin, exhibits inducible expression and competes with HSV glycoprotein D for binding to herpesvirus entry mediator, a receptor expressed on T lymphocytes
LPS	Lipopolysaccharide
m	Mouse
MFI	Mean fluorescence intensity
MHC	Major histocompatibility complex
MSX	Methionine sulphoximine
N-glycan	Amine-linked glycan
N-terminus	Amine-terminus
NFAT	Nuclear factor of activated T-cells
NK	Natural killer
NFκB	Nuclear factor kappa-light-chain-enhancer of activated B-cells
NHS-ester	N-hydroxysuccinimide ester
Ni-NTA	Nickel-nitrilotriacetic acid
O-linked	Oxygen-linked
PAMP	Pathogen-associated molecular pattern
PBMCs	Peripheral blood mononuclear cells
PBS	Phosphate-buffered saline
PCR	Polymerase chain reaction
PRR	Pattern recognition receptors
PD1	Programmed cell death protein 1
PDL1	Programmed death ligand 1
pH	Potential hydrogen
pMHC	peptide-bound MHC protein
r	Rat
RNA	Ribonucleic acid
RT	Room temperature
ScFv	Single chain variable fragment
SDS-PAGE	Sodium dodecyl sulphate polyacrylamide gel electrophoresis
SH2	Src homology 2
SHIP1	Src homology 2 domain containing inositol polyphosphate 5-phosphatase 1
SHP1	Src homology 2 domain containing protein tyrosine phosphatase-1
Taq	Thermus aquaticus
TCR	T-cell receptor
TLR	Toll like receptor
TNF	Tumour necrosis factor
TNFSF	Tumour necrosis factor superfamily
TNFR	Tumour necrosis factor receptor
TNFRSF	Tumour necrosis factor receptor superfamily

Chapter 1 Introduction

1.1. Introduction to the immune system

Humans have evolved in a world teeming with microbial life. Our immune system exists primarily as a mechanism to protect us from the small subset of microorganisms that might do us harm, termed pathogens. The system is made up of multiple lines of defence ranging from simple mechanical barriers to sophisticated cellular war machines capable of detecting short peptide sequences specific to a particular pathogen and equipped with an array of effector arms to neutralize the threat [1]. Given the potential to inflict great damage on both pathogens and the body itself, it is crucial that the immune system is kept in check by a complex collection of control mechanisms that prevent attack on benign or self-tissue and that can restore quiescence following target clearance when immune activation is no longer required. The ability of immune cells to discriminate between the harmful and the harmless is imparted largely by the repertoire of receptors on their surface, which enable them to interact with their surroundings. Danger signals received from unfamiliar molecules, or those known to be associated with pathogens, and from inflammatory mediators prompt an activation response, whilst the detection of self-molecules or regulatory cytokines can counteract this with an inhibitory signal. The processes that lead to immune non-responsiveness to harmless and self-molecules is known as immune tolerance [2] and the breakdown of this tolerance is the root cause of a range of pathologies broadly classified as autoimmune diseases. These diseases present a huge societal burden [3], and cause very significant patient morbidity, and there remains a need to develop novel and more effective therapies.

1.1.1. Mechanical and chemical barriers to infection

The external surface of the human body includes both the skin that we can see and the linings of the gut, respiratory and urogenital tract that also face the outside world. This entire surface is covered by a closely packed layer of epithelial cells that keeps the vast majority of microorganisms out. In the gut and urinary tract the one-way flow of fluids aids in expelling potential pathogens from the body. Similarly, in the lungs and nasal cavities the coordinated action of brush-like cilia acts to sweep dirt and pathogens, caught up in a protective layer of mucus, out of the body. These barriers are not just mechanical but also produce an array of chemical deterrents. The skin is coated in a layer of fatty acids that create a hostile environment for bacterial growth, and the very low pH of the stomach provides an even greater hurdle to bacterial survival. Enzymes such as lysozyme and phospholipase A_2 secreted into saliva, tears and the gut act to break down bacterial cell walls and membranes. Furthermore, epithelial cells produce various antimicrobial peptides such as defensins, cathelicidins, histatins and lectins that can integrate into the cell membrane of microbes, by electrostatic interactions or by binding to microbial sugars, and form pores that disrupt the integrity of the membrane [4].

Despite the creation of such a harsh environment, a vast number of commensal microbes do still live and grow on top of our epithelial coat, but whilst they stay on the outside they generally cause us no harm. When the barrier is damaged by injury or a pathogen manages to break through it is met by yet more chemical defences. A collection of hepatically-produced proteins that together make up the complement

cascade identify invaders either by directly binding to their surface or via other proteins that mark them for destruction, such as lectins which recognize bacterial sugars and antibodies which highlight previously encountered foreign structures. Once the complement system is activated a series of amplification steps, involving proteolytic cleavage of the next protein in the chain, leads to three branches of effector mechanism that deal with the threat [5]. Firstly, a collection of complement proteins group together to form a membrane-attack-complex that directly lyses the coated cell. Secondly, cleaved complement proteins, denoted anaphylatoxins, act as chemoattractants bringing inflammatory cells to the vicinity. Thirdly, other cleaved peptides remain stuck to the surface of the pathogen and, via binding to complement receptors, stimulate uptake by phagocytic cells in a process called opsonisation.

As an additional line of defence, damage to blood vessels and inflammation at the entry site leads to initiation of the coagulation cascade which clots off efferent blood vessels and traps bacteria in a fibrin network at the site of infection [6]. Activated endothelial cells also release pro-inflammatory mediators such as bradykinin that increase afferent blood flow and increase the permeability of blood vessels leading to an influx of immune cells [7].

1.1.2. Innate immune cells

Alongside the body's mechanical and chemical barriers, the immune system has evolved a repertoire of defensive cell types to further protect against microbial invasion. These cell types are dichotomised into two groups, based upon whether the primary receptors that they use to detect microbes are encoded in the germline

(innate cells) or generated quasi-randomly via genetic recombination events (adaptive cells). The innate cells include neutrophils, macrophages, dendritic cells (DCs), mast cells, eosinophils, basophils, natural killer (NK) cells and innate lymphoid cells (ILCs).

One route by which these cells can become activated is via receptors, on their surface or intracellular, that recognise molecules not present on healthy human tissue. These receptors are known as pattern recognition receptors (PRRs) and include both pathogen-associated-molecular-pattern (PAMP) receptors that recognise molecular structures expressed only on microbes and damage-associated-molecular pattern (DAMP) receptors that recognise molecules indicative of damaged or stressed cells. One key example is the toll-like receptor TLR4 which binds to the lipopolysaccharide (LPS) found in the outer membrane of gram-negative bacteria [8]. Other ligands for PRRs include bacteria-specific sugars and proteins such as flagellin, and nucleic acids specific to the pathogens such as viral double stranded RNAs and bacterial unmethylated CpG dinucleotides [9].

Innate immune cells can also be alerted to a threat via receptors that recognise complement proteins or antibodies coating the surface of pathogens. Once alerted they have a number of means to deal with invaders. Firstly, they can directly attack pathogens by releasing toxic mediators that damage cell membranes or pass through damaged membranes to inflict intracellular damage. Secondly, they can physically engulf pathogens in a process called phagocytosis, and once taken up destroy them by exposure to hydrolytic enzymes and reactive oxygen species in the low pH

environment of the phagolysosome. Finally, innate cells can raise the alarm by the release of inflammatory mediators such as cytokines and chemokines that stimulate the production, migration and activation of other immune cells. Furthermore, they can present on their cell surface short peptides derived from engulfed material that are recognised by T cells and enable the induction of an adaptive immune response.

1.1.3. The adaptive immune system

The germline encoded receptors of the innate immune system have evolved over many millennia to recognise common pathogen molecules. However, evolution in multicellular organisms is a slow process and by far outpaced by the speed at which pathogens such as viruses and bacteria can evolve. Accordingly, our immune system has developed a sophisticated mechanism to recognise any potential invader, even if entirely new. The B- and T-cells of the adaptive immune system each generate a key surface receptor by near random recombination of genetic building blocks in a process capable of generating a vast diversity of target binding sites [10]. Any specific molecule that these receptors recognise is referred to as an antigen. Each B- or T-cell clone stably expresses its own unique recognition receptor and clones can be selected to activate, proliferate and persist if they encounter their specific antigen in the appropriate context. In this way an accelerated Darwinian-like selection process is established within a single individual's immune system that is able to keep pace with novel and rapidly changing threats.

B cells develop in the bone marrow and express on their surface a bivalent B-cell receptor (BCR) that recognises cognate antigen in its native form. They also produce

antibodies, a secreted version of the BCR, which can bind to antigen and link up to other effector mechanisms of the immune system via binding to complement or to Fc receptors on other immune cells.

T cells develop initially in the bone marrow then mature in the thymus. They express on their surface a monovalent T-cell receptor (TCR) that recognises short peptides presented in the context of specialised receptors, known as MHC (major histocompatibility complex) molecules, on the surface of other self cells [11]. MHC class II molecules present peptides derived from endocytosed proteins and are recognised by helper T-cells, defined by their expression of the co-receptor CD4. MHC class I molecules generally present peptides derived from self-proteins inside the cell or from intracellular pathogens such as viruses, and they are recognised by CD8-expressing cytotoxic T-cells. In professional antigen presenting cells, such as dendritic cells, class I molecules can also present endocytosed material in a process known as cross-presentation which enables DCs to prime CD8 T-cells with viral material taken up from their surroundings even when they are not themselves infected [12].

1.1.4. Orchestration of an adaptive immune response

In damaged or infected tissues, dendritic cells take up antigens and become activated by the inflammatory milieu created by the innate immune system. The activated DCs traffic to regional lymphoid tissue with antigen presented on their surface. Naïve T-cells, having left the thymus, circulate through the blood and lymphatic system. If they encounter their cognate peptide-MHC on the surface of an activated DC they are

triggered to proliferate and differentiate into various subtypes of effector T-cell. Some primed T-cells then leave the lymph nodes and traffic to the site of infection.

Effector CD8 T-cells recognise their cognate peptide-MHC on the surface of infected cells and form a synapse with these cells into which they release pre-formed chemicals called perforins that damage the target cell membrane and granzymes that pass through the damaged membrane to induce apoptosis in the targeted cell [13]. They also upregulate the membrane bound molecule Fas-ligand which binds to the death receptor Fas on target cells inducing apoptosis [14].

Effector CD4 T-cells, after recognising their antigen on the surface of professional antigen presenting cells, produce cytokines that enhance the effector mechanisms and antigen presentation function of innate immune cells. For example IFNγ produced by CD4 T-cells can activate macrophages to increase their production of reactive oxygen species, boosting their ability to destroy phagocytosed bacteria [15]. Naïve CD4 T-cells can differentiate into different subtypes of effector helper T-cell, dependent on the nature of the inflammatory environment in which they are primed. These different effector cells (such as Th1, Th2 and Th17 cells) subsequently direct the on-going immune response in different ways, via the production of subset specific cytokines [16].

Some primed CD4 T-cells, termed T-follicular-helper (Tfh) cells, stay in the secondary lymphoid tissues and migrate to the B-cell area. Naïve B-cells recognise their cognate antigen via their surface-expressed BCR, which acts both as an activating receptor

and also aids endocytosis of the antigen. Following internalisation the antigen is degraded and peptides presented on class II MHC molecules on the B-cell surface. CD4 T-cells that recognise this peptide-MHC produce cytokines and upregulate activatory ligands on their cell surface, which provide the help signal that B cells need to become fully activated. The activated B-cells then either differentiate to become antibody producing plasma cells or enter a germinal centre where they undergo a process called somatic hypermutation. This involves the targeted mutation of BCR-encoding genes and a combination of rapid proliferation and clonal selection steps that ultimately lead to the production of B cells with higher affinity receptors for the target antigen [17]. T-cell help signals can also direct B cells to permanently switch the isotype of the antibody they produce. Antibodies of different isotype induce different effector responses dependent on their differential ability to engage complement and on the expression pattern on innate cells of the specific Fc receptors to which they bind [18], as described in more detail in the section below.

During an adaptive immune response a subset of activated B - and T-cells also differentiate into memory cells that persist in a primed state long after the offending pathogen has been cleared and enable an accelerated response to occur if the same pathogen, or a pathogen expressing similar antigens, is ever encountered again [19].

1.2. Antibody isotypes and Fc receptors

Antibodies are glycoproteins consisting of two heavy chains and two lights chains arranged into a homodimeric Y-shaped structure as depicted in Figure 1-1. The light chains consist of one variable and one constant immunoglobulin domain, whilst the

heavy chains consist of one variable and three or four constant domains. The portion of the molecule consisting of the light chain paired to the first two domains of the heavy chain is referred to as a Fab (fragment responsible for antigen binding). The portion consisting of the remaining heavy chain domains paired together is referred to as the Fc (fragment crystallisable) and is the part of the molecule that is responsible for effector functions by binding to complement proteins or Fc receptors. The two Fabs are connected to the Fc by the flexible hinge region of the heavy chains.

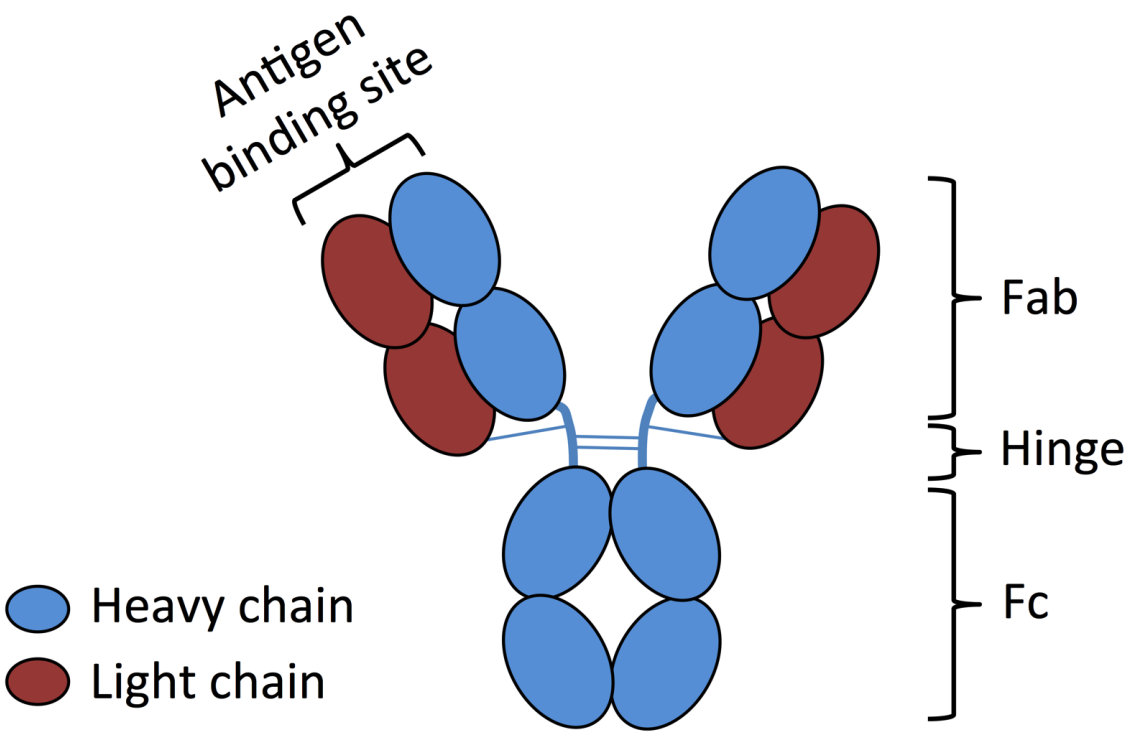


Figure 1-1: Structure of a human IgG1 antibody. Disulphide stabilised homodimeric structure of an IgG antibody. A light chain paired with the first two heavy chain domains comprises a Fab fragment, which contains the antigen-binding site. The remaining heavy chain domains pair to form the Fc region, which binds to complement proteins and Fc receptors to elicit effector functions.

In mammals, antibodies are divided into 5 main isotypes based on the type of heavy chain that they contain. These isotypes (IgM, IgD, IgE, IgA and IgG) differ in their biological properties and functional localisation [4]. IgM and IgD are the isotypes expressed during B cell development and by naïve B cells. IgD exists mainly in the surface bound B cell receptor form whilst IgM is also produced at significant levels in the secreted form. IgM molecules do not have a flexible hinge but instead contain four constant domains in their heavy chain. They can form pentamers (held together by an additional J-chain [20]) binding to antigens with high avidity, and also efficiently activating the complement cascade, so providing an early B cell defence against pathogens. IgA is the most abundant isotype in mucous secretions such as saliva, tears, milk and the intestine. IgA can exist either as a monomer or a dimer, held together by the J-chain, and can also bind to a secretory component that facilitates its transport across epithelial cells [21]. IgE (which like IgM has four constant domains in the heavy chain rather than a flexible hinge) is only found at low levels in serum but is present on the surface of basophils and mast cells, captured by Fc epsilon receptors, and plays a role in immunity to parasites and in type 1 hypersensitivity reactions and allergy [22].

IgG is the antibody isotype predominant in serum, comprising around 80% of the total immunoglobulin pool. In humans there are four subclasses of IgG (IgG1, IgG2, IgG3 and IgG4) whereas mice express up to five subclasses (IgG1, IgG2a, IgG2b, IgG2c and IgG3). The subclasses have different effector functions dependent on their differential ability to fix complement and to bind to the various Fc gamma receptors (FcγRs). These FcγRs are widely expressed on the surface of immune cells and when

engaged by antibody can mediate endocytosis, as well as delivering either an activating or inhibitory signal to the cell dependent on the particular motif in their cytoplasmic tail or in the tail of the adapter protein to which they bind. In mice and humans there is a single high affinity activating receptor (FcγRI) and several low affinity activating receptors (FcγRIIA, FcγRIIC, FcγRIIIA and FcγRIIIB in humans, and FcγRIII and FcγRIV in mice) [23]. There is also a single low affinity inhibitory receptor FcγRIIB, which like the other FcγRs is expressed on a variety of myeloid cells but is also uniquely expressed on B cells where it can negatively regulate BCR signalling [24]. The *in vivo* effector activity of IgG antibody subclasses is in part determined by the ratio of binding affinity to activating versus inhibitory FcγRs [25]. IgG molecules also bind to the neonatal Fc receptor (FcRn), which rescues them from intracellular degradation via a cellular recycling pathway, contributing to their long serum half life [26].

1.3. Immune tolerance

An unavoidable consequence of the adaptive immune system's random approach to receptor generation is that B- and T-cell receptors are sometimes produced with specificity for self-antigens. Cells expressing these receptors must be rendered safe or removed from the system to prevent catastrophic self-destruction. The immune system mostly succeeds in achieving this delicate task of removing potentially self-reactive cells from its diverse repertoire by interpreting the signals delivered by antigen-recognition-receptors in the context that they are received [27].

1.3.1. Central tolerance

The first step in this process is known as central tolerance, and utilizes the fact that antigens encountered in central lymphoid tissue straight after antigen receptors are first expressed are most likely to be self-antigens. If a newly rearranged B-cell receptor encounters a multivalent cognate antigen in the bone marrow as the B cell is developing, then the signal from the BCR drives the cell to initiate a second attempt at gene rearrangement to produce a new BCR with a different specificity, in a process known as receptor editing [28]. If this fails to produce a new non-self-reactive receptor then the cell undergoes apoptosis. In the case of a soluble monomeric cognate antigen the B cell may escape apoptosis and migrate to the periphery but in a functionally inert state known as anergy. Similarly, if a developing T-cell receives a strong signal from its TCR in the thymus then it is driven to undergo apoptosis, or occasionally may be directed to differentiate into a regulatory phenotype and then migrate to the periphery and function to suppress immune responses [29]. In the thymus, the transcription factor AIRE (autoimmune regulator) drives the production of a wide range of self-antigens that are usually tissue restricted in their expression, which further increases the capacity of central tolerance to remove potentially autoreactive T-cell clones [30].

1.3.2. Peripheral tolerance and co-stimulatory receptors

Despite the process of central tolerance, B- and T-cells with self-specificity do still occasionally emerge from the central lymphoid organs. However, when they encounter their cognate antigen in the periphery they are not automatically activated but instead interpret the signal in the context of their environment. Antigen

encountered in the absence of danger signals, which arise from activated innate immune cells, does not lead to activation but instead to clonal deletion, anergy or differentiation into a regulatory phenotype.

For effective activation of a naïve T-cell, it is proposed that three types of signal are required. The first signal results from antigen recognition by the T-cell receptor. TCR signalling drives the activation of transcription factors that upregulate cell activation genes, as well as profound cytoskeletal rearrangements and changes in cell adhesion receptors, but alone it is insufficient to produce durable T-cell activation [31]. A second signal is delivered by co-stimulatory receptors on the T-cell surface, which amplify the downstream pathways of TCR signalling. These receptors recognise co-stimulatory ligands which are upregulated on antigen presenting cells during an innate immune response, and so provide context to the T cell about the surrounding inflammatory milieu [32]. Numerous different activatory receptors can contribute to signal two, such as CD28, ICOS and the TNF receptor superfamily receptors. However, there are also many inhibitory receptors on the T-cell surface that bind to self-ligands and negatively regulate responses. The T-cell signalling machinery integrates the signals from positive and negative receptors and it is the net result that determines the cell's fate. The third signal is delivered by inflammatory cytokines which direct the T cell towards specific pathways of effector differentiation [33].

1.3.3. The breakdown of tolerance leading to autoimmune disease

There is a delicate balance between removing or inactivating potentially self-reactive lymphocytes whilst maintaining a diverse repertoire to fight pathogens, which

themselves are constantly evolving to evade the immune response. Despite the processes of central and peripheral tolerance, diseases in which the immune system loses control and attacks self-tissues are common. Examples of some of the more prevalent autoimmune diseases include psoriasis, rheumatoid arthritis, type-1-diabetes, Graves' disease, systemic lupus erythematosus, Sjögren's syndrome, Crohn's disease, ulcerative colitis and multiple sclerosis. In all of these cases a combination of genetic and environmental factors contribute to the breakdown of self-tolerance, and a primary driver of disease is the inappropriate activation of self-reactive T- or B-cells. Genetic factors alter the likelihood of autoreactive lymphocytes being present in the immune repertoire, as well as the threshold for lymphocyte activation. The central importance of T cells is highlighted by the fact that MHC haplotypes are the strongest determinant of autoimmune risk [34]. Environmental factors are less well understood, but may include infections or other foreign antigens that contribute to the initial break down in self-tolerance by creating an inflammatory environment in which autoreactive cells can inappropriately be activated [35].

1.3.4. Existing therapies for autoimmune disease

Multiple therapeutic options for the treatment of autoimmune disease have been developed in the last century, either by serendipity or through mechanistic understanding [36]. The mainstay of treatment for severe acute autoimmunity has long been, and remains, the use of high-dose corticosteroids. These agents bind to the intracellular glucocorticoid receptor and have wide ranging effects on the immune system via the regulation of transcription factors necessary for cytokine synthesis [37]. Whilst highly effective across a range of diseases, steroids come with a

multitude of adverse effects that limit their utility as long-term immunosuppressives. Another non-specific approach to cytokine inhibition that has become established in recent years is the use of small molecule inhibitors of the Janus kinases that mediate signalling downstream of cytokine receptors, exemplified by the drug Tofacitinib [38]. Again, the non-specific mechanism of action of these drugs leads to broad immunosuppression and dose-limiting toxicities. The advent of monoclonal antibodies as therapeutics has allowed the development of more targeted inhibitors of cytokine pathways. Particularly successful have been biologics that block the cytokine TNFα, a master regulator of the inflammatory cytokine cascade [39]. These agents have exhibited remarkable efficacy across a range of diseases including rheumatoid arthritis, psoriasis and inflammatory bowel disease. However, across all diseases there is still a significant fraction of patients who do not obtain a satisfactory response and as yet we have no reliable means of predicting non-responders. Furthermore, whilst TNFα blocking agents are generally well tolerated, the importance of this cytokine to the control of intracellular pathogens leads to an increased susceptibility to tuberculosis (TB) infection or reactivation, which is particularly a limitation in less-developed nations where the prevalence of TB remains high.

Cytokine targeting agents have become invaluable tools in the arsenal against autoimmune disease, however they are rarely able to achieve long-term drug-free remission but rather keep disease severity under control [40]. Theoretically, agents targeting the self reactive lymphocytes that are often the initial drivers of disease could be more effective at restoring tolerance than targeting the downstream

inflammatory mediators. A number of therapeutics have been developed that target lymphocytes, with varying degrees of specificity. The crudest of these agents are those that target DNA synthesis, taking advantage of the increased replicative rate of activated adaptive immune cells, including methotrexate, mycophenolate, azathioprine, leflunomide and cyclophosphamide. Clearly, by virtue of their non-specific mechanism of action, the efficacy of these agents is complicated by the associated dose-limiting toxicity. More specific, are compounds that target the unique signalling pathways of lymphocytes. Cyclosporin and Tacrolimus for example block calcineurin dependent transcriptional activation downstream of the T-cell receptor and by reducing T-cell activation have significantly improved the management of organ transplantation, although their use is limited by off target effects on vasculature and by renal toxicity. Another approach has been to target lymphocyte trafficking, for example the sphingosine-1-phosphate receptor modulator fingolimod that blocks T-cell egress from lymphoid tissue has shown some efficacy in multiple sclerosis (MS) and the integrin blocker Natalizumab that inhibits lymphocyte migration into tissues is approved for the treatment of MS and Crohn's disease. More specific still, are therapeutic antibodies that selectively deplete immune cells by binding to uniquely expressed surface antigens such as the anti-CD20 B cell-depleting agent Rituximab and the anti-CD52 antibody Alemtuzumab that depletes both B- and T-cells (as well as NK cells and dendritic cells). The complete depletion of T cells however poses significant infection risk, as well as the risk of reactive autoimmunity following therapy cessation as T-cell populations re-expand. Furthermore, total T-cell depletion may not be as effective as expected due to the removal of both effector and regulatory arms of the immune response. A final approach, and the one closest to that

explored in this thesis, is the manipulation of co-stimulatory pathways to regulate excess T-cell activation without major disruption of immune cell populations, as exemplified by the CTLA4-Ig fusion protein Abatacept that inhibits CD28 co-stimulatory signalling, and is approved for the treatment of severe rheumatoid arthritis. However, similar to complete T-cell depletion this drug targets a pathway that is also important to regulatory T-cells (Tregs) [41] and greater efficacy could perhaps be achieved by manipulation of co-stimulatory or inhibitory pathways that spare Treg function.

Despite the multitude of available treatment options many patients still fail to respond adequately to multiple lines of medical therapy, as demonstrated for example in ulcerative colitis where around 15% of patients eventually require colectomy [42, 43]. In part, the failure rates of first line therapy are a result of the heterogeneity within clinically defined diseases, as generally treatments are prescribed based on clinical presentation without taking account of differences in underlying disease pathobiology between patients. Response rates will no doubt increase with more targeted prescribing as our understanding of disease mechanisms improves, alongside the availability of biomarkers and sophisticated investigations to better characterise patient-specific biology. However, there also remains a need for more effective therapies with more tolerable side effect profiles than our existing immunosuppressive agents. Furthermore, as our ability to target therapeutics more specifically to underlying pathology improves there will be clear benefits in having available a diverse repertoire of agents that can modulate different aspects of the aberrant immune response.

1.4. Immunoreceptors

Immune cells interact with their surroundings primarily via receptors on their cell surface that bind to compounds on the outside, span the cell membrane and deliver a signal to the inside. These receptors fall into many different families, including G-protein-coupled receptors, ligand gated ion channels, cytokine receptors, TNF receptors and receptor tyrosine kinases, which all signal in different ways and play important roles in determining cell behaviour [44]. One family of receptors that is of particular importance to immune cells is a family known as immunoreceptors (or more descriptively they have been referred to as non-catalytic tyrosine-phosphorylated receptors or NTRs) [45]. This group of receptors includes the BCR and TCR and many of the co-stimulatory and co-inhibitory receptors that contribute to signal two during lymphocyte activation. They have in common that their signalling depends on the phosphorylation of cytoplasmic motifs by extrinsic tyrosine kinases.

Immunoreceptors have a modular structure consisting of an extracellular region (that is usually small and binds surface-bound ligands), a transmembrane region and a cytoplasmic tail that contains tyrosine-based motifs which when phosphorylated recruit signalling machinery that can transduce activating or inhibitory signals. This modular structure has enabled the family to expand during our evolutionary history by coupling numerous different extracellular regions, with different ligand specificities, to the same signalling machinery. So whilst there are over one hundred receptors of this type they tend to share just a few conserved tyrosine-containing

motifs, primarily immunoreceptor tyrosine-based activation, inhibitory, and switch motifs (ITAMs, ITIMs, and ITSMs). Phosphate groups are added to these motifs by extrinsic SRC-family kinases, such as Lck, and removed by receptor-type-phosphatases such as CD45. Once phosphorylated, these motifs recruit SH2 (Src-homology-2) domain containing proteins, which transduce the downstream signals.

ITAMs have the sequence Yxx(L/I)x6–8 Yxx(L/I) and recruit Syk-family kinases, which once brought to the membrane phosphorylate various substrates in a cascade leading to cellular activation [46]. ITIMs have the sequence (S/I/V/L)xYxx(I/V/L) and can recruit the protein phosphatases SHP1 and SHP2 which counteract the activity of ITAM containing receptors by dephosphorylating both the ITAMs themselves and their downstream targets [47]. Alternatively they can recruit the phosphoinositide phosphatase SHIP1 that hydrolyses PIP3 (phosphatidylinositol (3,4,5)-trisphosphate) and so counteracts PI3K (phosphoinositide 3-kinase) dependent pathways of cellular activation. ITSMs have the sequence TxYxx(I/V) and can recruit protein and inositol phosphatases like ITIMs, but can also recruit SLAM-associated protein (SAP) family adapters that in turn recruit activating molecules such as Src-family kinases and protein kinase C [48]. Therefore, ITSMs can have either an inhibitory or activating effect on immune cell function depending on the context and availability of downstream substrates. For all ITAM, ITIM and ITSM containing receptors the precise affinity for different downstream signalling molecules depends on the exact sequence of their motif.

Immunoreceptors generally bind to ligands expressed on the surface of other cells. At a cell-cell interface, such as a T-cell / APC contact, many such receptors co-localise enabling the integration of their disparate signals at the cell membrane.

1.5. Models of immunoreceptor triggering

The process by which ligand binding to an immunoreceptor's extracellular domain leads to phosphorylation of its cytoplasmic motifs is known as receptor triggering. There are several different, though not necessarily mutually exclusive, models for how this process occurs. Initially these models were proposed and explored in relation to the TCR, but it is increasingly appreciated that the same mechanisms may apply across all immunoreceptors.

It has long been known that the TCR can be triggered by the addition to cells of the phosphatase inhibitor pervanadate [49]. The ability to trigger immunoreceptors by the removal of phosphatase activity suggests that at rest a balance exists between the kinases that constitutively add phosphate groups to the tyrosine motifs and the abundant phosphatases that remove them. Recognising that this balance exists can perhaps help to unify the different models that have been proposed with regards to immunoreceptor triggering and explain how they may each play a role in different contexts, by tipping this balance in favour of kinase activity when receptor binds to ligand.

1.5.1. Aggregation models

Separate to immunoreceptors, there are other families of receptor, including cytokine receptors and receptor tyrosine kinases (such as the epidermal growth factor receptor), which also signal via phosphorylation of cytoplasmic tyrosine-containing motifs, and which trigger by dimerization when they bind to their dimeric ligands [50]. They are able to trigger via dimerization because they contain intrinsic kinase activity that cross-phosphorylates motifs on their dimer-partner when the two halves are brought together. Whilst immunoreceptors do not themselves contain intrinsic kinase activity it has been suggested that at rest they can be loosely associated with extrinsic kinases and so aggregation can again increase the local concentration of kinases and lead to receptor triggering [51, 52]. This is supported by the well-known fact that certain activating receptors such as the TCR and CD28 can be triggered by bivalent antibodies, and the activating effect further increased by higher order cross-linking with secondary anti-Fc antibodies. Furthermore, at the immune synapse TCRs can be observed in clusters on the surface of activated T-cells. However, as most immunoreceptors bind to monovalent ligands, it is unclear whether this mechanism of triggering is relevant in a physiological setting. For the many immunoreceptors that are inhibitory and associate with phosphatases rather than kinases, it is also harder to imagine how clustering could lead to a local increase in the kinase concentration.

1.5.2. Conformational change models

Ligand gated ion channels and G-protein-coupled receptors are examples of receptor families that trigger by undergoing conformational changes on ligand binding, which

alter their ability to bind to or process downstream molecules [53]. Unlike these receptors, immunoreceptors often have very simple single pass transmembrane regions, which would appear to place significant restriction on their ability to transduce signals across the membrane via conformational changes. However, at least in the case of the TCR, it has been proposed that traction forces applied to the receptor by ligand binding could transmit a signal via a piston-like movement of the rigid transmembrane domain. Indeed, applying direct force to tethered TCRs can trigger them [54] and there is some evidence from crystallographic studies that conformational changes are seen in the TCRα constant domain on ligand binding [55], although numerous other crystallographic studies have failed to see any significant conformational changes on ligand binding for either the TCR or other immunoreceptors [56]. Theoretically such conformational changes could lead to ITAM phosphorylation by releasing parts of the cytoplasmic tail that are buried in the membrane at rest [57, 58], and so effectively tip the local balance in favour of kinases by increasing kinase access to the motifs. Alternatively, conformational changes in the extracellular region may enable receptors to cluster and so promote triggering as suggested in aggregation models [59].

1.5.3. Segregation models

Segregation models of immunoreceptor triggering propose that on ligand engagement, phosphatases and kinases in the membrane are differentially separated from the receptor such that the local balance of activity is tipped in favour of kinases. The most compelling of these models is the kinetic segregation (KS) model [60]. This model proposes that upon binding to a surface-bound ligand the receptor is held in a

close contact zone between the apposing surfaces and receptor-type phosphatases like CD45, which have large and rigid extracellular domains [61] are physically excluded from the area, whilst kinases such as Lck which are bound to the inner leaflet of the membrane are not impeded from entry (Figure 1-2a). The exclusion of phosphatases therefore takes the brakes off the system and allows tyrosine phosphorylation to last long enough for downstream signalling machinery to be recruited.

In support of the KS model several groups have demonstrated that CD45 is excluded from close contact areas [61, 62] and that truncating the extracellular domain of CD45 both prevents this steric exclusion and prevents immunoreceptor triggering [63, 64]. It has also been demonstrated that triggering of the TCR is dependent on the size of the peptide-MHC complex, with elongation of the complex leading to reduced signalling, presumably because CD45 is less effectively excluded when the contact zone between surfaces is wider [65, 66]. The need for an apposing surface to create the close contact zone is demonstrated by the fact that surface bound monomeric ligand can trigger TCR signalling but soluble monomeric antigen can not [67]. The predictions of the model also appear to apply to more artificial systems of T-cell activation; Chimeric antigen receptor (CAR) T-cells (which express an artificially constructed immunoreceptor) targeting the surface antigen CD22 are more effective when they bind to epitopes closer to the membrane and so create a narrower gap between T cell and target cell [68]. Furthermore, chimeric antigen receptors become increasingly less effective as the size of the spacer in their extracellular domain is increased [69, 70]. Similarly, bi-specific T-cell engagers (BiTes), which are bivalent

molecules linking a target antigen to the TCR, are more effective when they bind to membrane proximal epitopes on their target antigen [71, 72].

Example evidence that the model applies to immunoreceptors other than the TCR and CARs comes from studies on NK cells, which integrate signals from multiple activating and inhibitory receptors in determining their fate. Köhler *et al* showed that elongating the ligand for the activating receptor NKG2D abrogated signalling [73]. They also showed that for the inhibitory receptor KIR2DL1 to inhibit NKG2D signalling, the size of the inhibitory receptor-ligand complex had to match the size of the activating receptor-ligand complex.

Another segregation based model of immunoreceptor triggering, proposed in relation to the TCR, suggests that following ligand engagement the receptor becomes associated with discrete areas of the membrane known as lipid rafts that are composed of particular types of lipid and enriched in signalling components such as Lck, with the overall effect again of an increase in the local kinase to phosphatase ratio [74]. However, the mechanism via which ligand engagement may lead to receptor accumulation into lipid rafts is unclear and it is possible that the enrichment of stimulated TCRs in lipid rafts that has been observed could be a downstream consequence of receptor triggering rather than its cause.

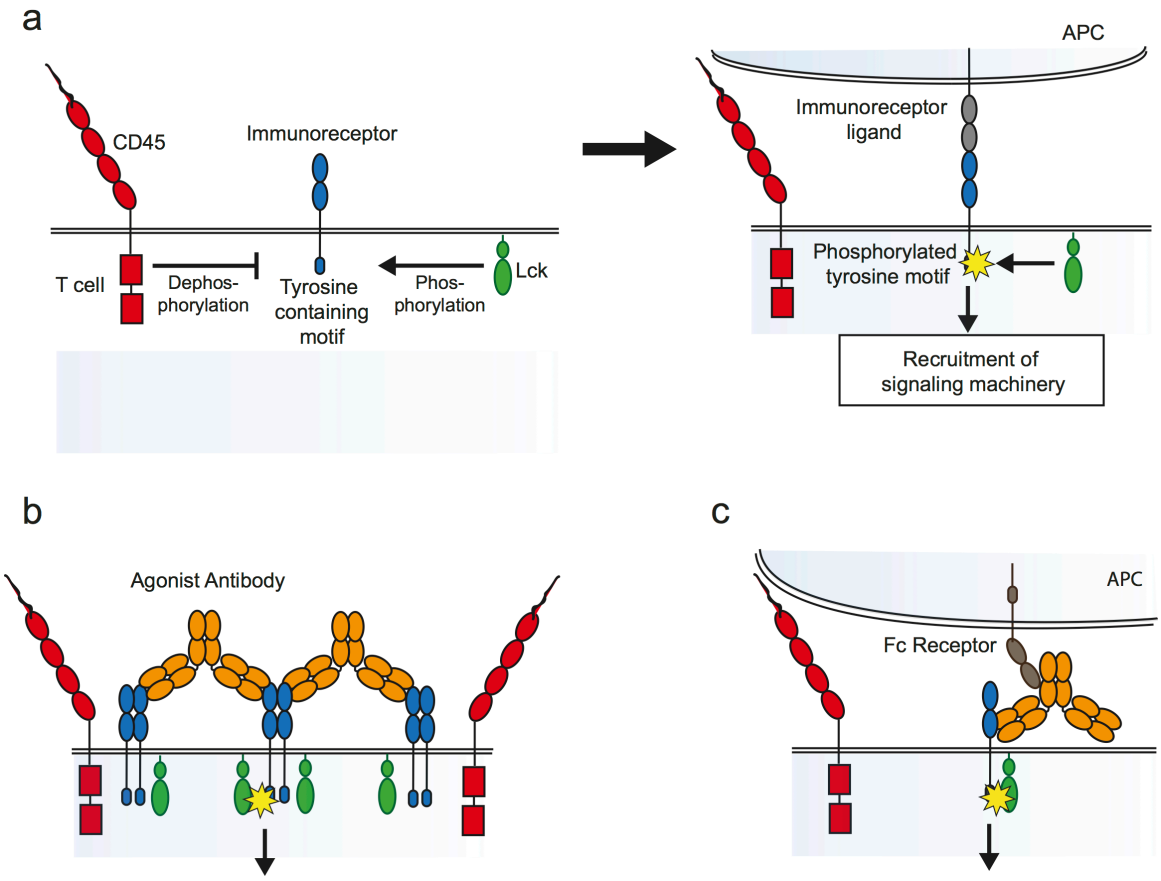


Figure 1-2: Immunoreceptor triggering in the physiological context and by agonist antibodies (adapted from [75]) (a) The kinetic-segregation model. *(Left)* Immunoreceptors contain intracellular tyrosine motifs that are phosphorylated by small membrane associated kinases (e.g. Lck) but dephosphorylated by abundant phosphatases (e.g. CD45), with no net signalling. (*Right*) When the receptor encounters its ligand on an opposing cell the balance of kinase and phosphatase activity is tipped in favour of kinases, for example by steric exclusion of bulky phosphatases from the contact zone, resulting in net phosphorylation of the tyrosine motifs and subsequent recruitment of signalling machinery. (b) Antibody triggering by aggregation. An agonist compound may cause receptor triggering by densely clustering kinase-associated receptors so that bulky phosphatases are again sterically excluded. (c) Triggering by an Fc receptor immobilized compound. An agonist that binds to Fc receptors on an apposing cell could lead to triggering by holding the receptor in a close contact zone that phosphatases cannot enter.

1.6. Immunoreceptor triggering by antibodies

The models described above have been investigated primarily in the context of physiological receptor triggering by endogenous ligand, but these principles can also be applied to understanding how agonistic antibodies modulate immunoreceptor function. Antibodies that trigger the TCR or CD28 are commonly used in cell culture to artificially activate T cells, and similarly antibodies against the BCR can be used to activate B cells *in vitro*. Bivalent antibodies can trigger these receptors in soluble format (and higher order crosslinking with secondary antibody further increases the signal) suggesting that receptor aggregation is sufficient to induce signalling of these ITAM containing receptors. This could be because these receptors are loosely associated with kinases at rest and so clustering enables cross-phosphorylation or it could be that clustering of the receptors creates an area of densely packed membrane into which bulky phosphatases cannot diffuse (Figure 1-2b). In this latter scenario even ITIM containing receptors, which would not be associated with kinases at rest, could be activated by clustering. However, it is also clear that by immobilizing these antibodies on plastic or via presentation on Fc receptor expressing cells the strength of the signal they deliver can be significantly increased. This may be because immobilizing the antibody effectively increases its valency enhancing aggregation, though this would require very dense packing of the antibody on the immobilisation surface. Alternatively, enhanced signalling in this situation may be due to the antibodies acting via a kinetic segregation mechanism and trapping the receptor in a close contact zone between the two surfaces from which CD45 is excluded (Figure 1-2c).

Much of the understanding of how antibodies can trigger immunoreceptors comes from work carried out leading up to and in the wake of TeGenero's ill-fated trial of the CD28 'superagonist' antibody TGN1412 at Northwick Park in 2006. This antibody very successfully triggers CD28 on T cells *in vivo* and led to a severe cytokine storm in the healthy volunteers who received it, which had not been predicted in preclinical studies [76] (the compound had been intended to preferentially activate regulatory T-cells and be of use in the treatment of autoimmune disease). CD28 antibodies fall into two categories – superagonists, which are independently mitogenic (i.e. can activate T cells in the absence of a TCR signal) and conventional agonists, which are co-mitogenic (i.e. can deliver a costimulatory signal but also require TCR signal for full T-cell activation) [77]. Analysis of panels of CD28 antibodies identified that the superagonists bind to epitopes on the 'side' of the receptor whilst conventional antibodies bind to epitopes on the 'top' of CD28 [78, 79]. Therefore, in an extension of the kinetic segregation model, Davis *et al* proposed that the stronger signal delivered by superagonists may be the result of the more-compact complexes they form and consequently the more effective exclusion of phosphatases from the contact zone when they are immobilized on plastic or presented by Fc receptors [60].

Several groups have demonstrated that Fc receptor engagement is critical to the function of CD28 superagonists [80-82]. TGN1412 has little effect on freshly isolated human PBMCs but strikingly activates PBMCs that have been pre-cultured at high density and this effect is dependent on the hypoxia-induced upregulation of FcγRIIB on monocytes in the culture [80, 81]. FcγRIIB on B cells can alternatively provide the necessary FcR engagement provided the B cells are added in to culture at high

density. It has subsequently been shown that any of the human FcγRs other than FcγRI can support TGN1412's superagonistic function when present at sufficient levels [82]. The reason why FcγRI does not support superagonism is not known, but it is interesting to note that, compared to all other FcRs, FcγRI has one additional immunoglobulin superfamily domain C-terminal to its Fc binding site suggesting that it may make a less compact complex with antibody and so create a wider contact zone between cells which does not effectively exclude phosphatases. FcγRI also binds to antibody with a much higher affinity than other FcRs, which may limit its ability to support superagonism by preventing serial engagement of multiple receptor–antibody complexes. The dramatic outcome of TeGenero's clinical trial is a clear demonstration that the FcR environment *in vivo* in humans is supportive of superagonism, even for hIgG4 antibodies such as TGN1412.

Aside from agonist antibodies targeting CD28 numerous preclinical studies have also demonstrated that agonist antibodies can be made against ITIM containing inhibitory receptors [75], and this is discussed in more detail later. However, in these various studies, very little further has been done to understand the mechanism by which the antibodies trigger receptor signalling, with the focus instead primarily on the functional effects of enhancing inhibitory receptor signalling.

1.7. Targeting immunoreceptors in cancer

The immune system plays an important role in protecting us from cancer, as evidenced by the fact that immunodeficiency imparts a heightened cancer risk and evolving cancers undergo a selective pressure for immune-evading mutations [83].

The idea of therapeutically enhancing the immune response to treat cancer is known as immunotherapy and was first scientifically explored in 1891 by the orthopaedic surgeon William Coley who showed that some sarcoma patients could be treated by immune-stimulating injections of bacterial products [84]. After a rather disappointing lull over the following one hundred years, the field of immunotherapy has recently been re-ignited by the dramatic success of 'checkpoint inhibitors'. These therapeutic antibodies block inhibitory immunoreceptors (also known as immune checkpoint receptors) taking the brakes off the anti-tumour immune response. Initially, antibodies blocking the receptor CTLA4 were shown to have efficacy in treating metastatic malignant melanoma [85] and, subsequently, blocking the receptor PD1, or its ligand PDL1, was shown to be even more effective [86]. These new drugs have revolutionised melanoma therapy and offer the hope of durable remission to a subset of patients, in a disease that just a decade ago was invariably terminal. PD1 or CTLA4 blockade has subsequently shown promise in multiple other cancer types [87] and, whilst the list of licenced indications for these drugs continues to grow, multiple other inhibitory immune receptors are being explored as potential novel targets [88].

By removing an inhibitory signal, checkpoint inhibitors effectively lower the threshold for T-cell activation, but as well as enhancing anti-tumour responses this can lead to a range of autoimmune side effects. These immune related adverse events (IRAEs) can affect almost any organ but most commonly affect the skin, gut, liver and endocrine organs [89]. This highlights the important role that immune checkpoint receptors normally play in the maintenance of self-tolerance, and raises the question

of whether defects in these pathways might contribute to the development of spontaneous autoimmune disease.

Following on from the success of checkpoint inhibitors there has also been interest in trying to develop agonist antibodies against activatory co-receptors to enhance anti-cancer immune responses. Several antibodies targeting the ITAM-containing immunoreceptor ICOS are in clinical trials [90]. There are also numerous agonists under investigation targeting TNFR-superfamily members such as CD40, OX40, 4-1BB, CD27 and GITR [91]. These receptors, unlike the immunoreceptors described above, signal by trimerisation when they bind to their trimeric ligands. This timerisation provides the docking sites for downstream adaptor proteins [92]. It is likely that agonist antibodies against this family of receptors function by facilitating aggregation of the receptors in the same way as the natural ligand and it has been shown that this clustering is dependent on binding of the antibody to a scaffold of FcγRIIB on adjacent cells [93]. Agonist antibodies can therefore be improved by Fc mutations which selectively enhance binding to FcγRIIB [94]. Separately, FcR independent agonism can be achieved by an isoform of hIgG2 in which the first constant domain of the heavy chain is linked via a disulphide bond to the hinge region, conferring a more compact structure that may aid tighter packing of bound receptors on the cell surface [95]. It is important to note that, due to the very different mechanism of signalling of this family of receptors, understanding about the action of TNFRSF agonist antibodies cannot be extrapolated to agonists targeting the tyrosine-motif-containing immunoreceptors.

1.8. Inhibitory immunoreceptor associations with autoimmune disease

The fact that inhibitory receptor blockade frequently leads to autoimmunity raises the possibility that defects in immune checkpoint signalling may be a contributing factor in spontaneous autoimmune disease. The only monogenic disease where this association is clearly seen in humans is in patients with heterozygous loss of function mutations in CTLA4 who develop widespread immune dysregulation [96]. CTLA4 knock-out mice also develop severe disease, with massive lymphoproliferation, and die of multiorgan autoimmune tissue destruction early in life [97]. PD1 deficiency in mice is less severe with specific manifestations dependent on the strain; BALB/c mice develop autoimmune cardiomyopathy [98] whilst C57BL/6 mice develop a lupus-like disease in late life [99]. Disease associations with PD1 in humans are less striking, but regulatory polymorphisms in the PDCD1 gene are linked to susceptibility for a range of autoimmune conditions including multiple sclerosis (MS) [100], systemic lupus erythematosus (SLE) [101], atopy and rheumatoid arthritis (RA) [102, 103]. Intriguingly, auto-antibodies against PDL1 are found in some patients with RA and correlate with disease severity [104]. Conversely, treatment with IFN-β in MS leads to upregulation of PDL1 and this may contribute to its beneficial effect [105].

Beyond PD1 and CTLA4, there are many other inhibitory immune receptors that regulate immune function. B- and T-lymphocyte attenuator (BTLA) is an inhibitory receptor expressed at high levels on B and T cells and at lower levels on a range of myeloid cells [106]. BTLA knockout mice develop a hepatitis-like disease and multi-organ inflammatory infiltrates in old age [107], and they have heightened susceptibility to induced autoimmune disease such as imiquimod induced psoriasis

[108]. In humans, single nucleotide polymorphisms (SNPs) in the BTLA gene, one of which was shown to reduce inhibitory function, are associated with RA risk [109, 110]. In genome wide association studies the ligand for BTLA, herpes virus entry mediator (HVEM), has been highlighted as a potential risk gene for ulcerative colitis (UC) [111], RA and coeliac disease [112], MS [113] and primary sclerosing cholangitis (PSC) [114]. In Behcet's disease BTLA expression on DCs and CD4 T-cells is reduced, correlating with increased Th17 and Th1 responses [115]. Conversely, in MS patients the drug fingolimod induces upregulation of BTLA in B cells, which is correlated with reduction in disease severity [116].

T-cell Immunoreceptor with Ig and ITIM domains (TIGIT) knockout mice do not develop spontaneous autoimmunity but do have heightened immune responses when challenged, for example in experimental autoimmune encephalitis (EAE) [117]. Polymorphisms of T-cell immunoglobulin and mucin domain 3 (TIM-3) in humans are linked with risk of MS [118], RA [119] and ankylosing spondylitis (AS) [120]. The Siglecs are a family of sialic acid binding receptors expressed across the immune system, many of which are ITIM-containing inhibitory receptors, and variation in these receptors or the enzymes that produce their ligands also affects risk of developing allergy and autoimmune disease [121]. CD300a is another widely expressed inhibitory receptor and a polymorphism in its extracellular domain that reduces binding to its lipid ligands has been reported to increase risk for psoriasis [122]. FcγRIIB is itself an ITIM containing inhibitory receptor and a functional polymorphism in its transmembrane region is one of the strongest genetic associations with SLE [123]. Overall there are over fifty inhibitory immune receptors

expressed across the immune system [45], each with an apparently unique role in immune regulation, and together they contribute to the differentiation of self and non-self and set the threshold for immune activation.

1.9. Targeting inhibitory receptors for the treatment of autoimmunity

The association of inhibitory receptors with autoimmune disease in humans and the autoimmunity induced by 'knocking out' these receptors experimentally in mice or therapeutically in cancer patients all provide evidence of the critical role these pathways play in the normal maintenance of self tolerance. This raises the possibility that therapeutic agents capable of enhancing signalling through these pathways might be beneficial in the treatment of autoimmune disease. Whilst this approach has not yet been tested in efficacy trials in the clinic it has been explored preclinically for a number of targets (reviewed in [75]) and some agonist antibodies targeting inhibitory receptors have recently entered early phase clinical trials. The clinical success of the CTLA4-Ig fusion protein Abatacept provides proof of principle that manipulating costimulatory pathways can have a meaningful impact on human autoimmune disease. This compound, which is used in the treatment of severe RA [124], is not a receptor agonist but rather acts by binding to the ligands CD80 and CD86 with a high affinity and preventing their binding to CD28. Competition for these costimulatory ligands is likely to be an important part of CTLA4's physiological mechanism of action, as supported by the fact that soluble CTLA4-Fc can compensate for CTLA4 haploinsufficiency [125]. Whether or not CTLA4 also has a significant intrinsic signalling function, which would be required for it to be an appropriate target for agonism, is still a matter of debate [126].

Several different approaches have been taken to developing agonistic agents against inhibitory receptors. These include compounds based on the natural ligand, agonist antibodies, novel engineered agonist constructs and bi-specific agents that co-localise an inhibitory receptor to an activating receptor on the same cell. For the most part such compounds have been targeted to murine inhibitory receptors and tested in mouse models of autoimmunity as proof of concept, but without being directly translatable into human cells.

1.9.1. Natural ligand based inhibitory agonists

With respect to natural ligand based agonist agents, the vast majority that have demonstrated efficacy preclinically have been Fc fusion proteins, where the ligand is linked to the hinge region, CH2 and CH3 domains of an IgG heavy chain. This has the effect of dimerising the ligand and consequently increasing its avidity for the target receptor, as well as providing the extended serum half-life that recycling of Fc via the FcRn pathway confers [26]. The ability of an Fc fusion protein to be captured by Fc receptors also provides the apposing surface that the kinetic segregation model predicts would be necessary for phosphatase exclusion and consequent receptor triggering.

In mice a PDL1-Fc fusion protein was shown to reduce collagen-specific T-cell responses and ameliorate disease in a collagen-induced arthritis (CIA) model [127, 128], as well as treating two different experimental colitis models [129]. The Fc used in this construct was based on a mIgG2a with three mutations (E318A, K320A,

K322A) to reduce C1q binding and an L235E mutation to reduce FcR binding, in order to minimise effector functions. Given the evidence described previously that FcR binding is important to agonist function it would be interesting to investigate whether a mIgG1 Fc (which maintains inhibitory FcR binding without significant effector function) could be a more effective construct.

Fc fusions of HVEM have also demonstrated some promise as agonists for BTLA. Human or mouse HVEM-IgG1 fusion proteins inhibited T-cell activation *in vitro*, but only when crosslinked by secondary antibody or when high molecular weight aggregates were present [130]. A mHVEM-mIgG1 fusion protein reduced disease severity in a graft-versus-host disease (GVHD) model [131] but a mHVEM-hIgG1 construct exacerbated CIA [132], perhaps due to inflammatory signalling through the activating receptor LIGHT which also binds HVEM.

CD200-Fc fusions targeting the predominantly myeloid cell receptor CD200R1 have also demonstrated efficacy in CIA [133, 134] and EAE [135], although in some of these studies it was not specified whether the mIgG2a-Fc used contained mutations to reduce effector function so complement or ADCC-mediated depletion of CD200R1 expressing cells may have contributed to the effect.

The rare exception to ligand-Fc-fusion based agonists is Galectin-9 (the ligand for the T cell exhaustion receptor TIM-3), which has demonstrated efficacy as a soluble protein without Fc-fusion in EAE [136], CIA [136] and in prolonging allograft survival [137, 138]. Galectin-9 does have two carbohydrate recognition domains so can bind

TIM-3 dimerically to cluster receptors, which might also enhance signalling indirectly by increasing the half-life of the receptor on the cell surface [139]. But galectins also have promiscuous binding patterns, often capable of binding to glycans on multiple different proteins, so it is difficult to definitively attribute the effects of Galectin-9 to TIM-3 binding rather than manipulation of an alternative binding partner [140].

1.9.2. Agonist antibodies targeting inhibitory receptors

Compared to natural ligands agonist antibodies have many theoretical advantages as therapeutic agents. They are stable and easy to produce proteins, with an impressive serum half-life and a proven track record in the clinic. They can be produced with much higher affinity for target than the endogenous ligand allowing high receptor occupancy at low doses. For paired receptor systems, in which activating and inhibitory receptors share the same ligand, antibodies can be produced with specificity for only the intended inhibitory receptor and with no undesirable cross-reactivity with the activating partner. For several murine inhibitory receptors preclinical studies have demonstrated that agonist antibodies can be produced that inhibit T-cell responses and ameliorate disease in models of autoimmunity.

A hamster-IgG targeting mouse BTLA prevented disease in a model of GVHD [141] and was shown to do so whilst still allowing engraftment of allogeneic cells and without abrogating responses to subsequent challenge with virus or tumour, suggesting that BTLA agonism raised the threshold for T-cell activation sufficiently to prevent attack on benign allogeneic tissue but that the increased costimulation associated with malignant or infected cells could overcome this immunosuppresion.

It is interesting to note that this antibody (clone 6A6) had previously been shown to block binding of the natural ligand HVEM [142] suggesting that even ligand-blocking antibodies which might be expected to enhance immune responses can in fact deliver a net agonist signal. Albring *et al* showed that 6A6 could prevent GVHD induced by $HVEM^{-/-}$ cells in $HVEM^{-/-}$ recipients indicating that the antibody's effect was independent of its ability to block the BTLA-HVEM interaction and was rather a result of a direct action on BTLA expressing cells [141]. They also showed that 6A6 was not depleting, further supporting the idea that the antibody acts as an agonist, enhancing BTLA's inhibitory signal to prevent activation and proliferation of effector T-cells. This same antibody was shown to reduce severity of an imiquimod-induced model of psoriasis via inhibition of γδ T-cells [108] and to ameliorate LPS-induced toxic shock via inhibition of TLR4 signalling in innate cells [143], as well as reducing inflammation in a model of cerebral malaria [144].

Another hamster IgG anti-mouse BTLA antibody (clone 3C10) was shown to inhibit T-cell responses in a mixed lymphocyte reaction and to prolong cardiac allograft survival, perhaps in part by inhibiting Th1 responses whilst stimulating Treg development [145]. Furthermore a non-depleting mIgG1 BTLA agonist was shown to synergise with CTLA4-Ig in prolonging islet cell allograft survival [146]. This antibody, whilst not depleting did lead to significant downregulation of BTLA expression on targeted cells.

Also targeting murine BTLA, Krieg *et al* screened a panel of eight rat antibodies and identified one with significant agonist activity *in vitro* [147]. When immobilised on

plastic this antibody was able to inhibit T-cell proliferation and IL2 production even if delivered 24 hours after initial T-cell activation, and was noted to have a more striking effect on CD4 rather than CD8 T-cells. A mouse IgG2a antibody against human BTLA was similarly shown to inhibit both primary and secondary T-cell activation when plate bound [148]. In both these studies the effect of BTLA agonism could be overcome by increasing the strength of the TCR activation signal or by adding high levels of CD28 costimulation.

In all the above studies the antibodies are capable of binding to murine Fc-receptors and are tested in settings where FcRs are present, or in settings where the antibody is immobilised on plastic. Thus, the apposing surface predicted to be a requirement for phosphatase exclusion by the KS model (be it another cell or a plastic surface) is always present.

Eli Lilly and Company has also announced that they have a BTLA agonist antibody in a phase 1 clinical trial. Although little information is publicly available about this agent, a relevant patent application assigned to the company describes three anti-human BTLA agonist antibodies, one that is ligand blocking and two that are not [149]. These antibodies were shown to reduce disease in models of psoriasis, lupus nephritis and GVHD. They were investigated on a hIgG4 backbone with one mutation to prevent Fab arm exchange (S228P) and two mutations to reduce effector function (F234A and L235A). The efficacy studies were conducted either in a murine FcR environment or with antibody immobilised on plastic, so whether efficacy will be translated to the clinic when tested in a human FcR environment remains to be seen.

Another inhibitory receptor that has been successfully targeted in mice with agonist antibodies is CD200R1. A rat IgG1 antibody (OX110) improved symptoms in arthritic mice [150] and reduced severity of influenza-induced innate inflammation [151]. A different rat IgG1 antibody (DX109) was able to suppress macrophage activation and reduce tissue damage in experimental autoimmune uveitis [152]. This antibody could also inhibit degranulation of murine mast cells overexpressing CD200R1, whilst a rat anti-human CD200R antibody (DX183) suppressed human mast cells [153]. The effect of these agonists was enhanced by cross-linking with a secondary antibody and further enhanced by co-crosslinking the receptor to the activating FcεR1 suggesting that both receptor aggregation and co-localisation to activating receptors may be important for the action of CD200R. Interestingly the agonist action appeared to be independent of FcR binding. Separately, it was shown that a CD200R agonist was most effective on a hIgG2 isotype in the constrained hinge format (CH1 to hinge disulphide) [154] as has been shown for TNFRSF agonists, again suggesting that receptor aggregation may be important for CD200R agonism.

Dixon *et al* explored a panel of antibodies against the T- and NK-cell inhibitory receptor TIGIT and identified ligand-blocking mIgG1 antibodies that could be either agonistic (treating EAE) or antagonistic (treating cancer) depending on the context [155]. In this paper, antibodies were first screened for ligand blockade on the assumption that only antibodies binding to the physiological ligand-binding site would have functional effects.

Agonist antibodies targeting several other checkpoint receptors have also been described. For example, targeting the receptor VISTA (PD1H) with a hamster IgG prevented GVHD [156] whilst a mIgG1 agonist suppressed Concanavalin-A (Con A) induced hepatitis [157]. A mIgG2a agonist targeting the human receptor NKG2A inhibited Th2 activation *in vitro* [158]. Agonist antibodies targeting CD300A have been shown to inhibit activation across a number of immune cell types on which it is expressed [122]. It is reasonable to assume, given the likely shared mechanism of triggering of immunoreceptors, that most of these receptors are feasible targets for antibody agonists.

Intriguingly, given the clinical success of PD1 and CTLA4 blockade, there is a conspicuous paucity of literature describing agonist antibodies against these receptors. For CTLA4 this adds weight to the argument that it functions predominantly via competition for CD80 and CD86 rather than having intrinsic signalling function (and the clinical effect of blocking antibodies may also in part be due to Treg depletion [159]). However, membrane bound anti-CTLA4 ScFv constructs have been reported to suppress T-cell activation if expressed on the same cells as TCR ligands [160, 161], suggesting that it may be possible to develop an agonist antibody. For PD1, previous work in our lab has identified an anti-human agonist antibody that inhibits T-cell responses *in vitro* and *in vivo* (in human receptor knock-in transgenic mice) but which did not show efficacy in an EAE model, perhaps due to downregulation of the receptor following binding of the high affinity antibody, which may have prevented prolonged signalling [162]. Aside from this work, the pharmaceutical company Celgene, in partnership with AnaptysBio, have a PD1

agonist antibody in a phase 1 clinical trial which was shown to inhibit T-cell activation *in vitro* (patent application [163]) and was also shown to cause PD1 downregulation suggesting that this could be a common feature of high affinity PD1 agonist antibodies. A similar phenomenon has been observed with antibodies targeting multiple other immunoreceptors including CD5 and CD22 (Siglec2) [164] and FcγRIIB [165], and may in part be due to phosphorylation of the tyrosine motifs recruiting endocytosis machinery. If this process differs between inhibitory receptors, then receptors for which signalling and internalisation are decoupled may be more promising targets for agonism as they could be triggered for prolonged period without inducing downregulation.

1.9.3. Novel engineered agonist constructs

In addition to antibodies and natural ligand based agonists, several other novel constructs have been explored as agonists of inhibitory receptors. The CMV protein UL144 is a homolog of HVEM and has likely been acquired by the virus from the human genome during its evolution as an immune evasion mechanism, enabling it to switch off the immune response against it by boosting BTLA's inhibitory signal. Futhermore, it has evolved mutations that knock out binding to HVEM's other binding partners LIGHT and CD160, and so avoids delivering counterproductive immune activatory signals. Cheung *et al* demonstrated that UL144-Fc suppressed T cells *in vitro* more potently than HVEM-Fc [166]. Interestingly, UL144 binds to the same epitope on BTLA as HVEM does but with a lower affinity, so the increased inhibitory effect seen with UL144 may indicate that lower affinity enhances agonism, or alternatively could be explained by the fact that the extracellular domain of UL144 is

49 amino acids shorter than HVEM and so, as per the KS model, may create a more compact complex with the receptor and lead to more effective exclusion of phosphatases when immobilized on plastic or by Fc receptors. Šedý *et al* used the structure of UL144 to guide mutagenesis of HVEM-Fc and produced a mutein capable of binding BTLA with 10 fold increased affinity and no detectable binding to LIGHT or CD160, and this inhibited B-, T- and NK-cell activation *in vitro* [167]. The fact that human herpes viruses have evolved checkpoint ligands to evade the immune response highlights the potential therapeutic merit of this approach for switching off unwanted immunity.

In a very different approach to checkpoint agonism Prodeus *et al* produced DNA aptamers targeting CD200R1 and demonstrated that these could inhibit a mixed lymphocyte reaction *in vitro*, and when pegylated could prolong allograft survival *in vivo* [168]. How these small monomeric constructs could trigger CD200R1 is not clear but it may be that they either aggregate (and consequently cluster the receptor), or are non-specifically captured by plastic or cell surfaces (and consequently trigger the receptor via a KS-based mechanism) or alternatively they may be acting by blocking signalling of the structurally similar activating receptors CD200R2-5.

Dendritic cells transfected to overexpress a checkpoint ligand have also been explored as a potentially tolerising agent. Dendritic cells overexpressing PDL1 alongside myelin oligodendrocyte glycoprotein (MOG) were able to reduce the severity of MOG-induced EAE [169]. Similarly dendritic cells expressing PDL1 and

GAD65 tolerised mice to this antigen leading to diminished responses when T cells were subsequently challenged *ex vivo* [170].

Whilst not strictly agonism, several different studies have also examined the merit of co-localising an inhibitory to an activatory signal in cis on the same cell surface using a bispecific agent. For example, a dual-affinity retargeting (DART) molecule linking FcγRIIB and CD79B (a component of the B-cell receptor signalling complex) was able to inhibit B-cell activation and prevent the development of CIA [171]. Similarly, a bispecific antibody linking CD300A to IgE was able to inhibit IgE induced mast cell degranulation [172]. A different bivalent approach was taken by Gorczynski *et al*, linking two immunosuppressive compounds in a construct, comprising CD200-Fc fused to TGF-β1, which showed more effective immunosuppression than either compound alone, by triggering CD200R on APCs and TGF-β receptor on T cells [173].

All these novel approaches to checkpoint agonism provide interesting proof of concept and help to better understand the important attributes of an agonist. However, such agents would present far greater hurdles to further development compared to standard format antibodies, in terms of stability, immunogenicity, expression yield, pharmacokinetics and regulatory acceptability. As such, despite efficacy in preclinical models of autoimmunity, most of these agents are unlikely to ever reach the clinic.

1.10. The inhibitory receptors explored in this thesis

1.10.1. PD1

Programmed cell death protein 1 (PD1 or CD279) is an immunoglobulin superfamily (IgSF) protein and member of the B7-CD28 family. It consists of a single extracellular IgV-like domain, a single pass transmembrane region and a cytoplasmic tail that contains an ITIM and an ITSM (Figure 1-3). It is monomeric on the cell surface as it lacks the extracellular cysteine found in CD28, CTLA4 and ICOS that allows these molecules to form covalent homodimers [174]. PD1 is so named because it was first identified as an upregulated transcript in T-cell lines undergoing programmed cell death [175]. It is also expressed on cells across the immune system including CD4 T-cells, CD8 T-cells, B cells, NKT cells, monocytes, macrophages and dendritic cells. It is briefly upregulated on acutely activated T-cells and persistently upregulated on exhausted T-cells [176].

PD1 binds to two ligands called PDL1 (CD279 or B7-H1) and PDL2 (CD273 or B7-DC) which each contain two IgSF domains in their extracellular region. PDL1 is constitutively expressed on professional antigen presenting cells (APCs) such as DCs, macrophages and B cells and can be induced on non-haematopoeitic cells during inflammation to limit tissue damage [177], but is also often upregulated on cancer cells enabling them to dampen anti-tumour immune responses [178]. PDL2 is only expressed at relevant levels on activated APCs [177]. PD1 binds to its ligands with low micromolar monomeric affinities [179] and whilst PDL2 has approximately 4 fold

higher affinity it likely has a less important physiological role due to its much lower and more restricted expression.

On binding to its ligands PD1's intracellular tyrosine motifs become phosphorylated and the phosphorylated ITSM in particular is able to recruit the protein phosphatase SHP2 (and possibly SHP1) [180]. Once recruited to the cell surface SHP2 negatively regulates cell signalling by dephosphorylating the ITAMs of activatory receptors (in particular CD28 [181, 182]) and other downstream mediators of activatory signalling. As well as suppressing activation of T cells, PD1 signalling also plays a role in the generation of regulatory T-cells (Tregs) [183].

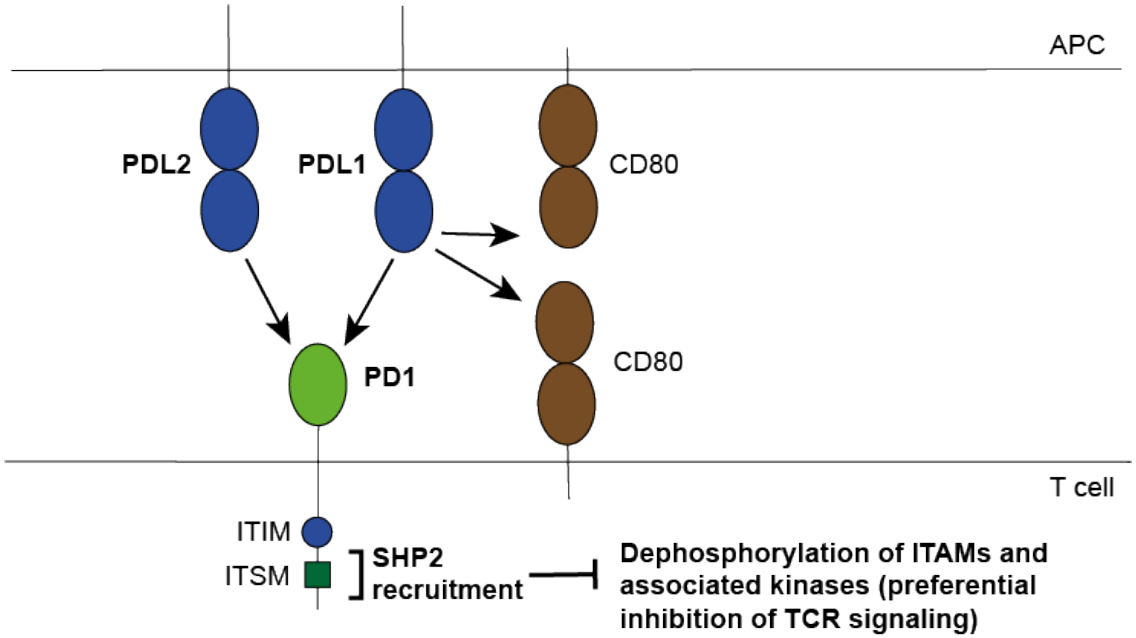


Figure 1-3: Ligand interactions and signalling pathways of PD1. PD1 engagement by either of its ligands PDL1 or PDL2 induces receptor phosphorylation and subsequent recruitment of SH2 domain containing phosphatases such as SHP2, which in turn inhibit activatory signaling cascades at the cell surface.

1.10.2. BTLA

B- and T-lymphocyte attenuator (BTLA or CD272) is also an IgSF member and part of the CD28 family [106]. It consists of a single IgV-like extracellular domain, a transmembrane domain and a cytoplasmic tail that contains both an ITIM and ITSM and also a Grb2 binding domain (one in mice, two in humans) (Figure 1-4). BTLA is expressed across the immune system on lymphoid and myeloid cells [184] and unlike PD1 is expressed constitutively on resting T-cells. On T-cell activation BTLA is initially upregulated but, in humans, following differentiation into effector phenotypes the expression falls to below the levels found on naïve cells [185]. In mice, expression is maintained at high levels on Th1 and anergic T-cells [142].

As BTLA is a member of the B7-CD28 family, when first identified it was assumed that its ligand would be a B7 homolog and B7x was identified as a potential candidate based on differential binding to WT vs BTLA$^{-/-}$ T-cells [106]. However, subsequent studies were unable to detect a direct interaction with B7x and instead identified a TNFRSF member called herpes virus entry mediator (HVEM or TNFRSF14) as BTLA's ligand [130, 186]. HVEM also binds to the trimeric TNFSF ligands LIGHT and LTα (as well as the HSV1 glycoprotein D which gives it its name), which in turn have their own additional binding partners (Figure 1-4). BTLA binds to the first of four cysteine rich domains (CRD1) of HVEM whilst LIGHT (TNFSF14) and LTα bind to CRD2 and CRD3 on the opposite face of HVEM, enabling BTLA to bind simultaneously and potentially for three BTLA molecules to bind to the outside of the trimeric HVEM-LIGHT complex [130]. Furthermore, HVEM binds to another IgSF molecule called CD160 that competes with BTLA for the CRD1 binding site [187]. HVEM is expressed

on many of the same cell types as BTLA and may be able to bind to BTLA in *cis*, preventing *trans* interactions [188], which adds an extra layer of complexity to the regulation of this already complex network.

LIGHT binding to HVEM, like other TNFSF interactions, leads to costimulatory signalling through HVEM and may also induce reverse activatory signalling through the ligand LIGHT [189]. HVEM binding to BTLA on the other hand leads to an inhibitory signal through BTLA, as BTLA's cytoplasmic tyrosine motifs become phosphorylated and recruit inhibitory downstream machinery. Unlike PD1, which in T cells appears to preferentially recruit SHP2 and inhibit CD28, BTLA recruits both SHP1 and SHP2 and potently regulates both the TCR and CD28 signal [182]. This effect is dependent on the tyrosines in both the ITIM and ITSM motifs [190-192]. There is some evidence that the Grb2 binding motifs of BTLA deliver a positive pro-survival signal via recruitment of PI3K and activation of Akt [192-194] and it has also been suggested than BTLA binding to HVEM can deliver an activatory signal through HVEM [195]. BTLA knockout T-cells paradoxically display a survival defect *in vivo* that can be corrected by expression of a truncated form of BTLA lacking the intracellular signalling domains, supporting a role for BTLA as an activating ligand for HVEM in T-cell / T-cell interactions [196]. However, the hyperproliferative T-cell responses and increased susceptibility to autoimmune disease seen in BTLA deficient mice indicates that the negative signalling effect dominates, and this is again supported by the efficacy of BTLA agonists in suppressing immune responses as described above. HVEM binding to CD160 also delivers an inhibitory signal to T cells [187] but delivers an activatory signal to NK cells [197] which may have evolved as a

host defence mechanism to counteract viruses such as CMV, which have acquired BTLA agonist proteins to evade the immune response.

The HVEM-BTLA axis is a crucial regulator of the immune response as highlighted by the disease associations described previously and the numerous studies in mice that have been carried out to investigate the pathway. BTLA knockout mice develop spontaneous multi-organ auto-inflammatory infiltrates in late life [107] and have increased sensitivity to experimental disease models including EAE [106], psoriasis [108], and lung inflammation [198]. HVEM deficient mice similarly are more susceptible to EAE and Con A induced hepatitis [199]. HVEM expression is particularly high in the gut mucosa where it also regulates immune responses via BTLA signalling [200]. In germinal centres HVEM-BTLA signalling is also of key importance in restraining T-cell help and setting the threshold for B-cell selection [201], and mutations in this pathway are often involved in the development of B-cell lymphomas [202].

BTLA is not just involved in the regulation of conventional T-cell responses but also negatively regulates multiple other immune cell types. As the name suggests it is capable of dampening B-cell responses [203]. BTLA has also been shown to have an important role in γδ T-cell function in psoriasis [108], as well as in regulating NKT activation [204]. It is also involved in the tolerogenic function of dendritic cells [205, 206] and plays a role in dampening innate immune responses via regulation of TLR4 signalling [143]. The prominent inhibitory roles of BTLA across a whole repertoire of

immune cell types could all contribute to its efficacy as a target for agonist agents in autoimmunity.

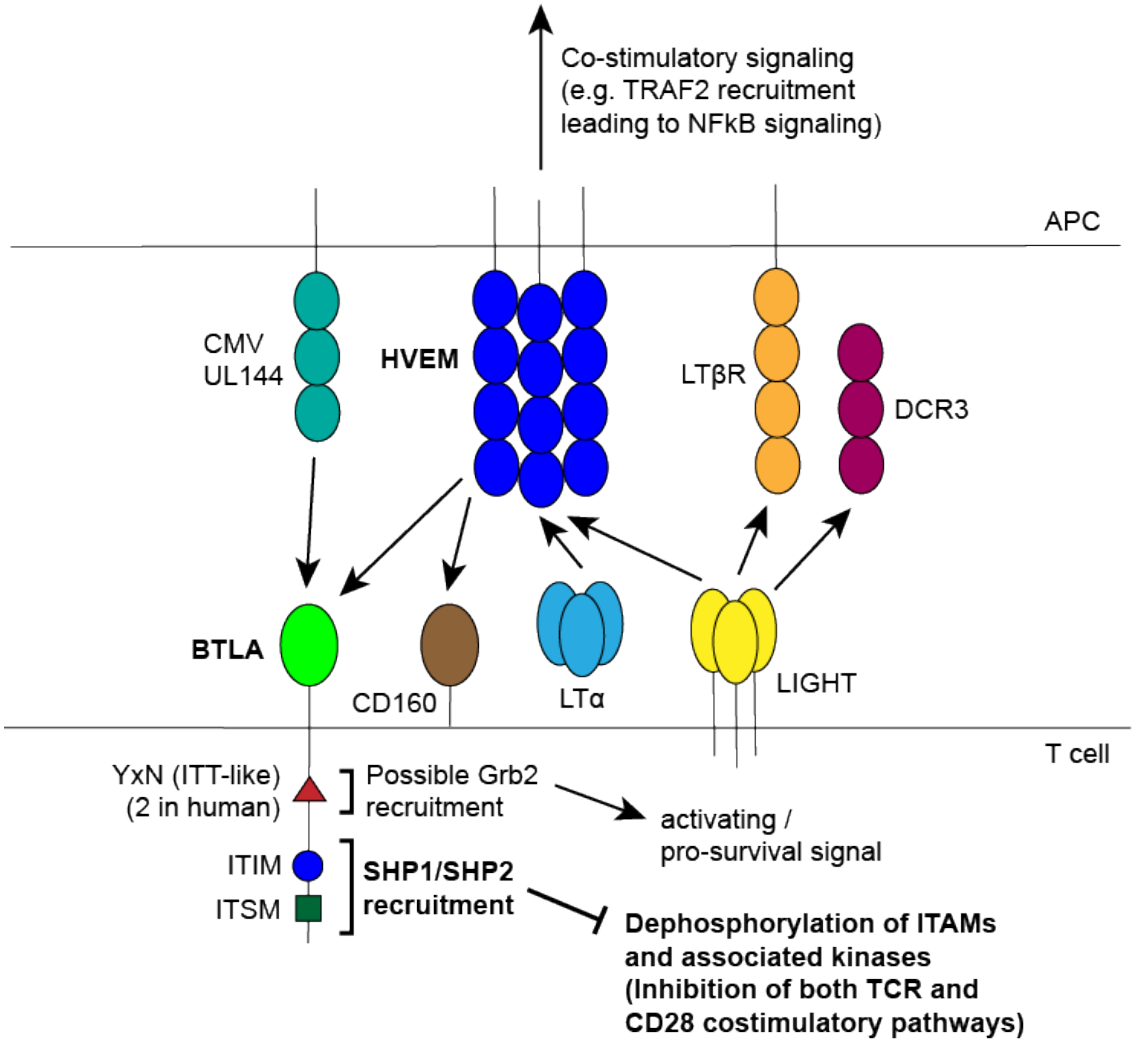


Figure 1-4: Ligand interactions and signalling pathways of BTLA. BTLA binds to the TNFR superfamily molecule HVEM, leading to phosphorylation of the tyrosine containing motifs in BTLA's tail and subsequent recruitment of downstream signalling machinery. BTLA can also be engaged by the cytomegalovirus protein UL144. HVEM also has multiple other binding partners and is itself a costimulatory receptor, delivering a positive signal when trimerised by binding to the trimeric ligands LIGHT or LTα.

1.10.3. TIGIT

TIGIT (also known as Vstm3, VSIG9 or WUCAM) is a more recently described IgSF member [207, 208]. It has a single IgV-like extracellular domain, a transmembrane region and a cytoplasmic tail containing an ITIM and an immunoglobulin-tail-tyrosine (ITT)-like motif (Figure 1-5). It is expressed primarily on activated and memory T-cells, NK cells, NKTs and Tregs [207].

TIGIT binds with highest affinity to the widely expressed poliovirus receptor (PVR or CD155) and may also bind with lower affinity to PVRL2 (CD112) and PVRL3 (CD113) [207], although others observed no binding to PVRL3 [208] and no binding to PVRL2 or PVRL3 in mice [209]. TIGIT competes for PVR with the activating receptor CD226 (DNAM1), and this competition may be in part responsible for its inhibitory activity, as supported by the fact that soluble TIGIT blocks T-cell activation and improves CIA [210]. Furthermore the positive impact of TIGIT blockade in some contexts is dependent on the presence of CD226 [211]. TIGIT also competes for binding to PVR with another inhibitory receptor called CD96 that is expressed on NK cells and also inhibits their activation [212].

Phosphorylation of TIGIT's cytoplasmic motifs leads to the recruitment of SHIP1 and subsequent inhibition of PI3K signalling in NK cells [213, 214], and either of TIGIT's motifs seems to be capable of this effect [209]. The inhibitory effect of TIGIT agonist antibodies on T-cell function supports the notion that TIGIT also has intrinsic inhibitory function in T cells [210]. In a reporter assay system Jutz *et al* also demonstrated that expressing TIGIT on a Jurkat T-cell line rendered it susceptible to

inhibition by PVR expressed on a stimulator cell line [190]. TIGIT binding to PVR on dendritic cells also appears to drive DCs towards a tolerogenic state, via reverse signalling through PVR, with a subsequent reduction in T-cell activation [207]. TIGIT also contributes to the development of Tregs and identifies a Treg subset that is particularly potent at inhibiting Th1 and Th17 responses [215]. Overexpression of TIGIT on CD4 T-cells inhibits their activity *in vitro* and ameliorates a model of aplastic anaemia [216], and TIGIT overexpression also protects mice from EAE, whilst knockout mice have more severe disease [210]. TIGIT is upregulated on exhausted T-cells and on tumour infiltrating T-cells in multiple cancers and, unlike BTLA, blocking TIGIT has demonstrated significant efficacy in treating murine cancer models, synergising with PD1 blockade [155, 211].

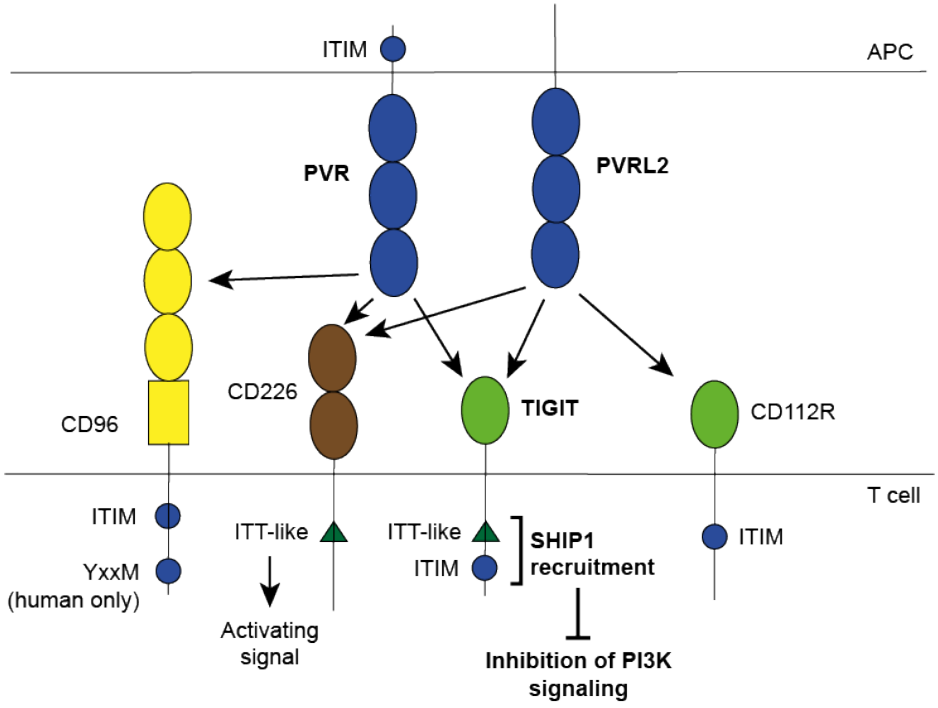


Figure 1-5: Ligand interactions and signalling pathways of TIGIT. TIGIT binds to the poliovirus receptor (PVR), competing with the activating receptor CD226 and another inhibitory receptor CD96. TIGIT may also bind to PVRL2 and PVRL3. Ligand engagement leads to phosphorylation of TIGIT's cytoplasmic motifs and subsequent recruitment of SH2 containing proteins including SHIP1.

1.10.4. CD200R

The CD200 receptor (CD200R) is an IgSF member but differs very substantially from the receptors described above. CD200R consists of two extracellular IgSF domains, a transmembrane region and a cytoplasmic tail that contains three tyrosines. None of these tyrosines is in an ITIM or ITSM motif but one sits in an NPXY motif, which has been described to regulate cellular activation via recruitment of the adaptors Dok-1 and Dok-2 and subsequent inhibition of the Ras-MAPK pathway [217, 218] (Figure 1-6). CD200R is expressed at highest levels on myeloid cells including monocytes, macrophages, DCs and granulocytes [219] but it is also expressed at lower levels in B- and T-cells [220].

CD200R binds to CD200, which itself has two IgSF domains in its extracellular region but has only a short cytoplasmic tail with no signalling function. In humans there is one closely related gene called CD200RLa that has a short cytoplasmic tail and a charged residue in its transmembrane region suggesting it could interact with the activating adaptor DAP12. However, it lacks two key extracellular cysteines and likely cannot be expressed as a functional protein [219]. In mice the system is more complicated with four CD200R like genes termed CD200RLa-d (or CD200R2-5), at least two of which can pair with DAP12 to transmit activatory signals [219]. There was initially some data to suggest that CD200 could also bind to these activating receptors [221] but subsequent thorough investigation concluded that there is no significant binding [222]. It seems likely that the activating receptors have evolved as a host defence against viruses that have developed CD200 orthologs to suppress the

immune response, although an investigation of two such herpesvirus orthologs demonstrated that they could not bind the activating receptors either [223].

As reviewed by Gorczynski [224], CD200R has been shown to play a role in regulating both myeloid and lymphoid immune responses. CD200R knockout mice have no resting phenotype and CD200 knockout mice have only a minor expansion of myeloid cell populations, but both strains display heightened immune responses to challenge, for example in CIA or EAE [225]. CD200 overexpressing mice conversely are protected from autoimmune disease. The key role CD200R plays in regulating the immune response is further highlighted by the many studies described previously in which it has been successfully targeted with agonist agents in models of autoimmune disease.

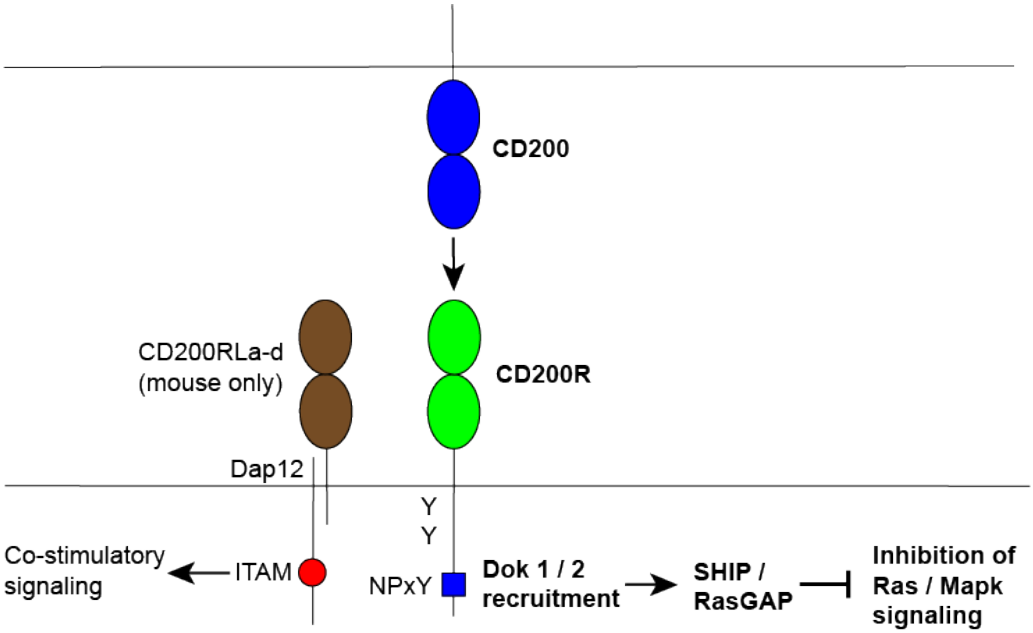


Figure 1-6: Ligand interactions and signalling pathways of CD200R. CD200R engagement by the ligand CD200 leads to phosphorylation of the tyrosine in its NPxY motif and subsequent recruitment of Dok1 and Dok2, which in turn lead to inhibition of the MAP kinase signaling pathway. In mice there are four homologous activating receptors (CD200RLa-d) but they do not bind CD200.

1.11. Work leading up to this project

Previous work in our lab (described in the PhD thesis of Billur Akkaya [162] and US patent 8927697 [226]) characterised an anti-human-PD1 agonist antibody termed Clone 19. The effects of this antibody were assessed both *in vitro* and *in vivo* using a transgenic mouse strain that expresses the extracellular domain of human PD1 in place of the murine extracellular domain. The antibody was shown to inhibit T-cell responses to various activation stimuli, but it demonstrated limited efficacy in an EAE disease model.

To enable investigation of the therapeutic potential of agonist antibodies against other human inhibitory receptors work was then undertaken to produce similar human receptor 'knock-in' mouse strains for three additional targets that the literature suggests are important regulators of immunity; BTLA, TIGIT and CD200R. The strategy for creation of these mice was devised by Dr Consuelo Anzilotti and their production was outsourced to InGenious Targeting Laboratory. Each strain was designed to express the human extracellular domain of the relevant target as a chimera with the murine transmembrane and signalling domains. This was achieved by gene targeting using homologous recombination in iTL IC1 (C57BL/6) embryonic stem (ES) cells to replace the genomic sequence in the endogenous gene locus with genomic sequence encoding the chimera (Figure 1-7 – 1-9). To maintain correct splicing in the mice a short section of murine sequence was maintained at each end of the inserted human exons (complete sequences of the chimeric transcripts can be found in the appendix). The targeting vector also contained a neomycin (Neo) resistance module for positive selection of transfected ES cells, which was flanked by

flippase recognition target (FRT) sites. Targeted ES cells were microinjected into Balb/c blastocysts and resulting chimeras with a high percentage of black coat colour were mated to flippase (FLP) expressing C57BL/6 mice to remove the Neo cassette. Offspring with black coat colour were selected for presence of the transgene and absence of the Neo cassette. These mice were subsequently mated with wildtype (WT) C57BL/6 mice and offspring again selected for presence of the transgene, absence of the Neo cassette and absence of the FLP transgene. Mice were then bred to homozygosity for the humanised transgene. Furthermore, each of these new human-knock-in strains was also crossbred with humanised-PD1 mice until homozygosity for both transgenes.

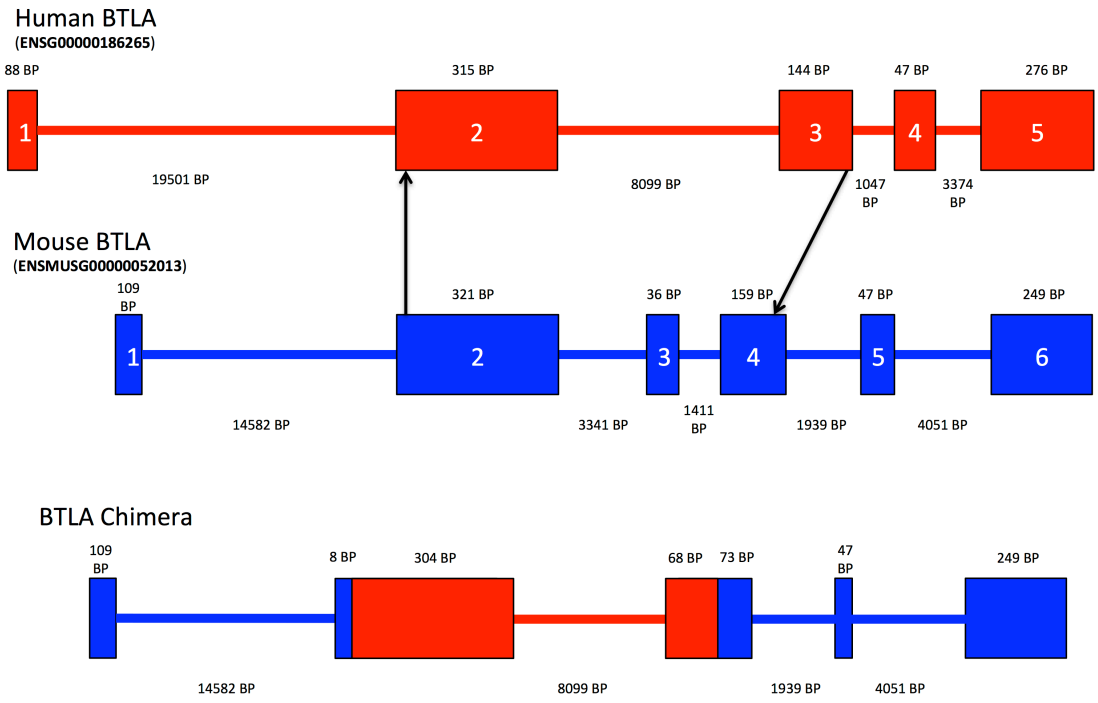


Figure 1-7: Design of the chimeric receptor expressed in the humanised BTLA mice. Genomic DNA encoding the human extracellular domain replaces the equivalent murine genomic DNA. To maintain appropriate splicing murine sequence is retained at each end of the inserted exons.

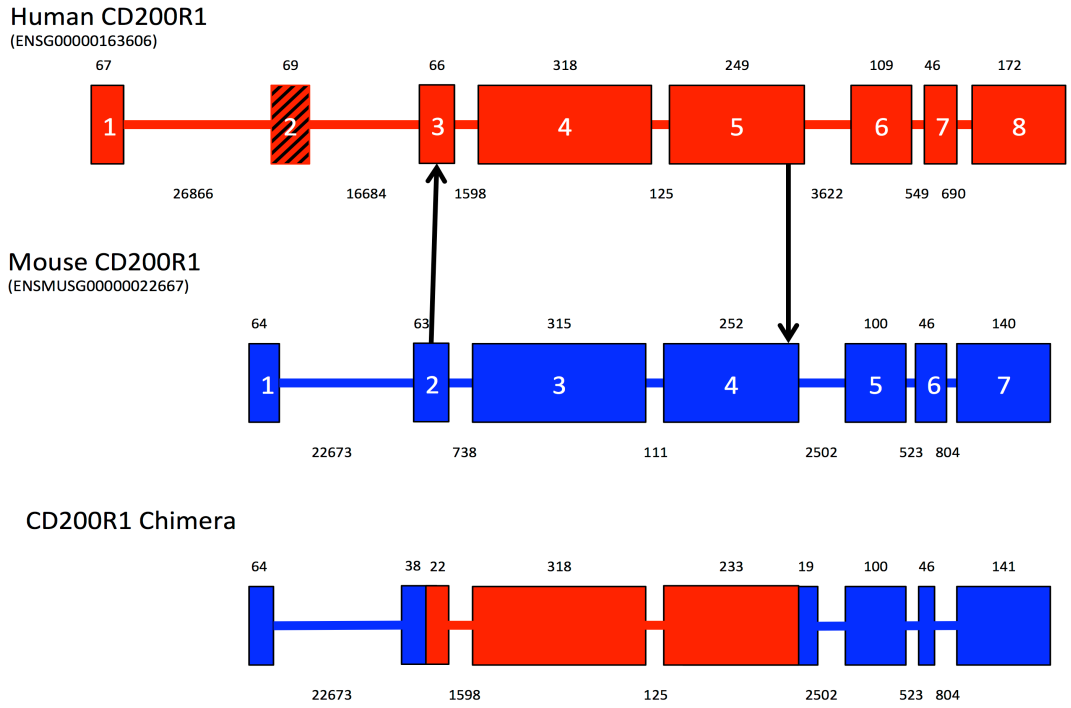


Figure 1-8: Design of the chimeric receptor expressed in the humanised CD200R mice. Genomic DNA encoding the human extracellular domain replaces the equivalent murine genomic DNA. To maintain appropriate splicing murine sequence is retained at each end of the inserted exons. (Human exon 2 is alternatively spliced and likely not expressed at a protein level [227])

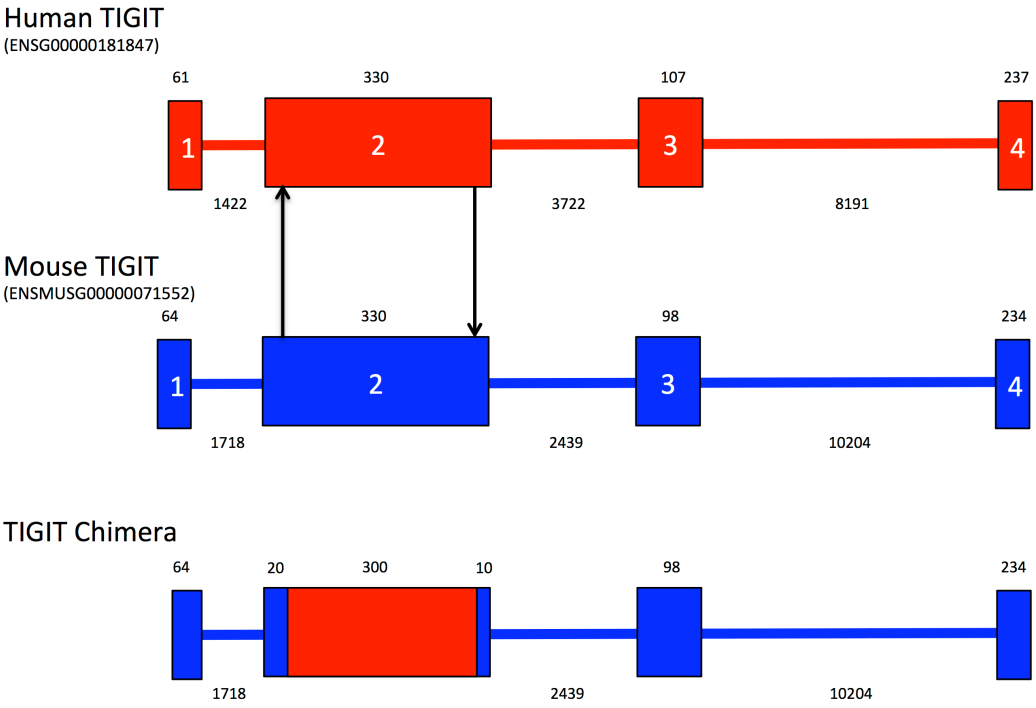


Figure 1-9: Design of the chimeric receptor expressed in the humanised TIGIT mice. Genomic DNA encoding the human extracellular domain replaces the equivalent murine genomic DNA. To maintain appropriate splicing murine sequence is retained at each end of the inserted exons.

Objectives of this thesis

As described above, several groups have explored the therapeutic potential of inhibitory receptor agonists in mouse models of autoimmune disease. Out of necessity these studies have been carried out using anti-murine antibodies, which could not be translated to the clinic. This thesis aims firstly to characterise three new strains of humanised checkpoint 'knock-in' mice to evaluate whether they can provide a functional tool for testing anti-human antibodies in a physiological *in vivo* setting. Secondly, it aims to assess panels of antibodies against these three human checkpoints (BTLA, CD200R and TIGIT) to explore whether agonist antibodies against these targets can be identified and whether any of these receptors may serve as more effective targets than PD1 in models of autoimmunity. Finally, by correlation of functional affects with binding characteristics, it aims to further elucidate the properties of an antibody required to confer agonist activity.

Chapter 2 Materials and Methods

2.1. Buffers and reagents

2.1.1. General reagents

PBS: 0.01 M phosphate buffer, 0.0027 M KCl, 0.137 M NaCl, pH 7.4 (either purchased sterile or made up using PBS tablets in de-ionised water)

PBS 0.5 M NaCl: 0.01 M phosphate buffer, 0.0027 M KCl, 0.5 M NaCl, pH 7.4 (made up by adding additional NaCl to PBS)

HBS-P buffer: 0.01 M HEPES pH 7.4, 0.15 M NaCl, 0.005% v/v Surfactant P20, 0.05% Na Azide

TBE buffer: 0.1 M Tris, 0.1 M borate, 2 mM EDTA

R2 media: RPMI containing 2% heat inactivated fetal calf serum (FCS), antibiotics (50 U / ml penicillin, 50 µg / ml streptomycin, 100 µg /ml neomycin), 10 mM HEPES

FACS buffer: PBS, 2% FCS, 0.05% sodium azide

MACS buffer: PBS, 2% FCS, 2 mM EDTA

ACK lysis buffer: 155 mM ammonium chloride, 10 mM potassium bicarbonate, 0.1 mM EDTA (generally purchased from ThermoFisher Scientific)

Cell freezing solution: 10% dimethyl sulfoxide, 90% FCS

2x SDS PAGE sample buffer (non-reducing): 1 ml 0.5 M Tris-HCl pH 6.8, 1.6ml 10% SDS, 0.8 ml glycerol, bromophenol blue to colour.

2x SDS PAGE sample buffer (reducing): 1 ml 0.5 M Tris-HCl pH 6.8, 1.6ml 10% SDS, 0.8 ml glycerol, bromophenol blue to colour, 0.4 ml β-mercaptoethanol

12% acrylamide resolving gel (recipe for 1 gel): 1.75 ml dH2O, 1.25 ml Tris/HCl pH 8.8 SDS resolving buffer, 2 ml acrylamide/bis-acrylamide 30% solution, 25 µl freshly prepared 10% ammonium persulphate, 5 µl TEMED.

4% acrylamide stacking gel (recipe for 1 gel): 1.55 ml dH2O, 625 µl Tris/HCl pH 6.8 SDS stacking buffer, 325 µl acrylamide/bis-acrylamide 30% solution, 12.5 µl freshly prepared 10% ammonium persulphate, 5 µl TEMED

Ear punch buffer: 50 mM Tris pH8, 2 mM NaCl, 10 mM EDTA, 1% SDS

2.1.2. Cell culture media

HEK293T cells were grown in DMEM medium supplemented with 10% heat inactivated FCS, 2 mM glutamine and antibiotics (50 units penicillin and 50 µg streptomycin per mL). When supernatant was being collected for protein purification the FCS percentage was reduced to 2%.

CHO-K1 cells were grown in DMEM medium supplemented with 10% heat inactivated FCS, 1mM Sodium Pyruvate, 2 mM glutamine, antibiotics (50 units penicillin and 50 µg streptomycin per mL) and 1x mixture of non-essential amino acids & nucleosides (Sigma-Aldrich). When selecting for stably transfected cells using the glutamine synthetase selection system FCS was replaced with 10% dialysed FCS and media without L-glutamine was used.

Primary murine immune cells (e.g. splenocytes) were cultured in R10 media consisting of RPMI-1640 supplemented with 2 mM L-glutamine, 10% heat inactivated FCS, antibiotics (50 units penicillin and 50 µg streptomycin per mL), 10 mM HEPES, 50 µM β-mercaptoethanol, 100 µM non-essential amino acids solution and 100 µM sodium pyruvate.

B-cell hybridomas were cultured in RPMI-1640 medium supplemented with 15% FCS, 10 mM HEPES, 1 mM sodium pyruvate, 2 mM L-glutamine, 100 µM hypoxanthine- 16 µM thymidine supplement (HT supplement), 100 µM non-essential amino acids solution and antibiotics (50 units penicillin, 50 µg streptomycin and 100 µg neomycin per mL). When collecting supernatant for antibody purification FCS was replaced with 10% ultra-low-IgG FCS.

2.2. Generation of B-cell hybridomas

The work to generate hybridomas producing antibodies against human CD200R, BTLA and TIGIT was outsourced to two contract research organizations (Biogenes AG and Generon Ltd). Hybridomas were generated by immunizing mice with serial injections of the extracellular domain of the target receptor and fusing immunised spleens with the myeloma cell line Sp2/0-Ag14. Following selection in HAT medium and limited dilution cloning, positive clones were identified by ELISA of supernatants. For each target a panel of several hybridomas was produced to enable characterization of a diverse range of antibodies with different binding characteristics and functional effects. The proteins used as immunogens were

produced by thrombin cleavage of Fc-fusions of each target receptor (the sequences of these constructs are in the appendix). Hybridomas with alphanumerical clone names (e.g. ID2) were produced by Generon, whilst hybridomas with entirely numerical clone names (e.g. 2.8.6) were produced by Biogenes.

2.3. Molecular biology techniques

2.3.1. Molecular Cloning

Template DNA for constructs was ordered as DNA strings (GeneArt, Thermo Fisher Scientific) or alternatively cDNA from human PBMCs was used. Protein sequences were obtained from UniProt and for gene synthesis DNA was codon optimized for the species of the intended expression cell line. When using cDNA as a template sequences were identified by searching online databases such as EMBL-EBI's European nucleotide Archive (ENA) or NCBI GenBank (usually linked from the UniProt entry). Primers complementary to the 5' or 3' ends of the sequence of interest and containing the desired restriction sites were designed to have matching melting temperatures in the range of 65-70°C (as calculated by NEB's online Tm calculator). Additional base pairs (typically TAGTAG) were added outside restriction sites to enable efficient cutting. DNA was amplified by PCR with Phusion High Fidelity DNA polymerase (ThermoFisher) using recommended protocols, adapted as required for different constructs.

PCR products were separated at 80 mA on ethidium-bromide stained 2% agarose gels in TBE buffer, alongside a DNA size marker. Bands of the correct size were excised and DNA extracted using the QiaQuick gel extraction kit (Qiagen).

Restriction digestion of inserts and vectors was carried out using NEB restriction enzymes following recommended protocols. Following digestion vector DNA was 5' dephosphorylated with Antarctic Phosphatase and then both vector and insert digests were cleaned up using the QiaQuick gel extraction kit.

Ligase reactions were typically carried out at 16°C for at least 2 hours using different ratios of insert to vector (generally 1x, 3x or 5x insert to vector), before transformation of chemically competent Top 10 E-coli using ligase product. Transformed cells were spread onto LB-agar plates containing the relevant selection antibiotic and incubated overnight at 37°C. The following day colonies were picked with a pipette tip, dropped into LB broth and again incubated overnight (the volume of LB broth being dependent on the desired quantity of vector DNA). DNA was extracted from bacterial cultures using PureLink HiPure Plasmid Miniprep / Midiprep / Maxiprep kits (ThermoFisher Scientific). Sequencing of the inserted DNA was carried out using SourceBioscience's Sanger sequencing service and primers designed to cover the inserted sequence and cloning sites. Sequences were read using 4Peaks software and checked against intended sequence using the online NCBI Basic Local Alignment Search Tool (BLAST) tool.

Other online tools used for sequence design and analysis included:

- RestrictionMapper.org to assess sequences for the presence of restriction sites.
- The ExPASy translate tool to perform DNA to peptide sequence translation

- reverse-complement.com to perform reverse complementation of DNA sequences for 3' primer design

2.3.2. Antibody Isotyping

Antibody isotypes were determined from hybridoma supernatant or purified antibody using Pierce Rapid Mouse Antibody Isotyping Kit (ThermoFisher), as per the provided protocol.

2.3.3. Hybridoma sequencing to obtain variable domain sequences

RNA was extracted from 10^7 hybridoma cells by trizol extraction. cDNA was prepared using Superscript II reverse transcriptase and reverse primers specific to IgG1 CH1 (TATGCAAGGCTTACAACCACA) or IgK constant domain (CTCATTCCTGTTGAAGCTCTTGACAAT). Variable sequences were then amplified by PCR using Phusion HF DNA polymerase. Primers were based on those used by Tiller *et al* [228] (*5′ mVkappa* and *3′ mCκ* for kappa chain, *5′ MsVHE* and *3′ Cγ1* outer for heavy chain, as all antibodies were known to be IgG1k isotype) . Hybridomas had been produced by fusion with Sp2/0-Ag14 myeloma cells and as such expressed a non-productively rearranged IgK transcript. This was present in large amounts and made amplification of the desired kappa chain difficult. To circumvent this we used a strategy described by Yuan *et al* [229] in which a primer specific to the aberrant chain CDR3 was included in the PCR reaction in 10x molar excess over other primers to terminate the reaction early. On a 1% agarose ethidium bromide gel, the correct length band was therefore enriched for the desired kappa chain. After gel extraction PCR products were sequenced using SourceBioscience's Sanger sequencing service.

The same forward and reverse primers used for PCR were also used for sequencing. The NCBI IgBlast tool was used to identify the germline V regions from which the antibodies had arisen and the start of the V region (upstream from the forward PCR primer) was assumed to be unchanged from germline.

2.3.4. Cell culture

All cell culture was performed using aseptic technique in HEPA filtered cell culture cabinets. All reagents were bought sterile or were filter-sterilised prior to being introduced into cell culture. Cells were grown at 37°C in 5% CO2. Cell viability and density were monitored regularly by microscopy and counting. Trypan blue (0.4%, Sigma Aldrich), a dye that penetrates dead but not viable cells, was mixed 1:1 with cells before counting in a haemocytometer.

For long-term storage, cell lines were kept in vapour phase liquid nitrogen. Typically, cells were pelleted by centrifugation for 5 minutes at 180 RCF and resuspended at 5 x 10^6 cells / ml in freezing solution. 1 ml was pipetted per cryovial and vials were transferred to isopropanol-filled freezing chambers in a -80°C freezer overnight before transfer to vapour phase liquid nitrogen.

2.3.5. Hybridoma culture for the production of murine antibodies

Hybridomas were initially grown up in standard tissue culture flasks in 15% FCS containing hybridoma media and then seeded (1 x 10^8 cells per flask) into 10 layer HYPERFlasks (Corning) in media containing ultra-low-IgG FCS. Supernatant was harvested after approx. 2 weeks once cells had reached high density. Supernatant was

centrifuged to pellet out cellular debris prior to antibody purification by Protein G affinity chromatography.

2.3.6. Lentiviral transduction of HEK293T cells

A lentiviral expression system was used to obtain high yields of soluble proteins for SPR experiments. The human immunodeficiency virus (HIV)-derived system used consists of three separate plasmids that were first transfected into HEK293T cells to produce self-inactivating virus, which was subsequently used to transduce HEK293Ts, integrating into the genome and driving expression of the gene of interest. The p8.91 vector contains the structural proteins and enzymes needed to generate infectious viral particles. The pMDG vector contains viral coat proteins for packaging. The pHR vector contains the gene of interest, cloned into the multiple-cloning-site, flanked by long terminal repeats and under control of the cytomegalovirus (CMV) promoter.

For transfection of HEK293Ts, cells were seeded in 6 well plates in 2 mL medium per well. The following day, for each well a mixture of 100 µL unsupplemented DMEM, 0.5 µg p8.91, 0.25 µg pMDG, 0.5 µg pHR and 3µL GeneJuice transfection reagent was incubated at room temperature for 20 minutes and then added to the cells. 48 hours later the supernatant containing virus was harvested, filtered through a 0.45 µm syringe filter and kept at 4°C. Fresh media was added to cells and again harvested and filtered the following day, and collated with the initial supernatant. For transduction of HEK293Ts this supernatant (4 ml total) was added to cells that had been seeded 24

hours earlier in a 25 cm^2 flask. Cells were subsequently grown up and supernatant collected for protein purification.

2.3.7. Stable transfection of CHOK1 cells

For some soluble proteins, to create stable CHOK1 cell lines expressing high levels of the protein a glutamine synthetase (GS) based system of selection was used, utilising the Lonza PEE14 vector. This vector contains the GS gene, leading to high GS expression in transfected cells, which can therefore survive the addition of L-Methionine sulfoximine (MSX), an inhibitor of GS activity, which kills non-transfected cells in glutamine free media.

4 x 10^6 CHOK1 cells in 20 ml media were seeded in a 75 cm^2 tissue culture flask and the following day media was changed to glutamine free media with dialysed FCS. A mixture of 500 µl DMEM, 10 µg PEE14 vector (containing the gene of interest) and 30 µl Genejuice was incubated for 20 minutes at room temperature and then added to the cells. The following day cells were detached using trypsin, centrifuged and resuspended in media, then plated out at 1 x 10^6 cells per plate in 96 well flat bottomed plates (in 100 µl media per well). MSX was added at 2x final concentration in 100 µl media per well, to create plates at 30 µM, 35 µM and 40 µM concentration (3 plates per concentration). 7 days after plating out, 100 µl media was removed and replaced with fresh MSX containing media. 1-2 weeks later (once supernatants had begun to turn orange in some wells) plates were assessed, selecting an MSX concentration at which most wells were dead, but some contained single colonies of live cells.

Protein concentration in supernatants was measured using a dot-blot technique. 5 µL from each well was pipetted onto a nitrocellulose membrane in a 12 x 8 grid (matching the plate layout). The membrane was blocked in 1 % skimmed milk in PBS for 1 hour at RT, then incubated with anti-penta-His antibody at 0.2 µg/ml in blocking buffer for 45 minutes at RT (the expressed proteins all contained a His tag for purification). The membrane was then washed 3x with PBS 0.05% Tween-20, and incubated with horseradish peroxidase conjugated secondary antibody at 1 µg/ml in blocking buffer for 30 minutes. Washed again 3x with PBS-Tween then developed with Pierce™ ECL Western blotting substrate and exposed to an X-ray film using darkroom development techniques. Highly expressing clones were identified by a strong signal on the dot blot and subsequently grown up to collect supernatant for protein purification and to freeze down vials for long term storage in liquid nitrogen.

2.3.8. Transient transfection of HEK293T cells using POPIN and pFUSE vectors

To recombinantly express Fab fragments, sequences encoding heavy and light variable domains were cloned into pOPINVH and pOPINVL vectors respectively, which contain a µ-phosphatase secretion leader upstream of the cloning site and the CH1 or CK domain sequences immediately downstream of the cloning site. The CH1 sequence is followed by a 6x Histidine tag to enable Ni-NTA purification.

To recombinantly express full-length antibodies, sequences encoding heavy and light variable domains were cloned into pFuse vectors (InvivoGen) that contain a human IL2 signal sequence upstream of the cloning site and immunoglobulin constant

domains downstream (different vectors were used to express antibodies onto different human or mouse isotypes).

Heavy and light chain vectors at a 1:1 ratio were co-transfected into HEK293T cells using 25 kDa linear PEI as a transfection reagent. Typically a 1:3 ratio of DNA:PEI was used and approx. 20 μg total DNA per 2 x 10^7 cells. Supernatant was collected and refreshed for 7 – 10 days of culture. For full-length antibodies medium containing ultra-low-IgG FCS was used. Fabs were purified from supernatant using Ni-NTA affinity chromatography, murine isotype antibodies were purified using protein-G and human isotype antibodies were purified using protein-A.

2.3.9. Creation of epitope mapping panels by site directed mutagenesis

Wildtype sequences of the ECD of hBTLA, hCD200R and hTIGIT (fused to part of the mCD28 transmembrane and cytoplasmic region) were cloned into the pGFP^2-N3 vector (construct sequences in the appendix) for transient expression in HEK293Ts. From these templates a panel of single surface residue mutants of each receptor was created by site directed mutagenesis so that residues critical for antibody binding could be identified by flow cytometric staining of cells transfected with each mutant.

For hBTLA and hTIGIT x-ray crystallographic structures of the extracellular domain are available (PDB entries 2AW2 and 3Q0H respectively). For hCD200R an automated homology model based on the murine crystal structure was obtained from the Swiss-Model repository (entry number Q8TD46). The degree of surface exposure of each residue was calculated from the PDB file using the Naccess program

(http://wolf.bms.umist.ac.uk/naccess/). Residues with greater than 50% surface exposure were chosen for mutation (for CD200R only residues in the membrane proximal IgSF domain were mutated).

For each mutant, overlap extension PCR was performed with primers designed to introduce a drastic mutation – for most amino acids this meant a change to arginine, except for histidine, lysine and arginine which were mutated to aspartic acid. The panel of mutants for each receptor are listed in Table 2-1. The mutant PCR products were cloned back into the pGFP^2-N3 vector for transient transfection in HEK293T cells.

BTLA	TIGIT	CD200R
D35R	M22R	T152R
Y39R	M23R	E154R
K41E	T26R	V155R
R42E	E28R	T156R
Q43R	T29R	F158R
E45R	S34R	Q159R
S47R	E36R	N160R
L48R	S40R	R161E
D52R	I42R	V170R
P53R	H46E	P174R
E55R	S49R	H177E
E57R	T51R	S179R
A64R	Q53R	I181R
N65R	Q62R	E183R
H68E	D63R	D185R
T77R	A71R	A187R
T78R	D72R	T188R
V80R	H76E	K189E
K81E	P79R	Q190R
E83R	S80R	E191R
D84R	K82E	Y192R
Q86R	D83R	S194R
S88R	P87R	K201E
E91R	P89R	H205E
E92R	L91R	E207R
K93E	S97R	V208R
E103R	T99R	H209E
L106R	T103R	S212R
N108R	E105R	T213R
S112R	Y113R	L221R
Q120R	Y117R	K225E
S121R	T119R	S226R
L123R	E125R	Y228R
E125R	E128R	E230R
Y132R	S129R	
K137E		

Table 2-1: Mutants produced for epitope mapping. For each receptor, surface exposed residues were mutated with a drastic substitution to create a panel of single residue mutants to enable epitope mapping. Numbering of residues as per the UniProt database.

2.3.10. Epitope mapping by flow cytometry of the mutant panels

Each mutant receptor construct was transiently expressed in HEK293T cells by transfection of cells in 6 well plates. Cells were plated out at 3 x 10^5 cells per well and the following day transfected with 0.5 μg DNA and 1.5 μl of Genejuice transfection reagent per well. 48 hours later cells were harvested by vigorous pipetting in ice cold PBS. One well of a six well plate provided enough cells to split between up to 10 wells of a 96 well U-bottom plate, in which antibody staining was carried out (and so multiple antibodies could be epitope mapped in parallel). After pelleting in 96 well plates cells were resuspended in 25 μl of either hybridoma culture supernatant or purified antibody diluted to 10 μg /ml in FACS buffer, and incubated for 30 minutes on ice. Cells were then washed twice with FACS buffer and resuspended in 25 μl of FACS buffer containing a fluorescently conjugated secondary antibody (typically APC-goat-anti-mouse-IgG at 1 μg / ml) and a live-dead cell marker (typically Zombie Aqua Fixable Viability Dye, Biolegend). Incubated for 30 minutes on ice then washed and resuspended in FACS buffer for acquisition on a BD FACS Canto flow cytometer. Appropriate single stain controls were used for compensation calculation.

For each mutant construct, live GFP positive (transfected) cells were gated on and receptor staining geomean was normalized to GFP geomean (to normalize for different transfection efficiencies) and then normalized to wildtype receptor staining as per the below equation:

$$\frac{Mutant\ receptor\ staining\ geomean}{mutant\ tranfection\ GFP\ geomean} \div \frac{Wildtype\ receptor\ staining\ geomean}{wildtype\ tranfection\ GFP\ geomean}$$

Mutant constructs that led to significantly reduced staining for a given antibody were plotted onto the receptor structure using PyMol software, with a cluster of closely positioned detrimental mutations highlighting the likely epitope of the antibody. Mutant constructs that led to significantly reduced staining for all antibodies tested were removed from analysis on the basis that they likely induced significant structural changes in the extracellular domain or reduced surface expression, rather than indicating an epitope position.

2.3.11. Creation of lower affinity antibody variants by CDR mutagenesis

The NCBI IgBlast tool was used to identify the position of CDRs in variable domain sequences. The degree of surface exposure of each residue was calculated using the Naccess program and the three most exposed residues in each CDR was chosen for mutation. Overlap extension PCR was used to introduce drastic mutations (all residues to arginine, except for histidine, lysine and arginine which were mutated to aspartic acid). Mutated variable domain sequences were cloned into POPIN or pFUSE vectors to allow expression as His-tagged Fab fragments or full length antibodies. Mutants were screened by SPR to assess the impact on target receptor affinity and mutations that reduced binding affinity were combined by further rounds of cloning, to further reduce affinity.

2.3.12. Nickel purification

Proteins expressed with a 6x His tag were purified by Ni-NTA affinity chromatography. Collected supernatant was centrifuged at 3000 RCF for 20 minutes

to remove any residual cellular debris and then diluted in equal volume PBS. Supernatant was then flowed over Ni-NTA sepharose beads packed in a glass Econo-Column (Bio-Rad)(volume of beads and size of column selected based on estimated amount of protein to be purified). Column was then washed with 10x column volume of PBS 10 mM Tris pH 8.0, followed by pre-elution with 10 mM Imidazole, collecting fractions until OD at 280 nM reached zero (as assessed using a NanoDrop One sprectrophotometer). Desired protein was then eluted with 250 mM imidazole in fractions equal to 1 x bead volume, again until no further protein eluted. Fractions from 10 mM and 250 mM elutions were checked on SDS-PAGE gels and desired fractions collated and concentrated (using a 10 kDa cut-off Millipore Amicon Ultra centrifugation filter unit), then run over FPLC using a Superdex 300 column to separate from aggregate and buffer exchange.

To regenerate Ni-NTA beads they were subjected to the following series of washes in an Econo-Column:

- 5x column volume of 250 mM Imidazole
- 5x column volume of dH2O
- 10x column volume of 0.5 M NaOH
- 5x column volume of dH2O
- 3x 5x column volume of 2% SDS
- 5x column volume of dH2O
- 5x column volume of 100 mM EDTA pH 8.0
- 5x column volume of dH2O
- Recharge column with 2x volume of 100 mM NiSO4
- 5x column volume of dH2O

For immediate use, then equilibrated with 5x volume of suitable buffer (eg PBS). For storage washed with 2x volume of 30% ethanol.

2.3.13. Protein G purification

Murine antibodies and mIgG1-Fc fusion proteins lacking a His-tag were purified using Protein G affinity chromatography. Collected supernatant was centrifuged at 3000 RCF for 20 minutes to remove any residual cellular debris and then diluted in equal volume PBS. Supernatant was then flowed over Protein G sepharose beads packed in a glass Econo-Column (Bio-Rad)(volume of beads and size of column selected based on estimated amount of protein to be purified). Washed with 10 x column volume PBS 0.5 M NaCl pH 7.4, then bound antibody eluted in 5 ml fractions of 0.1 M glycine pH 2.5 until no further protein coming off in eluent (as assessed by measuring OD at 280 nm with a NanoDrop One sprectrophotometer). Eluted fractions immediately neutralized with 2.75 M Tris pH 8.5 (approx. 200 µl / fraction). Fractions analysed by SDS-PAGE and desired fractions collated, concentrated using a 10 kDa cut-off Millipore Amicon Ultra centrifugation filter unit, then run over FPLC using a Superdex 300 column to separate from aggregate and buffer exchange into PBS.

Beads cleaned with further washes of 0.1 M glycine then neutralized with PBS azide and stored in PBS azide, or for long-term storage in 20% ethanol.

2.3.14. Protein A purification

Human isotype antibodies were purified using Protein A purification. Collected supernatant was centrifuged at 3000 RCF for 20 minutes to remove any residual cellular debris and then diluted in equal volume PBS. Supernatant was then flowed over Protein A sepharose beads packed in a glass Econo-Column (Bio-Rad)(volume of

beads and size of column selected based on estimated amount of protein to be purified). Washed with 10 x column volume PBS 0.5 M NaCl pH 7.4, then bound antibody eluted in 1 ml fractions of 0.1 M Citric Acid pH 3.0 until no further protein coming off in eluent (as assessed by measuring OD at 280 nm). Eluted fractions immediately neutralized with 2.75 M Tris pH 8.5. Fractions analysed by SDS-PAGE and desired fractions collated, concentrated using a 10 kDa cut-off Millipore Amicon Ultra centrifugation filter unit, then run over FPLC using a Superdex 300 column to separate from aggregate and buffer exchange into PBS.

Beads cleaned with further washes of 0.1 M Citric Acid then neutralized with PBS azide and stored in PBS azide, or for long-term storage in 20% ethanol.

2.3.15. Thrombin cleavage of Fc-fusion proteins

Fusion proteins were expressed linked to mIgG1-Fc-His by a thrombin cleavage site (sequence LVPRG). Cleaved by overnight incubation at room temperature with 1 unit thrombin (GE healthcare) per 100 µg of protein. Digest stopped by addition of PMSF at a final concentration of 1 mM. Separated from Fc-His by flowing over Ni-NTA beads packed in a glass Econo-Column (Bio-Rad).

2.3.16. Quantification of protein concentrations

Protein concentrations were determined by spectrophotometry, measuring absorbance at 280 nm on a NanoDrop One. Extinction coefficients were calculated using the ExPASy ProtParam online tool.

2.3.17. Gel electrophoresis

Mass and purity of purified proteins was assessed by running on SDS-PAGE gels alongside protein markers of known size. 10 µL of protein sample (at less than 0.5 mg/mL) was diluted in an equal volume of reducing or non-reducing 2x loading buffer. Samples were boiled at 95°C for 5 minutes then 15 µL was loaded per well of a 15-well, 12% SDS-PAGE gel. Electrophoresis was carried out at 150 V in a Tris/glycine/SDS-PAGE running buffer. 12% SDS-PAGE gels consisted of a 12% resolving gel topped with a 4% stacking gel. Gels were subsequently subjected to Western blotting or stained with Coomassie Brilliant Blue. The gel was placed in 0.1% Coomassie Brilliant Blue in a 10% acetic acid, 40% methanol solution for 15 minutes, then destained in a 10% acetic acid, 12% methanol solution until no background was visible. Gels were then dried using the GelAir Drying System (BioRad) for documentation in lab books.

2.3.18. FPLC

Proteins were mostly separated by size-exclusion chromatography on an ÄKTA Pure chromatography system using Superdex-75 or Superdex-300 columns, depending on the size of protein and resolution required. An appropriate buffer was used for downstream application (e.g. HBS with azide for SPR proteins, or PBS without azide for proteins to be added to live cells). Antibodies intended for *in vivo* administration were separated in sterile PBS on an ÄKTA Start system that had never been used for bacterial expressed proteins and were handled only in pyrogen free plastic, to maintain as low an endotoxin level as possible. Collected fractions from FPLC runs were analysed by SDS-PAGE to confirm protein quality. Where possible

proteins were used for experimentation (e.g. SPR assays) shortly after FPLC without undergoing freeze-thaw cycles. Purified antibodies were generally diluted to 1 mg / ml and frozen immediately after FPLC in small aliquots at -80°C and thawed immediately prior to use. Where required, proteins were concentrated in Millipore Amicon Ultra centrifugation filter units.

2.3.19. Biotinylation

Site specific biotinylation of proteins with a BirA site was carried out using the BirA biotin-protein ligase standard reaction kit (BirA-500, Avidity) as per provided protocol. FPLC was then used to separate biotinylated protein from free biotin.

2.4. Surface plasmon resonance assays

All experiments were performed at 37°C in HBS-P buffer (0.01 M HEPES, 0.15 M NaCl, 0.005% v/v Surfactant P20, pH 7.4), on either a Biacore T200 or a Biacore 3000. In all experiments binding measurements were double-referenced, subtracting both the signal from a reference channel and the signal for a zero-concentration (blank) injection. In all experiments attempts were made to match the reference channel as closely as possible to the signal channel by immobilizing an equal RU of a structurally similar but non-binding protein. For example, when assessing antibody-antigen interactions an isotype matched control antibody was immobilized in the reference channel.

In different experiments different approaches were taken to ligand immobilization.

For direct immobilization of purified protein by amine coupling, a CM5 sensor chip was first activated by 5 minute injection of 75 mg/mL 1-Ethyl-3-(3-dimethylaminopropyl)carbodiimide hydrochloride (EDC-HCl) and 11.5 mg/mL N-Hydroxysuccinimide (NHS) mixed in a 1:1 ratio. The ligand was diluted in 10 mM sodium acetate pH 5.0, typically to around 10 µg/mL, immediately prior to injection over the freshly activated chip. Following immobilization the chip was inactivated by 5 minute injection of 1.0 M ethanolamine-HCl pH 8.5. Even if no matched reference protein was available the reference channel was still subjected to the same activation and de-activation protocol. For indirect immobilisation of Fc-fusion proteins or antibody the mouse-antibody capture kit (GE healthcare) was used, in which a polyclonal anti-Ig antibody is first directly immobilized by amine coupling and then Fc tagged protein can be captured straight from tissue culture supernatant or from purified protein stock. For indirect immobilization of biotinylated proteins streptavidin was first immobilized onto the chip directly by amine coupling (by 5 minute injection over the activated chip at 0.2 mg/ml in 10 mM sodium acetate pH 5.0).

Low affinity interactions such as the checkpoint receptor-ligand interactions were assessed by equilibrium analysis in which various concentrations of analyte were injected and binding at equilibrium (RU_{eq}) for each concentration was measured. The K_d was then calculated by non-linear curve fitting using a one-site specific-binding model on GraphPad Prism. Scatchard transformations were also performed, plotting RU_{eq}/concentration against RU_{eq} to provide a linear representation of the data. Using the values calculated from the non-linear curve fitting a line of gradient $-K_d$ which

crosses the X-axis at X = B_{max} is superimposed onto the Scatchard plot to allow visual inspection of the quality of fit to the calculated K_d.

High affinity interactions such as receptor-antigen binding were assessed using kinetic analysis, with injections at a minimum speed of 30µl /min. For either a single injection of analyte, or injections at several different concentrations (in a single cycle without regeneration or multiple cycles with regeneration in between), BiaEvaluation software was used to curve fit to the association and dissociation phase of binding, providing the on rate (k_{on}) and off rate (k_{off}), and the dissociation constant (K_d) was calculated as k_{off} / k_{on}.

2.5. Flow cytometry

The majority of flow cytometry was carried out on a BD FACS Canto and analysed using FlowJo software. Typically cells were pelleted by centrifugation (180 RCF for 2 minutes) in 96 well U-bottom plates, washed with FACS buffer then stained for 30 minutes on ice by resuspension in 25 µl of staining cocktail. Staining cocktails consisted of appropriate dilutions of each conjugated-antibody in FACS buffer. Culture supernatant from the 2.4G2 rat-anti-mouse CD16/32 hybridoma was added at a 1 in 50 dilution to block Fc Receptor binding. Zombie Aqua Fixable Viability Dye or Zombie NIR Fixable Viability Dye (Biolegend) was used as a live/dead marker. Following staining, cells were washed with FACS buffer, then resuspended in 200 µl FACS buffer and kept on ice until acquisition. For intracellular staining (cytokines and transcription factors) the True Nuclear Transcription Factor Staining kit (Biolegend) was used as per recommended protocol. When performing intracellular staining for

cytokines cells were first stimulated for 4-6 hours with PMA (5 ng/ml), ionomycin (500 ng/ml) and BD GolgiStop (0.75 µl / ml) in R10 media at 37 °C and 5% CO_2.

Antibodies against the following mouse antigens (clone) were purchased from Biolegend unless otherwise specified:

B220 (RA3-6B2) AlexaFluor700, BV605, PE-Cy7, PerCP-Cy5.5;
BP-1 PE from BD;
mBTLA (8F4) PE;
hBTLA (MIH26) PE;
CD1d (1B1) FITC;
CD3 (17-A2) PerCP-Cy5.5 and BV421;
CD4 (GK1.5) AlexaFluor700;
CD5 (53-7.3) BV421;
CD8 (53–6.7) AlexaFluor700, PerCP-Cy5.5 and PE;
CD11b (M1/70) APC;
CD11c (N418) FITC;
CD19 (6D5) AlexaFluor700;
CD20 (SA275A11) APC;
CD21/35 (7E9) APC-Cy7, BV-605;
CD23 (B3B4) PE-Cy7;
CD23 (EBVCS-5) PE from BD;
CD24 (M1/69) FITC, AlexaFluor700, V450, BV605;
CD25 (PC61) FITC, PE and BV421;
CD43 (S7) APC and PerCP-Cy5.5 from BD;
CD44 (IM7) FITC, APC-Cy7, Pacific Blue;
CD45.1 (A20) PE-Cy7 and APC-Cy7;
CD45.2 (104) APC, BV421 and BV605;
CD45RB (MB4B4) APC;
CD49b (DX5) PE;
CD62L (MEL14) FITC, APC;
CD69 (H1.2F3) PE, BV605;
CD93 (AA4.1) APC;
CD127 (A7R34) APC;
mCD200R (OX110) PE;
hCD200R (OX108) PE;
F4/80 (BM8) PE-Cy7;
FOXP3 (MF-14) PE;
KLRG1 (2F1/KLRG1q) FITC;
ICOS (C398.4A) PerCP-Cy5.5;
CXCR5 (L138D7) BV605;
GL7 (GL7) FITC;
CD95 (Jo2) PE-Cy7 from BD;

IFN-γ (XMG1.2) PE;
IgD (11–26 c.2a) APC-Cy7;
IgM (RMM-1) PE, BV421;
IgM (II/41) FITC from BD;
IgG1 (RMG1-1) APC;
IL17 (TC11-18H10.1) APC;
Ly6c (HK1.4) PerCP-Cy5.5;
Ly6g (1A8) AlexaFluor700;
NK1.1 (PK136) PE-Cy7;
mTIGIT (1G9) PE;
hTIGIT (A15153G) PE;

AF-647 and Pacific Blue antibody labeling kits were purchased from ThermoFisher Scientific. Lynx Rapid RPE antibody conjugation kit was purchased from Bio-Rad Antibodies.

2.6. Experiments using transgenic humanised mice

All experiments were carried out in accordance with Animal (Scientific Procedures) Act 1986, with procedures reviewed by the Oxford University Animal Welfare and Ethical Review Body (AWERB), and conducted under project licence PPL P79A4C5BA. Most procedures were carried out under personal licence PIL I42DD2FE4. Animals were housed in specific pathogen free conditions, with the only reported positives on health screening over the entire time course of these studies being for Helicobacter hepaticus and Entamoeba spp. All animals were housed in individually ventilated cages in social groups, provided with food and water ad-libitum and maintained on a 12 h light /12 h dark cycle (150–200 lux cool white LED light, measured at the cage floor). Adult mice (>8 weeks of age) were used for experiments, with gender matched between groups and age matched as closely as possible. The mIgG1 antibody clone MOPC-21, which has no known binding specificity, was used as an isotype control.

2.6.1. Genotyping of transgenic mice

Genotyping of transgenic mice was in most part carried out by Tanya Cheetham in the Cornall laboratory. Ear notches were incubated in 20 µl of ear punch buffer with 1 mg/ml proteinase K for 40 minutes at 55°, then at 100°C for 5 minutes to inactivate the proteinase K. For each strain, PCR using pairs of primers specific for the replaced mouse sequence or inserted human sequence were used to detect the mouse or human alleles, with products run on 2% agarose gels at 110 V for 30min.

The primers and conditions of the PCR were as follows:

BTLA:
Shared forward - TGT ACC ACA CTG GAA TAC TGA AGG
Murine reverse - TCC TGG CAG ACT GTT TGG AA (product 212 bp)
Human reverse - CCC ATT GTC ATT AGG AAG CAC TGG (product 398 bp)

CD200R:
Shared forward - CCT ACA AAG GAC CTG GCA AGA AGG
Murine reverse - TGT GTC AGA GGA GAT GAA CTG T (product 272 bp)
Human reverse - GAA AGT ATA GGA ACT TCG CGA CAC GGA C (product 725 bp)

PD1:
Murine forward - CTC ACA GTG TCA GAG GCA
Murine reverse - ACG GGT TGG CTC AAA CCA TTA C (product 150 bp)
Human forward - TCG TGG TGA CCG AAG GGG AC
Human reverse - GCA GGC TCT CTT TGA TCT GCG (product 300 bp)

TIGIT:
Shared forward - CAG GCA GAG GAA GAA AAA CTC TGG
Murine reverse – ATGACAGAGCCACCTTCCTC (product 249 bp)
Human reverse - GAA AGT ATA GGA ACT TCG CGA CAC GGA C (product 736 bp)

<u>PCR Master Mix</u>

Buffer	2.5µL
$MgCl_2$	1.25µL
dNTPs	0.625µL
Fwd primer (10µM)	0.75µL
Rev primer (10µM)	0.75µL
Taq polymerase	0.125µL
H_2O	18µL
DNA template	1µL

PCR programme

95°C		5min
95°C	10sec}	
55°C	30sec}	x 35
72°C	60sec}	
72°C		5min
16°C		hold

2.7. Mouse mixed lymphocyte reaction

Splenocytes from Balb/c mice (MHC haplotype H-2^d) were used as stimulators and splenocytes from humanised C57BL/6 mice (MHC haplotype H-2^b) were used as responders. Spleens were aseptically removed and single cell suspensions were prepared by pressing through a 70 μm nylon cell strainer. Balb/c splenocytes were treated with ACK lysis buffer (to lyse red blood cells), washed and resuspended in 1 ml cell culture media containing 50 μg/ml Mitomycin-C and incubated for 30 minutes at 37°C. They were then washed 4-5 times with cell culture media changing the tubes each time. Responder spleens were also processed to a single cell suspension and then T cells were isolated by negative selection using Mojosort Mouse CD3 T-cell isolation kit. Purified T-cells were washed in PBS, then labeled with CFSE or CTV cell proliferation dyes (ThermoFisher Scientific) at 5 μM in PBS for 7 minutes at room temperature. Labeled responder T-cells were mixed at a 1:2 ratio with stimulator cells and seeded into 96-well U-bottom plates at 2 x 10^5 cells per well in 100 μl of R10 media. Prior to addition of cells wells were filled with the test antibody (+/- ligand blocking antibodies) at 2x final concentration in 100 μl of R10 media. The cultures were incubated for 3-5 days at 37°C, 5% CO2.

In some experiments the responder cell population was made up of a 50:50 mix of T cells from humanised mice and T cells from CD45.1 allotype marked C57BL/6 mice (which express only murine checkpoint receptors and do not bind any of the anti-human checkpoint antibodies). In these experiments the ratio of proliferation of humanised to WT responder cells was calculated for each antibody condition and normalized to the ratio in the presence of isotype control. In some experiments a polyclonal goat-anti-mouse HVEM antibody (R&D Systems, Cat #AF2516) was added to stimulator cells prior to mixing (to a final concentrations of 2μg/ml) to block endogenous signalling through the HVEM-BTLA pathway.

2.8. Assessing upregulation of checkpoint receptors on stimulation

For experiments in which T cells were activated prior to staining in order to assess the upregulation of checkpoint receptors, the mCD3 antibody 145.2C11 and mC28 antibody 37.51 were used. 96-well U-bottom plates were coated with anti-CD3 antibody at 1 μg / ml in carbonate buffer for 2 hours at 37°C then washed 3 times with PBS before addition of ACK lysed splenocytes at 2x 10^6 per well in R10 media with soluble anti-CD28 at 0.5 μg / ml. Cells were cultured for 24 hours before assessment of receptor expression by flow cytometry. To assess the expression of CD200R on myeloid cells in different settings peritoneal exudate cells were stimulated overnight with LPS (1 μg/ml), LPS + IFNg (10 ng/ml) or IL4 (40 ng/ml).

2.9. Phenotyping immune cell subsets in humanised mice

Thymus, spleen and mesenteric lymph nodes were collected from adult mice and processed to single cell suspensions by pressing through a 70 μm nylon cell strainer.

Peritoneal exudate cells were collected from humanely sacrificed mice by injection of 4 ml of R2 media into the peritoneal cavity, agitation to mix the cells and then collection of media with a Pasteur pipette. Bone marrow cells were obtained from two femurs and two tibias per mouse by flushing with R2 media using a 5 ml syringe and 25G needle. Samples were treated with ACK lysis buffer, washed and counted with a haemocytometer prior to staining and flow cytometry. Antibody staining panels (using clones as listed in Section 2.5) are described in Table 2-2, made up in FACS buffer with the addition of Fc-block.

Laser	488nm				640nm			405nm		
Fluorochromes	FITC, AF488, GFP, CFSE	PE	PerCPCy5.5, PE-Cy5, 7AAD	PE-Cy7	APC, AlexaFluor647	AF700, APC-R700	APC-Cy7, APC-eFluor780, NIR L/D	BV421, PacificBlue	BV510, V500, Aqua L/D,	BV605, BV570, Qdot605
B cell (Bone marrow)	**IgM**	**BP-1**	**CD43**	**CD19**	**CD127**	**B220**	**IgD**	**CD24**	**L/D**	
dilution (1 in...)	500	200	100	1000	100	500	500	400	500	
B cell (spleen / PEC / MLN)	**CD1d**	**IgM (a)**	**CD19**	**CD23**	**CD93**	**B220**	**IgD**	**CD5**	**L/D**	**CD21**
dilution	400	500	1000	200	100	500	500	100	500	400
T cells	**CD44**	**CD25**	**CD8a**		**CD62L**	**CD4**		**CD3**	**L/D**	**CD69**
dilution	200	200	400		100	400		200	500	200
NK/NKT	**KLRG1**	**CD49b**	**CD3e**	**NK1.1**	**CD11b**	**B220**		**CD44**	**L/D**	
dilution	100	100	200	200	500	200		100	500	
Myeloid lineage	**CD11c**	**CD8a**	**Ly6c**	**F4/80**	**CD11b**	**Ly6g**		**CD3e**	**L/D**	**B220**
dilution	100	800	400	200	500	200		200	500	400
Germinal Centre	**GL7**	**IgM**	**B220**	**CD95**	**IgG1**	**CD19**	**IgD**		**L/D**	
dilution	50	500	500	200	100	200	500		500	
TfH	**CD25**	**CD69**	**ICOS**		**CD62L**	**CD4**	**CD44**		**L/D**	**CXCR5**
dilution	50	100	300		100	500	200		500	100

Table 2-2: Flow cytometry panels used for phenotyping of immune cell subsets in the transgenic mice.

2.10. Immunisation protocols

2.10.1. Sheep red blood cell (SRBC) immunisations

10 ml SRBC in Alsever's solution 50% v/v (First Link UK) were topped up to 50 ml with PBS and centrifuged for 5 min at 2000 RPM. Supernatant discarded and pellet resuspended in PBS. Repeated twice for a total of three washes in PBS then pellet resuspended in 10 ml PBS and 200 µl injected intraperitoneally (IP) per mouse. In experiments assessing the effect of checkpoint antibodies on the immune response antibodies were injected IP at 200 µg / mouse 24 hours after SRBC immunisation. Mice were culled 6 days after immunization and flow cytometry carried out on ACK lysed, single cell suspensions of splenocytes using the germinal centre and TfH panels described in Table 2-2**.** To assess BTLA expression, a Pacific Blue conjugated anti-hBTLA antibody was added to the panels (splenocytes from mice injected with 2.8.6 were stained with the non-competing clone 11.5.1 and vice versa).

2.10.2. NPCGG immunisations and NPCGG specific ELISA

0.5 mg/ml NP-CGG in PBS was added to an equal volume of Imject Alum Adjuvant (ThermoFisher Scientific) and stirred for 1 hour at 4°C. 200 µl of this mixture (50 µg NP-CGG) was then injected IP per mouse. In experiments to assess the effect of checkpoint antibodies on the immune response antibodies were injected IP at 200 µg per mouse 24 hours after NP-CGG immunisation. On days 14, 21 and 28 after immunization, tail-vein blood was collected into EDTA-containing capillary action blood collection tubes. After centrifugation at 13000 RPM for 10 minutes serum was aspirated off and stored at -20°C. On day 35 mice were 'boosted' by immunization

with 50 µg NP-CGG in 200 µl PBS. On day 42 mice were culled and blood collected by cardiac puncture, then centrifuged to obtain serum.

Serum NP-specific antibodies were quantified by indirect ELISA. ELISA plates were coated overnight at 4°C with NP25-BSA (5 µg/µl; Biosearch Technologies), washed 3x with PBS, then blocked with 5% (w/v) milk at 37°C for 2 hours. Again washed 3x with PBS, then incubated with serum samples serially diluted in 1% milk for 1 hour at room temperature. Serial dilutions of pooled sera from day 42 immunised mice were used to produce a standard curve. Plates washed 5x with PBS 0.05% Tween-20, then incubated for 1 hour with horseradish-peroxidase-conjugated goat antibody to mouse IgM or IgG1 (Southern Biotechnology) diluted in 1% milk. Again washed 5x with PBS 0.05% Tween-20 then developed with TMB Peroxidase Substrate and TMB Stop Solution (ThermoFisher). Absorbance was measured at 450 nm on a BioTek ELx808 ELISA plate reader.

2.11. Adoptive transfer assays

Mice humanised for both BTLA and PD1 were crossed onto OT2 TCR transgenic mice, which express a T-cell receptor specific for an ovalbumin peptide presented by MHC class 2, and therefore develop a CD4 T-cell compartment greatly enriched for ovalbumin specific cells [230]. The mice were bred until homozygous for both humanised receptors and heterozygous for the OT2 transgene (hBTLAhPD1_OT2). Separately OT2 mice were crossed onto transgenic mice that constitutively express GFP under the control of the ubiquitin C (UBC) promoter (UBC-GFP_OT2 mice).

CD4 T-cells were purified by negative selection, using the MojoSort Mouse CD4 T-cell Isolation Kit (Biolegend), from the spleens of hBTLAhPD1_OT2 transgenic mice and UBC-GFP_OT2 mice. These cells were mixed in a 1:1 ratio and 500,000 cells in 200µl PBS injected IV per mouse into CD45.1 allotype-marked recipient mice. 24 hours later recipient mice were immunised IP with 200 µg ovalbumin in 50% Imject Alum in PBS (v/v). 24 hours after this, the mice were injected IP with 200 µg of treatment antibody in 200 µl PBS. In experiments with combinations of treatment antibodies mice were injected with 200 µg of each antibody (400 µg total) in a total volume of 200 µl PBS. Six days later (8 days after the initial cell transfer) the recipient mice were culled and splenocytes assessed by flow cytometry. The population of transferred cells was identified as $CD45.2^{+}CD4^{+}$ and within this population the ratio of humanised (GFP^{-}) to non-humanised (GFP^{+}) cells was calculated, and normalized to the ratio in the isotype control treated mice**.**

2.12. Complement mediated cytotoxicity (CDC) assay

Spleens were obtained from hBTLA transgenic mice and pressed through 70 µm nylon cell strainers to produce a single cell suspension. 2 x 10^5 splenocytes per well (in a 96 well U-bottom plate) were incubated in R10 media with 10% baby rabbit complement (BioRad) at 37°C for 15 minutes in the presence of antibody at 10 µg/ml. A depleting anti-CD20 antibody (clone SA271G2, isotype rat-IgG2b) was used as a positive control and the mIgG1 mopc21 used as a negative control. Cells were then pelleted by centrifugation, washed in FACS buffer, and stained for flow cytometry using the following panel in Annexin V Binding Buffer (Biolegend) to assess viability of different cell populations:

CD62L FITC, Propidium Iodide solution, CD8 PerCP/Cy5.5, CD23 PE/Cy7, Annexin V APC, CD4 AF700, CD21 APC/Cy7, CD44 Pacific Blue, B220 BV605. Acquired on a BD FACS Canto Flow Cytometer.

2.13. Antibody-dependent cell mediated cytotoxicity (ADCC) assay

2 x 10^5 unfractionated hBTLA splenocytes (containing FcR expressing effector cells) per well were incubated in R10 media at 37°C for 24 hours in the presence of antibody at 10 µg/ml. Cells were then assessed by flow cytometry using the same panel as in the CDC assay (Section 2.12).

2.14. *In vivo* cytotoxicity assessment

The frequency of BTLA expressing cell populations in the spleen and bone marrow of humanised BTLA mice was assessed by flow cytometry, using the panels below, 24 hours after IP injection of clone 2.8.6 or MOPC-21 isotype control (200 µg/mouse).
Bone marrow B-cell panel: IgM FITC, hBTLA clone 11.5.1 PE, CD43 PerCP-Cy5.5, CD19 PE-Cy7, B220 AF700, IgD APC-Cy7, CD24 V450, Zombie Aqua Live Dead
Spleen B-cell panel: IgM FITC, hBTLA clone 11.5.1 PE, B220 PerCP-Cy5.5, CD23 PE-Cy7, CD19 AF700, IgD APC-Cy7, Zombie Aqua Live Dead, CD21 BV605
Spleen T-cell panel: CD25 FITC, hBTLA clone 11.5.1 PE, CD8 PerCP-Cy5.5, CD62L APC, CD4 AF700, CD44 Pacific Blue, Zombie Aqua Live Dead

2.15. T-cell transfer model of colitis

Spleens and mesenteric lymph nodes were obtained from adult female hBTLAhPD1 mice (approx. 1 donor per 2 recipients) and processed to single cell suspensions.

$CD4^+$ T-cells were enriched by negative selection using MojoSort Mouse CD4 T-cell Isolation Kit (Biolegend), and pooled. Cells were then stained for 30 minutes on ice in 1 ml PBS with CD4 FITC, CD25 PE, CD45RB APC and Zombie Aqua Live Dead (each at 1 in 100 dilution). Washed in PBS then resuspended at 1.5 x 10^7 cells/ml in PBS 2% FCS. Cells were then sorted by Jonathan Webber at the Kennedy Institute Flow Cytometry Facility, collecting live $CD45RB^{high}CD25^-CD4^+$ T-cells into polypropylene collection tubes containing 500 µl FCS. Sorted cells were pelleted by centrifugation and resuspended in PBS, then 4 x 10^5 cells/mouse were injected IP into female $RAG^{-/-}$ recipient mice. The negative control group of mice were injected with PBS only. Mice were initially weighed once per week, then with increasing frequency as they began to lose weight. Treatment antibodies were injected IP (200 µg/mouse) on days 7, 21, 35 and 49. Mice were culled on day 56 or when they reached a severity endpoint (which included weight loss of >15% from starting weight).

Colons were collected (from just distal of caecum to anus), emptied of faeces, weighed and measured to calculate a weight to length ratio. To extract lamina propria leukocytes (LPLs) colons were initially cut into 0.5 cm pieces in PBS 1% FCS in 50 ml falcon tubes. After sedimentation, supernatant was aspirated and pre-warmed (37°C) RPMI 5% FCS + 5mM EDTA was added, then tubes were incubated for 40 mins at 37°C in a shaking incubator. Supernatant (containing intraepithelial leukocytes) was then discarded and tissue again incubated in RPMI with EDTA for a further 10 minutes. This was again repeated for a final wash, before next incubating tissue for 1 hour at 37°C with RPMI 5% FCS + HEPES + collagenase D (1.5mg/ml, ThermoFisher) and DNAse I (100µg/ml). This time supernatant was collected and filtered into a new

tube through a 70 μm cell strainer. Following a wash with PBS 1% FCS the cells were resuspended in 3 ml Percoll 30% (v/v with PBS) then carefully pipetted onto the top of a Percoll gradient in 15 ml Falcon tube (3 ml Percoll 75% on the bottom, 4 ml Percoll 40% above and then cells in 30% Percoll layered on top). Centrifuged for 20 mins at 1800 RPM with no brake, then LPLs pipetted off from the interface between 75% and 40% Percoll. Counted and stained for flow cytometry using T cell and myeloid lineage panels as in Table 2-2**.**

2.16. Graft versus host disease model

Spleens and bone marrow (from tibia and femur) were collected from adult hBTLAhPD1 female donor mice. 2 x 10^7 bone marrow cells and 10^7 splenocytes were injected IV into recipient C57BL/6 x BALB/C first generation offspring female recipient mice, which had been irradiated the same day with two doses of 4.5 Gy spaced three hours apart. Following IV cell transfer mice were treated IP (on the same day) with 200 μg/mouse antibody in 200 μl PBS. Mice were weighed daily for the first 14 days after cell transfer then at least three times per week thereafter. Mice were culled 35 days after cell transfer, or sooner if they reached a severity endpoint (which included >15% weight loss from starting weight, or >20% in the first two weeks). Colon weight to length ratio was calculated as a marker of gut inflammation.

2.17. MC38 colorectal cancer model

The MC38 colorectal cancer model was carried out by the contract research organization, Crown Bioscience. MC38 cells were first expanded *in vitro* and then 1 x 10^6 cells/mouse were injected subcutaneously into the left flank of humanised

transgenic mice, in 100 µl PBS. Tumour size was measured three times per week using electronic callipers. Once average tumour volume reached 100 mm^3 mice were allocated to matched treatment groups and injected IP with 10 mg/kg antibody twice per week for two weeks. Mice were culled 35 days after tumour cell transfer or when they reached a severity endpoint if earlier. Mouse IgG1k isotype control (clone CB5) and anti-mouse-CTLA4 antibody (Syrian hamster IgG clone 9H10) were provided by Crown Bioscience.

2.18. Statistical analysis

All statistical analysis was carried out on GraphPad Prism software. Student's t-tests were used to compare two groups of parametric data. One-way ANOVA was used to compare three or more groups, with follow up tests dependent on the particular experiment.

Chapter 3 Characterisation of the humanised mice

3.1. Introduction

The development of novel therapeutics necessitates the preclinical testing of compounds in model systems that aim to represent human biology as closely as possible. Testing on human cells *in vitro* can provide important information about the effects on particular cell types or signalling pathways but cannot yet replicate the complex interplay of diverse cell subsets in a complete immune system. Therefore, animal models are still a crucial addition to the process and can yield information that furthers our understanding of human biology as well as predicting the likely impact of therapeutics prior to testing in humans. The first-line species of choice for such studies is usually mice. As would be expected after 65 million years of divergent evolution there are differences between the mouse and human immune systems [231] and it has become common to focus on these discrepancies, but in reality the mouse immune system is remarkably similar to ours. The vast majority of human immune genes have a functional counterpart in mice, and studies on mice have contributed to numerous breakthroughs in understanding human biology over the years [232]. The fast breeding, short life cycle and easy handling of mice also contributes to their suitability for research, and the long history of using experimental mice means that there is a now a large repertoire of well established and validated protocols for inducing models of autoimmune disease in mice.

Monoclonal antibodies present a particular challenge for the translation of medicines from mice to humans, as they bind with remarkable specificity to their cognate

epitope and so their binding is often affected by the sequence differences between species. Furthermore, as rodents are frequently used in immunization campaigns for the development of monoclonal antibodies, unless animals knocked-out for the target of interest are used, then the physiological effect of immune tolerance means that antibodies are usually raised against epitopes which are not shared between mouse and human. It is possible to employ techniques that enrich for antibodies cross-reacting with mouse and human targets (for example by immunizing in a third species with serial immunisations of the human and then mouse target or using phage display and serially panning for human and then mouse binders). However, this limits the pool of potential candidates to those that bind to shared epitopes and risks triaging out compounds that could have therapeutic benefit in humans because they cannot be assessed in mice. The extracellular domains of the three inhibitory receptors explored in this thesis are not that highly conserved between mouse and human; 46% for BTLA, 56% for CD200R and 65% for TIGIT (based on global alignment of UniProt sequences using the EMBOSS Needle global alignment tool) and the residues that are conserved are dominated by inward facing structurally important residues rather than surface residues. Therefore, selecting for antibodies that bind to shared epitopes would dramatically reduce the potential diversity of development candidates, and may miss out on unique biology displayed by antibodies binding to other, non-shared epitopes.

The development of mice humanised for each of these inhibitory receptors therefore potentially provides an invaluable tool for the *in vivo* assessment of any antibody targeting the human protein. However, in order for the mice to faithfully model the

effects of targeting these pathways it is important that the replacement of murine extracellular domain with human does not significantly impact the functioning of the system. The knocked-in receptors must be expressed on the cell surface, and on the right cells under appropriate transcriptional control. They must also maintain their binding to the endogenous ligands and their integration with the murine intracellular signalling machinery.

3.2. Assessing cross-reactivity of human receptors with mouse ligands

The transgenic mice are designed to express the human checkpoint receptors but they retain the endogenous murine ligands. In order for the pathways to remain functional it is therefore essential that the human receptors possess conserved binding to the mouse ligands, otherwise the mice would develop akin to receptor knock-out strains. Such a situation may still allow for the evaluation of agonist antibodies but the effects would likely be exaggerated (correcting a deficit of natural ligand) and not representative of the impact on a physiological immune system.

Whilst the extracellular domains do display numerous sequence differences between mouse and human, the ligand-binding site is an area with significant evolutionary pressure for conservation, and so is disproportionately more similar between species. For BTLA it has previously been demonstrated by FACS staining of transfected cells with Fc-fusion proteins that human BTLA can bind both human and mouse HVEM, whereas mouse BTLA can only bind the murine ligand [166, 186], though the monovalent affinities of these interactions were not measured. Similarly, for TIGIT it has been shown by staining of transfected cells that human TIGIT can bind to mouse

PVR but mouse TIGIT cannot recognize human PVR [209]. Finally, in the case of CD200R, the mouse receptor cross-reacts with human ligand, albeit with a lower affinity than mouse ligand, but the interaction of the human receptor with mouse ligand was not assessed [219].

In order to measure the monovalent affinities for each of the cross-species receptor-ligand interactions using surface plasmon resonance (SPR) we first produced each of the murine and human proteins as monomeric soluble proteins. Cloning and protein production was carried out with the assistance of Heather Brouwer in the Davis lab. Different approaches were required in each case to obtain good quality protein (the sequences of each of the constructs can be found in the appendix). The murine and human receptors were each expressed as Fc-fusion proteins with a mIgG1-Fc tagged with six histidines (Fc-His) in stably transfected CHOK1 cells, purified using Ni-NTA beads and then separated from the Fc-His portion using thrombin cleavage. The human and murine ligands PVR and CD200 were expressed as 6xHis-tagged proteins by lentiviral expression in HEK293T cells and purified using Ni-NTA affinity purification. They also contained a BirA site to enable site-specific biotinylation. In all cases, following affinity purification, proteins were next subjected to size exclusion chromatography (to separate from dimer or aggregate) and the collected fractions were run on reducing and non-reducing SDS-PAGE gels. Only fractions corresponding to monomeric soluble protein were used for SPR experiments. The ligand HVEM could not be expressed as a monomeric protein and instead was expressed as an Fc-fusion with Fc-His. Expression yields were insufficient to enable cleavage of the Fc-fusion protein and so this protein was immobilized as an Fc-fusion in SPR

experiments (as the soluble receptors injected over were monomeric, this still allowed for the assessment of true affinities).

For CD200R and TIGIT, interactions were assessed on a Biacore 3000. Biotinylated ligands were indirectly immobilized onto streptavidin-coated chips and monomeric soluble receptor was injected over at various concentrations, with measurement of double-referenced binding at equilibrium (Figure 3-1 and Figure 3-2). The K_d for each interaction was calculated by curve fitting on GraphPad Prism software, and a Scatchard linear transformation of the data was performed to allow visual inspection of the quality of fit to the calculated K_d.

For BTLA, interactions were assessed on a Biacore T200. HVEM-Fc fusion proteins were indirectly captured via an anti-mouse Ig capture kit and soluble receptors were injected over at increasing concentrations with K_d for each interaction calculated as above (Figure 3-3). Each interaction was assessed in at least 2 separate experiments with different batches of freshly purified protein and the summary data for all interactions is presented in (Table 3-1).

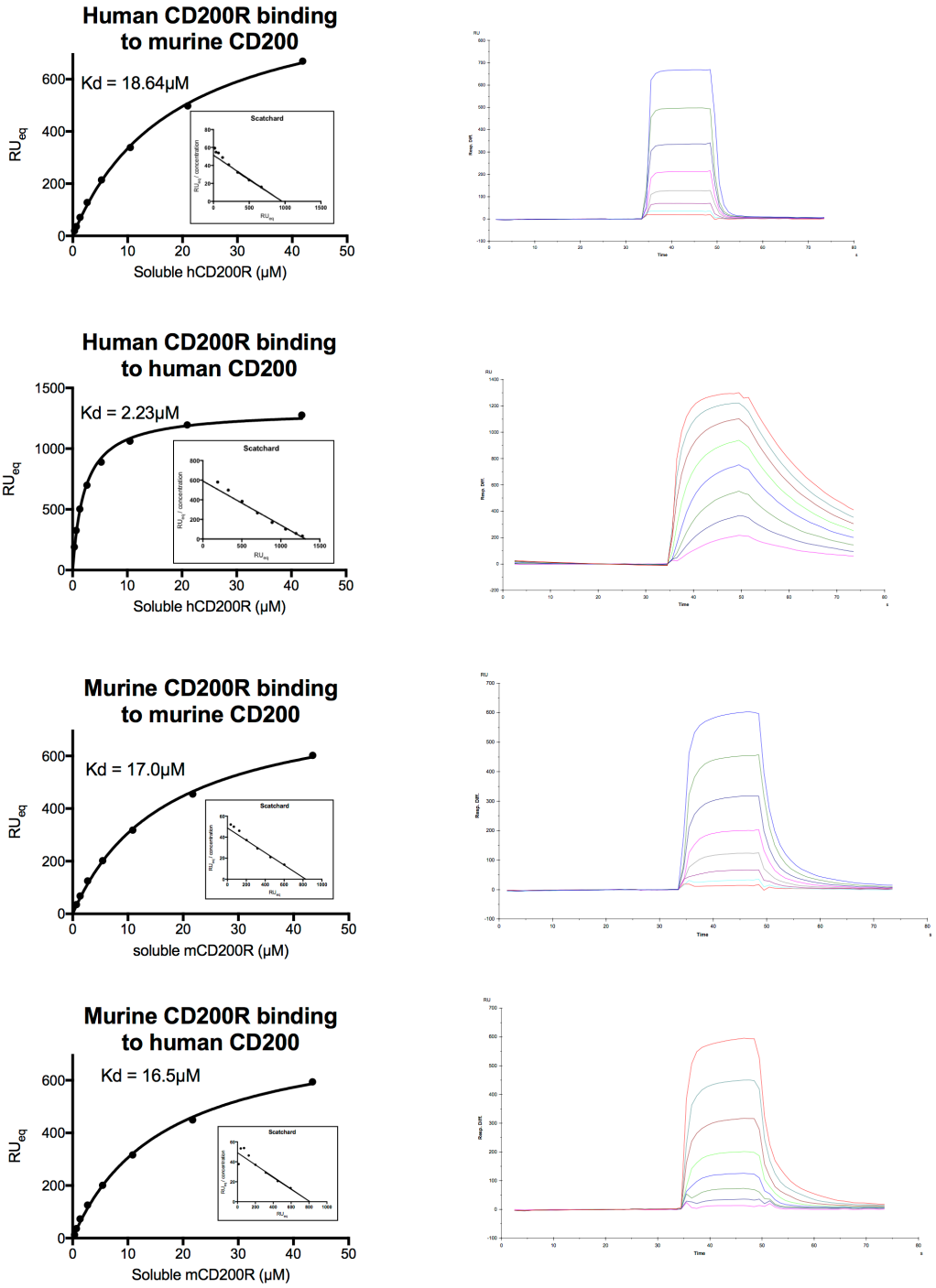


Figure 3-1: SPR assessment of CD200R-CD200 cross-species interactions. (Right) Soluble monomeric human or mouse CD200R was injected over immobilized human or mouse CD200 at various concentrations. (Left) Double-referenced binding at equilibrium was plotted against analyte concentration and the K_d for each interaction calculated by curve fitting on GraphPad Prism software; the inset Scatchard plots are a linear transformation of the data that allow visual inspection of the quality of fit to the calculated K_d.

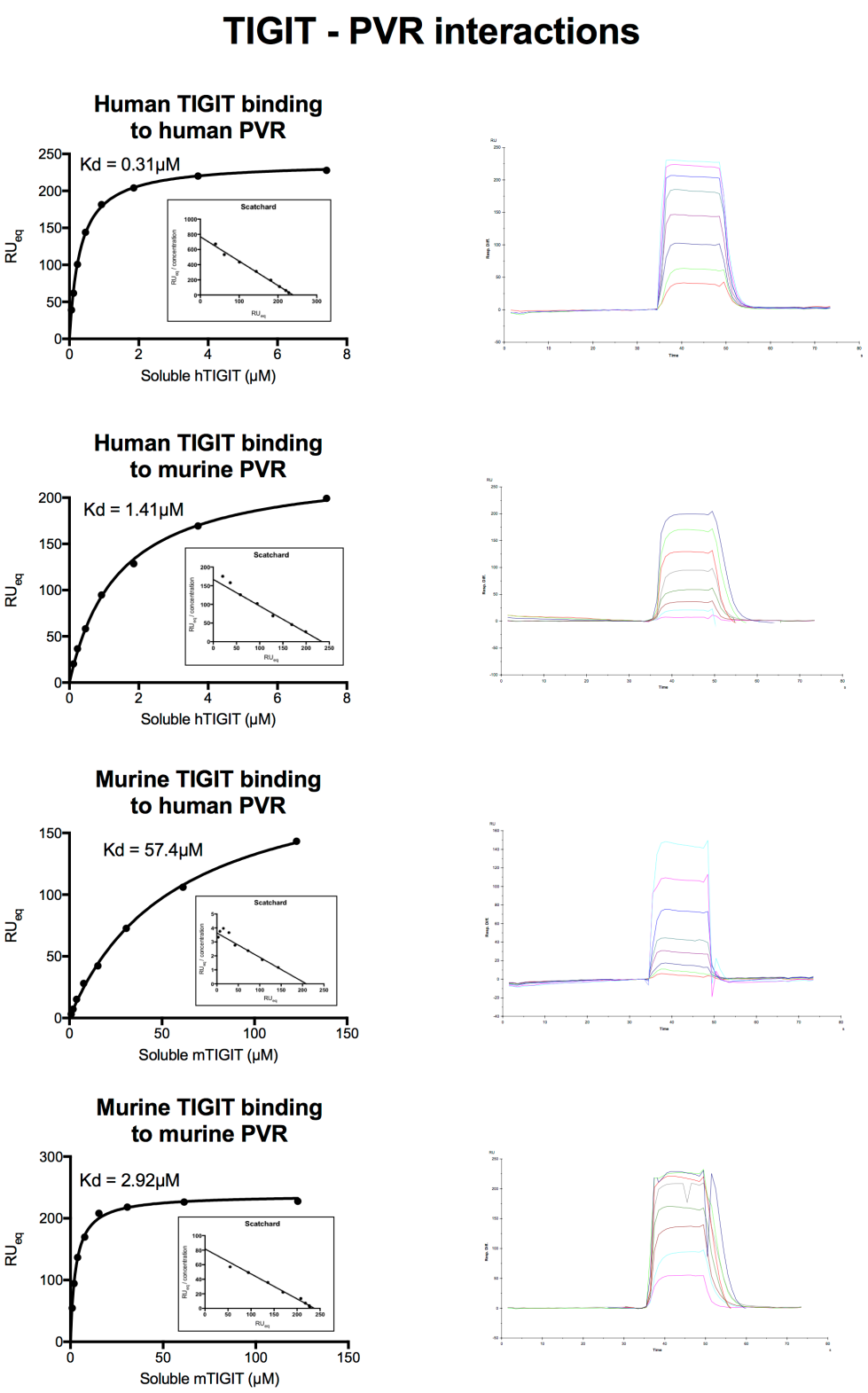


Figure 3-2: SPR assessment of TIGIT-PVR cross-species interactions. (Right) Soluble monomeric human or mouse TIGIT was injected over immobilized human or mouse PVR at various concentrations. (Left) Double-referenced binding at equilibrium was plotted against analyte concentration and the K_d for each interaction calculated by curve fitting on GraphPad Prism software; the inset Scatchard plots are a linear transformation of the data that allow visual inspection of the quality of fit to the calculated K_d.

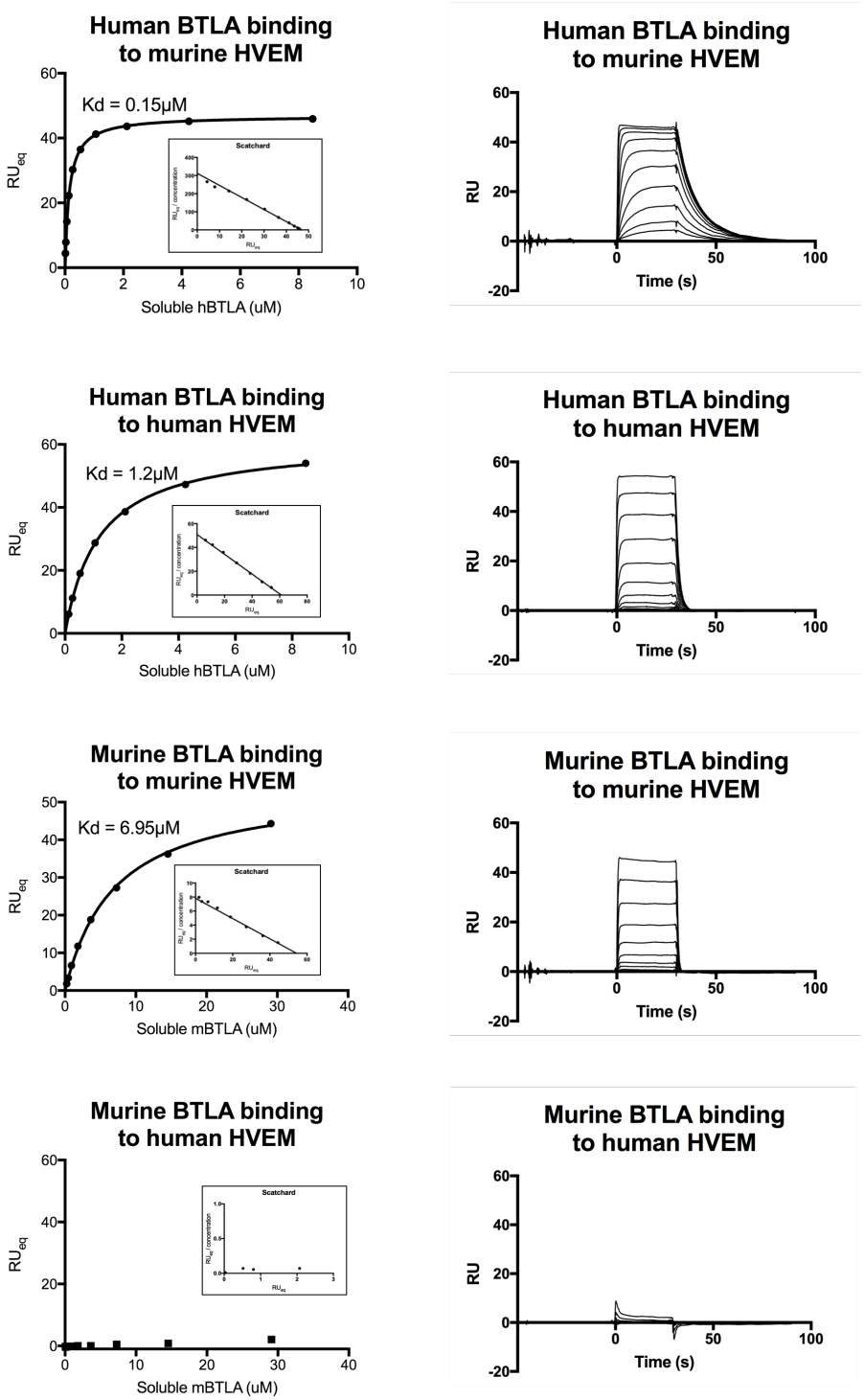


Figure 3-3: SPR assessment of BTLA-HVEM cross-species interactions. (Right) Soluble monomeric human or mouse BTLA was injected over immobilized human or mouse HVEM-Fc at various concentrations. (Left) Double-referenced binding at equilibrium was plotted against analyte concentration and the K_d for each interaction calculated by curve fitting on GraphPad Prism software; the inset Scatchard plots are a linear transformation of the data that allow visual inspection of the quality of fit to the calculated K_d.

	hBTLA	mBTLA	hCD200R	mCD200R	hTIGIT	mTIGIT
hHVEM	1.36 (0.23)	no binding				
mHVEM	0.17 (0.03)	6.03 (1.31)				
hCD200			2.29 (0.61)	19.27 (4.19)		
mCD200			22.39 (5.67)	17.62 (4.73)		
hPVR					0.37 (0.08)	48.68 (12.34)
mPVR					1.80 (0.54)	3.15 (0.32)

K_d in μM, with standard deviation in brackets

Table 3-1: Summary of interaction affinities for each of the cross-species receptor-ligand interactions

For all three pathways assessed the human form of the receptor exhibited cross-reactivity with the murine ligand. For CD200R and TIGIT the affinity of the human receptor for mouse ligand was very similar (within two-fold) of the native mouse interaction suggesting that the interactions in the transgenic mice should be very similar to wildtype mice. In both cases this interaction was of significantly lower affinity than the human interaction, which highlights the fact that there are differences in the biology of these pathways between mouse and human which need to be borne in mind when extrapolating from murine models to the human setting.

In the case of BTLA, the human receptor in fact binds to murine HVEM with significantly higher affinity (~30 fold) than the native mouse interaction, maintaining a binding affinity closer to the human system. The implications of this on signalling in the transgenic mice are difficult to predict, but it could mean that there will be a higher level of baseline signalling through the pathway leading to dampened immune responses in the mice and a consequent reduced sensitivity to the effects of agonist antibodies. Similarly, the increased affinity could lead to a homeostatic reduction in receptor expression.

3.3. Expression of the chimeric receptors in the transgenic mice

In order for the transgenic mice to provide a useful tool for the assessment of therapeutics it is essential that the chimeric humanised receptor is expressed and correctly folded at the cell surface. Furthermore, it is important that the introduction of human intronic DNA, when this occurs, has not affected transcriptional control so that the receptor is still expressed on the correct cell types and upregulated appropriately on cellular activation.

Cell types expected to express the receptor in question were isolated from wild type C57BL/6 and humanised mice and expression was assessed by flow cytometry using an antibody panel including antibodies targeting both the human and mouse extracellular domains. For BTLA and TIGIT, which are expressed on T cells and upregulated on activation, T cells were purified from spleens by negative selection magnetic cell sorting. These were then plated at 2 x 10^5 cells per well into 96-well U bottom plates that were either uncoated (giving 'resting' cells) or that had been coated with anti-CD3 antibody at 1 μg / ml in PBS for 2 hours at 37°C (producing 'activated' cells). Receptor expression was assessed after 24 hours of culture (Figure 3-4 and Figure 3-5).

For CD200R, which is expressed at highest levels on myeloid cells, peritoneal exudate cells were collected and cultured for 24 hours in flat-bottom plates either in medium alone or with the addition of IL-4 (M2 activation) or IFNγ and LPS (M1 activation). Receptor expression was assessed after 24 hours of culture (Figure 3-6a).

For all three of the transgenic strains the humanised receptor was detectable using anti-human antibody, and in these mice the murine receptor was no longer detectable, confirming the successful replacement of the murine extracellular domain with the human. Furthermore, each of the receptors exhibited expression levels at rest and on activation that were akin to the murine receptor in wild type mice. BTLA and TIGIT were present at low levels on resting CD4 T-cells and upregulated on activation, with expression also induced on CD8 T-cells following activation. Within the CD4 population, cells expressing the highest levels of these checkpoints correlated with activated $CD69^+$ cells.

Within the peritoneal exudate the population expressing high levels of CD200R correlated with $CD11b^+F4/80^+$ macrophages. Expression of CD200R on these cells was not affected by culturing in the presence of LPS and IFNγ but was increased by incubation with IL4 (Figure 3-6b), in keeping with previous observations that CD200R is associated with alternative (M2) macrophage activation [233].

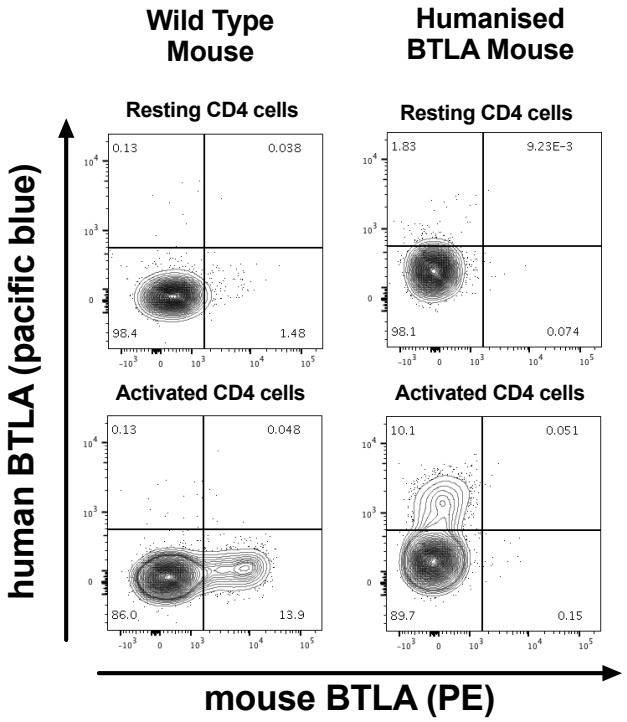


Figure 3-4: Chimeric BTLA expression. Expression of BTLA on wild type and humanised mouse splenic CD4 T-cells at rest (top two plots) and following activation for 24 hours with plate bound anti-CD3 and soluble anti-CD28 antibody (bottom two plots).

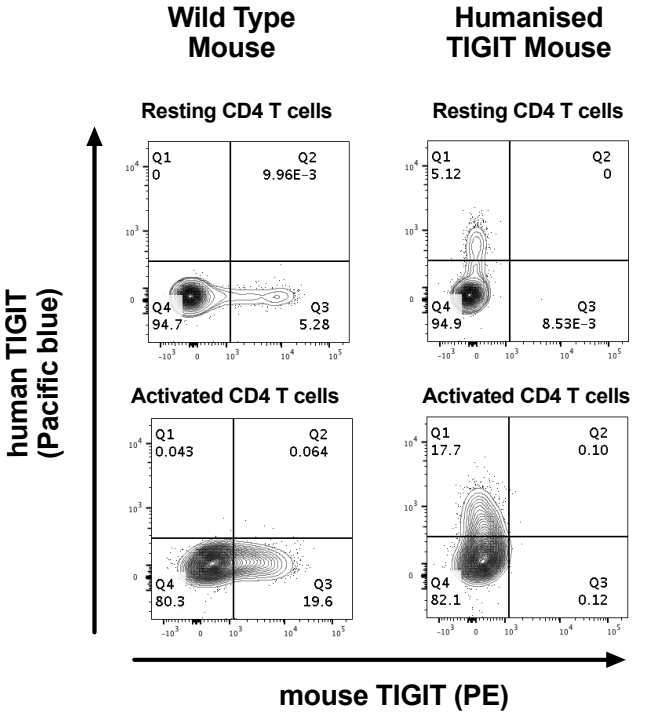


Figure 3-5: Chimeric TIGIT expression. Expression of TIGIT on wild type and humanised mouse splenic CD4 T-cells at rest (top two plots) and following activation for 24 hours with plate bound anti-CD3 and soluble anti-CD28 antibody (bottom two plots).

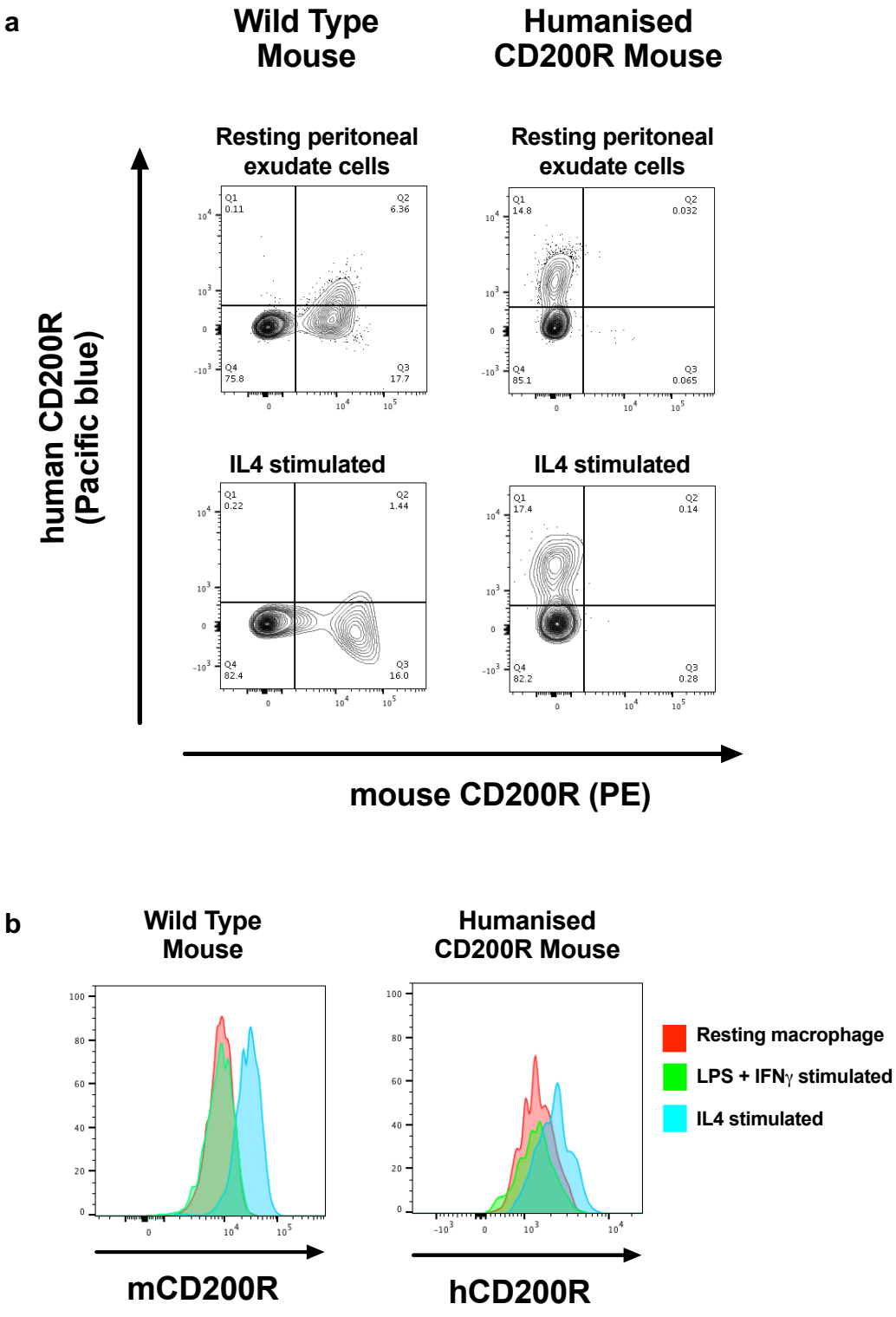


Figure 3-6: Chimeric CD200R expression (a) Expression of CD200R on wild type and humanised mouse peritoneal exudate cells at rest and following activation for 24 hours with 40 ng/ml recombinant IL4 (b) Comparison of CD200R expression on peritoneal macrophages cultured with media alone (resting), 40 ng/ml IL4 or 1 μg/ml LPS and 10 ng/ml IFNγ.

3.4. Immune system development in the transgenic mice

Detailed immunophenotyping of the transgenic strains was undertaken in order to assess whether they have any gross abnormalities in immune development that would complicate their use in modelling the immune response. Spleens, mesenteric lymph nodes, bone marrow (from the femurs and tibia of two legs), thymus and peritoneal exudate were collected from transgenic or wild type mice and processed into single cell suspensions. The total number of cells per organ was quantified by counting in a haemocytometer. Cells were stained with panels of antibodies as described in Section 2.9 to identify major immune cell subsets. For analysing flow cytometry data using FlowJo software all samples were first gated on live, nucleated, singlets (Figure 3-7 top).Differentiated subsets of CD4 and CD8 T-cells were measured in the periphery whilst T-cell developmental stages were quantified in the thymus, employing widely used gating strategies (Figure 3-7)**.** B-cell subsets in the periphery and developing fractions in the bone marrow were also enumerated (Figure 3-8), alongside myeloid populations and NK cells (Figure 3-9). For myeloid populations the gating strategy was based on that used by Rose *et al* to assess mouse splenic myeloid compartments [234]. The frequency of each population as assessed by flow cytometry was multiplied by total cell count to quantify the absolute number of each cell type in each organ**.** For each transgenic strain two separate experiments (with 4 -5 mice per group) were carried out to compare immune subsets to wildtype mice and representative data are plotted in (Figure 3-10 to 3-12). No statistically significant differences were seen between transgenic and wild type mice for any immune cell population suggesting an entirely normal development of the immune system in the presence of the chimeric receptors. Of note the hBTLA transgenic mice

did not exhibit the expanded B- and CD4 T-cell populations seen in hBTLA KO mice [107] and hCD200R transgenic mice did not have the expanded $CD11b^+$ population of myeloid cells seen in CD200 KO mouse spleens [225], again suggesting that the chimeric receptors are functional in the transgenic strains.

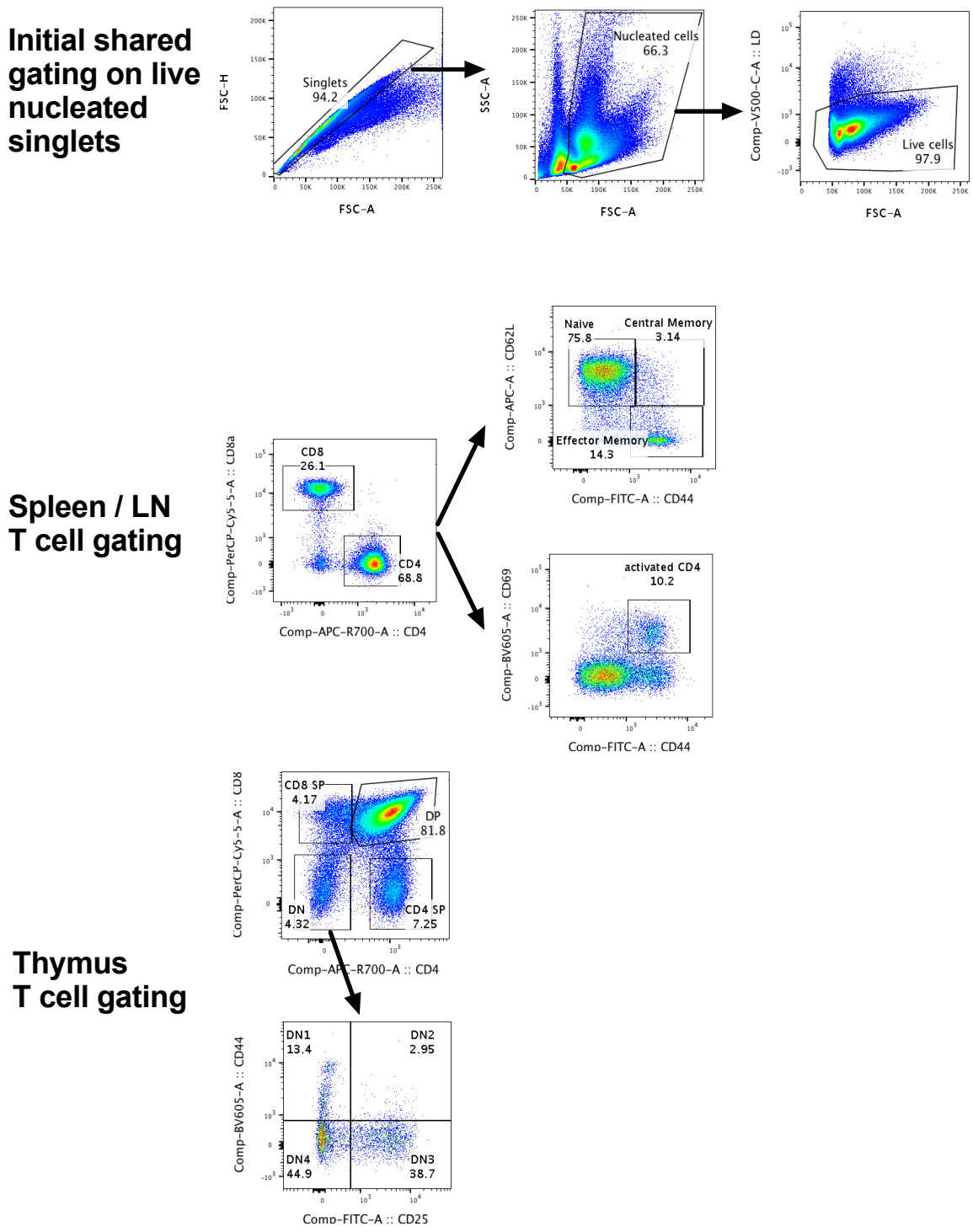


Figure 3-7: Flow cytometry gating strategies for immunophenotyping of transgenic mice. (Top) Gating on live singlet cells, which was used as the initial gating for all analyses. (Middle) T-cell gating strategy used in the spleen and lymph node to identify differentiation stages and activation status of CD4 and CD8 T cells. (Bottom) Gating used in the thymus to identify CD4/CD8 double negative, double positive and single positive populations and preceding T cell developmental stages within the double negative population.

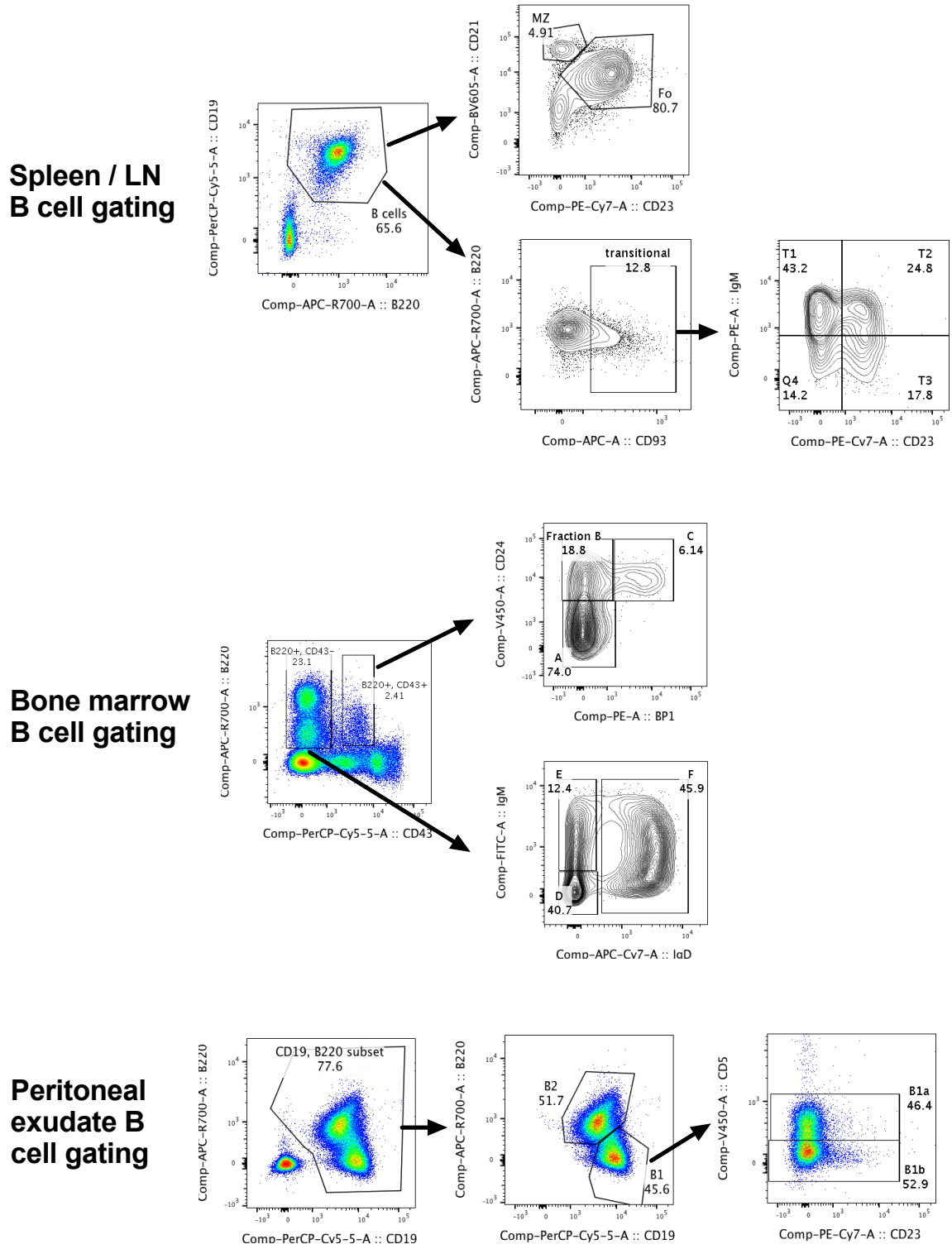


Figure 3-8: Flow cytometry gating strategies for phenotyping of B-cell populations and development. (Top) Gating to identify marginal zone ($CD21^{hi}CD23^{lo}$), follicular ($CD23^{hi}CD21^{int}$) and transitional ($CD93^{hi}$) B cells in the spleen and lymph nodes. (Middle) Gating on B cell development stages (Hardy Fractions A – F) in the bone marrow. (Bottom) Gating to identify B1a, B1b and B2 cell populations in the peritoneal exudate (bottom).

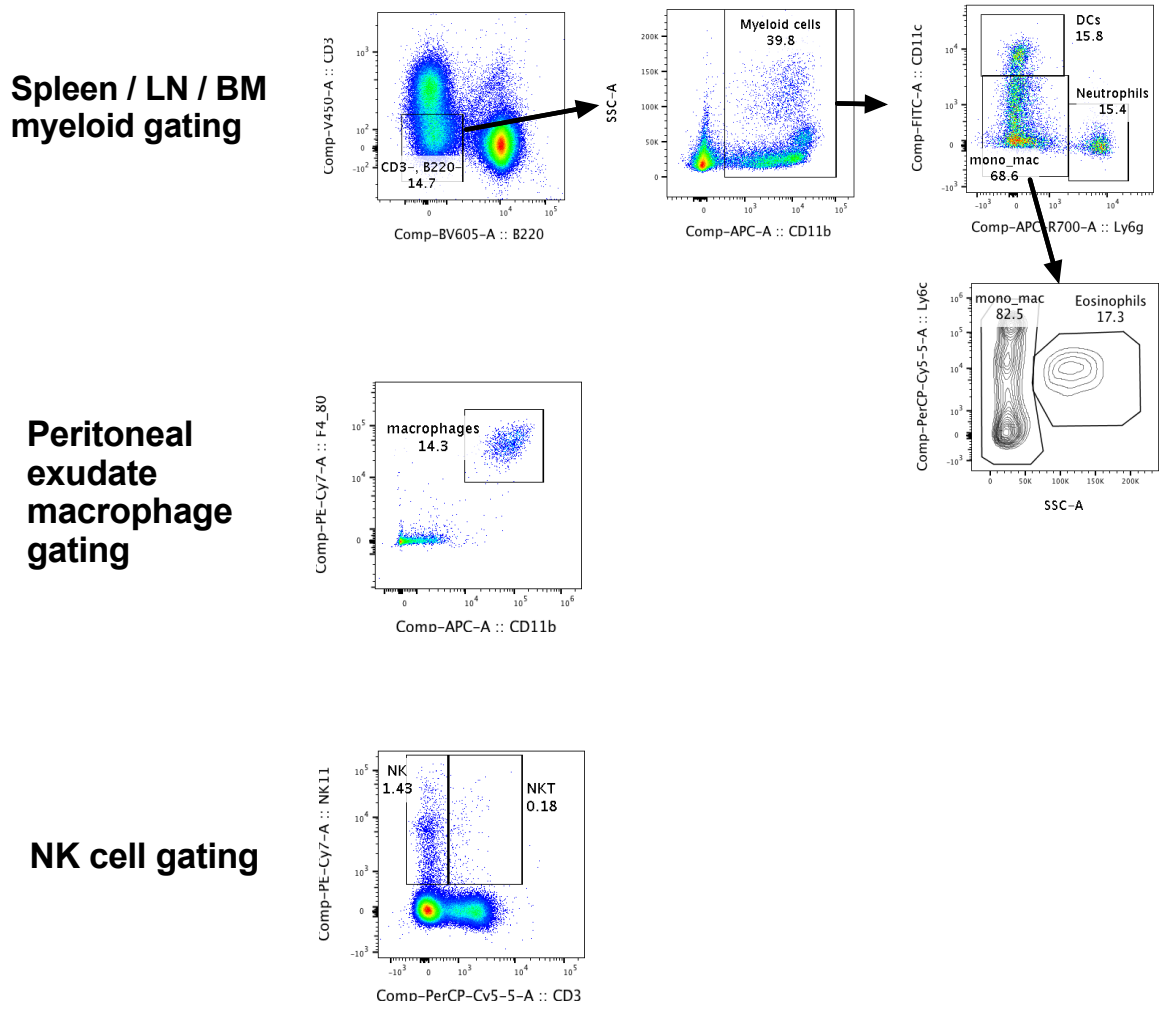


Figure 3-9: Flow cytometry gating strategies for myeloid cell populations and NK cells. (Top) Gating on $CD3^{-}B220^{-}CD11b^{+}$ myeloid cell populations used in the spleen, lymph nodes and bone marrow. (Middle) Gating on $F4/80^{+}$ macrophages in the peritoneal exudate. (Bottom) NK cell gating used in all organs.

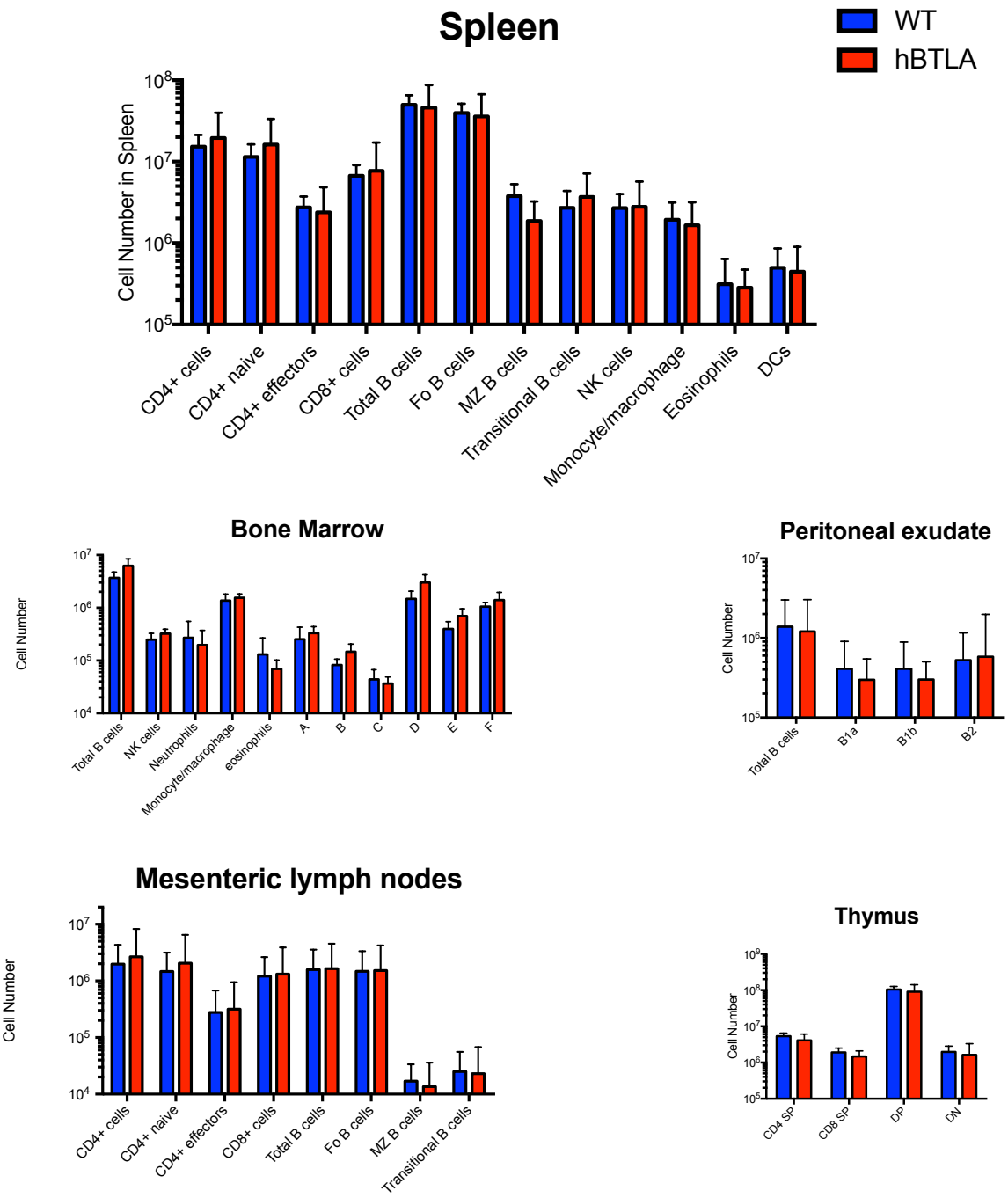


Figure 3-10: Humanised BTLA mice immune system development. Quantification of major immune cell subsets in primary and secondary lymphoid tissue in humanised BTLA compared to wild type mice. Representative data from 2 independent experiments with 4-5 mice per group. Plotted values are mean + SD. There were no significant differences in any immune cell population between groups.

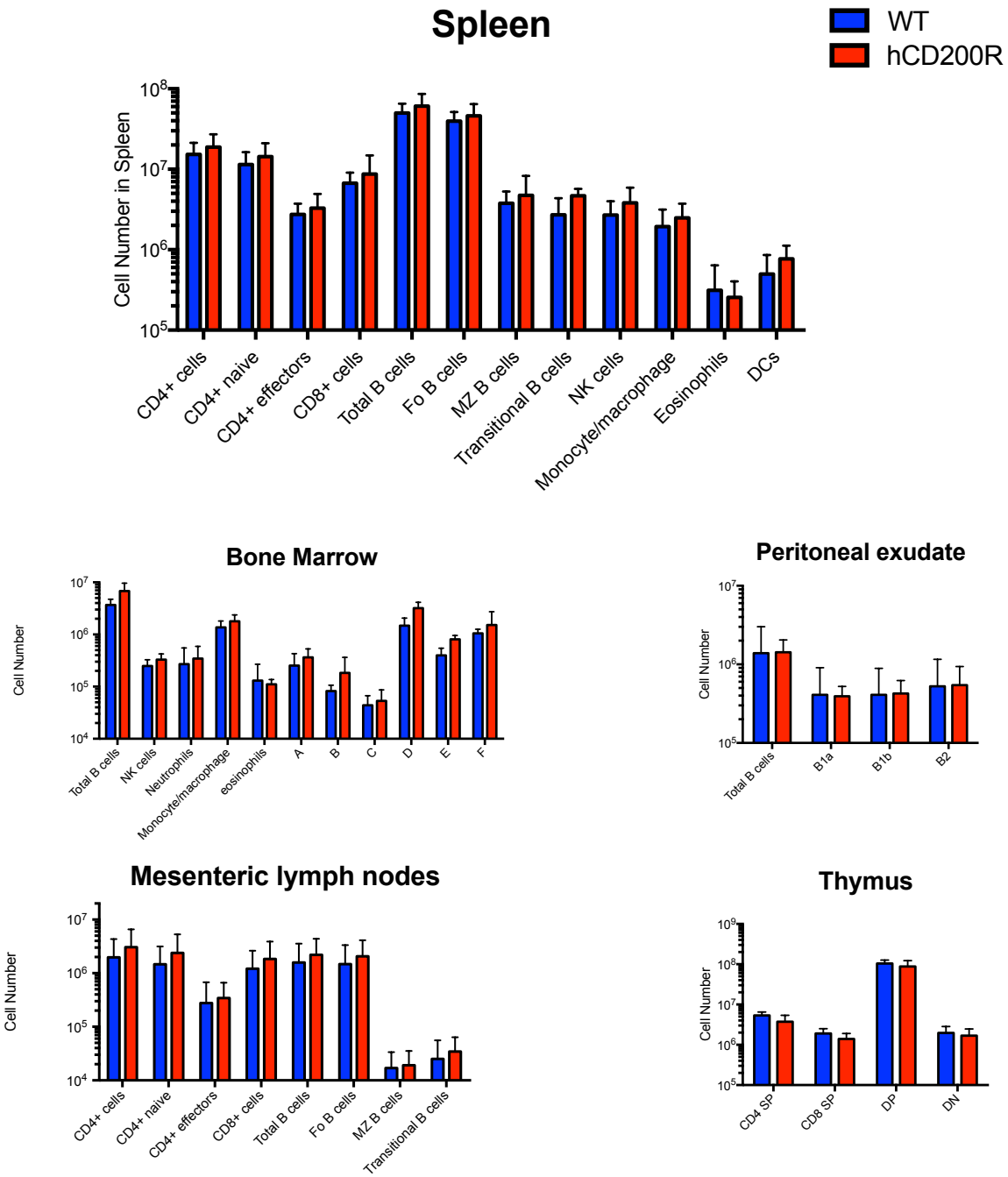


Figure 3-11: Humanised CD200R mice immune system development. Quantification of major immune cell subsets in primary and secondary lymphoid tissue in humanised CD200R compared to wild type mice. Representative data from 2 independent experiments with 4-5 mice per group. Plotted values are mean + SD. There were no significant differences in any immune cell population between groups.

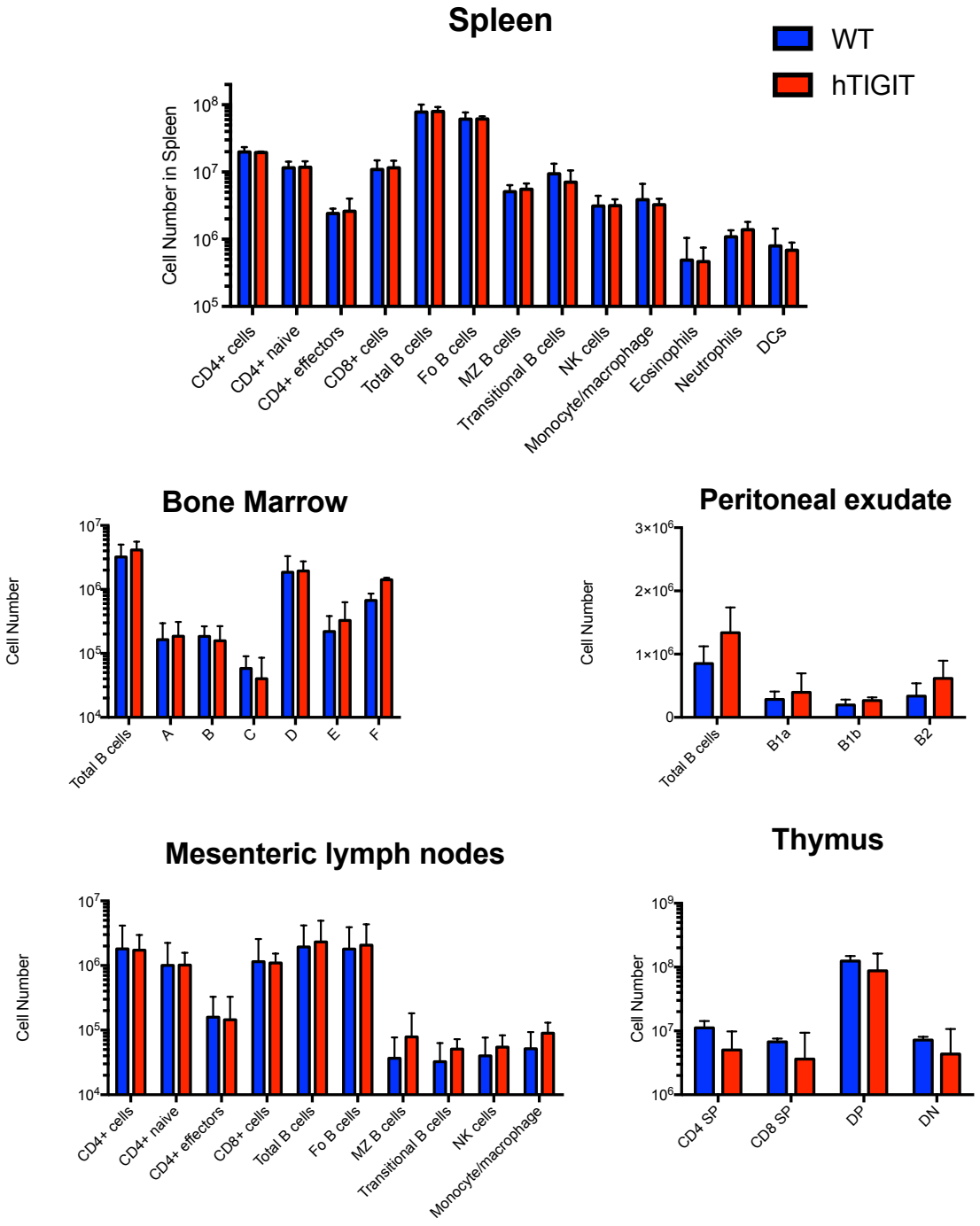


Figure 3-12: Humanised TIGIT mice immune system development. Quantification of major immune cell subsets in primary and secondary lymphoid tissue in humanised TIGIT compared to wild type mice. Representative data from 2 independent experiments with 4-5 mice per group. Plotted values are mean + SD. There were no significant differences in any immune cell population between groups.

3.5. Response to immune challenge

Knockout strains for each of these three checkpoint receptors exhibit only minor abnormalities in resting immune development, but these are exaggerated when the immune system is challenged [106, 117, 235]. In order to assess the response to immune challenge in our humanised strains we employed two widely used immunization models. Sheep red blood cells (SRBC) immunization induces a robust germinal centre response, which can be measured at its peak 6 – 8 days after injection. Immunisation with 4-hydroxy-3-nitrophenylacetyl (NP)- chicken gamma globulin (NP-CGG) in alum adjuvant similarly induces a strong germinal centre response but also allows for easy measurement of T-independent and T-dependent antibody production by ELISA of serum samples taken at time points after immunization. Adding a boosting NP-CGG injection 35 days after initial immunization also provides a readout of memory B-cell formation and function. Assessing these endpoints of the adaptive immune system also provides an indirect assessment of innate immune function, as priming and antigen presentation by the innate immune system is crucial to the development of a normal adaptive response.

Mice were sacrificed six days following immunization with SRBCs, and single cell suspensions of splenocytes were assessed by flow cytometry using antibody panels as described in Section 2.8 to quantify development of follicular helper T (TfH) cells and germinal centre (GC) B-cells. TfH cells were defined as $CD4^{+}ICOS^{hi}CXCR5^{hi}$ whilst GC B-cells were defined as $B220^{+}CD95^{+}GL7^{+}$ (Figure 3-13)**.** Responses in each transgenic strain were compared to wildtype mice in 2 separate experiments with 4-5 mice per

group, and no significant differences were seen in the frequency or absolute number of TfH cells or GC B-cells (Figure 3-14).

Following intraperitoneal injection with NP-CGG in Alum adjuvant, tail vein blood was taken from mice at days 14, 21 and 28. On day 35 a boosting NPCGG injection (without adjuvant) was given, and on day 42 mice were sacrificed and a terminal bleed taken. NP-specific serum IgM and IgG levels were assessed by indirect ELISA. Again, no significant difference in response was seen between transgenic and wild type mice (Figure 3-15). However, high levels of variation from mouse to mouse in this assay meant that it was insufficiently powered to detect small differences in response. Such variation is likely an inevitable consequence of both the natural variation between animals and the compounded experimental error of a protocol that involves 2 separate *in vivo* injections and an ELISA for antibody quantification. Larger numbers of mice could be used to provide more confidence of an entirely normal response. However, for the purposes of providing a tool for assessment of therapeutic antibodies it is sufficient to have confidence that the transgenic strains have no major disruptions in immune function; the possibility of subtle differences compared to wild type mice is not of concern.

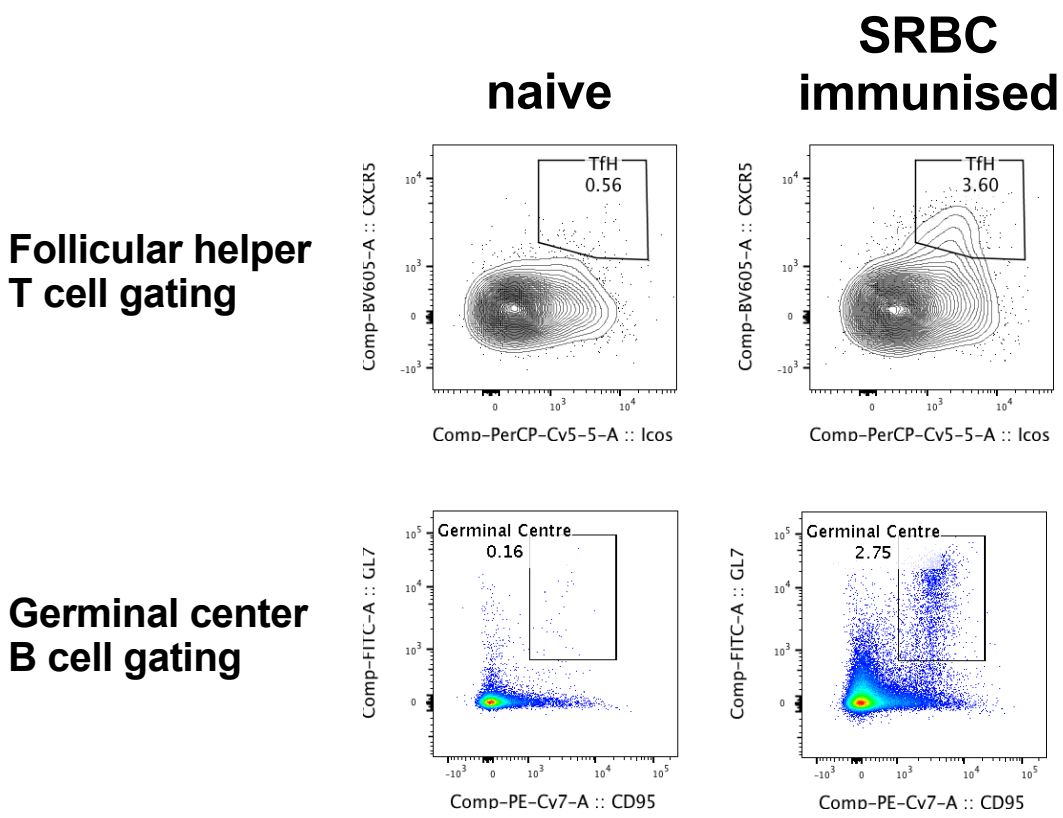


Figure 3-13: SRBC response FACS gating. Flow cytometry gating for splenic follicular helper T-cells ($ICOS^{hi}CXCR5^{hi}$) and germinal centre B-cells ($CD95^{+}GL7^{+}$) in response to SRBC immunisation.

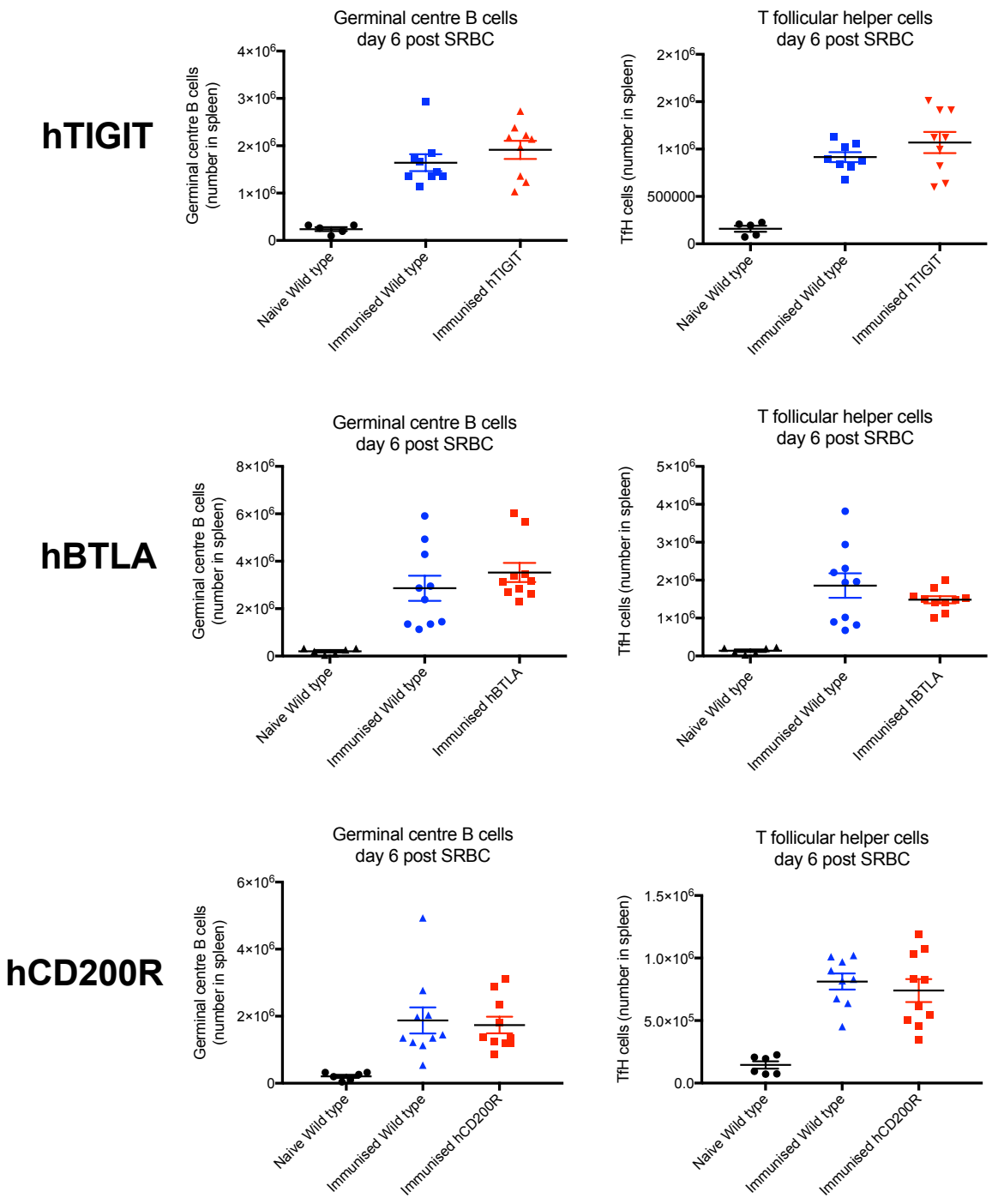


Figure 3-14: SRBC response in humanised strains. Quantification of absolute number of splenic GC B-cells and TfH cells in response to SRBC immunisations in humanised mouse strains compared to wild type C57BL/6 mice. Collated data from 2 independent experiments per receptor with 4-5 mice per group. Error bars show mean ± SD. There were no significant differences in response for any of the transgenic strains.

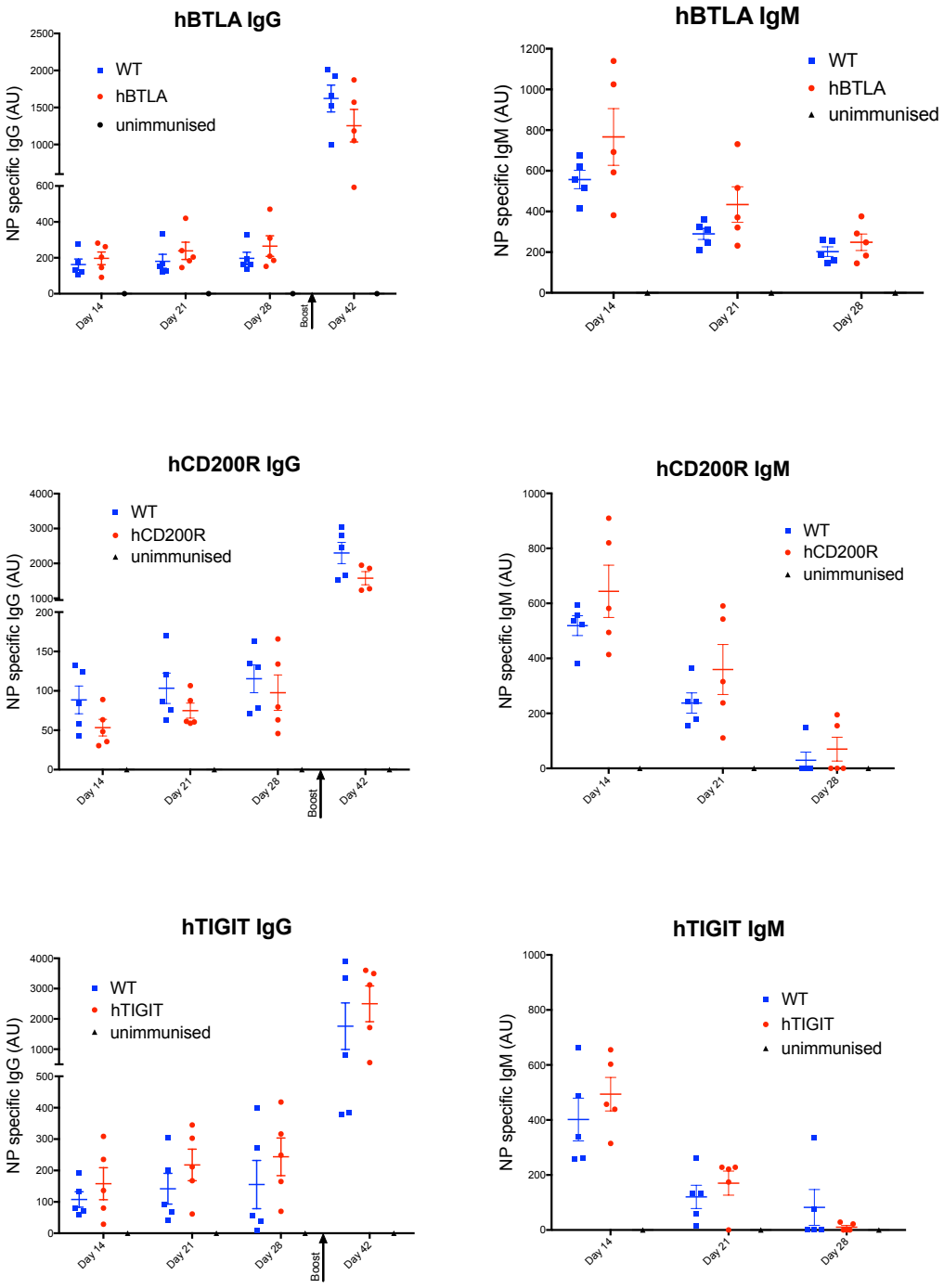


Figure 3-15: NP-CGG response in humanised strains. Serum NP specific IgG (left) and IgM (right) measured in arbitrary units by ELISA, in response to NP-CGG immunisations in the transgenic compared to wild type mice. NP-CGG in Alum was injected IP on day 0 and a boost of NP-CGG without adjuvant was injected IP on day 35. Error bars show mean ± SD. There were no significant differences in response for any of the transgenic strains.

3.6. Discussion

Analysis of the interactions of human checkpoint receptors with murine ligands confirmed that BTLA, TIGIT and CD200R all maintain the cross-species binding necessary to provide a functional pathway in our transgenic mouse strains. *Ex vivo* assessment of receptor expression on immune cells confirmed that the replacement of murine extracellular domain with human had been successfully achieved in the humanised mice and that this substitution had not affected the ability of the receptor to be expressed and correctly folded at the cell surface (as assessed by the binding of likely conformationally sensitive antibodies). Similarly, the observed changes in expression in response to activation stimuli confirm that the introduction of human genomic sequence has not significantly affected transcriptional control. Detailed immunophenotyping of the transgenic mice identified no significant abnormalities in immune system development or response to simple immunisation, providing further confidence that the inserted chimeric receptors are functional and exerting appropriate effects with respect to immune regulation. These data therefore suggest that the transgenic strains will provide a valid tool for the assessment of therapeutic antibodies modulating the human checkpoint receptors. In subsequent experiments exploring such antibodies, humanised mice will always be used for both treated and control groups, so that any subtle differences that might exist that were not detected between humanised and wild type mice will not confound interpretation of the antibody effects.

Mouse BTLA, CD200R and TIGIT are all located on chromosome 16, and closely linked, meaning that crossing these strains to produce double humanised mice was

not feasible. However, murine PD1 is located on chromosome 1, and so each of the new humanised strains was crossed onto the previously characterised humanised PD1 strain until homozygosity for both humanised receptors was obtained. This provides the opportunity to test combinations of human checkpoint modulating antibodies targeting PD1 and another checkpoint receptor.

Chapter 4 Characterisation of antibody panels

4.1. Introduction

To explore the potential utility of agonists targeting human CD200R, BTLA and TIGIT, we aimed to produce diverse panels of antibodies to screen. By characterizing in detail the binding properties of a series of antibodies in each case, we hoped first to identify candidate antibodies that would be predicted to have agonistic function, and secondly by correlating this binding data with observed functional effects we hoped to be able to better understand the fundamental properties of an antibody that confer upon it agonist activity.

The work to generate hybridomas producing antibodies against human CD200R, BTLA and TIGIT was outsourced to two contract research organizations (CROs); Biogenes AG and Generon Ltd. Hybridomas were generated by immunizing mice with serial injections of the extracellular domain of the target receptor, and then fusing immunised splenocytes with the myeloma cell line Sp2/0-Ag14. After selection in HAT medium and limited dilution cloning, positive clones were identified by ELISA of supernatants. For each target, a panel of several hybridomas was produced to enable characterization of a diverse range of antibodies with different binding characteristics and functional effects. Purified antibodies were obtained by Protein G affinity chromatography of hybridoma culture supernatant, followed by size exclusion chromatography to ensure removal of aggregated protein and running of reducing and non-reducing SDS-PAGE gels to assess protein purity. Antibodies of

interest were isotyped, either by the CRO that generated them, or using an antibody isotyping kit; the isotype information is included in Table 4-1.

4.2. Assessment of antibody affinities

Surface plasmon resonance (implemented on the Biacore) was used to assess the cognate antigen binding affinity and kinetics of each antibody. Antibodies were indirectly captured onto the sensor chip using a mouse antibody capture kit, in which a polyclonal anti-mouse-Ig is first immobilized by amine coupling. This allows for regeneration of the chip between the directly immobilized polyclonal and the indirectly captured monoclonal of interest, providing a high-throughput method for screening multiple antibodies.

For each target receptor, soluble, monomeric protein was produced as described in Section 3.2 and injected over immobilized antibody at various concentrations in a single cycle kinetic analysis. BiaEvaluation software was used to curve fit to the association and dissociation phases to measure on- and off-rate (k_{on} and k_{off}) from which the dissociation constant (K_d) was calculated. Example single cycle kinetic curves for a very high affinity and a lower affinity clone are displayed in Figure 4-1 and a summary of the kinetics for all antibodies targeting each of the receptors is provided in Table 4-1. In general the panels of antibodies assessed were comprised predominantly of high affinity clones, with most antibodies binding to their target receptor with dissociation constants in the low nanomolar range.

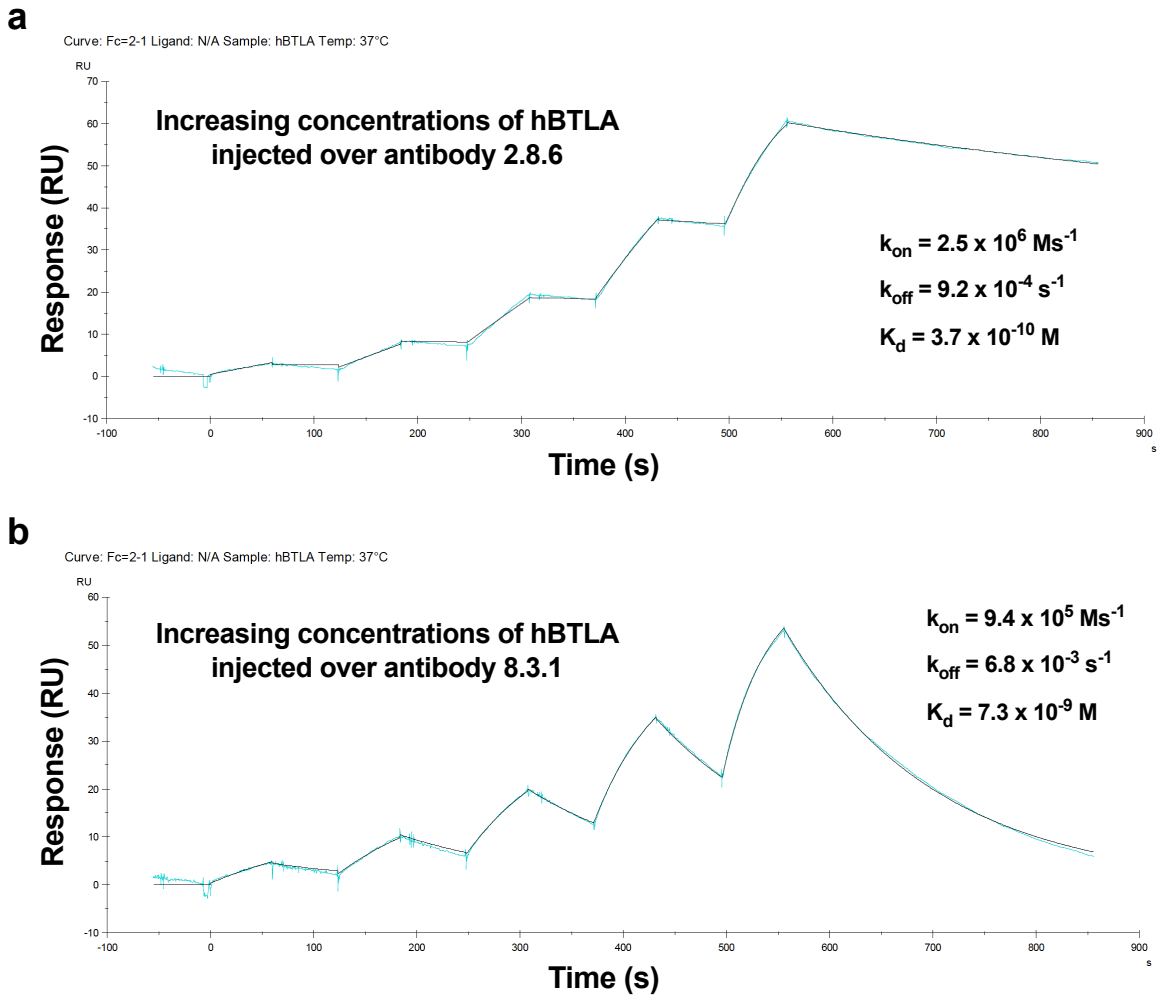


Figure 4-1: Example SPR data showing single cycle kinetics analysis of antibody binding to target receptor. Binding data (blue line) and curve fits (overlayed black line) are shown for increasing concentrations of hBTLA being injected over immobilized high affinity antibody 2.8.6 (a) or lower affinity antibody 8.3.1 (b). Curve fitting was performed using BiaEvaluation software to calculate the inset on and off rates.

receptor	Clone	Isotype	ligand blocking	Kon (1/Ms)	Koff (1/s)	Kd (nM)
hBTLA	2.8.6	mIgG1	no	2.5E+06	9.2E-04	0.4
	13.2.2	mIgG1	yes	8.1E+04	2.8E-03	34.1
	8.3.1	mIgG1	no	9.4E+05	6.8E-03	7.3
	9.9.3	mIgG1	yes	4.8E+04	9.4E-04	19.7
	11.5.1	mIgG1	yes	1.2E+06	6.4E-04	0.5
	4.6	-	yes	2.3E+05	3.8E-03	16.5
	6.2	-	no	6.8E+05	4.7E-04	0.7
	106.6	-	yes	2.1E+05	5.4E-04	2.6
	14.1	mIgG1	yes	7.2E+04	2.7E-03	37.3
	10.9	mIgG1	yes	2.2E+06	2.1E-03	0.9
	110.12	-	yes	1.7E+05	5.4E-04	3.2
hTIGIT	ID2	mIgG2a	yes	2.4E+06	5.9E-04	0.3
	IE5	mIgG1	yes	7.2E+05	7.3E-02	101.1
	2.7	mIgG1	yes	1.3E+05	9.2E-03	71.2
	8.4	mIgG1	yes	5.1E+06	2.1E-02	4.2
	CE10	mIgG1	no	1.6E+06	1.5E-03	0.9
	GE4	mIgG2a	yes	5.1E+05	2.9E-02	56.8
	FB3	-	no	1.2E+06	3.1E-03	2.5
	FF4	-	no	1.3E+06	3.1E-03	2.5
hCD200R	OX108	mIgG1	yes	3.0E+05	6.1E-03	20.4
	2.2.7	mIgG1	no	1.2E+05	3.3E-03	27.6
	21.3.1	mIgG1	no	1.4E+05	3.6E-05	0.3
	116.3	-	no	6.1E+04	1.5E-04	2.5
	1.1	-	no	1.4E+05	1.9E-04	1.3
	36.4	-	no	1.1E+05	3.1E-03	28.3
	180.1	-	no	9.0E+04	1.4E-02	160.8
	GC2	-	no	2.3E+05	2.4E-04	1.1
	FG4	-	no	3.3E+05	2.5E-02	76.1
	3.10	-	no	6.7E+05	2.7E-04	0.4
	10.2	-	no	3.2E+05	3.0E-04	0.9
	12.3	-	yes	1.8E+05	9.9E-04	5.4
	20.2	-	yes	2.4E+06	4.0E-03	1.7
	26.3	-	yes	1.6E+06	1.2E-03	0.7
	32.5	-	no	4.4E+05	4.8E-04	1.1
	40.7	-	no	5.5E+05	4.9E-04	0.9
	4.1	-	no	3.4E+05	1.1E-03	3.4
	42.15	-	no	4.0E+05	2.0E-03	5.0
	6.2	-	yes	2.8E+06	3.9E-03	1.4
	7.12	-	no	3.2E+05	9.3E-04	2.9
	24.1	-	no	2.9E+05	1.3E-03	4.3

Table 4-1: Summary of binding kinetics and ligand blockade for each antibody, as determined by surface plasmon resonance. The antibody isotype is provided for those antibodies where it was assessed. Red highlighting in the 'ligand blocking' column indicates clones that block the receptor interaction with its natural ligand. Dissociation constants are conditionally formatted with highest affinity antibody in green through to lowest affinity antibody in red.

4.3. Assessment of ligand blockade

A common mechanism by which therapeutic antibodies can exert biological effects is by sterically interfering with the interaction between their cognate antigen and its natural binding partners. For example, checkpoint-blocking antibodies such as Nivolumab and Pembrolizumab bind to PD1 and block its interaction with its natural ligands PDL1 and PDL2, hence blocking endogenous inhibitory signalling through this pathway. In order to correctly interpret the biological effects of our antibody panels we needed to know if they were capable of blocking the ligand interactions of their target receptor.

Surface plasmon resonance provides the ability to confidently assess whether antibody and ligand are able to simultaneously bind to receptor, and so confirms whether or not they bind to non-competing epitopes. For the majority of antibodies, this assessment was carried out by directly immobilising the target receptor onto the sensor chip by amine coupling. Then, in a single cycle, the cognate ligand was first injected over and allowed to bind and then dissociate to confirm baseline binding, followed by a saturating injection of antibody and finally by a repeat injection of ligand at the same concentration as the initial injection whilst all immobilized receptor remained saturated by antibody. The amount of ligand binding following antibody injection was compared to the amount of ligand binding prior to it. As expected, all antibodies tested fell into two discrete categories; those that did not affect ligand binding at all and those that completely abrogated ligand binding.

Representative SPR curves demonstrating a ligand blocking and a non-blocking antibody are displayed in Figure 4-2a.

For some antibodies, which were not purified but screened from supernatant, the concentration of antibody was insufficient to saturate the immobilized receptor, so ligand blockade was assessed in a different fashion. In these experiments, antibody was indirectly immobilised onto the sensor chip and then target receptor was injected over, followed by injection of the ligand. For non-blocking antibodies the ligand was able to bind to receptor captured by immobilized antibody, whereas for blocking antibodies no ligand binding was seen. These experiments were carried out at 25°C rather than 37°C to reduce the dissociation rate of the captured receptor from immobilized antibody, allowing more time for the subsequent ligand injection before receptor dissociation. Representative curves demonstrating a ligand-blocking and non-blocking antibody are shown in Figure 4-2b. For all antibodies tested, Table 4-1 describes whether or not they block ligand binding to receptor.

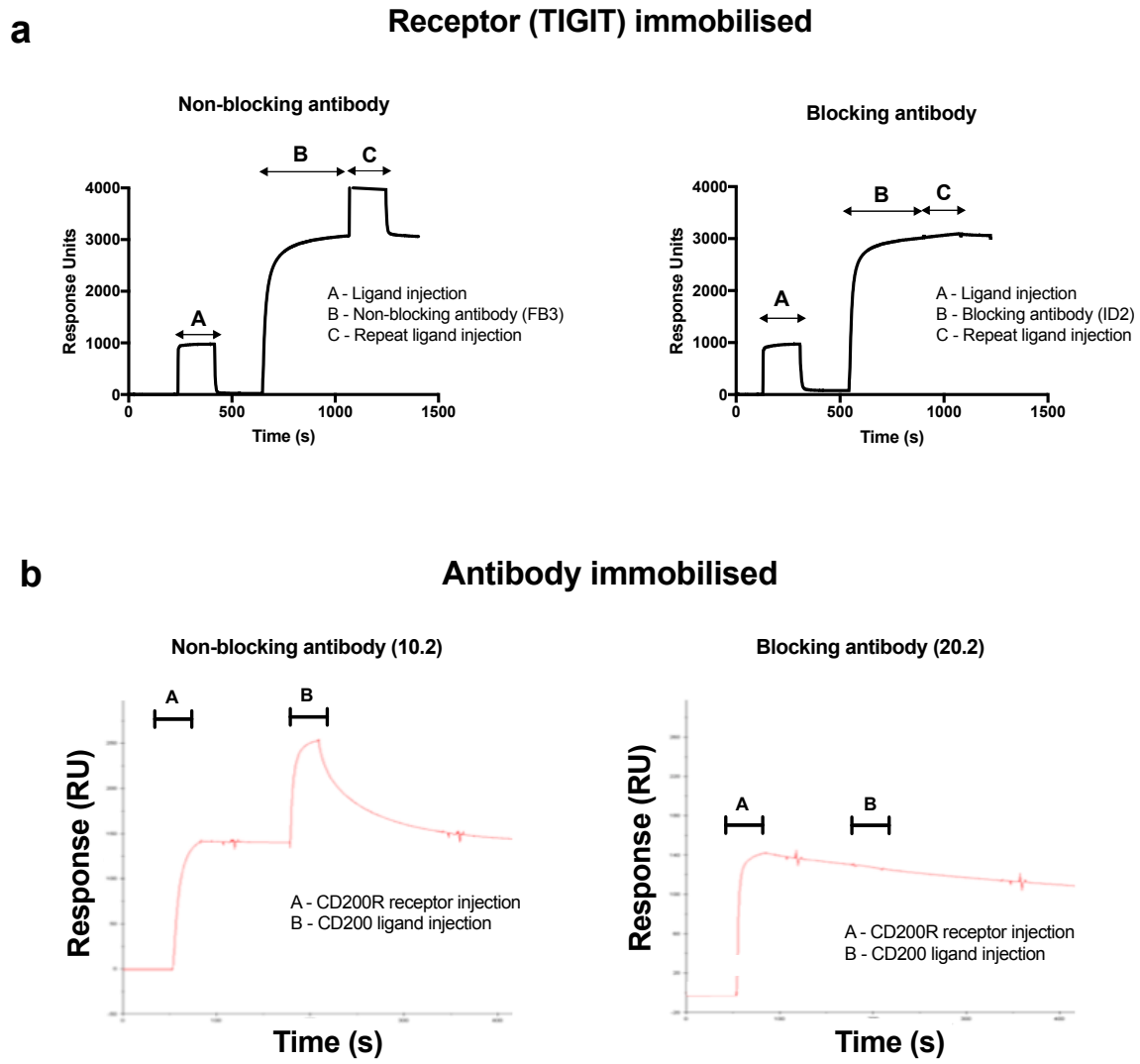


Figure 4-2: Two different methods for SPR assessment of ligand blockade by checkpoint antibodies. (a) Binding of ligand PVR to immobilized receptor TIGIT was measured before and after a saturating injection of the non-blocking antibody FB3 (left) or ligand-blocking antibody ID2 (right). (b) Receptor CD200R was captured by an immobilized non-blocking antibody (10.2, left) or a ligand-blocking antibody (20.2, right) and then binding of ligand CD200 to the captured receptor was assessed.

4.4. Epitope mapping

The precise part of a protein to which an antibody binds is known as the epitope, and in the case of antibodies targeting immunoreceptors it is probable that the particular epitope to which the antibody binds impacts its functional effects on the receptor. Most obviously, antibodies that bind to epitopes overlapping the ligand-binding site of the receptor are likely to interfere with ligand binding. It has also been proposed for both BTLA [167] and TIGIT [155] that in order for antibodies to act as agonists to a receptor that they should replicate the binding profile of the natural ligand (i.e. bind to the same epitope). However, given that there is little evidence conformational change of the receptor plays a role in triggering, it is not clear why binding to the endogenous ligand binding site would be beneficial for an antibody agonist, and indeed given that this will block endogenous signalling it would seem rather to be a detrimental characteristic for a therapeutic inhibitory receptor agonist.

Less intuitively, it is possible that the position of the epitope with respect to the cell membrane may influence the antibody's capacity for agonism. As introduced in Section 1.5, one mechanism by which antibodies could induce triggering of an immunoreceptor is by holding the receptor in a close contact zone between the cell on which it is expressed and an FcR expressing cell on which the antibody is immobilized; this would lead to steric exclusion of receptor-type phosphatases from the vicinity of the receptor and consequent phosphorylation of its cytoplasmic motifs, an extension of the kinetic segregation model. In the case of CD28, Evans *et al* demonstrated that a mitogenic Fab (which potently triggers the receptor) binds to a membrane proximal epitope and forms a compact complex close to the cell surface, in

comparison to non-mitogenic antibodies which bind more distally ([79] and Figure 4-3a). As a general principal therefore, antibodies that bind to membrane proximal epitopes of immunoreceptors may induce the most potent signalling by creating a compact complex that leads to efficient exclusion of phosphatases when the antibody is immobilized by binding to an FcR or to plastic (Figure 4-3b). This is most likely to be relevant to receptors with large extracellular domains, where the disparity between a membrane proximal epitope and a membrane distal one is greater. However, for receptors with small extracellular domains (such as BTLA and TIGIT, which have only a single IgSF domain) the more significant contributor to the dimensions of the receptor-antibody complex may be the orientation with which the antibody binds to the receptor. An epitope on the 'top' of the receptor leading to Fab pointing orthogonal to the membrane will create a much larger complex than an epitope on the 'side' of the receptor wherein the Fab lies parallel to the membrane.

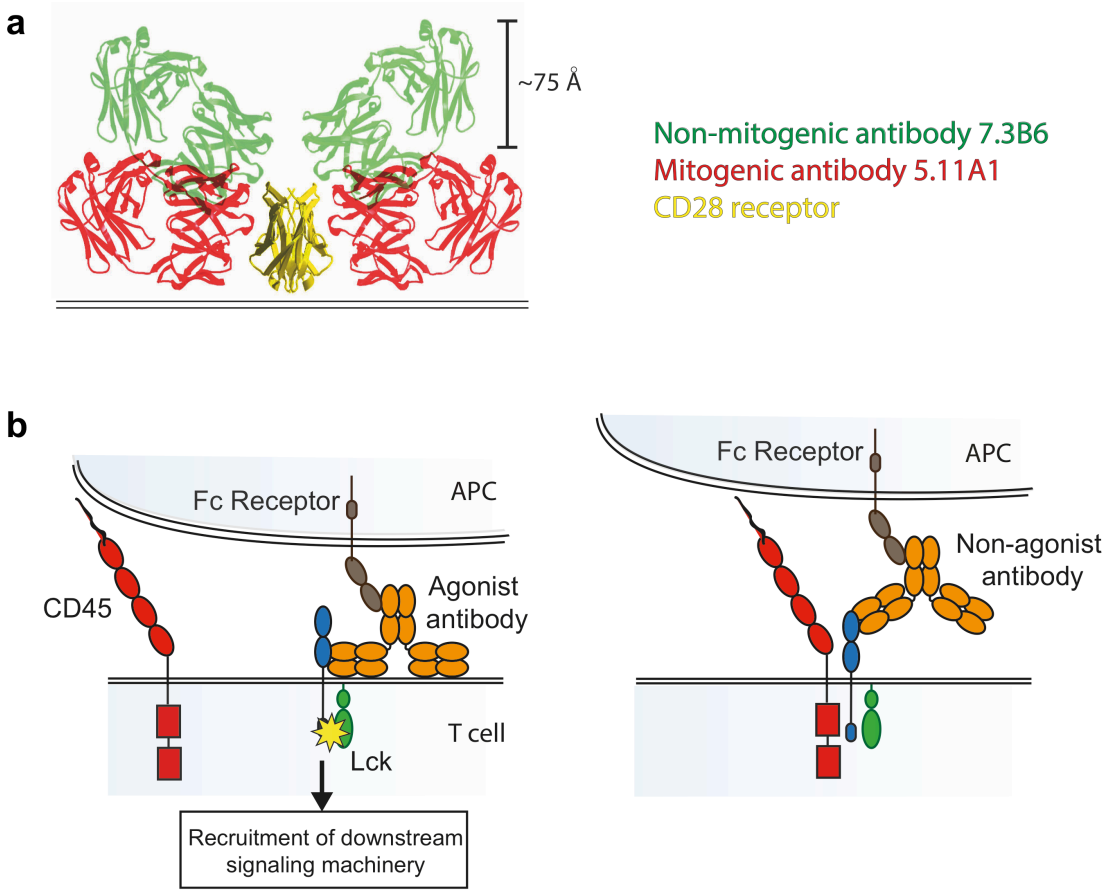
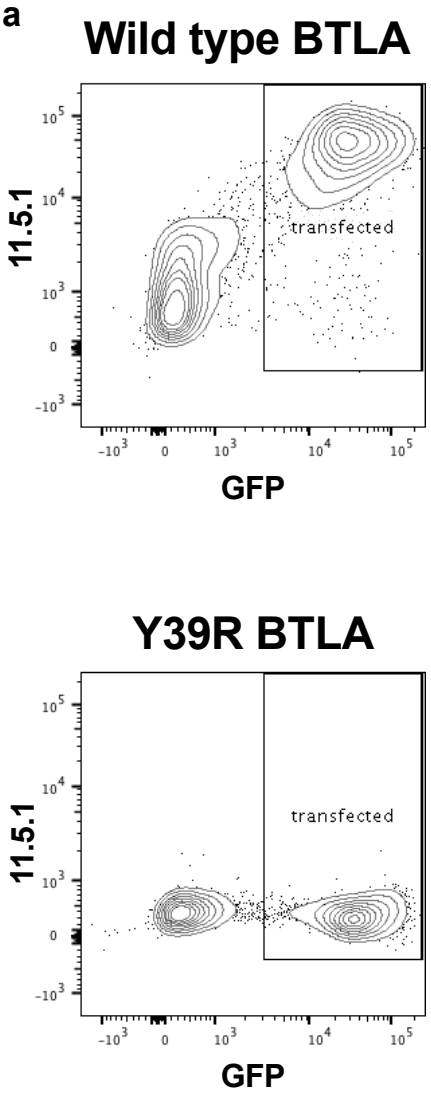


Figure 4-3: Hypothesised relevance of epitope position to agonist activity. (a) Adapted from [79]. Overlaid crystal structures of a mitogenic (superagonistic) and non-mitogenic anti-rat-CD28 antibody demonstrating that mitogenic CD28 antibodies bind to an epitope closer to the membrane and in an orientation that leads to the Fab lying closer to the membrane than for a non-mitogenic antibody. (b) Diagrammatic representation of how a membrane proximal epitope might allow for creation of a narrower gap between interacting cells, with more effective exclusion of phosphatases and hence more receptor triggering.

In order to identify the binding epitopes for each of our antibodies we employed an epitope-mapping technique in which a panel of single residue mutants of the cognate receptor was expressed on HEK293T cells and each mutant was assessed for its impact on antibody staining. For BTLA, TIGIT and CD200R, receptor variants with the surface-exposed residue mutations described in Table 2-1 were cloned into the pGFP^2-N3 vector, which allows transient expression of the mutant receptor labelled with an intracellular green-fluorescent-protein tag so that successfully transfected cells can be identified. HEK293Ts transfected with each of the mutants were stained with the antibody of interest and then with a fluorescently labelled secondary antibody, and assessed by flow cytometry. Within the GFP$^+$ transfected cell population, the staining geometric mean for each mutant was normalized to that for HEK293Ts transfected with the wild type receptor (Figure 4-4a). Having screened multiple antibodies against each target, mutations that abrogated binding for all antibodies were assumed to cause significant defects in receptor folding or expression rather than highlighting a specific epitope, and so these mutants were removed from analysis (Figure 4-4a). However, mutations that reduced binding of only particular antibodies were assumed to reveal the true epitope. For each antibody, the mutations that significantly impacted binding (reducing it to less than 10% of binding to wild type receptor) were plotted onto the structure of the receptor to depict the epitope; confidence is added to the assessment if several mutations that eliminate binding lie closely clustered together. For hBTLA and hTIGIT x-ray crystallographic structures of the extracellular domain are available (PDB entries 2AW2 and 3Q0H respectively). For hCD200R an automated homology model based on the murine crystal structure was obtained from the Swiss-Model repository (entry

number Q8TD46). For each receptor, at least one antibody was identified that had an epitope predicted to sit close to the membrane (if the receptor is orientated with the N-terminus most distal from, and C-terminus most proximal to the membrane, as would be expected for these type 1 membrane proteins) (Figure 4-5). Furthermore, for all antibodies assessed the epitope maps correlated with the SPR analysis of ligand blockade; antibodies with an epitope overlapping with areas of the receptor known to be involved in ligand binding also blocked ligand interactions according to the SPR measurements.

a



b

	Clone				
mutation	2.8.6	11.5.1	8.3.1	9.3.3	13.2.2
WT	100.0%	100.0%	100.0%	100.0%	100.0%
D35R	83.7%	71.2%	68.3%	28.4%	86.8%
Y39R	60.0%	0.8%	59.8%	56.3%	81.8%
K41E	91.4%	1.8%	96.6%	108.3%	115.3%
R42E	110.9%	72.3%	98.4%	141.9%	69.3%
Q43R	87.9%	55.2%	51.4%	47.7%	33.1%
E45R	96.3%	108.0%	92.5%	87.7%	87.2%
S47R	99.7%	107.5%	96.5%	141.0%	162.3%
L48R	102.5%	145.4%	125.4%	165.4%	106.1%
D52R	70.2%	128.6%	112.5%	110.9%	129.4%
P53R	55.6%	116.6%	1.7%	102.4%	126.7%
E55R	52.0%	60.5%	13.5%	42.1%	84.4%
E57R	76.3%	108.0%	76.3%	114.8%	154.6%
A64R	93.5%	148.2%	128.3%	116.3%	136.9%
N65R	89.0%	87.9%	80.3%	96.0%	78.8%
H68E	125.8%	81.3%	166.8%	72.3%	134.2%
T77R	26.7%	14.2%	13.1%	15.5%	12.2%
T78R	95.3%	108.5%	87.9%	95.5%	98.4%
V80R	71.6%	39.9%	40.0%	36.2%	33.1%
K81E	90.3%	115.8%	112.5%	53.7%	98.0%
E83R	98.8%	95.5%	75.6%	98.1%	58.8%
D84R	26.6%	15.0%	11.6%	12.9%	11.7%
Q86R	97.9%	132.0%	44.8%	156.6%	114.4%
S88R	5.3%	8.1%	0.8%	5.6%	11.4%
E91R	18.5%	12.6%	11.0%	12.8%	13.9%
E92R	62.2%	73.3%	73.1%	48.0%	66.6%
K93E	46.9%	24.8%	27.9%	24.9%	57.4%
E103R	79.0%	213.5%	0.8%	147.2%	110.0%
L106R	80.4%	135.4%	112.6%	112.3%	90.6%
N108R	107.2%	171.1%	159.0%	145.1%	93.3%
S112R	1.9%	2.6%	1.9%	1.4%	0.9%
Q120R	76.3%	89.9%	73.2%	62.2%	43.8%
S121R	67.9%	42.5%	36.5%	1.5%	32.7%
L123R	97.4%	116.0%	106.7%	77.9%	0.6%
E125R	11.4%	7.3%	6.4%	1.4%	0.6%
Y132R	68.2%	68.1%	60.5%	57.2%	47.4%
K137E	80.1%	55.6%	43.1%	44.7%	44.3%

Figure 4-4: Example epitope mapping data for antibodies against BTLA. (a) Binding of antibody 11.5.1 to HEK293Ts transfected with wildtype BTLA or Y39R mutated BTLA, which completely abrogates binding. The receptor constructs contain an intracellular GFP tag to enable gating on successfully transfected cells only. (b) Relative binding of five different anti-BTLA antibodies to the panel of surface mutants. Mutations highlighted in grey reduce binding to all antibodies suggesting a drastic effect on protein folding or expression rather than a specific epitope. Mutations (such as Y39R and K41E) that reduce binding of only certain antibodies reveal that antibody's epitope. Values are percentage of binding compared to binding to wildtype BTLA transfected cells and are conditionally formatted with 0-20% binding in red, 20-40% binding in yellow and >40% binding in green.

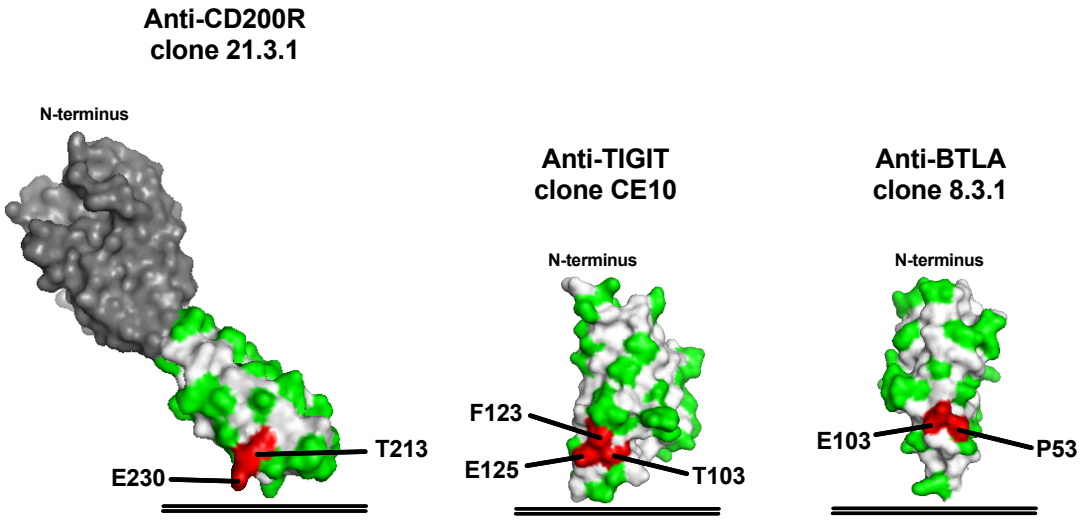


Figure 4-5: Epitope maps of membrane proximal binding antibodies to each of the three inhibitory receptors. Mutated surface residues that reduce binding of the antibody by >90% relative to wild type receptor are highlighted in red. Mutated residues that do not affect antibody binding are highlighted in green. The orientation of receptor with respect to cell membrane is predicted by positioning the C-terminus in proximity to the membrane and the N-terminus distal to the membrane. Molecular cloning to produce mutant constructs for the epitope mapping analysis, and mapping of some of the antibodies by flow cytometry, was carried out with the assistance of Heather Brouwer.

As shown in Figure 4-4 the epitope for the anti-BTLA antibody 2.8.6 could not be identified using this epitope mapping technique as none of the mutants significantly impacted binding. For this antibody the crystal structure of the Fab in complex with BTLA was solved by Ms Miki Iwamori and Prof Kimiko Fukuhara of Hokkaido University (unpublished data) revealing both the position of the epitope and the orientation with which the Fab binds to the receptor. When the residues on BTLA that are buried in the interface with 2.8.6 are plotted onto the structure of BTLA they highlight a membrane proximal epitope similar to the anti-BTLA clone 8.3.1 (Figure 4-6a).

A difficulty arises in trying to predict how an Fab binding to a receptor will sit in relation to the membrane, because these receptors contain flexible 'stalks' and the orientation in which they will be positioned on the cell surface is unpredictable. In the case of BTLA, the receptor binds to a ligand, HVEM, which is a TNFRSF member that binds in turn to a trimeric TNFSF ligand (LIGHT). The trimeric nature of the HVEM-LIGHT complex places a restriction on how these proteins must sit on the cell surface (as the three LIGHT 'stalks' must point in the opposite direction to the three HVEM 'stalks'). By superimposing the crystal structure of the HVEM-LIGHT complex (PDB entry 4RSU) onto the crystal structure of the BTLA-HVEM complex (PDB entry 2AW2) we could therefore more confidently predict how BTLA must sit on the cell surface, if it is to interact with HVEM. Furthermore, by superimposing our BTLA / 2.8.6 crystal structure onto this complex we could see how the Fab must lie in relation to the membrane if it binds to BTLA that is engaged by HVEM (Figure 4-6b). This model shows an antibody binding on the 'side' of the receptor with an orientation that

creates a complex close to the cell surface and which might be expected to lead to agonistic function, if the dimensions are important to signalling. The hinge of an IgG antibody, which begins at the end of the Fab, possesses a remarkably high degree of flexibility and the Fc region when bound by FcR lies parallel and close to the FcR-expressing cell membrane [236], and so the dimensions of the gap between the two cells will be largely determined by how far the C-terminal end of the Fab is from the surface of the target-receptor-expressing cell.

Figure 4-6c demonstrates that potentially three BTLA receptors can bind to the outside of the HVEM-LIGHT trimer, with an anti-BTLA Fab binding to each of these. Therefore, it is possible that lattices of HVEM-LIGHT-BTLA complexes could be stabilized by non-ligand-blocking BTLA antibodies, on cells that express the relevant proteins. The functional consequences of this (inhibitory or activatory) would depend on the relative degree to which signalling through BTLA, HVEM or LIGHT was enhanced by the artificial formation of these lattices.

TIGIT binds to the ligand PVR and has been reported to possibly form homodimers at the cell surface stabilized by trans-interactions with PVR homodimers [237], and as such non-blocking antibodies to TIGIT might also be able to stabilize higher order ligand-receptor lattices at cell-cell contacts. The CD200R monomer on the other hand binds to the monomeric ligand CD200 so an antibody to CD200R can only bring together two receptors at the cell surface rather than creating higher order complexes.

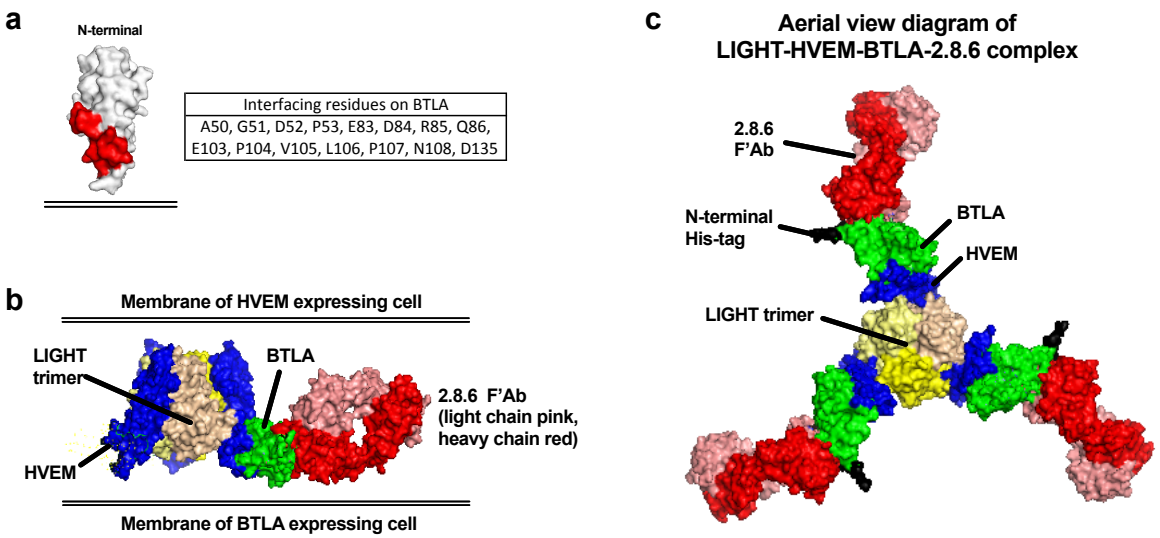


Figure 4-6: Binding of antibody 2.8.6 to BTLA (a) The residues buried in the interface of 2.8.6 and BTLA in the crystal structure are plotted onto the BTLA structure and reveal a potentially membrane proximal epitope. (b) Superimposing the crystal structures of the LIGHT-HVEM complex (PDB entry 4RSU), the BTLA-HVEM complex (PDB entry 2AW2) and the BTLA-2.8.6 complex using PyMol software provides further clarity as to the orientation of 2.8.6 with respect to the membrane. (c) Rotated view of the superimposed crystal structures (from 'above') demonstrating the higher-order complexes that might occur on the cell surface.

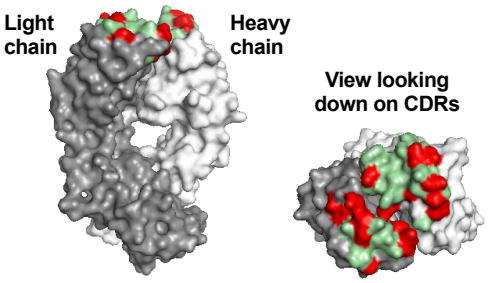
4.5. Generation of lower affinity mutants

High affinity antibodies have the advantage as therapeutics of requiring lower concentrations to reach high levels of receptor occupancy. This would be expected to translate into increased potency (i.e. a lower dose of antibody required to produce maximal effect). However, how antibody affinity impacts efficacy (i.e. the magnitude of the maximal effect) has not been widely explored. There is a possibility that low affinity interactions allow for serial engagement of multiple receptors, leading to greater maximal effect. Previous work with PD1 agonist antibodies (e.g. the PhD thesis of Billur Akkaya [162]) also suggested that perhaps high affinity antibodies lead to receptor internalization that limits the duration of agonist action, which might not be the case with lower-affinity interactions. It is interesting to note that the natural interactions of immunoreceptors with their endogenous ligands tend to be of relatively low affinity (K_ds in the low micromolar range) indicating that interactions of this strength can be very functionally relevant. Our antibodies (as outlined in Table 4-1) are all of much higher affinity than this (100 – 1000 fold higher affinity).

In order to create tool reagents to investigate the functional effect of antibody affinity I chose one of the membrane-proximal binding BTLA antibodies (clone 8.3.1) and produced an affinity series of mutated variants with a spectrum of reduced affinities. To achieve this, I first sequenced the variable domains of the antibody. The sequences were then modelled onto the crystal structure of an Fab with similar sequence (by Dr Yuan Lui, Davis laboratory) and the most surface exposed residues in the complementarity determining regions (CDRs) were identified. The three most surface exposed residues in each of the six CDRs were chosen for mutation (Figure 4-7a).

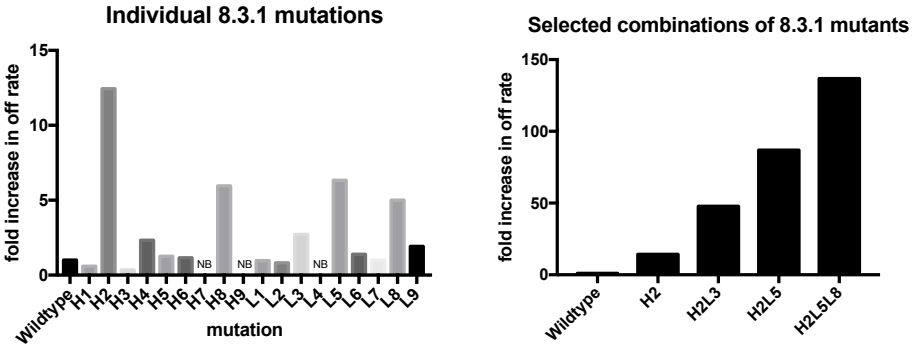
Overlap extension PCR was used to introduce drastic mutations (all residues to arginine, except for histidine, lysine and arginine which were mutated to aspartic acid). The mutants were then transiently expressed as Fab fragments in HEK293Ts. The affinity of each mutant for BTLA was assessed by SPR. Fab was indirectly captured from supernatant onto the sensor chip using a mouse antibody capture kit, and BTLA was injected over in a single concentration, allowing on- and off-rate calculation by curve fitting. Mutations that reduced affinity (i.e. increased off-rate) in this initial screen were combined to create variants with even greater changes in affinity (Figure 4-7b-d). For variants with greatly reduced affinity the K_d was also measured by equilibrium analysis as curve fitting to very fast off rates becomes quite inaccurate. Five antibodies in the series were selected for production as full-length antibody, with K_ds ranging from ~10nM to ~2μM. These will provide controlled tools to assess the functional impact of binding affinity, as they will all bind to the same epitope and with the same orientation and will vary only in their binding kinetics.

a

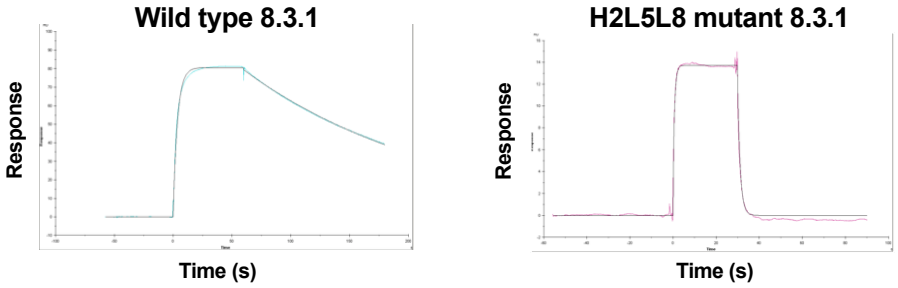


Heavy chain mutants		Light chain mutants	
H1	T29R	L1	S27R
H2	S30R	L2	S30R
H3	S33R	L3	N32R
H4	S54R	L4	R51D
H5	S56R	L5	T52R
H6	T57R	L6	S53R
H7	R101D	L7	I95R
H8	V105R	L8	P96R
H9	A108R	L9	L97R

b



c



d

	Ka (1/Ms)	Kd (1/s)	KD by kinetic analysis (nM)	KD by equilibrium analysis (nM)
Wildtype	6.12E+05	0.0059	9.7	
H2	8.16E+05	0.0850	104.2	
H2L3	4.99E+05	0.2839	568.8	1053
H2L5	4.09E+05	0.5157	1260.6	1319
H2L5L8	4.15E+05	0.81	1954.5	3430

Figure 4-7: Generation of an affinity series of mutant variants of the anti-BTLA clone 8.3.1. (a) Model demonstrating the CDRs of 8.3.1, made using PyMol software (pymol.org). Surface-exposed residues were predicted using Naccess (http://www.bioinf.manchester.ac.uk/naccess/). CDR residues that were not mutated are highlighted in green. Residues that were mutated to create affinity mutants are highlighted in red and itemized in the table on the right. (b) Increased off-rates of selected CDR mutants, as assessed by SPR, which have compounded effects when tested in combination. (c) Example SPR curves demonstrating the significantly increased off-rate of the compound mutant H2L5L8, which has one heavy chain and two light chain mutations. (d) Binding kinetics of the selected panel of affinity mutants, with affinities separately confirmed by equilibrium analysis.

4.6. Generation of Fc receptor knockout antibodies

It is common amongst immunoreceptors for the natural ligand-binding site to be located on the 'top' of the receptor, distal from the cell membrane. However, for small receptors such as BTLA, TIGIT and PD1 (which possess only a single IgSF domain) even the distal surface of the receptor is not far from the cell surface. If it is the case that antibody triggering of immunoreceptors results from the steric exclusion of phosphatases from close contact zones formed between receptor-expressing and FcR-expressing cells, then for such receptors it is possible that even ligand-blocking antibodies binding to this distal surface could create compact enough complexes to induce receptor triggering. If the intended purpose of these antibodies was to block signalling (as is the case with checkpoint blockers in immuno-oncology) then the capacity for artificially induced signalling by the antibody itself would be detrimental. The net effect would be a consequence of the signal that had been removed by blocking endogenous ligand, balanced out by the signal that had been created by antibody agonism, rather than complete blockade of the pathway. Given that the antibody agonism component in this scenario would be dependent upon Fc receptor engagement we proposed that ligand-blocking antibodies in which the Fc region had been mutated to reduce FcR binding might be more effective checkpoint blockers.

In order to explore this hypothesis we chose a high affinity ligand-blocking antibody against each of the three targets (clone 11.5.1 for BTLA, clone ID2 for TIGIT and clone OX108 for CD200R), sequenced the variable domains and then had the antibodies produced recombinantly (by the CRO, Absolute Antibody) on a mouse IgG1 backbone containing a point mutation from aspartate (D) to alanine (A) at position 265. The

D265A mutation has previously been shown to reduce binding to all murine FcRs [238-240] and in keeping with the above hypothesis it was demonstrated that a PD1 blocking antibody was more effective at treating murine cancer models when this mutation was introduced into the mIgG1 backbone [241], although in this paper the authors attributed the improved efficacy to reduced FcR dependent depletion of PD1 expressing tumour-specific T cells, rather than to removal of detrimental antibody agonism. Generation of these FcR-null blocking antibodies will provide the tools to further assess the importance of FcR interactions to checkpoint modulation in the transgenic mice.

4.7. Discussion

We have characterized diverse panels of antibodies against BTLA, TIGIT and CD200R to build a detailed picture of their binding position and kinetics and their impact on the receptors' natural ligand interactions. Such knowledge of the binding characteristics will be essential for the informed interpretation of the biological effects of these antibodies when they are subsequently assessed in functional assays using the transgenic mice. For each of the three receptors we have identified antibodies that are non-ligand blocking and that bind to membrane proximal epitopes, which we predict are most likely to confer agonist ability, and so could serve as promising development candidates for novel immunosuppressive therapeutics. We have also generated tool reagents to further explore the fundamental properties that determine antibody agonism, including a series of mutant variants of an anti-BTLA antibody to assess in a controlled fashion the

contribution of binding affinity, and a panel of FcR-null blocking antibodies to assess the relevance of FcR interactions to checkpoint modulation.

Chapter 5 Assessment of BTLA antibody effects on T cell responses

5.1. Introduction

Having demonstrated that the transgenic mice provide a valuable tool for assessing anti-human antibodies and having characterized panels of antibodies against each of the receptors, we undertook to explore the functional effects on the immune response of BTLA receptor modulating antibodies. These antibodies were assessed in a collection of *in vitro* and *in vivo* assays of T-cell function using immune cells from the transgenic mice.

5.2. Mixed lymphocyte reaction

The mixed lymphocyte reaction (MLR) is a commonly used *in vitro* assay that allows assessment of the impact of immunomodulatory agents on T-cell responses. Responder T-cells are cultured with allogeneic stimulator cells and the foreign major histocompatibility complex (MHC) antigens stimulate a T-cell response akin to transplant rejection in a dish, with proliferation of the T cells measured by incorporation of a radioactive label or dilution of a cell-tracker dye such as carboxyfluorescein succinimidyl ester (CFSE). In a one-way MLR the stimulator cells are either irradiated or treated with an anti-proliferative agent such as Mitomycin C to prevent any immune response against the responder cells. An advantage of the MLR for assessing the effects of agonist antibodies is that the stimulator cells are generally professional antigen presenting cells (APCs) that express on their surface Fc receptors, which may be necessary for the action of agonist antibodies. Cultures of T

cells alone (for example in assays using anti-CD3/CD28 antibodies or coated beads as the activation stimulus) would not contain Fc receptors at a significant level, so the agonist antibodies might need to be immobilized on plastic to have any detectable effect and this in turn may not faithfully replicate the potentially critical dimensions of physiological cell contacts.

In order to assess our mIgG1 anti-hBTLA antibodies, CFSE labelled purified T-cells from the humanised BTLA mice (which are on a C57BL/6 background) were used as responder cells and Mitomycin C treated unfractionated splenocytes from BALB/C mice were used as stimulator cells. Furthermore, to provide an internal control that nullifies any well-to-well variation (caused by factors such as position on the plate, endotoxin contamination of antibodies, or small differences in cell density or the stimulator-to-responder ratio) an additional population of responders was added to each well consisting of CFSE labelled purified T-cells from non-humanised C57BL/6 mice. These cells, to which the anti-human antibodies do not bind, were from allotype marked CD45.1 mice allowing separation during flow cytometry analysis (Figure 5-1a). Within each well, a ratio was calculated that indicated how the humanised cells proliferated compared to the non-humanised cells, and this was normalized to the mean ratio in the presence of isotype control antibody. This provides a highly controlled read-out of the direct effects of each antibody on humanised T-cell proliferation. Normalisation to the isotype control ratio also enables collation of data from independent experiments.

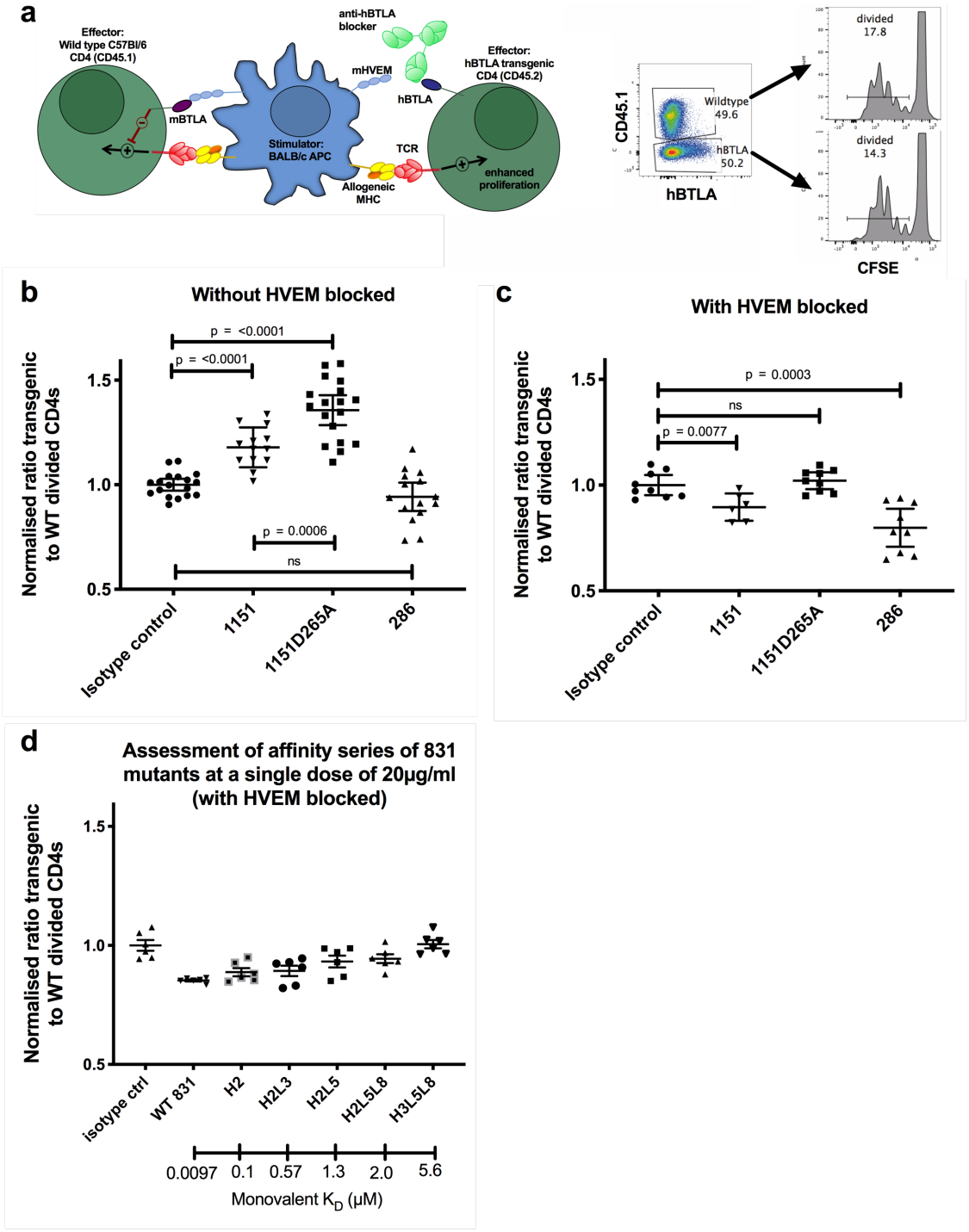


Figure 5-1: Mixed lymphocyte reaction (a) Diagrammatic representation of the internally controlled mixed lymphocyte reaction and flow cytometry gating strategy. 2x10^5 CFSE labelled responder T cells (a 50:50 mixture of humanised and wildtype C57BL/6) were mixed with 4x10^5 Mitomycin C treated BALB/c splenocytes in a U-bottom 96 well plate and incubated for 96 hours in the presence of 20 µg/ml BTLA antibody or isotype control. Proliferation was assessed by CFSE dilution and a ratio of division for humanised vs wildtype responders calculated. (b) Effect of anti-hBTLA antibodies on proliferation of humanised CD4 T-cells compared to non-humanised responder cells (c) Effect of anti-hBTLA antibodies in the presence of polyclonal HVEM antibody, which removes endogenous signalling (d) Assessment of reduced affinity mutants of antibody 8.3.1 in the MLR, with antibody affinity as determined by SPR inset below the x-axis. Data are normalized to the mean isotype control in each experiment and collated from 2 – 5 independent experiments with triplicate wells in each.

Initial screening of each of the BTLA antibodies in this assay (at a single high dose of 20μg/ml) showed no significant inhibitory effect with any antibody, even with clone 2.8.6, which from the binding characterization we had hypothesised might be agonistic. However, the ligand blocking antibody 11.5.1 did lead to significantly enhanced proliferation of humanised CD4 T-cells (with approximately 20% more cells dividing). This effect was more striking (approx. 35% more cells dividing) with the Fc mutated 11.5.1 D265A (which has significantly reduced FcR binding) (Figure 5-1b). The impact of blocking antibodies, and lack of impact of agonistic antibodies, suggested that there might be a high level of signalling through the HVEM-BTLA pathway at baseline in this assay and that the presence of ligand was not the rate-limiting step, as may be expected given that the stimulator cells are haematopoeitic cells which express HVEM at high levels [242].

To increase the sensitivity for detecting effects of BTLA agonists a polyclonal anti-HVEM antibody was added to each well to block binding of HVEM to BTLA and remove all baseline signalling through the pathway. The addition of HVEM antibody consistently led to enhanced proliferation of all responder cells suggesting that the net impact of HVEM in the MLR is inhibitory, and that BTLA (rather than the activating receptor LIGHT) is the dominant binding partner in this case. Furthermore, in the presence of HVEM blocking antibody the FcR null BTLA blocker 11.5.1 D265A no longer had any impact on humanised T-cell proliferation (Figure 5-1c) suggesting that indeed all baseline signalling through the pathway had been removed and there was none left to block. Furthermore, in this setting clone 2.8.6 now led to significantly

reduced proliferation of the humanised CD4 T-cells (approx. 30% fewer cells dividing) compared to non-humanised responders, demonstrating that it is able to deliver an agonist signal through BTLA and replace the signal that has been removed by blocking HVEM. The same pattern of results was seen when analysing CD8 proliferation, though with a smaller effect size. The ability of 2.8.6 to inhibit T cells in the presence of HVEM blocking antibody also suggests that 2.8.6's ability to trigger BTLA signalling is independent of BTLA's binding to HVEM, rather than a consequence of stabilizing the BTLA-HVEM interaction. These data are in keeping with previous observations that the impact of an anti-mouse BTLA agonist antibody on T cells activated ex-vivo in co-cultures with APCs is more striking when the APCs are derived from $HVEM^{-/-}$ mice [200].

In total, all 11 of the anti-BTLA antibodies listed in Table 4-1 were assessed in the MLR in the presence of HVEM blockade and, whilst none was more effective than 2.8.6, all FcR binding anti-BTLA antibodies tested, covering several different epitopes and including ligand blocking antibodies such as clone 11.5.1, demonstrated some degree of inhibition of humanised T-cells. As proposed in Section 4.6 this perhaps explains why the D265A mutated version of 11.5.1 demonstrates more effective blockade of the pathway in the original assay (Figure 5-1b), as the net effect of 11.5.1 will be a result of both the HVEM-dependent signal that it removes and the agonist signal that it delivers, whereas 11.5.1 D265A removes the endogenous signal and delivers no signal of its own. These data suggest that the *in vivo* effects of BTLA targeting antibodies are likely to be highly context dependent, affected by the relative

abundance of receptor and ligand as well as by the presence or absence of Fc receptors.

The affinity series of mutants of antibody 8.3.1 described in Section 4.5 was also assessed in the MLR. Whilst the parental clone 8.3.1 was not quite as effective as 2.8.6 at suppressing T-cell proliferation it did demonstrate a significant inhibitory effect in the presence of HVEM blockade. Testing each of the antibodies at a single dose of 20 μg/ml the mutants had a progressively smaller effect as the affinity was reduced. Whilst this quite possibly indicates a reduction in potency (i.e. the dose required to reach maximal effect) rather than efficacy (the magnitude of maximal effect), an *in vitro* dose of 20 μg/ml is high and effects requiring higher doses than this are unlikely to be clinically achievable [243]. There was certainly no indication in this case that reducing affinity improved function as we had hypothesized might be possible due to increased capacity for serial target engagement and reduced risk of receptor internalisation.

5.3. SRBC and NPCGG immunisations

Having selected clone 2.8.6 and clone 11.5.1 D265A as effective agonist and blocking antibodies respectively *in vitro*, we proceeded to assess their impact *in vivo*, initially returning to the sheep red blood cell (SRBC) and NP-CGG immunizations as assays of the immune response. Antibodies injected 24 hours after SRBC immunization had subtle but significant effects on the development of follicular helper T (TfH) cells, with 2.8.6 leading to a slight reduction in TfH number and 11.5.1. D265A leading to a slight increase (Figure 5-2a). This is in fitting with a recent publication that

demonstrated an inhibitory effect of BTLA signalling on TfH cells in the germinal centre [201]. No significant impact on the number of germinal centre B-cells generated was detected (Figure 5-2b). I also assessed BTLA expression on B- or T-cells by flow cytometry, using a staining antibody that did not compete with the injected BTLA antibody. 5 days following *in vivo* injection of the agonist antibody 2.8.6, BTLA expression had not been downregulated at all on B- or T-cells, and quite strikingly following injection of the blocking antibody 11.5.1 D265A, BTLA expression had been significantly upregulated (Figure 5-2c). This suggests firstly that the issue of antibody mediated receptor internalization that had previously been seen with PD1 agonist antibodies may not apply to BTLA, and secondly that the blocking antibody 11.5.1 may either stabilize BTLA expression on the cell surface or lead to a homeostatic feedback upregulation of the receptor. Staining splenocytes with an anti-mIgG1 antibody demonstrated that, in addition to the isotype switched B-cell population expected after SRBC immunization, immune cells from mice injected with 2.8.6 or 11.5.1 were coated with the therapeutically injected mIgG1 antibodies (Figure 5-2d). Even within the $B220^-$ non-B-cell population, cells stained positive for mIgG1. This again confirms that anti-BTLA antibodies are able to persist bound to BTLA on the cell surface (in this case for 5 days) without leading to downregulation of the receptor.

The impact of anti-BTLA antibodies injected alongside NP-CGG, on NP-specific antibody production was also tested. However, no significant effect of either agonistic or blocking antibody was discernible against the high mouse-to-mouse variation seen in this assay (Figure 5-2e).

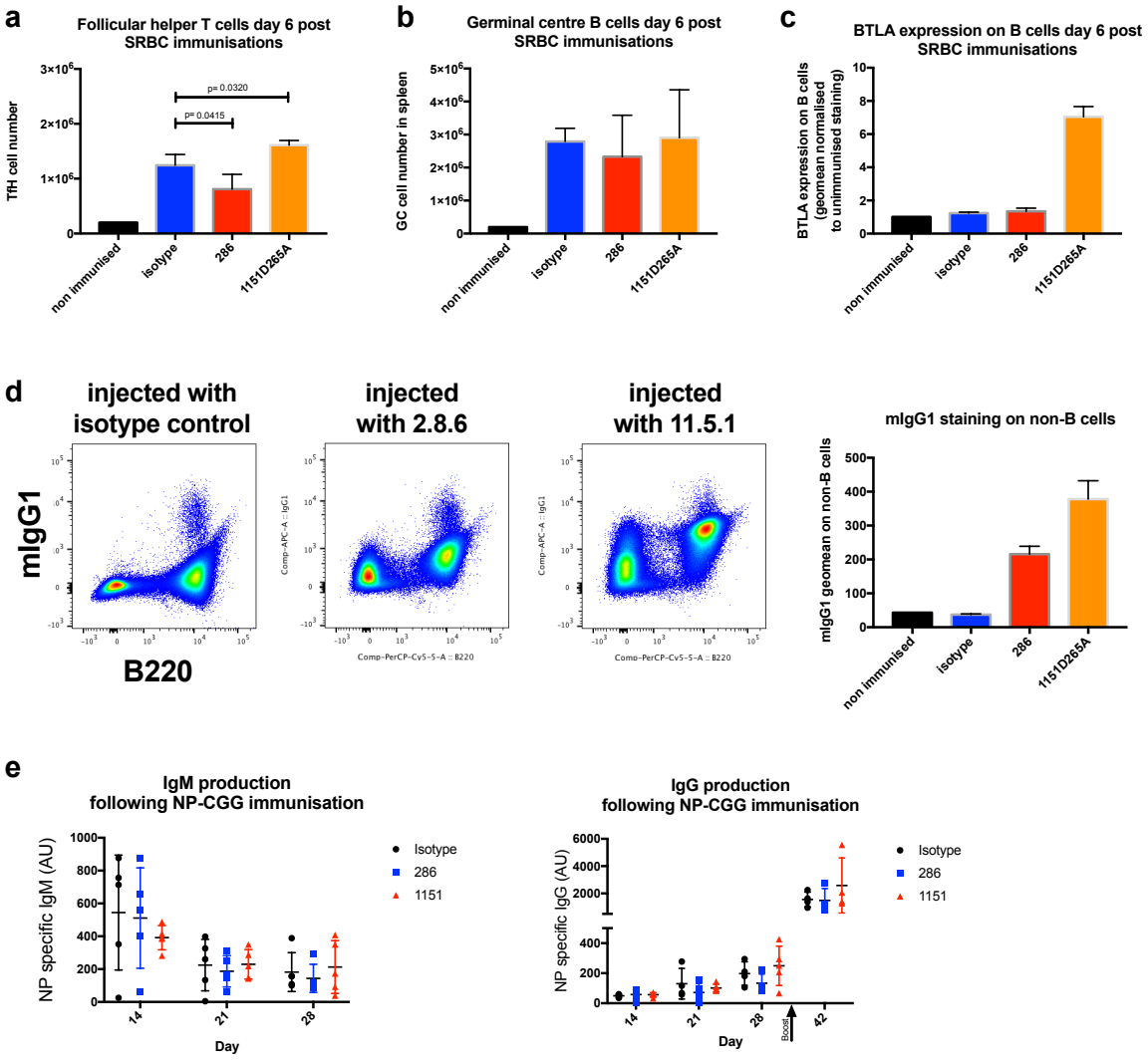


Figure 5-2: BTLA antibody impact on SRBC and NP-CGG immunisations (a,b) Quantification of splenic TfH (a) and germinal centre B-cell generation (b) in response to SRBC immunization (on day 0) in the presence of agonistic or blocking BTLA antibody (200 μg injected IP on day 1). (c) BTLA expression on B-cells following SRBC immunization and injection of BTLA antibodies (d) Staining of mIgG1 antibody on the surface of splenocytes 5 days following injection of mIgG1 monoclonals (e) Quantification of NP specific IgM (left) and IgG (right) at time points following NP-CGG in alum immunisation on day 0, and a boost with NP-CGG alone on day 35. BTLA antibody or isotype control was injected IP at a dose of 200 μg on day 1.

5.4. Adoptive transfer experiments

In order to assess antigen specific T-cell responses in a more controlled setting, mice humanised for both BTLA and PD1 were crossed onto OT2 TCR transgenic mice, which express a T-cell receptor specific for an ovalbumin peptide presented by MHC class 2, and therefore develop a CD4 T-cell compartment greatly enriched for ovalbumin specific cells [230]. The mice were bred until homozygous for both humanised receptors and heterozygous for the OT2 transgene. To work around the high level of mouse-to-mouse variation inherent in animal experiments we attempted to extrapolate the principle, from the MLR, of using an internal control population of responder cells that would not be impacted by anti-human antibodies. To this end, we mixed purified CD4 T-cells from the spleens of the hBTLAhPD1_OT2 transgenic mice with CD4 T-cells from non-humanised OT2 mice that constitutively expressed GFP under the control of the ubiquitin C promoter (UBC-GFP_OT2 mice), allowing identification of each population by flow cytometry. These mixed populations of CD4 T-cells were transferred intravenously into allotype-marked CD45.1 recipient mice and 24 hours later stimulated by immunizing the recipient mice intraperitoneally with ovalbumin in Alum adjuvant. 24 hours after this, the mice were treated with 200 µg of isotype control, anti-hBTLA antibody, anti-hPD1 antibody or combinations of the two. Six days later (8 days after the initial cell transfer) the recipient mice were culled and splenocytes assessed by flow cytometry. The population of transferred cells was identified by CD45.2 staining and within this population the ratio of humanised (GFP^-) to non-humanised (GFP^+) cells was calculated, and normalized to the ratio in the isotype control treated mice (Figure 5-3a).

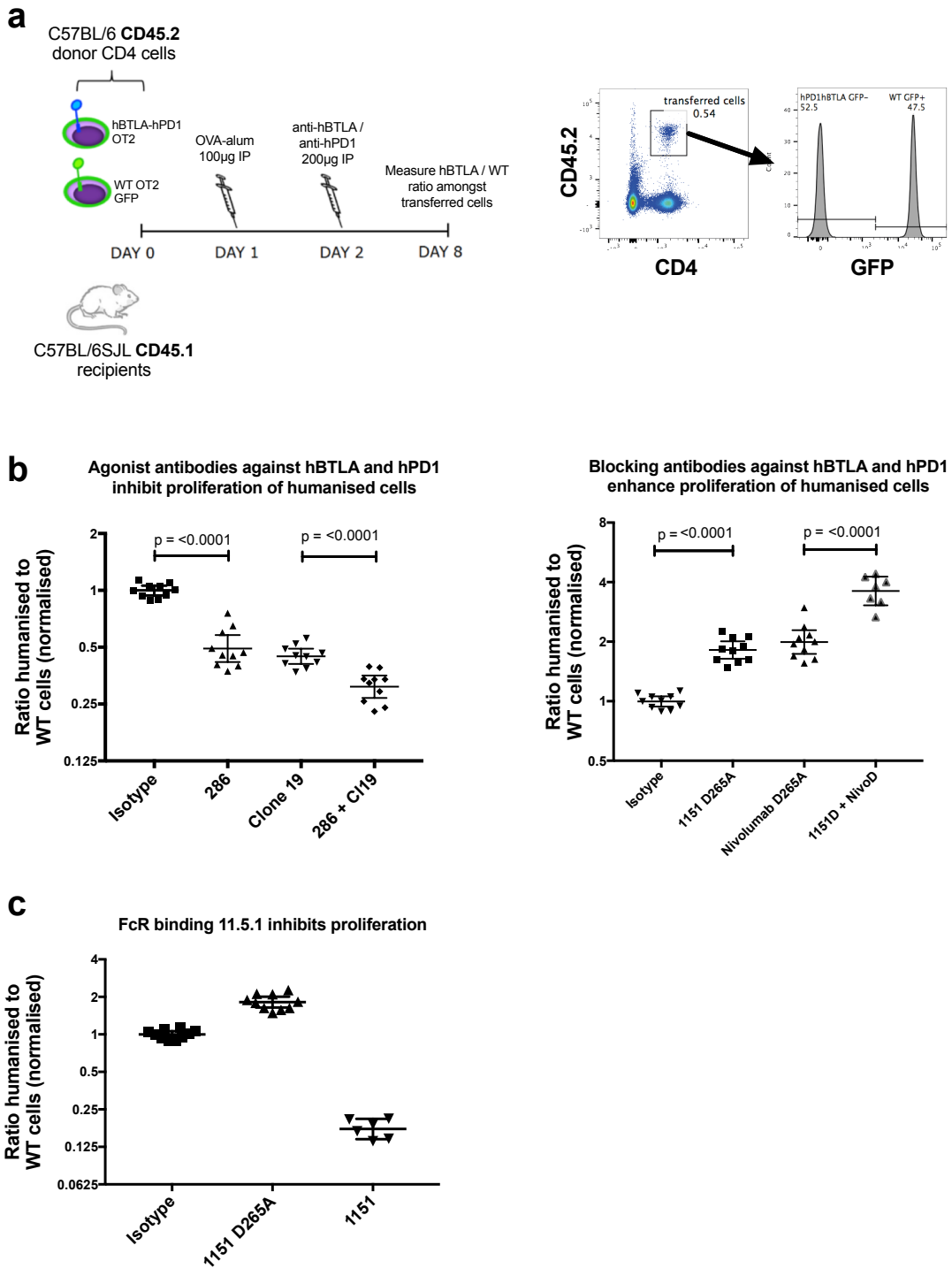


Figure 5-3: Adoptive transfers (a) Experimental protocol for the adoptive transfer assay and flow cytometry gating strategy. $5x10^5$ OT2 transgenic CD4 T cells (a 50:50 mixture of humanised and non-humanised GFP expressing) were injected IV into CD45.1 recipient mice on day 0. On day 1 mice were immunised IP with ovalbumin in alum and on day 2 treated IP with 200 µg checkpoint antibody or isotype control. On day 8, the ratio of humanised to non-humanised cells in the transferred ($CD45.2^+$) population was calculated and normalised to isotype control treated mice. (b) Impact of BTLA and PD1 agonist (left) and blocking (right) antibodies on expansion of humanised T-cells relative to non-humanised counterparts (c) Differential effect of Fc mutated (D265A) and FcR binding versions of the ligand blocking BTLA antibody 11.5.1. Data are collated from 2-3 independent experiments, normalized to the mean isotype control in each experiment. Each point represents one mouse.

In this adoptive transfer assay, the BTLA agonist 2.8.6 led to a 50% reduction in expansion of humanised CD4 T-cells relative to non-humanised cells (Figure 5-3b). This was comparable with the effect size of the hPD1 agonist antibody clone 19, and in combination the two antibodies had an additive effect (resulting in a 4-fold reduction of the humanised to non-humanised ratio). Conversely, FcR non-binding blocking antibodies targeting hBTLA or hPD1 each resulted in a 2-fold increase in expansion of humanised cells, and again had an additive effect in combination. For PD1 the blocking antibody used was a chimera of the variable domains of the clinically used checkpoint blocker Nivolumab on a D265A mutated mIgG1 Fc.

Whilst the FcR non-binding (D265A) version of 11.5.1 led to enhanced proliferation of humanised cells, the Fc competent mIgG1 version had the opposite effect, drastically reducing humanised T-cell expansion (Figure 5-3c). This was in fitting with the MLR data, suggesting that FcR-binding ligand-blocking antibodies can deliver an agonist signal and the net effect (inhibitory or activating) is context dependent. This has striking implications for the development of checkpoint blocking antibodies in the immuno-oncology field and demonstrates that the choice of isotype and Fc mutations is critical to function.

5.5. *In vitro* and *in vivo* cytotoxicity of anti-BTLA antibodies

One possible explanation for the reduced expansion of humanised cells seen with FcR competent anti-BTLA antibodies in the adoptive transfer assay is that the antibodies

are depleting cells by effector functions such as complement-dependent cytotoxicity (CDC) or antibody-dependent cellular cytotoxicity (ADCC). This is unlikely, firstly because the antibodies are all of the mIgG1 isotype, which has a high ratio of inhibitory to activatory FcR binding and is generally considered non-depleting [25], and, secondly, as we were able to demonstrate live cells coated in the mIgG1 2.8.6 antibody 5 days after antibody injection in the SRBC immunisation assays.

However, to further explore this possibility we assessed the ability of the mIgG1 antibodies 2.8.6 and 11.5.1 to deplete B cells (which express the highest levels of BTLA) *in vitro* and *in vivo*. To measure CDC, splenocytes incubated at 37°C for 15 minutes with rabbit complement in the presence of different antibodies were assessed by flow cytometry (Figure 5-4a). Whilst a positive control depleting anti-CD20 antibody (clone SA271G2, isotype rat-IgG2b) led to near complete depletion of B cells in this time frame the anti-BTLA antibodies had no impact on any cell population (Figure 5-4b). To assess ADCC, unfractionated splenocytes (therefore containing FcR expressing effector cells) were cultured at 37°C for 24 hours in the presence of different antibodies and again, whilst the positive control antibody effectively depleted B cells none of the anti-BTLA antibodies had any effect on the fraction of live B-cells compared to the isotype control-containing wells.

BTLA expressing cell populations were also assessed in the spleen and bone marrow 24 hours after *in vivo* injection of humanised BTLA mice with clone 2.8.6. Figure 5-5a demonstrates that, whilst B cells express high levels of BTLA, they are not depleted at all in this timeframe as would be expected with a depleting antibody. The number of

splenic CD4 T-cells, CD8 T-cells, and B cells, as well as B-cell developmental stages in the bone marrow, are unaffected 24 hours after 2.8.6 injection (Figure 5-5b) and BTLA expression on these cell types is also unaffected.

These data indicate that the mIgG1 anti-BTLA antibodies have no significant depleting effect *in vitro* or *in vivo* and support the idea that their inhibitory effect on T-cell expansion is due to their ability to trigger inhibitory signalling through the BTLA receptor.

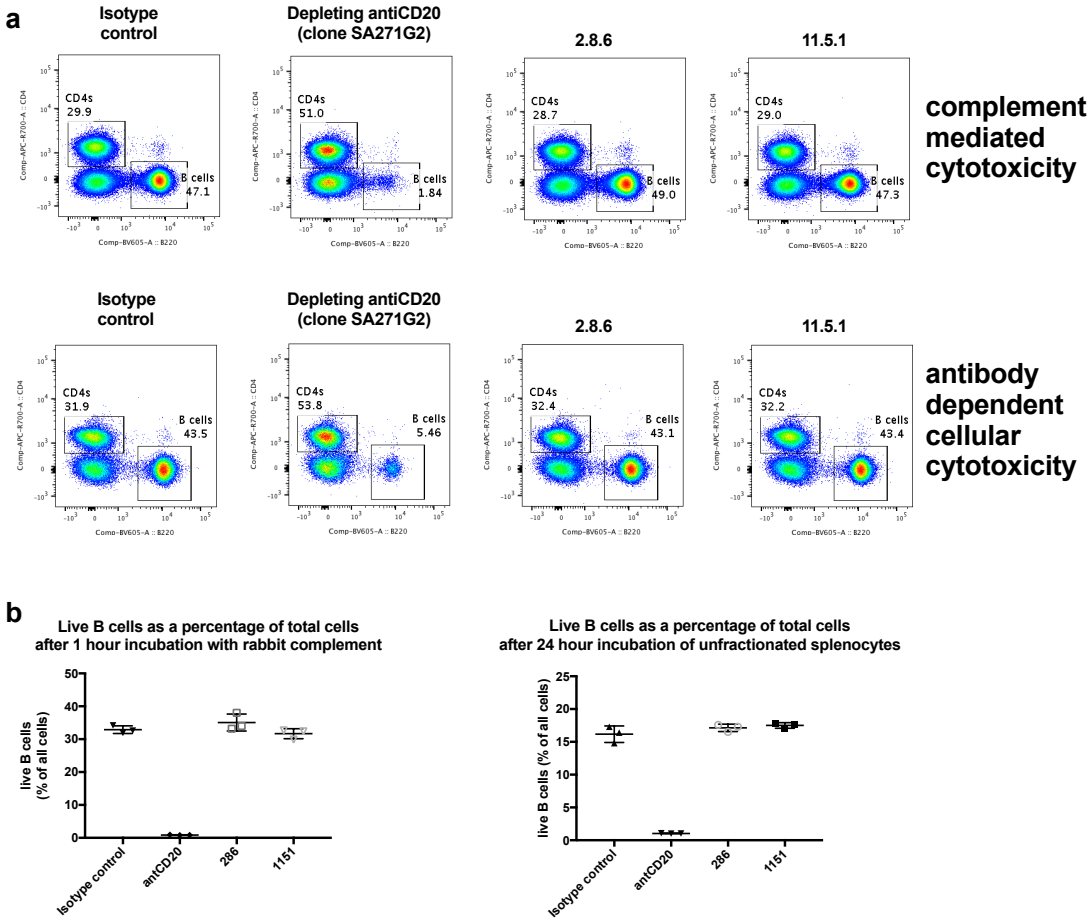


Figure 5-4: *In vitro* cytotoxicity assessment (a) Representative flow cytometry plots of unfractionated splenocytes incubated with rabbit complement for 15 minutes (top, CDC) or alone for 24 hours (bottom, ADCC) in the presence of different antibodies. (b) Frequency of live B-cells within the total cell population in the CDC (left) and ADCC (right) assays.

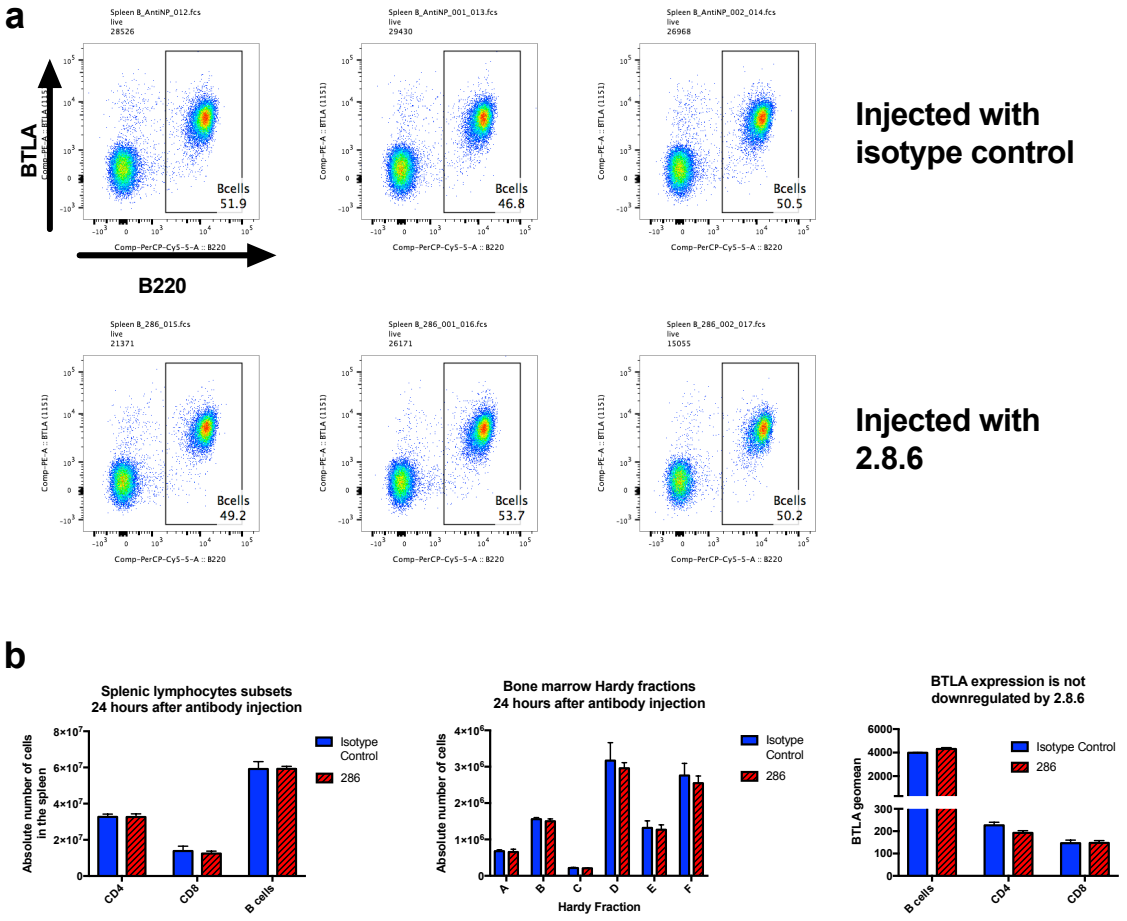


Figure 5-5: *In vivo* cytotoxicity assessment (a) Representative flow cytometry plots of splenocytes from mice injected with 200 µg isotype control (top) or 2.8.6 (bottom) demonstrating the high expression of BTLA on B cells and lack of depletion. (b) Quantification of different BTLA expressing cell populations in the spleen (left) and of B cell developmental fractions in the bone marrow (centre) 24 hours after 2.8.6 injection. BTLA expression on major lymphocyte subsets 24 hours after 2.8.6 injection (right).

5.6. Importance of antibody size to agonist function

Having identified clone 2.8.6 as a non-ligand-blocking BTLA agonist we chose to use it as a tool to further investigate the mechanisms of antibody agonism. If a kinetic segregation-based explanation for antibody action is correct then the dimensions of the complex formed between receptor, antibody and FcR would be critical and we hypothesized that reducing the size of the antibody in this complex might enhance agonist function. To investigate this we wished to express 2.8.6 as an ScFv-Fc, an antibody-like format in which the first constant domains of the heavy and light chain are removed and the variable domains are joined by a linker sequence (Figure 5-6a). The recombinant expression of this protein was outsourced to the CRO, Absolute Antibody. Based on their experience that human variable domains are more likely to successfully express in ScFv format than murine variable domains we chose to produce the construct using the variable domains of a humanised variant of clone 2.8.6. This humanised variant had already been created by CDR grafting of the parental 2.8.6 CDRs onto homologous human germline V regions (IGHV2-5*08 and IGKV3-11*01), as clone 2.8.6 has development potential as a therapeutic and humanization of variable domains reduces the risk of immunogenicity in humans. The humanised variant displays binding to BTLA with a K_d of ~2nM (approximately 3-fold lower affinity than the parental clone). The ScFv-Fc construct on a mIgG1-Fc expressed well and maintained the same binding affinity to BTLA (assessed by SPR) as the humanised 2.8.6, i.e. a 3-fold lower affinity than the non-humanised parental antibody (Figure 5-6b).

We compared the efficacy of the 2.8.6 ScFv-Fc to the parental murine 2.8.6 antibody in the adoptive transfer assay described in Section 5.4. Consistently, the ScFv-Fc format led to greater inhibition of T-cell expansion. The ScFv-Fc must bind to the same epitope on BTLA as the parental clone, albeit with slightly lower affinity and it comprises the same Fc region so will have the same FcR binding affinity. It is likely therefore that the different functional impact of this format can be attributed to the reduced dimensions of the antibody, which is strongly supportive of a kinetic segregation-based mechanism of receptor triggering.

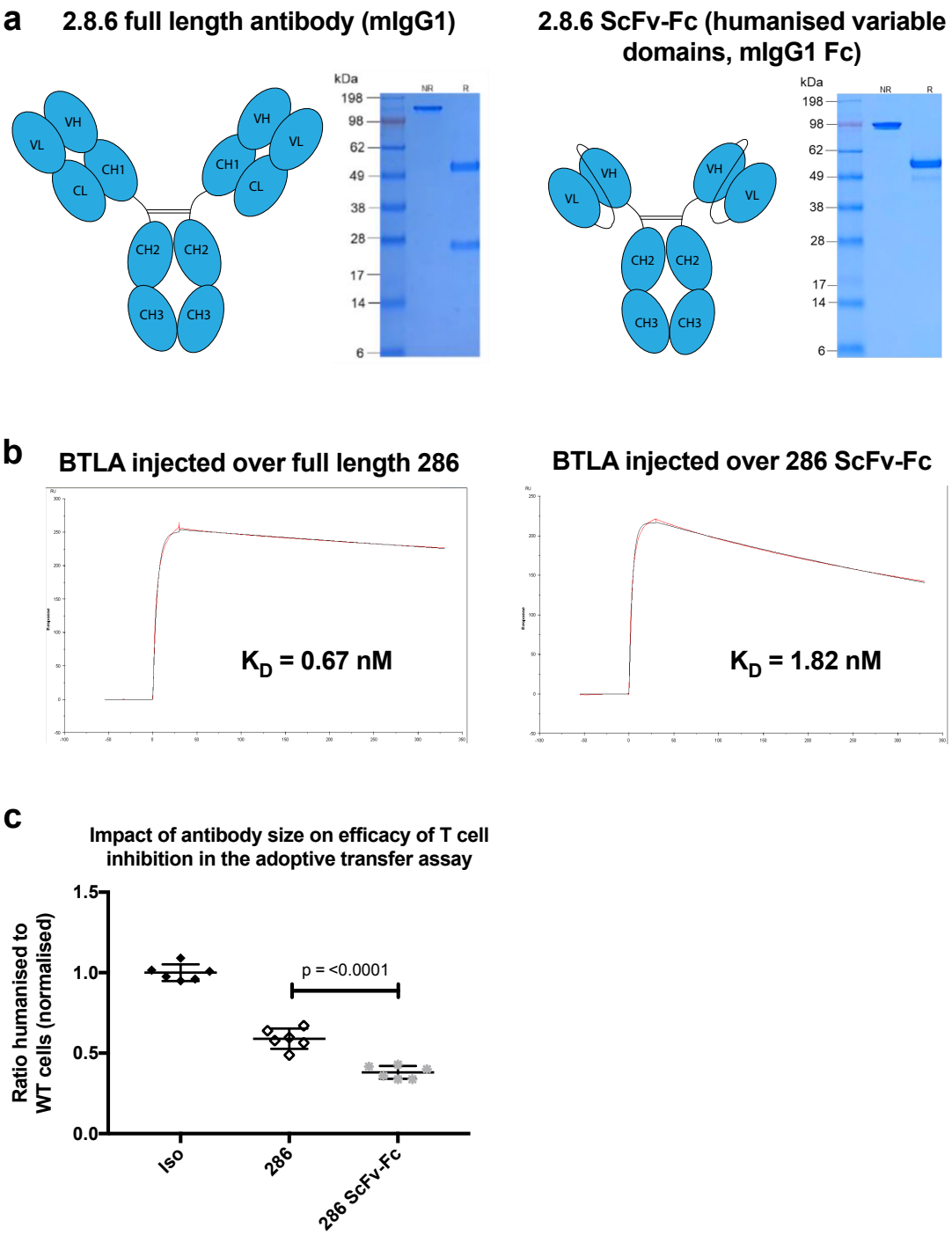


Figure 5-6: Impact of antibody size on agonistic function (a) Depiction of a full-length antibody compared to the ScFv-Fc format with inset non-reducing and reducing SDS-PAGE gels of full length 2.8.6 and ScFv-Fc humanised 2.8.6 (b) Example SPR curves showing hBTLA injected over immobilized 2.8.6 formats, with K_d inset (c) Enhanced inhibition of humanised OT2 T-cell proliferation (in response to ovalbumin) by 2.8.6 ScFv-Fc vs full length antibody, in the adoptive transfer assay described in Section 5.4.

5.7. Improving PD1 blockade by removal of antibody agonism

We observed in Section 5.4 that a ligand-blocking antibody targeting BTLA paradoxically inhibits T-cell responses, and to generate a truly antagonistic antibody Fc receptor binding had to be removed with a targeted Fc mutation. We wished to explore whether the phenomenon of antibody agonism limiting pathway blockade extended to antibodies against PD1. This would be of significant interest given that the clinically used PD1 antibodies Nivolumab and Pembrolizumab are both of the human IgG4 isotype (with only a S228P mutation to prevent Fab arm exchange) and so will have the capacity to bind Fc receptors *in vivo.* To investigate this using the humanised mice we produced a chimeric antibody comprising the Fab (variable domains plus first constant domains) of Nivolumab with a mouse IgG1 Fc, which would bind to Fc receptors in the transgenic mice. We also produced an Fc variant of this antibody with the D265A mutation to remove Fc receptor binding. Furthermore, we produced a final chimeric variant in which the dimensions of the Nivolumab mIgG1 antibody were increased by a 50 amino acid insertion in the hinge region, using rigid, mucin-like sequence from human CD43 (Figure 5-7a). This sequence insertion has previously been described, in the DPhil thesis of Meike Assmann [244], as increasing the physical size of an antibody without affecting antigen or Fc receptor binding. In that instance the insertion eliminated the superagonistic effect of an anti-CD28 antibody superagonist. Similarly, we hypothesized that if the parental antibody was inducing receptor triggering via a phosphatase exclusion-based mechanism then this effect could be removed by extending the dimensions of the antibody so that it could no longer create the narrow contact zone necessary for excluding the

phosphatases. Each of these variants of Nivolumab was produced and purified by the contract research organization, Absolute Antibody.

We used the adoptive transfer assay described in Section 5.4 to compare the effects on T-cell expansion of these three variants. Very similar to our observations with BTLA antibodies, the FcR binding mIgG1 variant of Nivolumab in fact led to reduced expansion of humanised T-cells (Figure 5-7b). Introduction of the D265A mutation created a true PD1 antagonist that enhanced expansion of the humanised T-cells. Similarly, the extended variant of Nivolumab also functioned as a true PD1 antagonist leading to enhanced T-cell proliferation. These data intriguingly suggest that the efficacy of PD1 blockade may be limited in some contexts by FcR dependent antibody agonism and raise the possibility that clinically used PD1 inhibitors could be improved by engineering approaches to remove this agonist effect. The fact that increasing the antibody size has the same impact as removing FcR binding is supportive of a KS-based explanation for the signalling activity rather than, for example, a receptor cross-linking effect of the antibody. The ability to improve blockade without removing FcR binding may in itself be useful, as most described Fc mutations on the IgG1 or IgG4 backbones do not completely abolish FcR binding [245] and removing the Fc region in its entirety leads to very significant reductions in serum half life (due to loss of interactions with the neonatal Fc receptor that is crucial to antibody half- life)[26]. Furthermore, the engagement of FcRs by a hinge-extended antibody could force exclusion of PD1 from narrow cell contacts and prevent ligand-independent signalling that could otherwise occur as a result of passive diffusion of the receptor into the synapse. Finally, combining this approach with Fc mutations

that enhance binding for the inhibitory Fc receptor (FcγRIIB) could allow the simultaneous blockade of this second inhibitory signal leading to an additional immune activating effect.

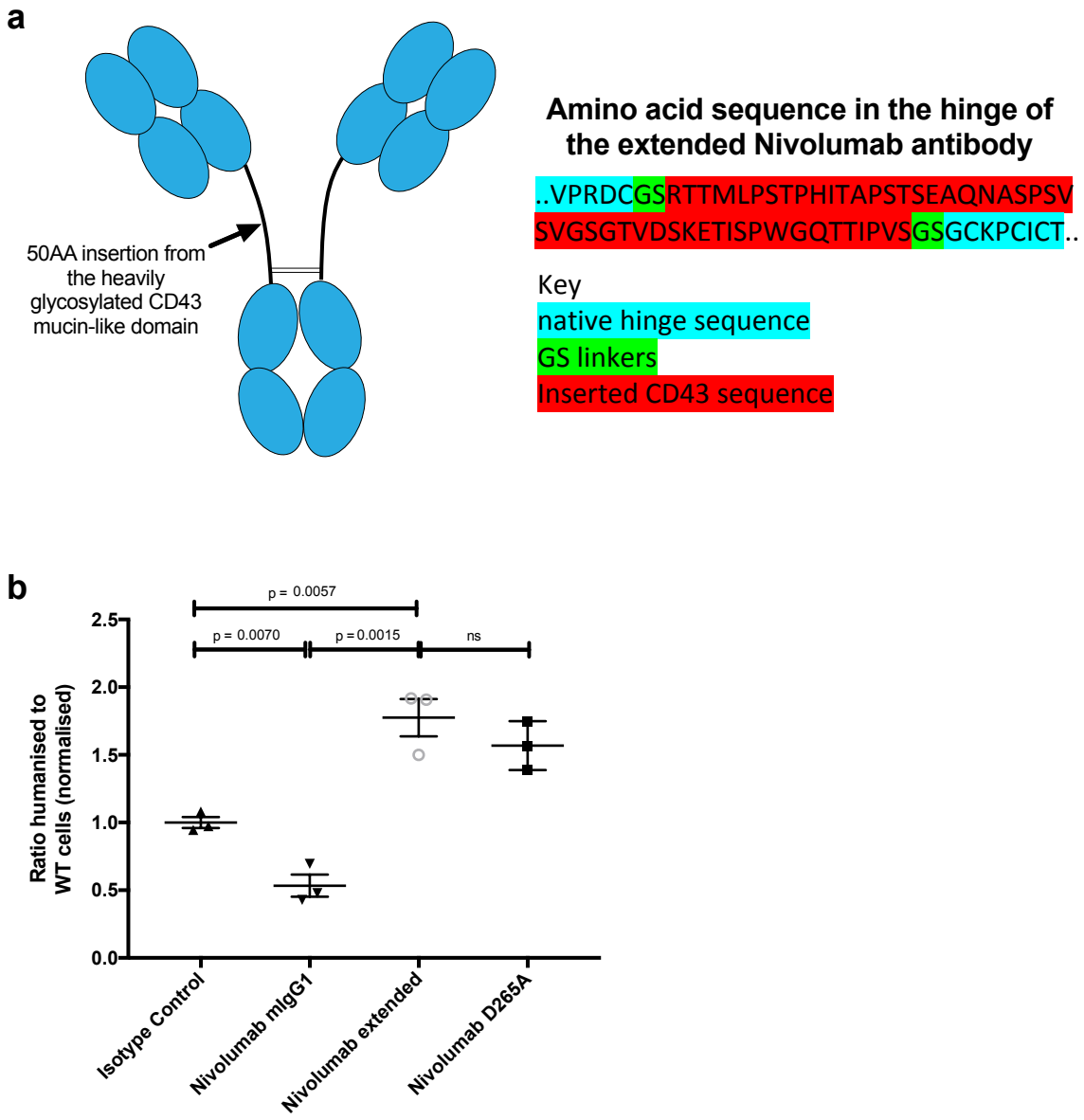


Figure 5-7: Effect of antibody size and FcR interaction on PD1 blockade (a) Description of the hinge insertion used to increase the dimensions of the extended Nivolumab mIgG1 construct. A 50 amino acid section of heavily glycosylated CD43 sequence was inserted into the hinge region of the mIgG1 antibody between the first and second cysteine. (b) Effect of different Nivolumab variants on humanised OT2 T-cell expansion (in response to ovalbumin) in the adoptive transfer assay described in Section 5.4.

5.8. Discussion

The data in this chapter demonstrate that BTLA receptor-modulating antibodies can have a significant impact on T-cell responses to activating stimuli. The fact that this modulation can be detected in immune cells from the transgenic mice confirms that the knocked-in chimeric BTLA receptor is functioning and able to deliver an inhibitory signal to the murine cells. In addition to providing the ability to perform *in vivo* assessment of anti-human antibodies the transgenic mice have created the opportunity to carry out highly controlled assessments of T-cell function in which non-humanised, but otherwise identical, responder cells serve as internal controls unaffected by the specific actions of the antibody of interest. This approach helps to tackle the issue of biological variation and enables the confident and consistent assessment of small but significant effects that otherwise might be lost in noise.

Key findings that can guide the development of checkpoint agonist antibodies have started to emerge from these experiments. It is clear that the agonist effect of these antibodies is critically dependent on FcR interactions, but also that the functional impact of receptor binding is context dependent. In settings where ligand is highly expressed and baseline signalling is high then agonist antibodies have little additional effect, but conversely in settings where there is no baseline signalling antibody agonism becomes relevant and even ligand-blocking antibodies can have a paradoxical immunosuppressive effect.

The importance of FcR binding to agonism, and the fact that simply reducing the size of an antibody can lead to enhanced agonism are both supportive of a kinetic segregation-based explanation for antibody agonism. And this is further supported by the fact that all FcR-binding antibodies against BTLA that we tested demonstrated some degree of agonism, regardless of the position of their epitope on the receptor, suggesting that it is merely the trapping of receptor in a narrow synapse between BTLA-expressing and FcR-expressing cells that leads to signalling, rather than, e.g. an epitope dependent conformational change in the receptor.

It has previously been observed that Fc mutated PD1 blocking antibodies with reduced FcR binding are more effective in treating murine tumours [241, 246]. Potential explanations for this that have been proposed previously include the possibility of antibody dependent depletion of PD1 expressing T-cells [241] or FcR dependent sequestering of antibody by macrophages [246]. We too have shown here that an Fc mutation that reduces FcR interactions significantly improves the ability of a PD1 blocking antibody to enhance T-cell proliferation. However, we have also shown that increasing the dimensions of the antibody without removing FcR binding can have the same effect and we propose that the enhanced blockade seen with either of these constructs is due to the removal of counterproductive FcR dependent antibody agonism. These observations could in part explain the significant fraction of cancer patients who do not respond to PD1 blockade and may have important implications for the design of novel checkpoint inhibitors against both PD1 and other targets.

The assessment of reduced affinity mutants of a BTLA agonist antibody revealed that reducing affinity from a nanomolar range to micromolar range dissociation constant can have a meaningful impact on functional effect, even when antibodies are assessed at high concentration *in vitro*. This is perhaps surprising, given that the endogenous ligand-receptor interactions for checkpoint receptors usually themselves have micromolar range dissociation constants. It may be explained by the requirement for Fc receptor engagement to support antibody agonist signalling. Fc-FcR interactions are also generally of low affinity and so the half-life of the complex between target receptor, antibody and FcR will be determined by the off-rate of both interactions, either of them falling apart would break down the complex needed for agonism. Conversely, the half-life of the interaction of an endogenous ligand (anchored in the membrane) binding to target receptor is determined by the single off-rate of this interaction. Similarly, a very high affinity antibody can bind stably to its target and so can still form complexes with an Fc receptor for long enough to induce signalling even though the Fc-FcR interactions themselves are short lived.

A further important observation from the experiments in this chapter is that antibody binding to BTLA does not appear to lead to receptor downregulation *in vivo,* with target cells remaining coated in antibody for at least 5 days after dosing. This is in contrast to previous observations with PD1 agonist antibodies and suggests that BTLA agonists may be more able to deliver prolonged inhibitory signalling, which might be necessary for a clinically effective therapeutic.

Chapter 6 Assessment of BTLA antibodies in models of disease

6.1. Introduction

The data presented in Chapter 5 revealed that BTLA agonist antibodies can suppress T-cell responses in simple activation assays. However, we did not observe a complete block of T-cell activation but rather a reduction (in the range of 20 – 50%) in the fraction of CD4 T-cells within a population that were induced to proliferate, likely representing an increase in the stimulation threshold required for activation. Furthermore, this effect was context dependent and not seen in settings where there was significant baseline signalling due to the presence of high levels of HVEM. We therefore set out to assess whether this degree of increased inhibitory pressure on the immune response could be therapeutically meaningful in the setting of autoimmune disease. To investigate this question we utilized the humanised mice in two well-validated models of T-cell driven pathology; the T-cell transfer model of colitis and a parent-to-F1 model of graft versus host disease.

Furthermore, in Chapter 5 we demonstrated that a BTLA antagonist antibody could enhance T-cell responses to antigen, with an effect equivalent to PD1 blockade. Given the clinical efficacy of PD1 blockade in cancer immunotherapy we also utilised the humanised mice to explore the efficacy of blocking BTLA, as well as the checkpoints CD200R and TIGIT, in a murine model of colorectal adenocarcinoma.

6.2. T-cell transfer model of colitis

Crohn's disease (CD) and ulcerative colitis (UC) are autoimmune conditions primarily affecting the intestines and are grouped together in the term inflammatory bowel disease (IBD). These two chronic diseases, with a peak onset in early adulthood, can be highly debilitating and whilst a number of management options exist (including lifestyle changes, and medical and surgical approaches) many patients remain refractory to multiple lines of therapy. There remains a need both for more effective treatments, and for more targeted utilization of current therapies, guided by a deeper understanding of patient-specific disease pathology.

A number of mouse models have been developed to investigate the pathogenesis of IBD and to assess the efficacy and mechanism of action of novel therapeutics [247]. Many of these models require inbred mouse strains with a specific genetic defect and so would not be easily applied to our humanised transgenic mice. Other commonly used models, such as Dextran sodium sulphate (DSS) colitis, involve administering a chemical agent that impairs intestinal epithelial integrity and induces an inflammatory response primarily driven by the innate immune system. The T-cell transfer model of colitis on the other hand is a model that can be induced using cells from non-transgenic strains and that provides a useful tool for assessing therapeutics that modulate pathogenic T-cell responses [248]. The model, first described by Powrie *et al* [249], involves the transfer of naïve T-reg depleted CD4 T-cells ($CD4^{+}CD45RB^{high}CD25^{-}$) into immunodeficient $RAG1^{-/-}$ mice. These cells are capable of trafficking to the gut where they become activated, expand and drive intestinal inflammation. The mice begin to develop diarrhoea and a chronic wasting disease

from 2-3 weeks after cell transfer. The majority of clinically used IBD therapies have been shown to be effective in the T-cell transfer model, at least when administered in a preventative setting [250].

In order to assess the effect of anti-human BTLA and PD1 antibodies we induced the disease in RAG1$^{-/-}$ recipient mice by transfer of CD45RB^{high}CD25^{-}CD4^{+} T-cells from the spleens of donor mice humanised for both BTLA and PD1 (Figure 6-1). This provides a model in which the disease-initiating T-cells are targetable with anti-human antibodies, although the disease-propagating innate immune cells in the recipient mice do not express the human checkpoint receptors. Treatment antibodies or isotype control were administered intraperitoneally every two weeks, starting one week after cell transfer, in a semi-preventative regime (allowing time for cells to engraft and traffick to the gut but before the onset of clinical disease). In addition to the BTLA agonist 2.8.6, we assessed the effect of a variant of the PD1 agonist antibody Clone 19 that has been mutated to reduce its affinity 70-fold (Clone 19 Fast-off) and has been shown to retain the ability to suppress T-cell responses *in vivo* but without inducing significant downregulation of the receptor (this is the work of Susan Yu, a DPhil student in the Davis laboratory, Oxford.)

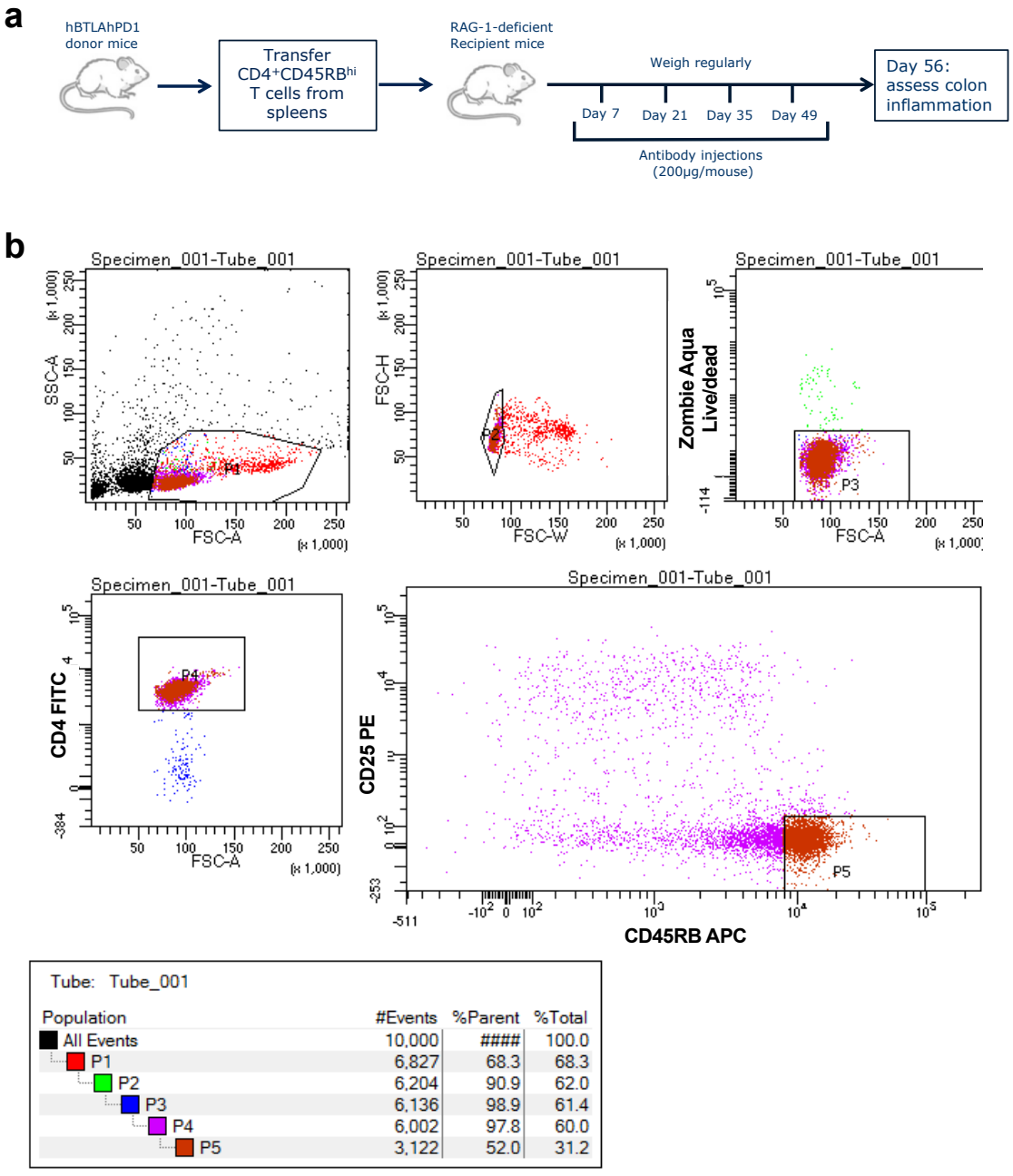


Figure 6-1: T-cell transfer model of colitis set up (a) Experimental protocol. 4x10^5 naïve CD45RB^{hi}CD25^{lo}CD4$^+$ T cells were transferred IV into RAG-1-deficient recipient mice, which were then treated with 200 µg antibody on days 7, 21, 35 and 49 before sacrifice and assessment of colon inflammation on day 56. (b) Flow cytometry gates to sort CD45RB^{hi}CD25$^-$CD4$^+$ cells for transfer. Prior to fluorescence-activated cell sorting, CD4$^+$ cells were enriched by negative selection using magnetic-activated cell sorting.

Mice that had not received transferred T-cells continued to put on weight throughout the eight week time course of the experiment, whilst mice that had received T cells and been treated with isotype control began to develop diarrhoea and lose weight between 20 and 40 days after transfer (Figure 6-2a,b). Eight weeks after cell transfer, or at the time of humane sacrifice if sooner, the large colon weight to length ratio was calculated, as a readily measurable outcome that correlates strongly with blinded histological score [251]. Mice that had received T-cell transfer had significantly higher colonic weight to length ratios than non-transferred mice, in fitting with the expected inflammatory infiltration and colonic thickening (Figure 6-2c).

Treatment with the PD1 agonist Clone 19 Fast-off did not lead to a significant reduction in weight loss or colonic inflammation. However treatment with the BTLA agonist 2.8.6 (or the combination of 2.8.6 and Clone 19 Fast-off) led to near complete abrogation of the clinical disease and prevented the associated increase in colon weight to length ratio. Furthermore, following processing of the colon to extract lamina propria leukocytes, significantly fewer white blood cells were isolated from the groups treated with 2.8.6 or the combination (Figure 6-2d). Analysing these extracted leukocytes by flow cytometry revealed that 2.8.6 treated mice had a significant reduction in the frequency of $CD11b^{+}Ly6G^{High}$ neutrophils, key downstream innate effectors of the inflammatory response. These data demonstrate the ability of an anti-human-BTLA agonist to ameliorate disease in an experimental model of colitis. This is in keeping with previous observations using an anti-mouse-BTLA agonist [200], however in those experiments the mouse BTLA agonist was shown to ameliorate the more severe disease induced in $HVEM^{-/-}$ recipient mice,

whilst here we have demonstrated that a BTLA agonist can deliver a beneficial additional inhibitory signal even in the presence of endogenous HVEM-BTLA signalling, suggesting that it could be therapeutically useful in human IBD even when there are no defects in the natural signalling pathway contributing to disease.

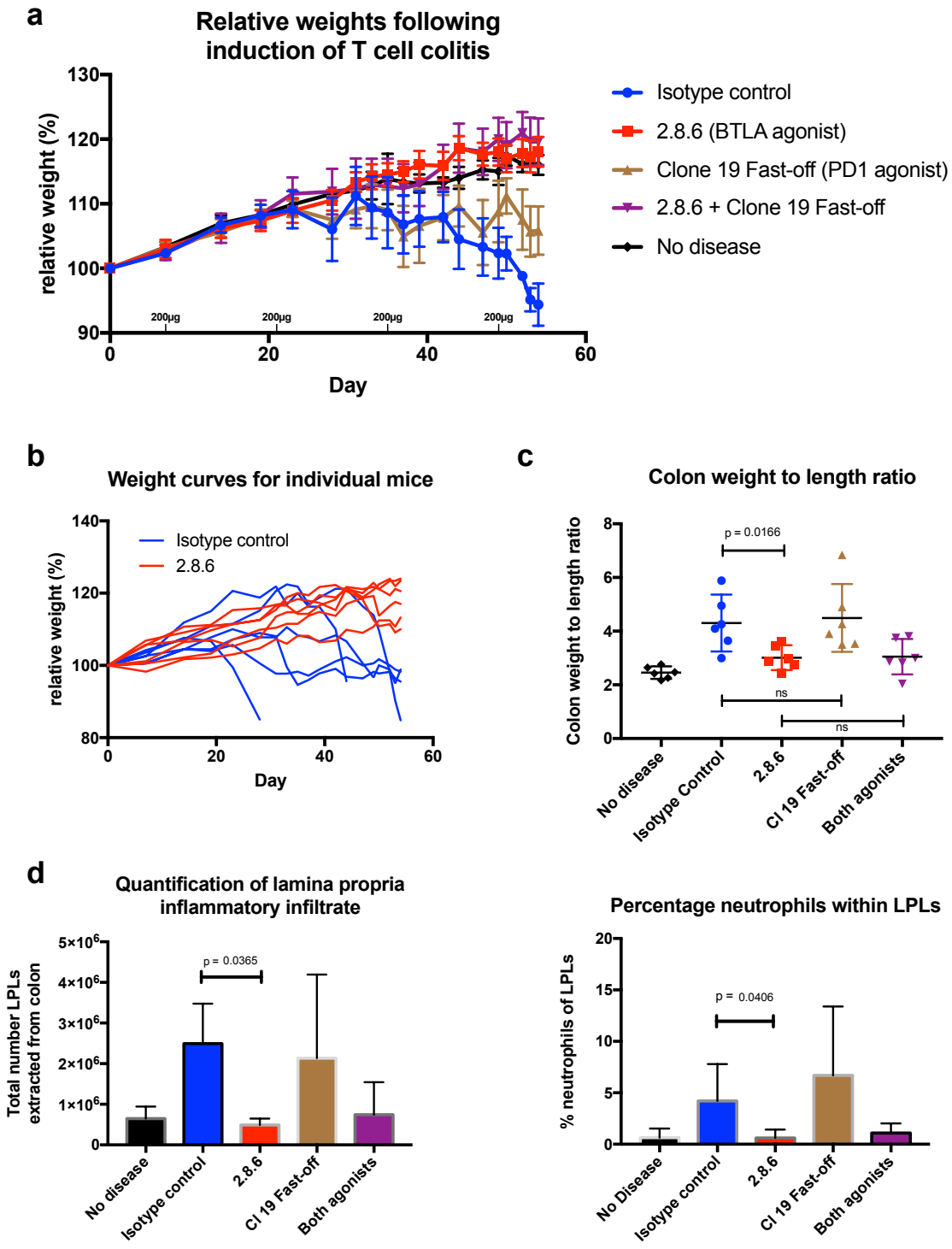


Figure 6-2: Antibody effects in T-cell transfer model of colitis (a) Weight curves normalized to starting weight following T-cell transfer (b) Relative weight curves for individual mice treated with isotype control or BTLA agonist 2.8.6 (c) Colon weight to length ratios (d) Total number of lamina propria leukocytes extracted from large colon (left) and frequency of neutrophils within these cells (right). Data are representative of two independent experiments with 5-6 mice per group. Plotted values are means ± SD.

6.3. Graft versus host disease

Graft versus host disease (GVHD) is a clinical complication encountered in patients who have undergone allogeneic stem cell transplant for the treatment of malignancy or a haematological disorder. The disease is caused by the appropriate, but unwanted, attack of transplanted immune cells against the recipient's tissues, with commonly affected organs including the gut, skin and liver [252]. T cells are the primary drivers of GVHD and disease incidence can be dramatically reduced by depletion of T cells from the transferred cells [253]. However, this depletion also reduces the rate of successful engraftment, increases infection risk and reduces the incidence of clinically beneficial graft versus tumour responses in the setting of treatment for haematological malignancy. Therefore, therapies that can modify T-cell activation without completely removing it are potentially more desirable, and currently agents such as methotrexate and cyclosporine are used to this end, often given prophylactically from the time of transplant. These small molecule agents however are accompanied by diverse side effects and more targeted therapeutics would be preferable. In theory a checkpoint agonist antibody could impose extra inhibitory pressure on transplanted T-cells, raising the activation threshold so that healthy 'non-self' tissues were no longer attacked, but malignant or microbial stimuli (providing a greater associated costimulatory signal) still induced a response. An anti-mouse BTLA agonist antibody was shown to effectively prevent acute GVHD in a mouse model whilst allowing successful engraftment of the transplanted immune system and sparing long term anti-viral and anti-tumour responses [141]. We employed a similar parent-to-F1 GVHD model to investigate whether an anti-human BTLA agonist could ameliorate disease induced by transfer of humanised mouse cells. Again, we

additionally explored the effects of an anti-human-PD1 agonist antibody alone or in combination with BTLA agonism.

To induce the disease, bone marrow and splenocytes from hBTLAhPD1 donor mice (on a C57BL/6 background, MHC haplotype H-2^b) were transferred intravenously into irradiated first generation (F1) offspring of C57BL/6 crossed with BALB/C (MHC haplotype H-2^d) mice (Figure 6-3a). These recipient mice (MHC haplotype H-$2^{b/d}$) therefore are recognised as foreign by the transferred cells. Recipient mice were weighed at least three times weekly for 35 days and humanely sacrificed if weight loss exceeded 15% of starting weight (or 20% in the first two weeks). Generally transplanted mice exhibited a rapid weight loss in the first 7 days (that was at least in part due to the conditioning irradiation as mice transplanted with syngeneic cells also lost weight), followed by a partial recovery and then more gradual weight loss from two weeks on. The majority of allogeneic transplanted mice treated with isotype control antibody had to be culled due to weight loss or disease severity before day 35, whilst no mice transplanted with syngeneic cells died (Figure 6-3b). As expected, diseased mice exhibited a significantly increased colon weight to length ratio at time of death compared to non-diseased mice (Figure 6-3c), in keeping with the gut inflammation seen in human GVHD. Treatment, on the day of cell transfer, with the PD1 agonist Clone 19 or the Fast-off variant of Clone 19 had no significant impact on disease severity. Conversely, treatment with the BTLA agonist 2.8.6, alone or in combination with Clone 19 Fast-off, significantly reduced weight loss, reduced colon inflammation and increased survival. Plotting the weights of individual mice reveals that there was not complete abrogation of disease but a reduction in the weight loss

observed (Figure 6-3d). Interestingly, the anti-BTLA antibody 11.5.1, despite being a ligand-blocking antibody, also significantly ameliorated disease. This is in keeping with the data presented in Chapter 5, which demonstrated that 11.5.1 (on an FcR binding mIgG1 isotype) can inhibit T-cell responses despite blocking the endogenous inhibitory signal. Whilst there was no significant difference between the effects of 2.8.6 and 11.5.1, the trend was towards greater efficacy with 11.5.1, which (if a true difference) could represent the removal of a positive signal delivered through HVEM by blocking the BTLA-HVEM interaction (in addition to the inhibitory signal 11.5.1 delivers through BTLA). This explanation would be in fitting with the less-severe disease seen when $HVEM^{-/-}$ T-cells are used to induce disease [200].

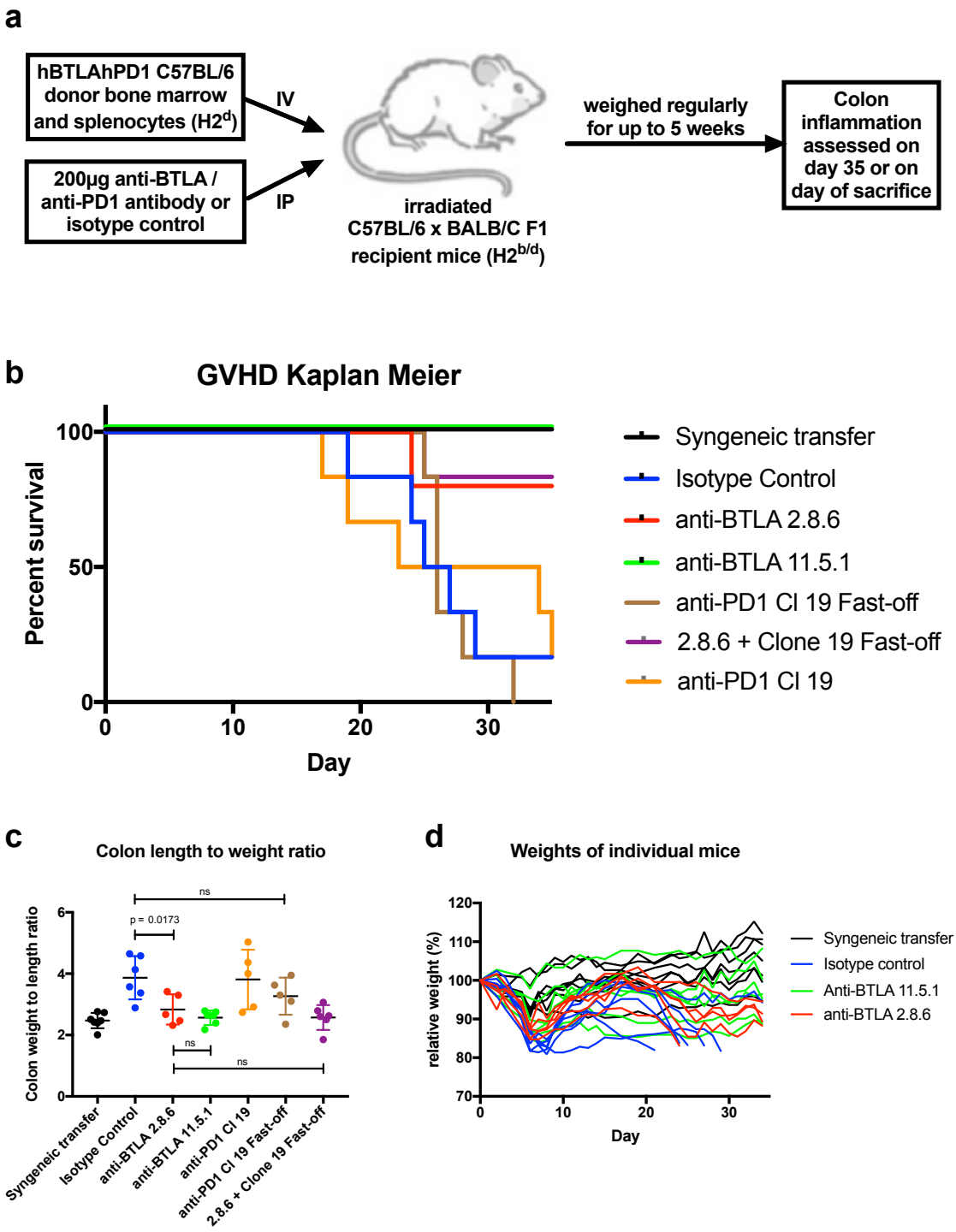


Figure 6-3: Parent-to-F1 model of GVHD (a) Experimental protocol for GVHD model. Recipient C57BL/6 x BALB/C first generation offspring female recipient mice were irradiated with two doses of 4.5 Gy spaced three hours apart. These mice were then injected with 2 x 10^7 bone marrow cells and 10^7 splenocytes from female hBTLAhPD1 C57BL/6 donors. The same day the mice were treated with 200 µg antibody IP. Mice were then weighed regularly for 5 weeks. On day 35 mice were culled and colon inflammation assessed by measuring weight to length ratios. (b) Kaplan Meier survival curves for different treatment groups (c) Colon length to weight ratios (d) Weight curves for individual mice treated with isotype control or BTLA antibodies. Data are representative of two independent experiments with 6-7 mice per group.

6.4. MC38 model of colorectal cancer

In Chapter 5 we demonstrated that BTLA blocking antibodies, when mutated to remove Fc receptor binding, could significantly enhance T-cell activation by removing the endogenous HVEM mediated inhibitory signal. Furthermore, *in vivo* this effect was equivalent to the activating effect of blocking PD1 on CD4 T-cells, and the two were additive in combination (Figure 6-4b). Given the striking clinical success of PD1 blockade in enhancing anti-tumour immune responses we wished to investigate whether BTLA blockade might also be beneficial in this context. Furthermore, having characterised ligand-blocking antibodies against the other inhibitory receptors TIGIT and CD200R, and having developed the humanised mouse models to explore these pathways we also had to the opportunity to explore the therapeutic potential of blocking these receptors in a cancer setting. For each of the receptors we chose a high affinity ligand-blocking antibody (clone 11.5.1 for BTLA, ID2 for TIGIT, OX108 for CD200R and the clinically used antibody Nivolumab for PD1) and expressed the variable domains onto a D265A mutated mIgG1 Fc region to minimise Fc receptor binding. We then assessed the impact of blocking each pathway, alone or in combination with PD1 blockade, in an MC38 model of colorectal cancer. This model involves the subcutaneous transfer of a colorectal adenocarcinoma cell line, originally derived from a C57BL/6 mouse, into syngeneic C57BL/6 recipient mice (in this case our humanised transgenic mice), and is widely used for the assessment of immune-modulating therapies as it is a cancer cell line that exploits checkpoint pathways as a tumour escape mechanism [254]. Furthermore, this model usually displays a partial but incomplete response to PD1 pathway blockade [255], providing the scope to

assess for enhanced efficacy with combination checkpoint blockade. We outsourced the running of this model to the contract research organisation, Crown Bioscience. Tumour volumes were measured using electronic callipers three times per week after cell transfer and mice were treated twice weekly with 10 mg/kg of each antibody for two weeks starting once the average tumour volume had reached 100 mm^3.

PD1 blockade consistently led to a halting of tumour growth (stable disease) in all three double-humanised mouse strains but alone did not lead to significant tumour shrinkage (partial or complete response) (Figure 6-4). Single pathway blockade of BTLA, TIGIT or CD200R on the other hand had no significant impact on tumour growth compared to isotype control. However, combining PD1 blockade with blockade of any of these other pathways led to a significant increase in the number of mice rejecting tumours (i.e. showing partial or complete response, defined as a >30% reduction in tumour volume). This effect was equivalent to the added benefit of combining PD1 blockade with an anti-mouse-CTLA4 antibody.

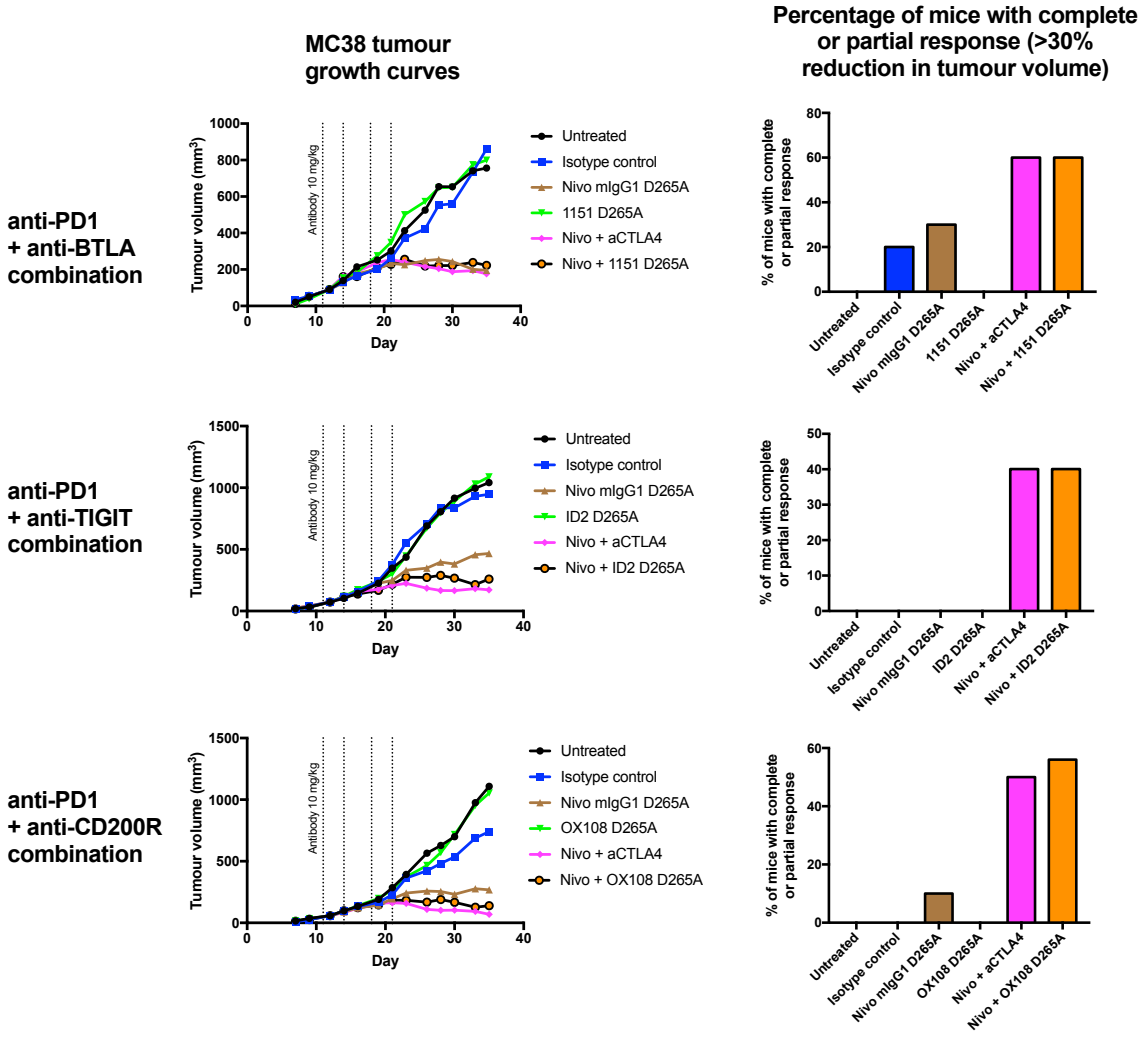


Figure 6-4: MC38 model of colorectal cancer. (Left) Tumour growth curves following treatment with checkpoint blocking antibodies alone or in combination. MC38 colorectal cancer cells were first expanded *in vitro* and then 1 x 10^6 cells/mouse were injected subcutaneously into the left flank of humanised transgenic mice, in 100 µl PBS. Tumour size was measured three times per week using electronic callipers. Once average tumour volume reached 100 mm^3 mice were allocated to matched treatment groups and injected IP with 10 mg/kg antibody twice per week for two weeks. (Right) Percentage of mice exhibiting complete or partial response (>30% reduction in tumour volume) in different treatment groups. N=10 mice per group.

6.5. Discussion

In this chapter we have demonstrated the therapeutic potential of modulating the BTLA pathway in murine models of human disease. In simplified but well-validated T-cell driven models of inflammatory bowel disease and graft versus host disease a BTLA agonist antibody (clone 2.8.6) displayed striking efficacy in ameliorating disease. Not only has this provided proof of concept for the approach, but the humanised transgenic mice have enabled us to assess an anti-human BTLA antibody and so the complementarity-determining regions (CDRs) from this antibody (which confer the epitope, orientation and affinity of binding) would be directly translatable into a clinical therapeutic. In both models the antibodies were assessed in a preventative setting, being administered prior to clinical disease onset, which might have exaggerated the impact compared to a treatment regime. However, the inability of even the most clinically successful IBD therapeutics (including TNF blockers and integrin inhibitors) to demonstrate efficacy in a treatment setting in the T-cell transfer model of colitis [250] highlights that such an experimental set up creates an excessively high bar for assessing efficacy that would lead to the unjustified side-lining of promising therapeutics. In the case of GVHD, immunosuppression to prevent excessive T-cell activation is given prophylactically (starting even prior to transplant) and so our experimental set up is representative of how a checkpoint agonist could be used clinically in this setting. Obviously, such simplified models of disease carried out in mice do not precisely replicate human disease biology, but they provide a promising indication that BTLA agonism can have a meaningful regulating effect on complex immune responses, and they provide a tool for further investigation into the mechanisms of this effect.

In contrast to BTLA, no efficacy was seen with a PD1 agonist antibody, suggesting that the PD1 pathway may not be as effective a target for this approach. The low affinity (fast off rate) PD1 agonist that was assessed does not induce significant receptor downregulation so this is unlikely to be the explanation for lack of efficacy, although the low affinity (and consequently higher IC50) may mean that antibody concentration in the target tissues did not reach the level required to induce significant signalling. In both of the models used, disease was induced by the transfer of humanised cells into non-humanised recipients, and so the only cells which could be affected by the administered antibodies were the transferred cells. Therefore, these models might under-represent the impact of PD1 agonism that would be seen if all PD1 expressing cells (including cells of the myeloid compartment) were available for modulation.

In contrast to the autoimmune model data, modulation of the PD1 pathway was unique in its impact on tumour growth in the MC38 cancer model, with the effect of PD1 blockade unrivalled by blockade of BTLA, CD200R or TIGIT. This observation is not surprising given the as yet unrivalled clinical success of PD1 pathway blocking antibodies, despite the vast resource that has been dedicated by the pharmaceutical industry to find novel checkpoint inhibitors that can match this success. Each of the checkpoint receptors (and their ligands) has their own unique expression profile and subtly different downstream signalling effects [256] and so the special role that the PD1 pathway plays in anti-tumour immunity might be due to its differential expression on immune-cell subsets important to tumour rejection, to its specific

effects on T-cell signalling or to the expression pattern of its ligands. However, blockade of BTLA, CD200R or TIGIT did display an additive effect on tumour rejection when combined with PD1 blockade that was equivalent to the effect seen with combined PD1 and CTLA4 blockade (a combination that certainly makes a clinically meaningful impact in human disease). For TIGIT this data is in line with previously published observations [155, 211], whereas for BTLA and CD200R this is a novel finding and suggests that these receptors do warrant further investigation as targets in cancer immunotherapy.

Chapter 7 General Discussion

Work described in this thesis builds upon previous studies investigating the functional effects of agonistic antibodies targeting immune checkpoint receptors. Whilst most previous work by necessity has focused on the assessment of anti-murine antibodies [75], the transgenic mouse strains characterised here have enabled the evaluation of clinically translatable anti-human antibodies. With a focus on the inhibitory receptor BTLA we have confirmed the therapeutic potential of checkpoint agonists. We have also contributed to defining the physical properties of an antibody that correlate with agonist function, which sheds light on the mechanism of action of these compounds and has important implications for the design of future therapeutics.

7.1. The humanised mice provide a tool for therapeutic antibody assessment

The development of new medicines benefits enormously from the availability of animal models representative of human biology, which provide the opportunity to explore pharmacodynamics and to identify unexpected adverse effects. Despite advances in cell culture systems, the complex interactions of diverse immune cell types in an intact immune system still cannot be replicated *in vitro* [257]. Mice have long served as a preferred model species due to their phylogenetic relatedness to humans, rapid breeding and easy maintenance [258], but in the case of monoclonal antibodies against cell surface proteins, sequence differences between species (and the fact that therapeutic antibodies are often initially made in mice) mean that

antibodies raised against human receptors often do not cross-react with the murine counterpart. In these situations human receptor knock-in mice can enable *in vivo* assessment of non cross-reactive compounds [259] and have for example been used to explore the functional effects of anti-human CTLA4 antibodies [260]. In this thesis, we described three new transgenic mouse strains expressing the human forms of the immune checkpoints BTLA, CD200R and TIGIT. In all three cases the human receptor exhibited cross-species binding to the murine ligand, satisfying the first requirement for these pathways to function in the transgenic mice. For BTLA and TIGIT this cross-species binding had previously been assessed by flow cytometry [166, 186, 209], but we have described for the first time the true affinities assessed by surface plasmon resonance. For CD200R binding of the human receptor to the mouse ligand has not previously been described in the literature. We showed that for all three transgenic strains the inserted chimeric receptor is expressed at the cell surface on appropriate cell types and transcriptionally controlled as expected. Normal development of the immune system, and responses to immune challenge comparable to wildtype mice, suggest that signalling through the checkpoint pathways remains intact, and this was confirmed in the BTLA transgenic mice by the enhanced T-cell proliferation observed in the presence of BTLA blocking antibody. These humanised mouse strains therefore provide valuable models for assessing the effect of checkpoint modulating antibodies, both agonistic and antagonistic. Crossing these three strains onto humanised PD1 mice has further provided the opportunity to assess combinations of antibodies targeting both PD1 and another of these inhibitory receptors.

7.2. BTLA agonist antibodies inhibit immune responses

BTLA was one of the first inhibitory lymphocyte receptors to be described [106] and several subsequent publications have contributed to defining this CD28 family member as an important regulator of T-cell function [189]. Agonistic BTLA antibodies have been described previously and shown to inhibit T-cell responses, particularly CD4 T-cells, *in vitro* [147, 148, 200, 261]. In keeping with these observations, in Chapter 5 we showed that anti-human BTLA agonist antibodies could inhibit CD4 T-cells from the humanised mice. Whereas all previous *in vitro* studies had involved activating T-cells with anti-CD3 or anti-CD28 antibodies, we showed for the first time functional effects of soluble BTLA agonists in a mixed lymphocyte reaction, which represents a more physiological assay of T-cell activation. These experiments also highlighted that the effects of BTLA agonists are context dependent, and contingent on the availability of natural ligand being a limiting factor, as we only saw significant effects when the natural ligand HVEM was blocked. This aligns with a previous study that showed the effects of a BTLA agonist antibody were more striking on immune cells from $HVEM^{-/-}$ mice [200]. This observation has implications for the therapeutic potential of agonistic BTLA antibodies and suggests that optimal disease indications would involve pathological T-cell activation in situations where BTLA is not already maximally engaged by HVEM. The fact that HVEM and BTLA are reciprocally regulated with BTLA increasing on T-cell activation and HVEM decreasing [189] may mean that in inflammatory conditions availability of ligand often is the limiting factor for signalling. Furthermore, it has been argued that BTLA and HVEM can interact in cis on the same cell surface restricting trans-binding [188] and in such a scenario BTLA could be available for artificial triggering by non-blocking agonist antibodies

that was not available for endogenous ligand-induced signalling. Genetic variation in the HVEM gene locus has been linked to autoimmune disease risk [111-114, 262, 263], but it is unclear whether some patients have reduced expression or mutations that affect binding to BTLA, which might render them particularly sensitive to BTLA agonists as a therapeutic intervention.

Anti-mouse BTLA agonists in the literature have also been shown *in vivo* to ameliorate mouse models of GVHD [141, 196] and colitis [200] and to improve cardiac allograft survival [145]. In Chapter 6 we demonstrated that anti-human BTLA agonist antibodies could similarly prevent disease in models of colitis and GVHD using the humanised BTLA mice. Of note, both ligand-blocking and non-blocking antibodies were capable of abrogating disease in the GVHD model, implying that the effect was not dependent on interference with the BTLA-HVEM interaction but a direct effect of antibody on BTLA signalling (having confirmed in Chapter 5 that the antibodies do not deplete BTLA expressing cells). Whilst the difference was not significant there was a trend towards greater effect with the ligand-blocking agonist, suggesting that there could be an additional inhibitory impact of blocking activatory reverse signalling through HVEM. This would be in keeping with previous studies that surprisingly demonstrated the BTLA-HVEM interaction can induce HVEM signalling, despite the fact that HVEM normally triggers via trimerisation following engagement with its trimeric ligand LIGHT [195]. In choosing an agonist BTLA antibody to develop as a therapeutic the potential of a ligand-blocking antibody to provide this additional inhibitory effect would have to be weighed against the risk that in other contexts it might have a counterproductive immune activatory effect by blocking the

endogenous ligand-dependent signalling pathway. This is highlighted in Chapter 5 by the fact that the ligand-blocking BTLA agonist 11.5.1 enhances T-cell proliferation in the MLR when HVEM itself is not blocked. The net effect of an antibody in different situations is likely to depend on the degree of baseline signalling through the pathway and the availability of Fc receptors to support antibody agonism (as discussed in Section 7.3).

Intriguingly, despite exhibiting a similar ability to inhibit CD4 T-cell proliferation, a PD1 agonist antibody did not abrogate disease in the same models of colitis and GVHD. Previously it has been demonstrated that PD1 agonist antibodies induce downregulation of the receptor that might limit their efficacy [162], a phenomenon that we did not observe *in vivo* with BTLA agonists. However, a fast off-rate variant of the PD1 antibody that does not induce significant receptor downregulation was also not able to prevent disease, suggesting that there are other differences between BTLA and PD1 responsible for their different effectiveness as targets. The two receptors clearly have different expression patterns on differentiated T-cell subsets [185] and preferentially inhibit different signalling pathways [264]. Furthermore, the high prevalence of autoimmune adverse events seen with PD1 blockade in the clinic suggests that there is significant signalling through this pathway regulating immune responses at baseline and so it may be that availability of ligand is not a rate-limiting factor and there is little scope for increasing inhibitory pressure on pathological immune responses with an artificial agonist.

Whilst some *in vitro* data suggests that blocking BTLA signalling could enhance anti-tumour T-cell responses [265, 266], antagonist antibodies against this target have not yet enjoyed the clinical success of PD1 or CTLA4 inhibitors in cancer immunotherapy [267]. In Chapter 6 we demonstrated in an MC38 colorectal cancer model that PD1 is particularly effective as a target for checkpoint blockade. As a single agent, an anti-human PD1 blocking antibody had a significant impact on tumour growth in the humanised mice, which was unrivalled by high-affinity blocking antibodies against BTLA, TIGIT or CD200R. This does support the conclusion that PD1 has a unique importance to cancer immunity. However, we did observe additive effects of combining PD1 blockade with an inhibitor of any of the three other receptors, equivalent to the effect of combining with CTLA4 blockade. Even in the most responsive tumour types, a significant fraction of patients still fail to respond to PD1 blockade [267] and so agents that could provide an additive effect would still be of significant therapeutic value.

7.3. Antibody agonism of checkpoint receptors is FcR dependent

Most of the published work assessing immune checkpoint agonists focuses on the functional effects of the agonistic molecules without exploring the fundamental properties of the compounds required for agonism [75]. Experiments in Chapter 5 elucidated some of the physical characteristics of an antibody that contribute to agonist function. Comparison of a wildtype mIgG1 to an FcR non-binding variant in assays of T-cell activation showed that FcR engagement is critical to the agonist action of antibodies against both BTLA and PD1. This observation tallies with the action of agonists against activating immunoreceptors (such as CD3 and CD28) for

which the role of FcR binding is well established [80, 81, 268]. We have assessed antibodies on a mouse IgG1 isotype in the presence of murine Fc receptors. To translate these compounds onto a human isotype, or when developing future inhibitory agonist therapeutics, the selection of an appropriate Fc region will be critically important. In humans (and mice) there are multiple different Fc receptors, the majority of which function as activating receptors via ITAM-dependent signalling, with the sole inhibitory receptor being FcγRIIB [23], which itself is an important regulator of immunity having strong genetic links to autoimmune disease [123]. In the context of trying to develop an immunosuppressive antibody, engagement and triggering of activating Fc receptors would induce a counterproductive immune activatory effect. An Fc region with specificity for FcγRIIB on the other hand would provide the FcR engagement necessary to support agonism whilst inducing an additional inhibitory signal in the FcR-expressing cell, and so would be preferable. Furthermore, in the case of the CD28 superagonist antibody TGN1412, it has recently been shown that different Fc receptors compete for binding to the antibody Fc region and that the high affinity FcγRI sequesters antibody but is not able to support antibody agonism [82], again suggesting that a high ratio of FcγRIIB to FcγRI binding affinity would be beneficial. Finally, it has previously been observed that excessively high affinity for FcγRIIB leads to rapid clearance via liver sinusoidal endothelial cells and so a drastic reduction in antibody serum half-life [269-271]. Therefore the optimal Fc region for a checkpoint agonist might be one that possesses a high ratio of inhibitory to activatory FcR binding without excessively high affinity for FcγRIIB. Much work has previously been carried out to assess the impact of Fc region mutations on FcR binding [272]. Following the observation that TNFRSF agonists

(being widely explored as candidates for cancer immunotherapy) are also dependent on FcγRIIB binding [93], attention has also been paid to identifying mutations that specifically enhance binding to this Fc receptor. Several combinations of mutations have been described that achieve this goal to varying degrees [273] and in the context of TNFRSF agonists have been shown to enhance function [94]. In future work it would be of interest to explore whether such mutations can similarly enhance the effect of immune checkpoint agonistic antibodies. Furthermore, in the case of TNFRSF agonists it has been shown that the structurally constrained hinge variant isoform of human IgG2 can confer FcR independent agonism, perhaps by enhancing clustering of target receptors [95]. Exploring whether this property translates to agonism of immune checkpoint receptors could shed further light on differences in the mechanism of triggering between these two different families of receptor.

Whilst there is significant cross species binding between human antibody isotypes and murine Fc receptors [274], the FcR binding profile of human antibodies in mice would not be representative of the human FcR environment. *In vivo* assessment of humanised antibodies in the presence of a more representative human FcR repertoire could be achieved by crossing our transgenic humanised mice onto mice humanised at the FcR loci [275] or alternatively by the use of severely immunocompromised mice reconstituted with human immune components via haematopoeitic stem cell transfer [276].

The observed requirement for FcR engagement to support antibody agonism also suggests that antibodies may only be able to trigger checkpoint signalling on cell

types that are making contacts with FcR expressing cells. T cells require priming by professional antigen presenting cells which invariably express FcRs [277] and so this stage of the immune response would always be available to target with checkpoint agonists against T-cell inhibitory receptors, though responses of effector differentiated T-cells in the periphery may not be, as these may involve interactions with non-haematopoeitic cells. Other cell types, such as B cells and granulocytes, are not classically described as being so dependent on interactions with FcR expressing cells and so receptors on the surface of these cell types might be harder to trigger with an agonist antibody. However, in reality the immune system is highly dynamic, with cells constantly on the move and continuously interacting with each other [278] and so it is probable that there will always be the availability of FcRs on apposing cell surfaces to support agonistic antibody activity.

7.4. Agonist activity does not require mimicry of ligand binding

In some prior studies in which checkpoint agonists were sought there has been an assumption that in order to trigger receptor an agonist compound must replicate the binding of the natural ligand (i.e. bind to the same epitope with a similar structural interface), an assumption presumably based on the hypothesis that a specific conformational change in the receptor, induced by ligand binding, transmits the signal. For example, Joller *et al* screened TIGIT antibodies for an ability to block ligand binding as a first step in searching for agonists [155]. Similarly, Šedý *et al* identified binding residues on BTLA shared by endogenous ligands and agonist antibodies and hypothesised that these must constitute a functional epitope that can induce signalling when engaged [167]. In marked contrast, in this thesis we have

described BTLA antibodies capable of inducing an agonist signal whilst binding to disparate epitopes on the receptor, and regardless of whether they block endogenous ligand binding or not. This strongly suggests that the antibodies are not functioning by inducing a specific conformational change in the receptor. Of the models for immunoreceptor triggering described in Section 1.4 this would be in fitting with either an aggregation dependent mechanism or a kinetic-segregation (KS) dependent mechanism. The additional observation that immobilisation via Fc receptors is a requirement for agonism is further support that agonism can be explained by an extension of the KS model, in which all that is required for triggering is trapping of the receptor between two apposing cell surfaces in a contact zone narrow enough to exclude receptor-type phosphatases. To further discriminate between the different possible mechanisms of antibody induced triggering it would be of value to explore whether a monovalent antibody-like construct could trigger signalling, as such as compound would still be able to act with a KS mechanism but could not cause aggregation of receptors.

7.5. Agonism of checkpoints is sensitive to antibody dimensions

If the hypothesis is correct that checkpoint antibody agonism can be explained by an extension of the kinetic segregation model, then it would be expected that agonist activity would be sensitive to the dimensions of the complex formed between receptor, antibody and Fc receptor on the apposing cell. In Chapter 5 we demonstrated that reducing the physical size of an agonist antibody can indeed lead to more effective agonist activity and we propose that this is likely due to more effective exclusion of phosphatases due to a more compact contact zone when

immobilised antibody engages the receptor. Conversely, we showed that extending the length of an antibody can remove its agonist function. These observations are strongly supportive of an explanation for antibody agonism based on the KS model, as changing the dimensions of the antibody would not be expected to affect its ability to either induce receptor aggregation or induce a conformational change.

For receptors such as BTLA and PD1 which have small, single IgSF domain-containing extracellular regions it is not surprising that antibodies binding anywhere on the receptor could create a compact enough complex to exclude phosphatases when immobilised. However, for receptors with much large extracellular domains, antibodies with the necessary epitope position to create such a small complex would be somewhat rarer. In future work, comparison of antibodies against a larger ITIM containing receptor (for example Siglec 2 that has 7 IgSF extracellular domains) could explore whether antibodies binding to the membrane proximal domain have enhanced agonistic activity compared to those binding to the membrane distal domain. In a similar vein it has previously been observed that CAR-T cells and bispecific T-cell engagers (BiTEs), which both work by artificially triggering an ITAM containing activating immunoreceptor, are more effective when targeting receptors with small extracellular domains or when targeting membrane proximal epitopes on larger receptors [71, 72].

7.6. Efficacy of checkpoint inhibitors could be limited by agonist activity

PD1 blocking antibodies have revolutionised the treatment of multiple cancer types but there remains a significant fraction of patients that do not respond [267]. Whilst these agents do induce a range of autoimmune side effects, they are generally well tolerated compared to cytotoxic chemotherapy. Given the severity of the underlying disease indications additional toxicity would likely be tolerable in exchange for additional efficacy, as highlighted by the fact that many patients are prescribed combined PD1 and CTLA4 blockade despite a disproportionate increase in adverse effects compared to anti-tumour response [279]. With this in mind, we were intrigued to observe that PD1 blocking antibodies, if expressed on an FcR binding mIgG1 isotype, could lead in some contexts to a paradoxical reduction in T-cell expansion suggesting suboptimal blockade of the pathway. Given the findings discussed above, it is not surprising for a small receptor like PD1 that even ligand-blocking antibodies could deliver an agonist signal, and that this might counteract the effect of blocking the native ligand interaction. The most widely used PD1 blockers in the clinic (Nivolumab and Pembrolizumab) are both IgG4 isotype antibodies [280] which, although selected due to low effector function, are still capable of binding FcRs [281]. Given that the CD28 superagonist TGN1412 is also an IgG4 isotype, this degree of FcR binding is clearly sufficient to support antibody agonism. Therefore, it is possible that these PD1 blocking agents are not achieving optimal blockade of the pathway and could be improved by engineering approaches to remove their agonist capacity.

7.7. Concluding remarks

In this thesis we have begun to explore the potential of checkpoint agonist antibodies, focusing on the receptors BTLA and PD1. The antibody characteristics that we have defined as being important for agonist function are in keeping with a mechanism of receptor triggering that is an extension of the kinetic-segregation model. These mechanistic insights can help to direct the rational design and optimisation of future drug candidates. We have characterised the tools necessary to expand this work to the receptors TIGIT and CD200R in the first instance, but this approach is potentially much more broadly applicable still, with very many more immunoreceptors available to target, both inhibitory receptors for the treatment of autoimmunity and activatory targets in the context of cancer immunotherapy [45]. Each unique target represents a potential switch to manipulate different elements of the immune response depending on the receptor's expression and function. A key advantage of a checkpoint agonist, in contrast to conventional antagonist based therapies, is that the targeted pathway does not need to be contributing to disease pathogenesis for the agent to be therapeutically beneficial. Rather than correcting specific abnormalities in the inflammatory cascade this approach seeks to enhance physiological regulatory signalling and to increase inhibitory pressure on the immune response, harnessing the system's natural control mechanisms in a way that few other therapeutics currently do.

Chapter 8 Appendix

8.1. Sequences of chimeric transcripts expressed in the transgenic mice

Key:

Blue highlighting: murine sequence

No highlighting: human sequence

Grey highlighting: exon-exon junction between these base pairs

8.1.1. BTLA

```
  1 ATGAAGACAGTGCCTGCCATGCTTGGGACTCCTCGGTTATTTAGGGAATTCTTCATCCTC
  1 -M--K--T--V--P--A--M--L--G--T--P--R--L--F--R--E--F--F--I--L-

 61 CATCTGGGCCTCTGGAGCATCCTTTGTGAGAAAGCTACTAAGAGGAATGATGAAGAGTGT
 21 -H--L--G--L--W--S--I--L--C--E--K--A--T--K--R--N--D--E--E--C-

121 GATGTACAGCTTTATATAAAGAGACAATCTGAACACTCCATCTTAGCAGGAGATCCCTTT
 41 -D--V--Q--L--Y--I--K--R--Q--S--E--H--S--I--L--A--G--D--P--F-

181 GAACTAGAATGCCCTGTGAAATACTGTGCTAACAGGCCTCATGTGACTTGGTGCAAGCTC
 61 -E--L--E--C--P--V--K--Y--C--A--N--R--P--H--V--T--W--C--K--L-

241 AATGGAACAACATGTGTAAAACTTGAAGATAGACAAACAAGTTGGAAGGAAGAGAAGAAC
 81 -N--G--T--T--C--V--K--L--E--D--R--Q--T--S--W--K--E--E--K--N-

301 ATTTCATTTTTCATTCTACATTTTGAACCAGTGCTTCCTAATGACAATGGGTCATACCGC
101 -I--S--F--F--I--L--H--F--E--P--V--L--P--N--D--N--G--S--Y--R-

361 TGTTCTGCAAATTTTCAGTCTAATCTCATTGAAAGCCACTCAACAACTCTTTATGTGACA
121 -C--S--A--N--F--Q--S--N--L--I--E--S--H--S--T--T--L--Y--V--T-

421 GATGTAAAAAGTGCCTCAGAACGACCCTCCAAGGACGAAATGGCAAGCAGACCCTGGCTC
141 -D--V--K--S--A--S--E--R--P--S--K--D--E--M--A--S--R--P--W--L-

481 CTGTATCGTTTGCTTCCTTTGGGGGCATTGCTTCTGCTCCTTGCCTGTGTCTGCCTGCTC
161 -L--Y--R--L--L--P--L--G--A--L--L--L--L--A--C--V--C--L--L-

541 TGCTTTCTGAAAAGGATCCAAGGGAAAGAAAAGAAGCCTTCTGACTTGGCAGGAAGGGAC
181 -C--F--L--K--R--I--Q--G--K--E--K--K--P--S--D--L--A--G--R--D-

601 ACTAACCTGGTTGATATTCCAGCCAGTTCCAGGACAAATCACCAAGCACTGCCATCAGGA
201 -T--N--L--V--D--I--P--A--S--S--R--T--N--H--Q--A--L--P--S--G-

661 ACTGGAATTTATGATAATGATCCCTGGTCTAGCATGCAGGATGAATCTGAATTGACAATT
221 -T--G--I--Y--D--N--D--P--W--S--S--M--Q--D--E--S--E--L--T--I-

721 AGCTTGCAATCAGAGAGAAACAACCAGGGCATTGTTTATGCTTCTTTGAACCATTGTGTT
241 -S--L--Q--S--E--R--N--N--Q--G--I--V--Y--A--S--L--N--H--C--V-

781 ATTGGAAGGAATCCAAGACAGGAAAACAACATGCAGGAGGCACCCACAGAATATGCATCC
261 -I--G--R--N--P--R--Q--E--N--N--M--Q--E--A--P--T--E--Y--A--S-

841 ATTTGTGTGAGAAGTTAA
281 -I--C--V--R--S--*-
```

8.1.2. TIGIT

```
  1 ATGCATGGCTGGCTGCTCCTGGTCTGGGTCCAGGGGCTGATACAGGCTGCCTTCCTCGCT
  1 -M--H--G--W--L--L--L--V--W--V--Q--G--L--I--Q--A--A--F--L--A-

 61 ACAGGAGCCACAGCAGGCACGATAGAAACAACGGGGAACATTTCTGCAGAGAAAGGTGGC
 21 -T--G--A--T--A--G--T--I--E--T--T--G--N--I--S--A--E--K--G--G-

121 TCTATCATCTTACAATGTCACCTCTCCTCCACCACGGCACAAGTGACCCAGGTCAACTGG
 41 -S--I--I--L--Q--C--H--L--S--S--T--T--A--Q--V--T--Q--V--N--W-

181 GAGCAGCAGGACCAGCTTCTGGCCATTTGTAATGCTGACTTGGGGTGGCACATCTCCCCA
 61 -E--Q--Q--D--Q--L--L--A--I--C--N--A--D--L--G--W--H--I--S--P-

241 TCCTTCAAGGATCGAGTGGCCCCAGGTCCCGGCCTGGGCCTCACCCTCCAGTCGCTGACC
 81 -S--F--K--D--R--V--A--P--G--P--G--L--G--L--T--L--Q--S--L--T-

301 GTGAACGATACAGGGGAGTACTTCTGCATCTATCACACCTACCCTGATGGGACGTACACT
101 -V--N--D--T--G--E--Y--F--C--I--Y--H--T--Y--P--D--G--T--Y--T-

361 GGGAGAATCTTCCTGGAGGTCCTAGAAAGCTCAGTGGCTCAGTTCCAGACTGCCCCGCTT
121 -G--R--I--F--L--E--V--L--E--S--S--V--A--Q--F--Q--T--A--P--L-

421 GGAGGAACCATGGCTGCTGTGCTGGGACTCATTTGCTTAATGGTCACAGGAGTGACTGTA
141 -G--G--T--M--A--A--V--L--G--L--I--C--L--M--V--T--G--V--T--V-

481 CTGGCTAGAAAGAAGTCTATTAGAATGCATTCTATAGAAAGTGGCCTTGGGAGAACAGAA
161 -L--A--R--K--K--S--I--R--M--H--S--I--E--S--G--L--G--R--T--E-

541 GCGGAGCCACAGGAATGGAACCTGAGGAGTCTCTCATCCCCTGGAAGCCCTGTCCAGACA
181 -A--E--P--Q--E--W--N--L--R--S--L--S--S--P--G--S--P--V--Q--T-

601 CAAACTGCCCCTGCTGGTCCCTGTGGAGAGCAGGCAGAAGATGACTATGCTGACCCACAG
201 -Q--T--A--P--A--G--P--C--G--E--Q--A--E--D--D--Y--A--D--P--Q-

661 GAATACTTTAATGTCCTGAGCTACAGAAGCCTAGAGAGCTTCATTGCTGTATCGAAGACT
221 -E--Y--F--N--V--L--S--Y--R--S--L--E--S--F--I--A--V--S--K--T-

721 GGCTAA
241 -G--*-
```

8.1.3. CD200R

```
  1 ATGTTTTGCTTTTGGAGAACTTCTGCCCTAGCAGTGCTCTTAATATGGGGGGTCTTTGTG
  1 -M--F--C--F--W--R--T--S--A--L--A--V--L--L--I--W--G--V--F--V-

 61 GCTGGGTCAAGTTGTACTGATAAGAATCAAACAACACAGAACTACTCGAAAGTACTCGCA
 21 -A--G--S--S--C--T--D--K--N--Q--T--T--Q--N--Y--S--K--V--L--A-

121 GAAGTTAACACTTCATGGCCTGTAAAGATGGCTACAAATGCTGTGCTTTGTTGCCCTCCT
 41 -E--V--N--T--S--W--P--V--K--M--A--T--N--A--V--L--C--C--P--P-

181 ATCGCATTAAGAAATTTGATCATAATAACATGGGAAATAATCCTGAGAGGCCAGCCTTCC
 61 -I--A--L--R--N--L--I--I--I--T--W--E--I--I--L--R--G--Q--P--S-

241 TGCACAAAAGCCTACAAGAAAGAAACAAATGAGACCAAGGAAACCAACTGTACTGATGAG
 81 -C--T--K--A--Y--K--K--E--T--N--E--T--K--E--T--N--C--T--D--E-

301 AGAATAACCTGGGTCTCCAGACCTGATCAGAATTCGGACCTTCAGATTCGTACCGTGGCC
101 -R--I--T--W--V--S--R--P--D--Q--N--S--D--L--Q--I--R--T--V--A-

361 ATCACTCATGACGGGTATTACAGATGCATAATGGTAACACCTGATGGGAATTTCCATCGT
121 -I--T--H--D--G--Y--Y--R--C--I--M--V--T--P--D--G--N--F--H--R-

421 GGATATCACCTCCAAGTGTTAGTTACACCTGAAGTGACCCTGTTTCAAAACAGGAATAGA
141 -G--Y--H--L--Q--V--L--V--T--P--E--V--T--L--F--Q--N--R--N--R-

481 ACTGCAGTATGCAAGGCAGTTGCAGGGAAGCCAGCTGCGCATATCTCCTGGATCCCAGAG
161 -T--A--V--C--K--A--V--A--G--K--P--A--A--H--I--S--W--I--P--E-

541 GGCGATTGTGCCACTAAGCAAGAATACTGGAGCAATGGCACAGTGACTGTTAAGAGTACA
181 -G--D--C--A--T--K--Q--E--Y--W--S--N--G--T--V--T--V--K--S--T-

601 TGCCACTGGGAGGTCCACAATGTGTCTACCGTGACCTGCCACGTCTCCCATTTGACTGGC
201 -C--H--W--E--V--H--N--V--S--T--V--T--C--H--V--S--H--L--T--G-

661 AACAAGAGTCTGTACATAGAACTGAGTAGAGGTGGTAACCAATCATTACGACCATATATT
221 -N--K--S--L--Y--I--E--L--S--R--G--G--N--Q--S--L--R--P--Y--I-

721 CCATACATCATACCATCAATTATCATTTTGATCATCATAGGATGCATTTGTCTTTTGAAA
241 -P--Y--I--I--P--S--I--I--I--L--I--I--I--G--C--I--C--L--L--K-

781 ATCAGTGGCTTCAGAAAATGCAAATTGCCAAAATTAGAAGCTACTTCAGCTATTGAGGAG
261 -I--S--G--F--R--K--C--K--L--P--K--L--E--A--T--S--A--I--E--E-

841 GATGAAATGCAGCCTTATGCTAGCTATACAGAGAAGAGCAATCCACTCTATGATACTGTG
281 -D--E--M--Q--P--Y--A--S--Y--T--E--K--S--N--P--L--Y--D--T--V-

901 ACTAAGGTGGAGGCATTTCCAGTATCACAAGGCGAAGTCAATGGCACAGACTGCCTTACT
301 -T--K--V--E--A--F--P--V--S--Q--G--E--V--N--G--T--D--C--L--T-

961 TTGTCGGCCATTGGAATCTAG
321 -L--S--A--I--G--I--*-
```

8.2. Sequences of soluble proteins used for surface plasmon resonance

KOZAK sequence CTCAAGCAGGCCACC (from rat CD4 UTR) used for all proteins.

Predicted signal peptides highlighted in yellow.

Relevant ECD in red.

Additional tag sequence in blue.

8.2.1. hCD200RmFc-His

MLCPWRTANLGLLLILTIFLVAASSSLCMDEKQITQNYSKVLAEVNTSWPVKMATNAVLCC
PPIALRNLIIITWEIILRGQPSCTKAYKKETNETKETNCTDERITWVSRPDQNSDLQIRTVAIT
HDGYYRCIMVTPDGNFHRGYHLQVLVTPEVTLFQNRNRTAVCKAVAGKPAAHISWIPEGD
CATKQEYWSNGTVTVKSTCHWEVHNVSTVTCHVSHLTGNKSLYIELLPVPGAKKSAKLVP
RGSGSKPSISTVPEVSSVFIFPPKPKDVLTITLTPKVTCVVVDISKDDPEVQFSWFVDDVEVH
TAQTQPREEQFNSTFRSVSELPIMHQDWLNGKEFKCRVNSAAFPAPIEKTISKTKGRPKAP
QVYTIPPPKEQMAKDKVSLTCMITDFFPEDITVEWQWNGQPAENYKNTQPIMDTDGSYFV
YSKLNVQKSNWEAGNTFTCSVLHEGLHNHHTEKSLSHSPGKHHHHHH-

8.2.2. mCD200RmFc-His

MFCFWRTSALAVLLIWGVFVAGSSCTDKNQTTQNNSSSPLTQVNTTVSVQIGTKALLCCFSI
PLTKAVLITWIIKLRGLPSCTIAYKVDTKTNETSCLGRNITWASTPDHSPELQISAVTLQHEG
TYTCETVTPEGNFEKNYDLQVLVPPEVTYFPEKNRSAVCEAMAGKPAAQISWSPDGDCVTT
SESHSNGTVTVRSTCHWEQNNVSDVSCIVSHLTGNQSLSIELSRGGNQSLRPLVPRGSGSKP
SISTVPEVSSVFIFPPKPKDVLTITLTPKVTCVVVDISKDDPEVQFSWFVDDVEVHTAQTQPR
EEQFNSTFRSVSELPIMHQDWLNGKEFKCRVNSAAFPAPIEKTISKTKGRPKAPQVYTIPPP
KEQMAKDKVSLTCMITDFFPEDITVEWQWNGQPAENYKNTQPIMDTDGSYFVYSKLNVQ
KSNWEAGNTFTCSVLHEGLHNHHTEKSLSHSPGKHHHHHH-

8.2.3. hTIGITmFC-His

MRWCLLLIWAQGLRQAPLASGMMTGTIETTGNISAEKGGSIILQCHLSSTTAQVTQVNWEQ
QDQLLAICNADLGWHISPSFKDRVAPGPGLGLTLQSLTVNDTGEYFCIYHTYPDGTYTGRIF
LEVLESSVAEHGARFQIPLVPRGSGSKPSISTVPEVSSVFIFPPKPKDVLTITLTPKVTCVVVDI
SKDDPEVQFSWFVDDVEVHTAQTQPREEQFNSTFRSVSELPIMHQDWLNGKEFKCRVNSA
AFPAPIEKTISKTKGRPKAPQVYTIPPPKEQMAKDKVSLTCMITDFFPEDITVEWQWNGQP
AENYKNTQPIMDTDGSYFVYSKLNVQKSNWEAGNTFTCSVLHEGLHNHHTEKSLSHSPGK
HHHHHH-

8.2.4. mTIGITmFc-His

MHGWLLLVWVQGLIQAAFLATAIGATAGTIDTKRNISAEEGGSVILQCHFSSDTAEVTQVD
WKQQDQLLAIYSVDLGWHVASVFSDRVVPGPSLGLTFQSLTMNDTGEYFCTYHTYPGGIYK
GRIFLKVQESSDDRNGLAQFQTAPLGLVPRGSGSKPSISTVPEVSSVFIFPPKPKDVLTITLTP
KVTCVVVDISKDDPEVQFSWFVDDVEVHTAQTQPREEQFNSTFRSVSELPIMHQDWLNGK
EFKCRVNSAAFPAPIEKTISKTKGRPKAPQVYTIPPPKEQMAKDKVSLTCMITDFFPEDITVE

WQWNGQPAENYKNTQPIMDTDGSYFVYSKLNVQKSNWEAGNTFTCSVLHEGLHNHHTE
KSLSHSPGKHHHHHH-

8.2.5. His-hTIGIT (bacterial expression and refold)

HHHHHHSSGLVPRGSHMMTGTIETTGNISAEKGGSIILQCHLSSTTAQVTQVNWEQQDQLL
AICNADLGWHISPSFKDRVAPGPGLGLTLQSLTVNDTGEYFCIYHTYPDGTYTGRIFLEVLE-

8.2.6. His-hTIGIT-BirA (bacterial expression and refold)

HHHHHHSSGLVPRGSHMMTGTIETTGNISAEKGGSIILQCHLSSTTAQVTQVNWEQQDQLL
AICNADLGWHISPSFKDRVAPGPGLGLTLQSLTVNDTGEYFCIYHTYPDGTYTGRIFLEVLEG
GSGGSGLNDIFEAQKIEWHEGRTLE-

8.2.7. His-mTIGIT (bacterial expression and refold)

HHHHHHSSGLVPRGSHTIDTKRNISAEEGGSVILQCHFSSDTAEVTQVDWKQQDQLLAIYSV
DLGWHVASVFSDRVVPGPSLGLTFQSLTMNDTGEYFCTYHTYPGGIYKGRIFLKVQESSDDR
NGLAQFQTAPLG-

8.2.8. hBTLAmFc-His

MKTLPAMLGTGKLFWVFFLIPYLDIWNIHGKESCDVQLYIKRQSEHSILAGDPFELECPVKY
CANRPHVTWCKLNGTTCVKLEDRQTSWKEEKNISFFILHFEPVLPNDNGSYRCSANFQSNL
IESHSTTLYVTDVKSASERPSKDEMASRLVPRGSGSKPSISTVPEVSSVFIFPPKPKDVLTITL
TPKVTCVVVDISKDDPEVQFSWFVDDVEVHTAQTQPREEQFNSTFRSVSELPIMHQDWLN
GKEFKCRVNSAAFPAPIEKTISKTKGRPKAPQVYTIPPPKEQMAKDKVSLTCMITDFFPEDIT
VEWQWNGQPAENYKNTQPIMDTDGSYFVYSKLNVQKSNWEAGNTFTCSVLHEGLHNHH
TEKSLSHSPGKHHHHHH-

8.2.9. mBTLAmFc-His

MKTVPAMLGTPRLFREFFILHLGLWSILCEKATKRNDEECPVQLTITRNSKQSARTGELFKI
QCPVKYCVHRPNVTWCKHNGTICVPLEVSPQLYTSWEENQSVPVFVLHFKPIHLSDNGSYS
CSTNFNSQVINSHSVTIHVTERTQNSSEHPLITVSDIPDATNASGPSTMEERPGRLVPRGSGS
KPSISTVPEVSSVFIFPPKPKDVLTITLTPKVTCVVVDISKDDPEVQFSWFVDDVEVHTAQTQ
PREEQFNSTFRSVSELPIMHQDWLNGKEFKCRVNSAAFPAPIEKTISKTKGRPKAPQVYTIP
PPKEQMAKDKVSLTCMITDFFPEDITVEWQWNGQPAENYKNTQPIMDTDGSYFVYSKLNV
QKSNWEAGNTFTCSVLHEGLHNHHTEKSLSHSPGKHHHHHH-

8.2.10. hBTLA-His-BirA (bacterial expression and refold)

MSCDVQLYIKRQSEHSILAGDPFELECPVKYCANRPHVTWCKLNGTTCVKLEDRQTSWKEE
KNISFFILHFEPVLPNDNGSYRCSANFQSNLIESHSTTLYVTDVKHHHHHHHHGSGGSGLND
IFEAQKIEWHEGRT-

8.2.11. hHVEMmFc-His

MEPPGDWGPPPWRSTPRTDVLRLVLYLTFLGAPCYAPALPSCKEDEYPVGSECCPKCSPGY
RVKEACGELTGTVCEPCPPGTYIAHLNGLSKCLQCQMCDPAMGLRASRNCSRTENAVCGCS
PGHFCIVQDGDHCAACRAYATSSPGQRVQKGGTESQDTLCQNCPPGTFSPNGTLEECQHQT
KCSWLVTKAGAGTSSSHLVPRGSGSKPSISTVPEVSSVFIFPPKPKDVLTITLTPKVTCVVVDI
SKDDPEVQFSWFVDDVEVHTAQTQPREEQFNSTFRSVSELPIMHQDWLNGKEFKCRVNSA
AFPAPIEKTISKTKGRPKAPQVYTIPPPKEQMAKDKVSLTCMITDFFPEDITVEWQWNGQP
AENYKNTQPIMDTDGSYFVYSKLNVQKSNWEAGNTFTCSVLHEGLHNHHTEKSLSHSPGK
HHHHHH-

8.2.12. mHVEMmFc-His

MEPLPGWGSAPWSQAPTDNTFRLVPCVFLLNLLQRISAQPSCRQEEFLVGDECCPMCNPGY
HVKQVCSEHTGTVCAPCPPQTYTAHANGLSKCLPCGVCDPDMGLLTWQECSSWKDTVCRC
IPGYFCENQDGSHCSTCLQHTTCPPGQRVEKRGTHDQDTVCADCLTGTFSLGGTQEECLPW
TNCSAFQQEVRRGTNSTDTTCSSQLVPRGSGSKPSISTVPEVSSVFIFPPKPKDVLTITLTPKV
TCVVVDISKDDPEVQFSWFVDDVEVHTAQTQPREEQFNSTFRSVSELPIMHQDWLNGKEF
KCRVNSAAFPAPIEKTISKTKGRPKAPQVYTIPPPKEQMAKDKVSLTCMITDFFPEDITVEW
QWNGQPAENYKNTQPIMDTDGSYFVYSKLNVQKSNWEAGNTFTCSVLHEGLHNHHTEKS
LSHSPGKHHHHHH-

8.2.13. hPVR-BirA-His

MARAMAAAWPLLLVALLVLSWPPPGTGDVVVQAPTQVPGFLGDSVTLPCYLQVPNMEVT
HVSQLTWARHGESGSMAVFHQTQGPSYSESKRLEFVAARLGAELRNASLRMFGLRVEDEG
NYTCLFVTFPQGSRSVDIWLRVLAKPQNTAEVQKVQLTGEPVPMARCVSTGGRPPAQITW
HSDLGGMPNTSQVPGFLSGTVTVTSLWILVPSSQVDGKNVTCKVEHESFEKPQLLTVNLTV
YYPPEVSISGYDNNWYLGQNEATLTCDARSNPEPTGYNWSTTMGPLPPFAVAQGAQLLIRP
VDKPINTTLICNVTNALGARQAELTVQVKEGPPSEHSGMSRNLEGGSGGSGLNDIFEAQKIE
WHHHHHH-

8.2.14. mPVR-BirA-His

MAQLARATRSPLSWLLLLFCYALRKAGGDIRVLVPYNSTGVLGGSTTLHCSLTSNENVTITQ
ITWMKKDSGGSHALVAVFHPKKGPNIKEPERVKFLAAQQDLRNASLAISNLSVEDEGIYECQ
IATFPRGSRSTNAWLKVQARPKNTAEALEPSPTLILQDVAKCISANGHPPGRISWPSNVNGS
HREMKEPGSQPGTTTVTSYLSMVPSRQADGKNITCTVEHESLQELDQLLVTLSQPYPPENV
SISGYDGNWYVGLTNLTLTCEAHSKPAPDMAGYNWSTNTGDFPNSVKRQGNMLLISTVED
GLNNTVIVCEVTNALGSGQGQVHIIVKEKPENMQQNTRLHLEGGSGGSGLNDIFEAQKIEW
HEGRTKHHHHHH-

8.2.15. hCD200-BirA-His

MERLVIRMPFCHLSTYSLVWVMAAVVLCTAQVQVVTQDEREQLYTPASLKCSLQNAQEALI
VTWQKKKAVSPENMVTFSENHGVVIQPAYKDKINITQLGLQNSTITFWNITLEDEGCYMCL
FNTFGFGKISGTACLTVYVQPIVSLHYKFSEDHLNITCSATARPAPMVFWKVPRSGIEDSTVT

LSHPNGTTSVTSILHIKDPKNQVGKEVICQVLHLGTVTDSKQTVNKGLEGGSGGSGLNDIFE
AQKIEWHEGRTKHHHHHH-

8.2.16. mCD200-BirA-His

MGSLVFRRPFCHLSTYSLIWGIAAVALSTAQVEVVTQDERKALHTTASLRCSLKTSQEPLIVT
WQKKKAVSPENMVTYSKTHGVVIQPAYKDRINVTELGLWNSSITFWNTHIGDGGCYMCLF
NTFGSQKVSGTACLTLYVQPIVHLHYNYFEHHLNITCSATARPAPAITWKGTGTGIENSTES
HFHSNGTTSVTSILRVKDPKTQVGKEVICQVLYLGNVIDYKQSLDKGLEGGSGGSGLNDIFEA
QKIEWHEGRTKHHHHHH-

8.3. Constructs for epitope mapping

8.3.1. Wildtype hBTLAmCD28-GFP² (cloned into pGFP²-N3 vector)

MKTLPAMLGTGKLFWVFFLIPYLDIWNIHGKESCDVQLYIKRQSEHSILAGDPFELECPVKY
CANRPHVTWCKLNGTTCVKLEDRQTSWKEEKNISFFILHFEPVLPNDNGSYRCSANFQSNL
IESHSTTLYVTDVKSASERPSKDEMASRPWLLYSLLPLGGLPLLITTCFCLFCCLRRNRLLQS
DYMNMTPRRPGLTRKPYQPYAPARDFAAYRPGVPRARDPPVATMVSKGEELFTGVVPILV
ELDGDVNGHKFSVSGEGEGDATYGKLTLKFICTTGKLPVPWPTLVTTLSYGVQCFSRYPDH
MKQHDFFKSAMPEGYVQERTIFFKDDGNYKTRAEVKFEGDTLVNRIELKGIDFKEDGNILG
HKLEYNYNSHNVYIMADKQKNGIKVNFKIRHNIEDGSVQLADHYQQNTPIGDGPVLLPDNH
YLSTQSALSKDPNEKRDHMVLLEFVTAAGITLGMDELYK-

8.3.2. Wildtype hTIGITmCD28-GFP²

MRWCLLLIWAQGLRQAPLASGMMTGTIETTGNISAEKGGSIILQCHLSSTTAQVTQVNWEQ
QDQLLAICNADLGWHISPSFKDRVAPGPGLGLTLQSLTVNDTGEYFCIYHTYPDGAYTGRIF
LEVLESSVAEHGARFQIPFWALVVVAGVLFCYGLLVTVALCVIWTNSRRNRLLQSDYMNMT
PRRPGLTRKPYQPYAPARDFAAYRPGVPRARDPPVATMVSKGEELFTGVVPILVELDGDVN
GHKFSVSGEGEGDATYGKLTLKFICTTGKLPVPWPTLVTTLSYGVQCFSRYPDHMKQHDFF
KSAMPEGYVQERTIFFKDDGNYKTRAEVKFEGDTLVNRIELKGIDFKEDGNILGHKLEYNY
NSHNVYIMADKQKNGIKVNFKIRHNIEDGSVQLADHYQQNTPIGDGPVLLPDNHYLSTQSA
LSKDPNEKRDHMVLLEFVTAAGITLGMDELYK-

8.3.3. Wildtype hCD200RmCD28-GFP²

MLCPWRTANLGLLLILTIFLVAASSSLCMDEKQITQNYSKVLAEVNTSWPVKMATNAVLCC
PPIALRNLIIITWEIILRGQPSCTKAYKKETNETKETNCTDERITWVSRPDQNSDLQIRTVAIT
HDGYYRCIMVTPDGNFHRGYHLQVLVTPEVTLFQNRNRTAVCKAVAGKPAAHISWIPEGD
CATKQEYWSNGTVTVKSTCHWEVHNVSTVTCHVSHLTGNKSLYIELLPVPGAKKSAKLFW
ALVVVAGVLFCYGLLVTVALCVIWTNSRRNRLLQSDYMNMTPRRPGLTRKPYQPYAPARD
FAAYRPGVPRARDPPVATMVSKGEELFTGVVPILVELDGDVNGHKFSVSGEGEGDATYGKL
TLKFICTTGKLPVPWPTLVTTLSYGVQCFSRYPDHMKQHDFFKSAMPEGYVQERTIFFKDD
GNYKTRAEVKFEGDTLVNRIELKGIDFKEDGNILGHKLEYNYNSHNVYIMADKQKNGIKVN
FKIRHNIEDGSVQLADHYQQNTPIGDGPVLLPDNHYLSTQSALSKDPNEKRDHMVLLEFVT
AAGITLGMDELYK-

Chapter 9 References

1. Parkin, J. and B. Cohen, *An overview of the immune system.* Lancet, 2001. **357**(9270): p. 1777-89.
2. Waldmann, H., *Immunological Tolerance*, in *Reference Module in Biomedical Sciences*. 2014, Elsevier.
3. Hayter, S.M. and M.C. Cook, *Updated assessment of the prevalence, spectrum and case definition of autoimmune disease.* Autoimmun Rev, 2012. **11**(10): p. 754-65.
4. Murphy, K., et al., *Janeway's immunobiology*. 8th ed. 2012, New York: Garland Science.
5. Sarma, J.V. and P.A. Ward, *The complement system.* Cell Tissue Res, 2011. **343**(1): p. 227-35.
6. Massberg, S., et al., *Reciprocal coupling of coagulation and innate immunity via neutrophil serine proteases.* Nat Med, 2010. **16**(8): p. 887-96.
7. Bhoola, K.D., C.D. Figueroa, and K. Worthy, *Bioregulation of kinins: kallikreins, kininogens, and kininases.* Pharmacol Rev, 1992. **44**(1): p. 1-80.
8. Pålsson-McDermott, E.M. and L.A. O'Neill, *Signal transduction by the lipopolysaccharide receptor, Toll-like receptor-4.* Immunology, 2004. **113**(2): p. 153-62.
9. Mogensen, T.H., *Pathogen recognition and inflammatory signaling in innate immune defenses.* Clin Microbiol Rev, 2009. **22**(2): p. 240-73, Table of Contents.
10. Brandt, V.L. and D.B. Roth, *G.O.D.'s Holy Grail: discovery of the RAG proteins.* J Immunol, 2008. **180**(1): p. 3-4.
11. Neefjes, J., et al., *Towards a systems understanding of MHC class I and MHC class II antigen presentation.* Nat Rev Immunol, 2011. **11**(12): p. 823-36.
12. Joffre, O.P., et al., *Cross-presentation by dendritic cells.* Nat Rev Immunol, 2012. **12**(8): p. 557-69.
13. Zhang, N. and M.J. Bevan, *CD8(+) T cells: foot soldiers of the immune system.* Immunity, 2011. **35**(2): p. 161-8.
14. Strasser, A., P.J. Jost, and S. Nagata, *The many roles of FAS receptor signaling in the immune system.* Immunity, 2009. **30**(2): p. 180-92.
15. Green, A.M., R. Difazio, and J.L. Flynn, *IFN-γ from CD4 T cells is essential for host survival and enhances CD8 T cell function during Mycobacterium tuberculosis infection.* J Immunol, 2013. **190**(1): p. 270-7.
16. Raphael, I., et al., *T cell subsets and their signature cytokines in autoimmune and inflammatory diseases.* Cytokine, 2015. **74**(1): p. 5-17.
17. Gatto, D. and R. Brink, *The germinal center reaction.* J Allergy Clin Immunol, 2010. **126**(5): p. 898-907; quiz 908-9.
18. Schroeder, H.W., Jr. and L. Cavacini, *Structure and function of immunoglobulins.* J Allergy Clin Immunol, 2010. **125**(2 0 2): p. S41-52.
19. Gasper, D.J., M.M. Tejera, and M. Suresh, *CD4 T-cell memory generation and maintenance.* Crit Rev Immunol, 2014. **34**(2): p. 121-46.
20. Davis, A.C. and M.J. Shulman, *IgM--molecular requirements for its assembly and function.* Immunol Today, 1989. **10**(4): p. 118-22; 127-8.
21. Phalipon, A., et al., *Secretory component: a new role in secretory IgA-mediated immune exclusion in vivo.* Immunity, 2002. **17**(1): p. 107-15.

22. Galli, S.J. and M. Tsai, *IgE and mast cells in allergic disease.* Nat Med, 2012. **18**(5): p. 693-704.
23. Bruhns, P., *Properties of mouse and human IgG receptors and their contribution to disease models.* Blood, 2012. **119**(24): p. 5640-9.
24. Veri, M.C., et al., *Monoclonal antibodies capable of discriminating the human inhibitory Fcgamma-receptor IIB (CD32B) from the activating Fcgamma-receptor IIA (CD32A): biochemical, biological and functional characterization.* Immunology, 2007. **121**(3): p. 392-404.
25. Nimmerjahn, F. and J.V. Ravetch, *Divergent immunoglobulin g subclass activity through selective Fc receptor binding.* Science, 2005. **310**(5753): p. 1510-2.
26. Ghetie, V. and E.S. Ward, *Multiple roles for the major histocompatibility complex class I- related receptor FcRn.* Annu Rev Immunol, 2000. **18**: p. 739-66.
27. Goodnow, C.C., et al., *Cellular and genetic mechanisms of self tolerance and autoimmunity.* Nature, 2005. **435**(7042): p. 590-7.
28. Nemazee, D., *Mechanisms of central tolerance for B cells.* Nat Rev Immunol, 2017. **17**(5): p. 281-294.
29. Xing, Y. and K.A. Hogquist, *T-cell tolerance: central and peripheral.* Cold Spring Harb Perspect Biol, 2012. **4**(6).
30. Anderson, M.S., et al., *Projection of an immunological self shadow within the thymus by the aire protein.* Science, 2002. **298**(5597): p. 1395-401.
31. Smith-Garvin, J.E., G.A. Koretzky, and M.S. Jordan, *T cell activation.* Annu Rev Immunol, 2009. **27**: p. 591-619.
32. Chen, L. and D.B. Flies, *Molecular mechanisms of T cell co-stimulation and co-inhibition.* Nat Rev Immunol, 2013. **13**(4): p. 227-42.
33. Curtsinger, J.M., et al., *Inflammatory cytokines provide a third signal for activation of naive CD4+ and CD8+ T cells.* J Immunol, 1999. **162**(6): p. 3256-62.
34. Fernando, M.M., et al., *Defining the role of the MHC in autoimmunity: a review and pooled analysis.* PLoS Genet, 2008. **4**(4): p. e1000024.
35. Mueller, D.L. and M.K. Jenkins, *Autoimmunity: when self-tolerance breaks down.* Curr Biol, 1997. **7**(4): p. R255-7.
36. Wiseman, A.C., *Immunosuppressive Medications.* Clin J Am Soc Nephrol, 2016. **11**(2): p. 332-43.
37. Rhen, T. and J.A. Cidlowski, *Antiinflammatory action of glucocorticoids--new mechanisms for old drugs.* N Engl J Med, 2005. **353**(16): p. 1711-23.
38. Dhillon, S., *Tofacitinib: A Review in Rheumatoid Arthritis.* Drugs, 2017. **77**(18): p. 1987-2001.
39. Taylor, P.C. and M. Feldmann, *Anti-TNF biologic agents: still the therapy of choice for rheumatoid arthritis.* Nat Rev Rheumatol, 2009. **5**(10): p. 578-82.
40. Sorrentino, D., et al., *Stopping anti-TNF agents in patients with Crohn's disease in remission: is it a feasible long-term strategy?* Inflamm Bowel Dis, 2014. **20**(4): p. 757-66.
41. Glatigny, S., et al., *Abatacept Targets T Follicular Helper and Regulatory T Cells, Disrupting Molecular Pathways That Regulate Their Proliferation and Maintenance.* J Immunol, 2019. **202**(5): p. 1373-1382.

42. Targownik, L.E., et al., *The epidemiology of colectomy in ulcerative colitis: results from a population-based cohort.* Am J Gastroenterol, 2012. **107**(8): p. 1228-35.
43. Parragi, L., et al., *Colectomy Rates in Ulcerative Colitis are Low and Decreasing: 10-year Follow-up Data From the Swiss IBD Cohort Study.* J Crohns Colitis, 2018. **12**(7): p. 811-818.
44. Uings, I.J. and S.N. Farrow, *Cell receptors and cell signalling.* Mol Pathol, 2000. **53**(6): p. 295-9.
45. Dushek, O., J. Goyette, and P.A. van der Merwe, *Non-catalytic tyrosine-phosphorylated receptors.* Immunol Rev, 2012. **250**(1): p. 258-76.
46. Isakov, N., *Immunoreceptor tyrosine-based activation motif (ITAM), a unique module linking antigen and Fc receptors to their signaling cascades.* J Leukoc Biol, 1997. **61**(1): p. 6-16.
47. Daeron, M., et al., *Immunoreceptor tyrosine-based inhibition motifs: a quest in the past and future.* Immunol Rev, 2008. **224**: p. 11-43.
48. Le Borgne, M. and A.S. Shaw, *SAP signaling: a dual mechanism of action.* Immunity, 2012. **36**(6): p. 899-901.
49. Imbert, V., et al., *Induction of tyrosine phosphorylation and T-cell activation by vanadate peroxide, an inhibitor of protein tyrosine phosphatases.* Biochem J, 1994. **297 (Pt 1)**: p. 163-73.
50. Lemmon, M.A. and J. Schlessinger, *Cell signaling by receptor tyrosine kinases.* Cell, 2010. **141**(7): p. 1117-34.
51. Tolar, P., et al., *The constant region of the membrane immunoglobulin mediates B cell-receptor clustering and signaling in response to membrane antigens.* Immunity, 2009. **30**(1): p. 44-55.
52. Krogsgaard, M., et al., *Agonist/endogenous peptide-MHC heterodimers drive T cell activation and sensitivity.* Nature, 2005. **434**(7030): p. 238-43.
53. Erlandson, S.C., C. McMahon, and A.C. Kruse, *Structural Basis for G Protein-Coupled Receptor Signaling.* Annu Rev Biophys, 2018.
54. Li, Y.C., et al., *Cutting Edge: mechanical forces acting on T cells immobilized via the TCR complex can trigger TCR signaling.* J Immunol, 2010. **184**(11): p. 5959-63.
55. Kjer-Nielsen, L., et al., *A structural basis for the selection of dominant alphabeta T cell receptors in antiviral immunity.* Immunity, 2003. **18**(1): p. 53-64.
56. Rudolph, M.G., R.L. Stanfield, and I.A. Wilson, *How TCRs bind MHCs, peptides, and coreceptors.* Annu Rev Immunol, 2006. **24**: p. 419-66.
57. Dobbins, J., et al., *Binding of the cytoplasmic domain of CD28 to the plasma membrane inhibits Lck recruitment and signaling.* Sci Signal, 2016. **9**(438): p. ra75.
58. Xu, C., et al., *Regulation of T cell receptor activation by dynamic membrane binding of the CD3epsilon cytoplasmic tyrosine-based motif.* Cell, 2008. **135**(4): p. 702-13.
59. Tolar, P. and S.K. Pierce, *A conformation-induced oligomerization model for B cell receptor microclustering and signaling*, in *Immunological Synapse*, T. Saito and F.D. Batista, Editors. 2010, Springer Berlin Heidelberg: Berlin, Heidelberg. p. 155-69.

60. Davis, S.J. and P.A. van der Merwe, *The kinetic-segregation model: TCR triggering and beyond.* Nat Immunol, 2006. **7**(8): p. 803-9.
61. Chang, V.T., et al., *Initiation of T cell signaling by CD45 segregation at 'close contacts'.* Nat Immunol, 2016. **17**(5): p. 574-82.
62. Varma, R., et al., *T cell receptor-proximal signals are sustained in peripheral microclusters and terminated in the central supramolecular activation cluster.* Immunity, 2006. **25**(1): p. 117-27.
63. Irles, C., et al., *CD45 ectodomain controls interaction with GEMs and Lck activity for optimal TCR signaling.* Nat Immunol, 2003. **4**(2): p. 189-97.
64. Cordoba, S.-P.P., et al., *The large ectodomains of CD45 and CD148 regulate their segregation from and inhibition of ligated T-cell receptor.* Blood, 2013. **121**(21): p. 4295-4302.
65. Choudhuri, K., et al., *Peptide-major histocompatibility complex dimensions control proximal kinase-phosphatase balance during T cell activation.* J Biol Chem, 2009. **284**(38): p. 26096-105.
66. Choudhuri, K., et al., *T-cell receptor triggering is critically dependent on the dimensions of its peptide-MHC ligand.* Nature, 2005. **436**(7050): p. 578-82.
67. Ma, Z., et al., *Surface-anchored monomeric agonist pMHCs alone trigger TCR with high sensitivity.* PLoS Biol, 2008. **6**(2): p. e43.
68. James, S.E., et al., *Antigen sensitivity of CD22-specific chimeric TCR is modulated by target epitope distance from the cell membrane.* J Immunol, 2008. **180**(10): p. 7028-38.
69. Hudecek, M., et al., *Receptor affinity and extracellular domain modifications affect tumor recognition by ROR1-specific chimeric antigen receptor T cells.* Clin Cancer Res, 2013. **19**(12): p. 3153-64.
70. Hudecek, M., et al., *The nonsignaling extracellular spacer domain of chimeric antigen receptors is decisive for in vivo antitumor activity.* Cancer Immunol Res, 2015. **3**(2): p. 125-35.
71. Bluemel, C., et al., *Epitope distance to the target cell membrane and antigen size determine the potency of T cell-mediated lysis by BiTE antibodies specific for a large melanoma surface antigen.* Cancer Immunol Immunother, 2010. **59**(8): p. 1197-209.
72. Li, J., et al., *Membrane-Proximal Epitope Facilitates Efficient T Cell Synapse Formation by Anti-FcRH5/CD3 and Is a Requirement for Myeloma Cell Killing.* Cancer Cell, 2017. **31**(3): p. 383-395.
73. Köhler, K., et al., *Matched sizes of activating and inhibitory receptor/ligand pairs are required for optimal signal integration by human natural killer cells.* PLoS One, 2010. **5**(11): p. e15374.
74. He, H.T., A. Lellouch, and D. Marguet, *Lipid rafts and the initiation of T cell receptor signaling.* Semin Immunol, 2005. **17**(1): p. 23-33.
75. Paluch, C., et al., *Immune Checkpoints as Therapeutic Targets in Autoimmunity.* Front Immunol, 2018. **9**: p. 2306.
76. Suntharalingam, G., et al., *Cytokine storm in a phase 1 trial of the anti-CD28 monoclonal antibody TGN1412.* N Engl J Med, 2006. **355**(10): p. 1018-28.
77. Siefken, R., R. Kurrle, and R. Schwinzer, *CD28-mediated activation of resting human T cells without costimulation of the CD3/TCR complex.* Cell Immunol, 1997. **176**(1): p. 59-65.

78. Lühder, F., et al., *Topological requirements and signaling properties of T cell-activating, anti-CD28 antibody superagonists.* J Exp Med, 2003. **197**(8): p. 955-66.
79. Evans, E.J., et al., *Crystal structure of a soluble CD28-Fab complex.* Nat Immunol, 2005. **6**(3): p. 271-9.
80. Bartholomaeus, P., et al., *Cell contact-dependent priming and Fc interaction with CD32+ immune cells contribute to the TGN1412-triggered cytokine response.* J Immunol, 2014. **192**(5): p. 2091-8.
81. Hussain, K., et al., *Upregulation of FcγRIIb on monocytes is necessary to promote the superagonist activity of TGN1412.* Blood, 2015. **125**(1): p. 102-10.
82. Dudek, S., et al., *Human Fcγ receptors compete for TGN1412 binding that determines the antibody's effector function.* Eur J Immunol, 2019. **49**(7): p. 1117-1126.
83. Corthay, A., *Does the immune system naturally protect against cancer?* Front Immunol, 2014. **5**: p. 197.
84. McCarthy, E.F., *The toxins of William B. Coley and the treatment of bone and soft-tissue sarcomas.* Iowa Orthop J, 2006. **26**: p. 154-8.
85. Hodi, F.S., et al., *Improved survival with ipilimumab in patients with metastatic melanoma.* N Engl J Med, 2010. **363**(8): p. 711-23.
86. Robert, C., et al., *Nivolumab in previously untreated melanoma without BRAF mutation.* N Engl J Med, 2015. **372**(4): p. 320-30.
87. Gong, J., et al., *Development of PD-1 and PD-L1 inhibitors as a form of cancer immunotherapy: a comprehensive review of registration trials and future considerations.* J Immunother Cancer, 2018. **6**(1): p. 8.
88. Le Mercier, I., J.L. Lines, and R.J. Noelle, *Beyond CTLA-4 and PD-1, the Generation Z of Negative Checkpoint Regulators.* Front Immunol, 2015. **6**: p. 418.
89. Michot, J.M., et al., *Immune-related adverse events with immune checkpoint blockade: a comprehensive review.* Eur J Cancer, 2016. **54**: p. 139-148.
90. Amatore, F., L. Gorvel, and D. Olive, *Inducible Co-Stimulator (ICOS) as a potential therapeutic target for anti-cancer therapy.* Expert Opin Ther Targets, 2018. **22**(4): p. 343-351.
91. Melero, I., et al., *Agonist antibodies to TNFR molecules that costimulate T and NK cells.* Clin Cancer Res, 2013. **19**(5): p. 1044-53.
92. Li, J., Q. Yin, and H. Wu, *Structural basis of signal transduction in the TNF receptor superfamily.* Adv Immunol, 2013. **119**: p. 135-53.
93. Li, F. and J.V. Ravetch, *A general requirement for FcγRIIB co-engagement of agonistic anti-TNFR antibodies.* Cell Cycle, 2012. **11**(18): p. 3343-4.
94. Dahan, R., et al., *Therapeutic Activity of Agonistic, Human Anti-CD40 Monoclonal Antibodies Requires Selective FcγR Engagement.* Cancer Cell, 2016. **29**(6): p. 820-831.
95. White, A.L., et al., *Conformation of the human immunoglobulin G2 hinge imparts superagonistic properties to immunostimulatory anticancer antibodies.* Cancer Cell, 2015. **27**(1): p. 138-48.
96. Kuehn, H.S., et al., *Immune dysregulation in human subjects with heterozygous germline mutations in CTLA4.* Science, 2014. **345**(6204): p. 1623-1627.

97. Tivol, E.A., et al., *Loss of CTLA-4 leads to massive lymphoproliferation and fatal multiorgan tissue destruction, revealing a critical negative regulatory role of CTLA-4.* Immunity, 1995. **3**(5): p. 541-7.
98. Nishimura, H., et al., *Autoimmune dilated cardiomyopathy in PD-1 receptor-deficient mice.* Science, 2001. **291**(5502): p. 319-22.
99. Nishimura, H., et al., *Development of lupus-like autoimmune diseases by disruption of the PD-1 gene encoding an ITIM motif-carrying immunoreceptor.* Immunity, 1999. **11**(2): p. 141-51.
100. Kroner, A., et al., *A PD-1 polymorphism is associated with disease progression in multiple sclerosis.* Ann Neurol, 2005. **58**(1): p. 50-7.
101. Prokunina, L., et al., *A regulatory polymorphism in PDCD1 is associated with susceptibility to systemic lupus erythematosus in humans.* Nat Genet, 2002. **32**(4): p. 666-9.
102. James, E.S., et al., *PDCD1: a tissue-specific susceptibility locus for inherited inflammatory disorders.* Genes Immun, 2005. **6**(5): p. 430-7.
103. Lee, Y.H., et al., *Meta-analysis of genetic polymorphisms in programmed cell death 1. Associations with rheumatoid arthritis, ankylosing spondylitis, and type 1 diabetes susceptibility.* Z Rheumatol, 2015. **74**(3): p. 230-9.
104. Dong, H., et al., *Costimulating aberrant T cell responses by B7-H1 autoantibodies in rheumatoid arthritis.* J Clin Invest, 2003. **111**(3): p. 363-70.
105. Schreiner, B., et al., *Interferon-beta enhances monocyte and dendritic cell expression of B7-H1 (PD-L1), a strong inhibitor of autologous T-cell activation: relevance for the immune modulatory effect in multiple sclerosis.* J Neuroimmunol, 2004. **155**(1-2): p. 172-82.
106. Watanabe, N., et al., *BTLA is a lymphocyte inhibitory receptor with similarities to CTLA-4 and PD-1.* Nat Immunol, 2003. **4**(7): p. 670-9.
107. Oya, Y., et al., *Development of autoimmune hepatitis-like disease and production of autoantibodies to nuclear antigens in mice lacking B and T lymphocyte attenuator.* Arthritis Rheum, 2008. **58**(8): p. 2498-510.
108. Bekiaris, V., et al., *The inhibitory receptor BTLA controls γδ T cell homeostasis and inflammatory responses.* Immunity, 2013. **39**(6): p. 1082-1094.
109. Oki, M., et al., *A functional polymorphism in B and T lymphocyte attenuator is associated with susceptibility to rheumatoid arthritis.* Clin Dev Immunol, 2011. **2011**: p. 305656.
110. Lin, S.C., C.C. Kuo, and C.H. Chan, *Association of a BTLA gene polymorphism with the risk of rheumatoid arthritis.* J Biomed Sci, 2006. **13**(6): p. 853-60.
111. Anderson, C.A., et al., *Meta-analysis identifies 29 additional ulcerative colitis risk loci, increasing the number of confirmed associations to 47.* Nat Genet, 2011. **43**(3): p. 246-52.
112. Coenen, M.J., et al., *Common and different genetic background for rheumatoid arthritis and coeliac disease.* Hum Mol Genet, 2009. **18**(21): p. 4195-203.
113. Sawcer, S., et al., *Genetic risk and a primary role for cell-mediated immune mechanisms in multiple sclerosis.* Nature, 2011. **476**(7359): p. 214-9.
114. Folseraas, T., et al., *Extended analysis of a genome-wide association study in primary sclerosing cholangitis detects multiple novel risk loci.* J Hepatol, 2012. **57**(2): p. 366-75.

115. Ye, Z., et al., *Decreased B and T lymphocyte attenuator in Behcet's disease may trigger abnormal Th17 and Th1 immune responses.* Sci Rep, 2016. **6**: p. 20401.
116. Piancone, F., et al., *B Lymphocytes in Multiple Sclerosis: Bregs and BTLA/CD272 Expressing-CD19+ Lymphocytes Modulate Disease Severity.* Sci Rep, 2016. **6**: p. 29699.
117. Joller, N., et al., *Cutting edge: TIGIT has T cell-intrinsic inhibitory functions.* J Immunol\, 2011. **186**\(3\): p. 1338-42\.
118. Yaghoobi, E., et al., *TIM-3 Rs10515746 (A/C) and Rs10053538 (C/A) Gene Polymorphisms and Risk of Multiple Sclerosis.* Iran J Public Health, 2016. **45**(5): p. 644-9.
119. Chae, S.C., et al., *The polymorphisms of Th1 cell surface gene Tim-3 are associated in a Korean population with rheumatoid arthritis.* Immunol Lett, 2004. **95**(1): p. 91-5.
120. Wang, M., et al., *Tim-3 polymorphism downregulates gene expression and is involved in the susceptibility to ankylosing spondylitis.* DNA Cell Biol, 2014. **33**(10): p. 723-8.
121. Macauley, M.S., P.R. Crocker, and J.C. Paulson, *Siglec-mediated regulation of immune cell function in disease.* Nat Rev Immunol, 2014. **14**(10): p. 653-66.
122. Zenarruzabeitia, O., et al., *The Biology and Disease Relevance of CD300a, an Inhibitory Receptor for Phosphatidylserine and Phosphatidylethanolamine.* J Immunol, 2015. **194**(11): p. 5053-60.
123. Smith, K.G. and M.R. Clatworthy, *FcgammaRIIB in autoimmunity and infection: evolutionary and therapeutic implications.* Nat Rev Immunol, 2010. **10**(5): p. 328-43.
124. Moreland, L., G. Bate, and P. Kirkpatrick, *Abatacept.* Nat Rev Drug Discov, 2006. **5**(3): p. 185-6.
125. Lee, S., et al., *Abatacept alleviates severe autoimmune symptoms in a patient carrying a de novo variant in CTLA-4.* J Allergy Clin Immunol, 2016. **137**(1): p. 327-330.
126. Walker, L.S. and D.M. Sansom, *Confusing signals: recent progress in CTLA-4 biology.* Trends Immunol, 2015. **36**(2): p. 63-70.
127. Raptopoulou, A.P., et al., *The programmed death 1/programmed death ligand 1 inhibitory pathway is up-regulated in rheumatoid synovium and regulates peripheral T cell responses in human and murine arthritis.* Arthritis Rheum, 2010. **62**(7): p. 1870-80.
128. Wang, G., et al., *The effects of PDL-Ig on collagen-induced arthritis.* Rheumatol Int, 2011. **31**(4): p. 513-9.
129. Song, M.Y., et al., *Protective effects of Fc-fused PD-L1 on two different animal models of colitis.* Gut, 2015. **64**(2): p. 260-71.
130. Gonzalez, L.C., et al., *A coreceptor interaction between the CD28 and TNF receptor family members B and T\ lymphocyte attenuator and herpesvirus entry mediator.* Proc Natl Acad Sci U S A\, 2005. **102**\(4\): p. 1116-21\.
131. Brown, G.R., et al., *IL-12-independent LIGHT signaling enhances MHC class II disparate CD4+ T cell alloproliferation, IFN-gamma responses, and intestinal graft-versus-host disease.* J Immunol, 2005. **174**(8): p. 4688-95.

132. Pierer, M., et al., *Herpesvirus entry mediator-Ig treatment during immunization aggravates rheumatoid arthritis in the collagen-induced arthritis model.* J Immunol, 2009. **182**(5): p. 3139-45.
133. Gorczynski, R.M., et al., *CD200 immunoadhesin suppresses collagen-induced arthritis in mice.* Clin Immunol, 2001. **101**(3): p. 328-34.
134. Simelyte, E., et al., *CD200-Fc, a novel antiarthritic biologic agent that targets proinflammatory cytokine expression in the joints of mice with collagen-induced arthritis.* Arthritis Rheum, 2008. **58**(4): p. 1038-43.
135. Liu, Y., et al., *CD200R1 agonist attenuates mechanisms of chronic disease in a murine model of multiple sclerosis.* J Neurosci, 2010. **30**(6): p. 2025-38.
136. Seki, M., et al., *Galectin-9 suppresses the generation of Th17, promotes the induction of regulatory T cells, and regulates experimental autoimmune arthritis.* Clin Immunol, 2008. **127**(1): p. 78-88.
137. He, W., et al., *Galectin-9 significantly prolongs the survival of fully mismatched cardiac allografts in mice.* Transplantation, 2009. **88**(6): p. 782-90.
138. Wang, F., et al., *The Tim-3 ligand galectin-9 negatively regulates CD8+ alloreactive T cell and prolongs survival of skin graft.* Cell Immunol, 2007. **250**(1-2): p. 68-74.
139. Belardi, B., et al., *Investigating cell surface galectin-mediated cross-linking on glycoengineered cells.* J Am Chem Soc, 2012. **134**(23): p. 9549-52.
140. Cooper, D.N. and S.H. Barondes, *God must love galectins; he made so many of them.* Glycobiology, 1999. **9**(10): p. 979-84.
141. Albring, J.C., et al., *Targeting of B and T lymphocyte associated (BTLA) prevents graft-versus-host disease without global immunosuppression.* J Exp Med, 2010. **207**(12): p. 2551-9.
142. Hurchla, M.A., et al., *B and T lymphocyte attenuator exhibits structural and expression polymorphisms and is highly Induced in anergic CD4+ T cells.* J Immunol, 2005. **174**(6): p. 3377-85.
143. Kobayashi, Y., et al., *B and T lymphocyte attenuator inhibits LPS-induced endotoxic shock by suppressing Toll-like receptor 4 signaling in innate immune cells.* Proc Natl Acad Sci U S A, 2013. **110**(13): p. 5121-6.
144. Lepenies, B., et al., *Ligation of B and T lymphocyte attenuator prevents the genesis of experimental cerebral malaria.* J Immunol, 2007. **179**(6): p. 4093-100.
145. Uchiyama, M., et al., *An agonistic anti-BTLA mAb (3C10) induced generation of IL-10-dependent regulatory CD4+ T cells and prolongation of murine cardiac allograft.* Transplantation, 2014. **97**(3): p. 301-9.
146. Truong, W., et al., *Negative and positive co-signaling with anti-BTLA (PJ196) and CTLA4Ig prolongs islet allograft survival.* Transplantation, 2007. **84**(10): p. 1368-72.
147. Krieg, C., et al., *Functional analysis of B and T lymphocyte attenuator engagement on CD4+ and CD8+ T cells.* J Immunol, 2005. **175**(10): p. 6420-7.
148. Otsuki, N., et al., *Expression and function of the B and T lymphocyte attenuator (BTLA/CD272) on human T cells.* Biochem Biophys Res Commun, 2006. **344**(4): p. 1121-7.
149. Atwell, S.K., A.C. Vendel, and V.H. Obungu, *Btla Agonist Antibodies and Uses Thereof (US Patent No. US2018334502 (A1))*. 2018, Lilly Co Eli.

150. Gorczynski, R.M., et al., *Anti-CD200R ameliorates collagen-induced arthritis in mice.* Clin Immunol, 2002. **104**(3): p. 256-64.
151. Snelgrove, R.J., et al., *A critical function for CD200 in lung immune homeostasis and the severity of influenza infection.* Nat Immunol, 2008. **9**(9): p. 1074-83.
152. Copland, D.A., et al., *Monoclonal antibody-mediated CD200 receptor signaling suppresses macrophage\ activation and tissue damage in experimental autoimmune uveoretinitis.* Am J Pathol\, 2007. **171**(2\): p. 580-8\.
153. Cherwinski, H.M., et al., *The CD200 receptor is a novel and potent regulator of murine and human mast cell \ function.* J Immunol\, 2005. **174**(3\): p. 1348-56\.
154. Grujic, O., et al., *Impact of antibody subclass and disulfide isoform differences on the biological activity of CD200R and βklotho agonist antibodies.* Biochem Biophys Res Commun, 2017. **486**(4): p. 985-991.
155. Dixon, K.O., et al., *Functional Anti-TIGIT Antibodies Regulate Development of Autoimmunity and Antitumor Immunity.* J Immunol, 2018.
156. Flies, D.B., T. Higuchi, and L. Chen, *Mechanistic Assessment of PD-1H Coinhibitory Receptor-Induced T Cell Tolerance to Allogeneic Antigens.* J Immunol, 2015. **194**(11): p. 5294-304.
157. Flies, D.B., et al., *Coinhibitory receptor PD-1H preferentially suppresses CD4⁺ T cell-mediated immunity.* J Clin Invest, 2014. **124**(5): p. 1966-75.
158. Freishtat, R.J., et al., *NKG2A inhibits TH2 cell effector function in vitro.* BMC Pulm Med, 2007. **7**: p. 14.
159. Arce Vargas, F., et al., *Fc Effector Function Contributes to the Activity of Human Anti-CTLA-4 Antibodies.* Cancer Cell, 2018. **33**(4): p. 649-663.e4.
160. Griffin, M.D., et al., *Blockade of T cell activation using a surface-linked single-chain antibody to CTLA-4 (CD152).* J Immunol, 2000. **164**(9): p. 4433-42.
161. Fife, B.T., et al., *Inhibition of T cell activation and autoimmune diabetes using a B cell surface-linked CTLA-4 agonist.* J Clin Invest, 2006. **116**(8): p. 2252-61.
162. Akkaya, B., *Modulation of the PD-1 pathway by inhibitory antibody superagonists (PhD Thesis)*. 2012.
163. Bennett, B., et al., *Pd-1 Binding Proteins and Methods of Use Thereof (Patent No. WO2017058859 (A1))*. 2017, Celgene Corp.
164. Sieber, T., et al., *Selective internalization of monoclonal antibodies by B-cell chronic lymphocytic leukaemia cells.* Br J Haematol, 2003. **121**(3): p. 458-61.
165. Vaughan, A.T., et al., *Activatory and inhibitory Fcγ receptors augment rituximab-mediated internalization of CD20 independent of signaling via the cytoplasmic domain.* J Biol Chem, 2015. **290**(9): p. 5424-37.
166. Cheung, T.C., et al., *Evolutionarily divergent herpesviruses modulate T cell activation by targeting the herpesvirus entry mediator cosignaling pathway.* Proc Natl Acad Sci U S A, 2005. **102**(37): p. 13218-23.
167. Šedý, J.R., et al., *A herpesvirus entry mediator mutein with selective agonist action for the inhibitory receptor B and T lymphocyte attenuator.* J Biol Chem, 2017. **292**(51): p. 21060-21070.
168. Prodeus, A., et al., *Agonistic CD200R1 DNA Aptamers Are Potent Immunosuppressants That Prolong Allogeneic Skin Graft Survival.* Mol Ther Nucleic Acids, 2014. **3**: p. e190.

169. Hirata, S., et al., *Prevention of experimental autoimmune encephalomyelitis by transfer of embryonic stem cell-derived dendritic cells expressing myelin oligodendrocyte glycoprotein peptide along with TRAIL or programmed death-1 ligand.* J Immunol, 2005. **174**(4): p. 1888-97.
170. He, F.R., et al., *Programmed death-1 ligands-transfected dendritic cells loaded with glutamic acid decarboxylase 65 (GAD65) inhibit both the alloresponse and the GAD65-reactive lymphocyte response.* Clin Exp Immunol, 2008. **151**(1): p. 86-93.
171. Veri, M.C., et al., *Therapeutic control of B cell activation via recruitment of Fcgamma receptor IIb (CD32B) inhibitory function with a novel bispecific antibody scaffold.* Arthritis Rheum, 2010. **62**(7): p. 1933-43.
172. Bachelet, I., A. Munitz, and F. Levi-Schaffer, *Abrogation of allergic reactions by a bispecific antibody fragment linking IgE to CD300a.* J Allergy Clin Immunol, 2006. **117**(6): p. 1314-20.
173. Gorczynski, R.M., et al., *Potent immunosuppression by a bivalent molecule binding to CD200R and TGF-betaR.* Transplantation, 2010. **90**(2): p. 150-9.
174. Zhang, X., et al., *Structural and functional analysis of the costimulatory receptor programmed death-1.* Immunity, 2004. **20**(3): p. 337-47.
175. Ishida, Y., et al., *Induced expression of PD-1, a novel member of the immunoglobulin gene superfamily, upon programmed cell death.* EMBO J, 1992. **11**(11): p. 3887-95.
176. Bally, A.P., J.W. Austin, and J.M. Boss, *Genetic and Epigenetic Regulation of PD-1 Expression.* J Immunol, 2016. **196**(6): p. 2431-7.
177. Francisco, L.M., P.T. Sage, and A.H. Sharpe, *The PD-1 pathway in tolerance and autoimmunity.* Immunol Rev, 2010. **236**: p. 219-42.
178. Chen, J., et al., *Regulation of PD-L1: a novel role of pro-survival signalling in cancer.* Ann Oncol, 2016. **27**(3): p. 409-16.
179. Cheng, X., et al., *Structure and interactions of the human programmed cell death 1 receptor.* J Biol Chem, 2013. **288**(17): p. 11771-85.
180. Chemnitz, J.M., et al., *SHP-1 and SHP-2 associate with immunoreceptor tyrosine-based switch motif of programmed death 1 upon primary human T cell stimulation, but only receptor ligation prevents T cell activation.* J Immunol, 2004. **173**(2): p. 945-54.
181. Hui, E., et al., *T cell costimulatory receptor CD28 is a primary target for PD-1-mediated inhibition.* Science, 2017. **355**(6332): p. 1428-1433.
182. Xu, X., et al., *BTLA and PD-1 employ distinct phosphatases to differentially repress T cell signaling.* bioRxiv, 2019: p. 669812.
183. Francisco, L.M., et al., *PD-L1 regulates the development, maintenance, and function of induced regulatory T cells.* J Exp Med, 2009. **206**(13): p. 3015-29.
184. Han, P., et al., *An inhibitory Ig superfamily protein expressed by lymphocytes and APCs is also an early marker of thymocyte positive selection.* J Immunol, 2004. **172**(10): p. 5931-9.
185. Fuertes Marraco, S.A., et al., *Inhibitory Receptors Beyond T Cell Exhaustion.* Front Immunol, 2015. **6**: p. 310.
186. Sedy, J.R., et al., *B and T lymphocyte attenuator regulates T cell activation through interaction with herpesvirus entry mediator.* Nat Immunol, 2005. **6**(1): p. 90-8.

187. Cai, G., et al., *CD160 inhibits activation of human CD4+ T cells through interaction with herpesvirus entry mediator.* Nat Immunol, 2008. **9**(2): p. 176-85.
188. Cheung, T.C., et al., *T cell intrinsic heterodimeric complexes between HVEM and BTLA determine receptivity to the surrounding microenvironment.* J Immunol, 2009. **183**(11): p. 7286-96.
189. Murphy, K.M., C.A. Nelson, and J.R. Sedý, *Balancing co-stimulation and inhibition with BTLA and HVEM.* Nat Rev Immunol, 2006. **6**(9): p. 671-81.
190. Jutz, S., et al., *A cellular platform for the evaluation of immune checkpoint molecules.* Oncotarget, 2017. **8**(39): p. 64892-64906.
191. Gavrieli, M., et al., *Characterization of phosphotyrosine binding motifs in the cytoplasmic domain of B and T lymphocyte attenuator required for association with protein tyrosine phosphatases SHP-1 and SHP-2.* Biochem Biophys Res Commun, 2003. **312**(4): p. 1236-43.
192. Ritthipichai, K., et al., *Multifaceted Role of BTLA in the Control of CD8.* Clin Cancer Res, 2017. **23**(20): p. 6151-6164.
193. Gavrieli, M. and K.M. Murphy, *Association of Grb-2 and PI3K p85 with phosphotyrosile peptides derived from BTLA.* Biochem Biophys Res Commun, 2006. **345**(4): p. 1440-5.
194. Hurchla, M.A., J.R. Sedy, and K.M. Murphy, *Unexpected role of B and T lymphocyte attenuator in sustaining cell survival during chronic allostimulation.* J Immunol, 2007. **178**(10): p. 6073-82.
195. Cheung, T.C., et al., *Unconventional ligand activation of herpesvirus entry mediator signals cell survival.* Proc Natl Acad Sci U S A, 2009. **106**(15): p. 6244-9.
196. Sakoda, Y., et al., *Dichotomous regulation of GVHD through bidirectional functions of the BTLA-HVEM pathway.* Blood, 2011. **117**(8): p. 2506-14.
197. Le Bouteiller, P., et al., *CD160: a unique activating NK cell receptor.* Immunol Lett, 2011. **138**(2): p. 93-6.
198. Deppong, C., et al., *Cutting edge: B and T lymphocyte attenuator and programmed death receptor-1 inhibitory receptors are required for termination of acute allergic airway inflammation.* J Immunol, 2006. **176**(7): p. 3909-13.
199. Wang, Y., et al., *The role of herpesvirus entry mediator as a negative regulator of T cell-mediated responses.* J Clin Invest, 2005. **115**(3): p. 711-7.
200. Steinberg, M.W., et al., *A crucial role for HVEM and BTLA in preventing intestinal inflammation.* J Exp Med, 2008. **205**(6): p. 1463-76.
201. Mintz, M.A., et al., *The HVEM-BTLA Axis Restrains T Cell Help to Germinal Center B Cells and Functions as a Cell-Extrinsic Suppressor in Lymphomagenesis.* Immunity, 2019.
202. Boice, M., et al., *Loss of the HVEM Tumor Suppressor in Lymphoma and Restoration by Modified CAR-T Cells.* Cell, 2016. **167**(2): p. 405-418.e13.
203. Vendel, A.C., et al., *B and T lymphocyte attenuator regulates B cell receptor signaling by targeting Syk and BLNK.* J Immunol, 2009. **182**(3): p. 1509-17.
204. Miller, M.L., Y. Sun, and Y.X. Fu, *Cutting edge: B and T lymphocyte attenuator signaling on NKT cells inhibits cytokine release and tissue injury in early immune responses.* J Immunol, 2009. **183**(1): p. 32-6.

205. Jones, A., et al., *Immunomodulatory Functions of BTLA and HVEM Govern Induction of Extrathymic Regulatory T Cells and Tolerance by Dendritic Cells.* Immunity, 2016. **45**(5): p. 1066-1077.
206. Yang, X., et al., *A BTLA-mediated bait and switch strategy permits Listeria expansion in CD8α(+) DCs to promote long-term T cell responses.* Cell Host Microbe, 2014. **16**(1): p. 68-80.
207. Yu, X., et al., *The surface protein TIGIT suppresses T cell activation by promoting the\ generation of mature immunoregulatory dendritic cells.* Nat Immunol\, 2009. **10**(1\): p. 48-57\.
208. Stanietsky, N., et al., *The interaction of TIGIT with PVR and PVRL2 inhibits human NK cell cytotoxicity.* Proc Natl Acad Sci U S A\, 2009. **106**(42\): p. 17858-63\.
209. Stanietsky, N., et al., *Mouse TIGIT inhibits NK-cell cytotoxicity upon interaction with PVR.* Eur J Immunol\, 2013. **43**(8\): p. 2138-50\.
210. Levin, S.D., et al., *Vstm3 is a member of the CD28 family and an important modulator of T-cell\ function.* Eur J Immunol\, 2011. **41**(4\): p. 902-15\.
211. Johnston, R.J., et al., *The immunoreceptor TIGIT regulates antitumor and antiviral CD8(+) T cell effector function.* Cancer Cell, 2014. **26**(6): p. 923-37.
212. Chan, C.J., et al., *The receptors CD96 and CD226 oppose each other in the regulation of natural\ killer cell functions.* Nat Immunol\, 2014. **15**(5\): p. 431-8\.
213. Li, M., et al., *T-cell immunoglobulin and ITIM domain (TIGIT) receptor/poliovirus receptor (PVR) \ ligand engagement suppresses interferon-gamma production of natural killer cells \ via beta-arrestin 2-mediated negative signaling.* J Biol Chem\, 2014. **289**(25\): p. 17647-57\.
214. Liu, S., et al., *Recruitment of Grb2 and SHIP1 by the ITT-like motif of TIGIT suppresses granule\ polarization and cytotoxicity of NK cells.* Cell Death Differ\, 2013. **20**(3\): p. 456-64\.
215. Joller, N., et al., *Treg cells expressing the coinhibitory molecule TIGIT selectively inhibit\ proinflammatory Th1 and Th17 cell responses.* Immunity\, 2014. **40**(4\): p. 569-81\.
216. Zhang, T., et al., *Increased expression of TIGIT on CD4+ T cells ameliorates immune-mediated bone\ marrow failure of aplastic anemia.* J Cell Biochem\, 2014. **115**(11\): p. 1918-27\.
217. Zhang, S., et al., *Molecular mechanisms of CD200 inhibition of mast cell activation.* J Immunol, 2004. **173**(11): p. 6786-93.
218. Zhang, S. and J.H. Phillips, *Identification of tyrosine residues crucial for CD200R-mediated inhibition of mast cell activation.* J Leukoc Biol, 2006. **79**(2): p. 363-8.
219. Wright, G.J., et al., *Characterization of the CD200 receptor family in mice and humans and their interactions with CD200.* J Immunol, 2003. **171**(6): p. 3034-46.
220. Rijkers, E.S., et al., *The inhibitory CD200R is differentially expressed on human and mouse T and B lymphocytes.* Mol Immunol, 2008. **45**(4): p. 1126-35.
221. Gorczynski, R., et al., *CD200 is a ligand for all members of the CD200R family of immunoregulatory molecules.* J Immunol, 2004. **172**(12): p. 7744-9.

222. Hatherley, D., et al., *Structures of CD200/CD200 receptor family and implications for topology, regulation, and evolution.* Structure, 2013. **21**(5): p. 820-32.
223. Kwong, L.S., et al., *Herpesvirus orthologues of CD200 bind host CD200R but not related activating receptors.* J Gen Virol, 2016. **97**(1): p. 179-84.
224. Gorczynski, R.M., *CD200:CD200R-Mediated Regulation of Immunity.* ISRN Immunology, 2012. **2012**: p. 18.
225. Hoek, R.M., et al., *Down-regulation of the macrophage lineage through interaction with OX2 (CD200).* Science, 2000. **290**(5497): p. 1768-71.
226. Davis, S. and K.-L. Tyson, *Pd-1 Specific Antibodies and Uses Thereof (granted patent)*. 2015, Isis Innovation.
227. Vieites, J.M., et al., *Characterization of human cd200 glycoprotein receptor gene located on chromosome 3q12-13.* Gene, 2003. **311**: p. 99-104.
228. Tiller, T., C.E. Busse, and H. Wardemann, *Cloning and expression of murine Ig genes from single B cells.* J Immunol Methods, 2009. **350**(1-2): p. 183-93.
229. Yuan, X., M.J. Gubbins, and J.D. Berry, *A simple and rapid protocol for the sequence determination of functional kappa light chain cDNAs from aberrant-chain-positive murine hybridomas.* J Immunol Methods, 2004. **294**(1-2): p. 199-207.
230. Barnden, M.J., et al., *Defective TCR expression in transgenic mice constructed using cDNA-based alpha- and beta-chain genes under the control of heterologous regulatory elements.* Immunol Cell Biol, 1998. **76**(1): p. 34-40.
231. Mestas, J. and C.C. Hughes, *Of mice and not men: differences between mouse and human immunology.* J Immunol, 2004. **172**(5): p. 2731-8.
232. Masopust, D., C.P. Sivula, and S.C. Jameson, *Of Mice, Dirty Mice, and Men: Using Mice To Understand Human Immunology.* J Immunol, 2017. **199**(2): p. 383-388.
233. Koning, N., et al., *Expression of the inhibitory CD200 receptor is associated with alternative macrophage activation.* J Innate Immun, 2010. **2**(2): p. 195-200.
234. Rose, S., A. Misharin, and H. Perlman, *A novel Ly6C/Ly6G-based strategy to analyze the mouse splenic myeloid compartment.* Cytometry A, 2012. **81**(4): p. 343-50.
235. Boudakov, I., et al., *Mice lacking CD200R1 show absence of suppression of lipopolysaccharide-induced tumor necrosis factor-alpha and mixed leukocyte culture responses by CD200.* Transplantation, 2007. **84**(2): p. 251-7.
236. Woof, J.M. and D.R. Burton, *Human antibody-Fc receptor interactions illuminated by crystal structures.* Nat Rev Immunol, 2004. **4**(2): p. 89-99.
237. Stengel, K.F., et al., *Structure of TIGIT immunoreceptor bound to poliovirus receptor reveals a\ cell-cell adhesion and signaling mechanism that requires cis-trans receptor\ clustering.* Proc Natl Acad Sci U S A\, 2012. **109**(14\): p. 5399-404\.
238. Baudino, L., et al., *Crucial role of aspartic acid at position 265 in the CH2 domain for murine IgG2a and IgG2b Fc-associated effector functions.* J Immunol, 2008. **181**(9): p. 6664-9.
239. Nimmerjahn, F., et al., *FcgammaRIV: a novel FcR with distinct IgG subclass specificity.* Immunity, 2005. **23**(1): p. 41-51.
240. Clynes, R.A., et al., *Inhibitory Fc receptors modulate in vivo cytotoxicity against tumor targets.* Nat Med, 2000. **6**(4): p. 443-6.

241. Dahan, R., et al., *FcγRs Modulate the Anti-tumor Activity of Antibodies Targeting the PD-1/PD-L1 Axis.* Cancer Cell, 2015. **28**(3): p. 285-95.
242. Steinberg, M.W., T.C. Cheung, and C.F. Ware, *The signaling networks of the herpesvirus entry mediator (TNFRSF14) in immune regulation.* Immunol Rev, 2011. **244**(1): p. 169-87.
243. Chames, P., et al., *Therapeutic antibodies: successes, limitations and hopes for the future.* Br J Pharmacol, 2009. **157**(2): p. 220-33.
244. Assmann, M., *Imaging-based analysis of antibody superagonism*. 2016, University of Oxford
245. Vafa, O., et al., *An engineered Fc variant of an IgG eliminates all immune effector functions via structural perturbations.* Methods, 2014. **65**(1): p. 114-26.
246. Arlauckas, S.P., et al., *In vivo imaging reveals a tumor-associated macrophage-mediated resistance pathway in anti-PD-1 therapy.* Sci Transl Med, 2017. **9**(389).
247. Kiesler, P., I.J. Fuss, and W. Strober, *Experimental Models of Inflammatory Bowel Diseases.* Cell Mol Gastroenterol Hepatol, 2015. **1**(2): p. 154-170.
248. Eri, R., M.A. McGuckin, and R. Wadley, *T cell transfer model of colitis: a great tool to assess the contribution of T cells in chronic intestinal inflammation.* Methods Mol Biol, 2012. **844**: p. 261-75.
249. Powrie, F., et al., *Inhibition of Th1 responses prevents inflammatory bowel disease in scid mice reconstituted with CD45RBhi CD4+ T cells.* Immunity, 1994. **1**(7): p. 553-62.
250. Lindebo Holm, T., et al., *Pharmacological Evaluation of the SCID T Cell Transfer Model of Colitis: As a Model of Crohn's Disease.* Int J Inflam, 2012. **2012**: p. 412178.
251. Kjellev, S., et al., *Reconstitution of Scid mice with CD4+CD25- T cells leads to rapid colitis: an improved model for pharmacologic testing.* Int Immunopharmacol, 2006. **6**(8): p. 1341-54.
252. Shlomchik, W.D., *Graft-versus-host disease.* Nat Rev Immunol, 2007. **7**(5): p. 340-52.
253. Saad, A. and L.S. Lamb, *Ex vivo T-cell depletion in allogeneic hematopoietic stem cell transplant: past, present and future.* Bone Marrow Transplant, 2017. **52**(9): p. 1241-1248.
254. Efremova, M., et al., *Targeting immune checkpoints potentiates immunoediting and changes the dynamics of tumor evolution.* Nat Commun, 2018. **9**(1): p. 32.
255. Tang, H., et al., *PD-L1 on host cells is essential for PD-L1 blockade-mediated tumor regression.* J Clin Invest, 2018. **128**(2): p. 580-588.
256. De Sousa Linhares, A., et al., *Not All Immune Checkpoints Are Created Equal.* Front Immunol, 2018. **9**: p. 1909.
257. Barré-Sinoussi, F. and X. Montagutelli, *Animal models are essential to biological research: issues and perspectives.* Future Sci OA, 2015. **1**(4): p. FSO63.
258. Fox, J.G., *The mouse in biomedical research*. 2nd ed. / edited by James G. Fox ... [et al.]. ed. 2007, Amsterdam ; London: Elsevier.
259. Sanmamed, M.F., et al., *Defining the optimal murine models to investigate immune checkpoint blockers and their combination with other immunotherapies.* Ann Oncol, 2016. **27**(7): p. 1190-8.

260. Lute, K.D., et al., *Human CTLA4 knock-in mice unravel the quantitative link between tumor immunity and autoimmunity induced by anti-CTLA-4 antibodies.* Blood, 2005. **106**(9): p. 3127-33.
261. Zhang, M., et al., *Monoclonal antibodies to B and T lymphocyte attenuator (BTLA) have no effect on in vitro B cell proliferation and act to inhibit in vitro T cell proliferation when presented in a cis, but not trans, format relative to the activating stimulus.* Clin Exp Immunol, 2011. **163**(1): p. 77-87.
262. Kurreeman, F.A., et al., *Use of a multiethnic approach to identify rheumatoid-arthritis-susceptibility loci, 1p36 and 17q12.* Am J Hum Genet, 2012. **90**(3): p. 524-32.
263. Dubois, P.C., et al., *Multiple common variants for celiac disease influencing immune gene expression.* Nat Genet, 2010. **42**(4): p. 295-302.
264. Celis-Gutierrez, J., et al., *Quantitative Interactomics in Primary T Cells Provides a Rationale for Concomitant PD-1 and BTLA Coinhibitor Blockade in Cancer Immunotherapy.* Cell Rep, 2019. **27**(11): p. 3315-3330.e7.
265. Hobo, W., et al., *B and T lymphocyte attenuator mediates inhibition of tumor-reactive CD8+ T cells in patients after allogeneic stem cell transplantation.* J Immunol, 2012. **189**(1): p. 39-49.
266. Fourcade, J., et al., *CD8(+) T cells specific for tumor antigens can be rendered dysfunctional by the tumor microenvironment through upregulation of the inhibitory receptors BTLA and PD-1.* Cancer Res, 2012. **72**(4): p. 887-96.
267. Darvin, P., et al., *Immune checkpoint inhibitors: recent progress and potential biomarkers.* Exp Mol Med, 2018. **50**(12): p. 165.
268. Austyn, J.M., K.G. Smith, and P.J. Morris, *T cell activation by anti-CD3 antibodies: function of Fc receptors on B cell blasts, but not resting B cells, and CD18 on the responding T cells.* Eur J Immunol, 1987. **17**(9): p. 1329-35.
269. Moore, G., L., Chu, S.Y., Pong, E., Wickramarachchi, D., Endo, N.A., Chan, E.W., Phung, S., Chen, H., Leung, I.W.L., Bonzon, C., Goetzmann, J.E., Carmichael, D.F., Szymkowksi, D. E., and Desjarlais, J.R., *Accelerated clearance of IgE in chimpanzees is mediated by XmAb7195, an Fc-engineered antibody with enhanced affinity for inhibitory receptor FcγRIIb. ATS International Conference (poster).* 2014
270. Foster. P., G.A., Goldwater. R., *A randomized, double-blinded, placebo-controlled, ascending dose study of the safety, tolerability, and pharmacokinetics of XmAb7195. ATS International Conference (poster).* 2016.
271. Ganesan, L.P., et al., *FcγRIIb on liver sinusoidal endothelium clears small immune complexes.* J Immunol, 2012. **189**(10): p. 4981-8.
272. Wang, X., M. Mathieu, and R.J. Brezski, *IgG Fc engineering to modulate antibody effector functions.* Protein Cell, 2018. **9**(1): p. 63-73.
273. Mimoto, F., et al., *Engineered antibody Fc variant with selectively enhanced FcγRIIb binding over both FcγRIIa(R131) and FcγRIIa(H131).* Protein Eng Des Sel, 2013. **26**(10): p. 589-98.
274. Overdijk, M.B., et al., *Crosstalk between human IgG isotypes and murine effector cells.* J Immunol, 2012. **189**(7): p. 3430-8.
275. Smith, P., et al., *Mouse model recapitulating human Fcγ receptor structural and functional diversity.* Proc Natl Acad Sci U S A, 2012. **109**(16): p. 6181-6.

276. Heuts, F. and N. Nagy, *Mice with Reconstituted Human Immune System Components as a Tool to Study Immune Cell Interactions in EBV Infection.* Methods Mol Biol, 2017. **1532**: p. 229-240.
277. Amigorena, S. and C. Bonnerot, *Fc receptor signaling and trafficking: a connection for antigen processing.* Immunol Rev, 1999. **172**: p. 279-84.
278. Batista, F.D. and M.L. Dustin, *Cell:cell interactions in the immune system.* Immunol Rev, 2013. **251**(1): p. 7-12.
279. Wolchok, J.D., et al., *Overall Survival with Combined Nivolumab and Ipilimumab in Advanced Melanoma.* N Engl J Med, 2017. **377**(14): p. 1345-1356.
280. Fessas, P., et al., *A molecular and preclinical comparison of the PD-1-targeted T-cell checkpoint inhibitors nivolumab and pembrolizumab.* Semin Oncol, 2017. **44**(2): p. 136-140.
281. Bruhns, P., et al., *Specificity and affinity of human Fcgamma receptors and their polymorphic variants for human IgG subclasses.* Blood, 2009. **113**(16): p. 3716-25.